frontiers | Research Topics

Microorganisms in sustainable and green agriculture: synergistic effect on carbon sequestration and crop productivity

Edited by
Jianling Fan and Yichao Shi

Coordinated by
Yunliang Li

Published in
Frontiers in Microbiology

ISSN 1664-8714
ISBN 978-2-8325-5339-8
DOI 10.3389/978-2-8325-5339-8

About Frontiers

Frontiers is more than just an open access publisher of scholarly articles: it is a pioneering approach to the world of academia, radically improving the way scholarly research is managed. The grand vision of Frontiers is a world where all people have an equal opportunity to seek, share and generate knowledge. Frontiers provides immediate and permanent online open access to all its publications, but this alone is not enough to realize our grand goals.

Frontiers journal series

The Frontiers journal series is a multi-tier and interdisciplinary set of open-access, online journals, promising a paradigm shift from the current review, selection and dissemination processes in academic publishing. All Frontiers journals are driven by researchers for researchers; therefore, they constitute a service to the scholarly community. At the same time, the *Frontiers journal series* operates on a revolutionary invention, the tiered publishing system, initially addressing specific communities of scholars, and gradually climbing up to broader public understanding, thus serving the interests of the lay society, too.

Dedication to quality

Each Frontiers article is a landmark of the highest quality, thanks to genuinely collaborative interactions between authors and review editors, who include some of the world's best academicians. Research must be certified by peers before entering a stream of knowledge that may eventually reach the public - and shape society; therefore, Frontiers only applies the most rigorous and unbiased reviews. Frontiers revolutionizes research publishing by freely delivering the most outstanding research, evaluated with no bias from both the academic and social point of view. By applying the most advanced information technologies, Frontiers is catapulting scholarly publishing into a new generation.

What are Frontiers Research Topics?

Frontiers Research Topics are very popular trademarks of the *Frontiers journals series*: they are collections of at least ten articles, all centered on a particular subject. With their unique mix of varied contributions from Original Research to Review Articles, Frontiers Research Topics unify the most influential researchers, the latest key findings and historical advances in a hot research area.

Find out more on how to host your own Frontiers Research Topic or contribute to one as an author by contacting the Frontiers editorial office: frontiersin.org/about/contact

Microorganisms in sustainable and green agriculture: synergistic effect on carbon sequestration and crop productivity

Topic editors

Jianling Fan — Nanjing University of Information Science and Technology, China

Yichao Shi — Ottawa Research and Development Centre, Agriculture and Agri-Food Canada (AAFC), Canada

Topic coordinator

Yunliang Li — University of Saskatchewan, Canada

Citation

Fan, J., Shi, Y., Li, Y., eds. (2025). *Microorganisms in sustainable and green agriculture: synergistic effect on carbon sequestration and crop productivity*. Lausanne: Frontiers Media SA. doi: 10.3389/978-2-8325-5339-8

Table of contents

frontiers | Frontiers in Microbiology

TYPE Editorial
PUBLISHED 08 August 2024
DOI 10.3389/fmicb.2024.1470240

OPEN ACCESS

EDITED AND REVIEWED BY
Jesús Navas-Castillo,
CSIC, Spain

*CORRESPONDENCE
Jianling Fan
✉ jlfan@nuist.edu.cn

RECEIVED 25 July 2024
ACCEPTED 31 July 2024
PUBLISHED 08 August 2024

CITATION
Fan J, Shi Y and Li Y (2024) Editorial: Microorganisms in sustainable and green agriculture: synergistic effect on carbon sequestration and crop productivity. *Front. Microbiol.* 15:1470240. doi: 10.3389/fmicb.2024.1470240

Editorial: Microorganisms in sustainable and green agriculture: synergistic effect on carbon sequestration and crop productivity

Jianling Fan[1]*, Yichao Shi[2] and Yunliang Li[3]

[1]Jiangsu Key Laboratory of Atmospheric Environment Monitoring and Pollution Control, Jiangsu Collaborative Innovation Center of Atmospheric Environment and Equipment Technology, School of Environmental Science and Engineering, Nanjing University of Information Science and Technology, Nanjing, China, [2]Ottawa Research and Development Centre, Agriculture and Agri-Food Canada, Ottawa, ON, Canada, [3]Department of Soil Science, University of Saskatchewan, Saskatoon, SK, Canada

KEYWORDS

soil, microorganisms, root, rhizosphere, inoculants and bio-stimulants

Editorial on the Research Topic
Microorganisms in sustainable and green agriculture: synergistic effect on carbon sequestration and crop productivity

Since the mid-20th century, chemical fertilizers have been widely used to enhance crop productivity, resulting in soil degradation, water pollution, and environmental harm. Microorganisms play a crucial role in soil nutrient cycling and subsequently influence crop productivity, carbon sequestration, soil fertility, and soil health. Specifically, the rhizosphere microbiome could significantly affect plant health, where Plant Growth-Promoting bacteria (PGPB) have emerged as vital allies in mitigating abiotic stresses, such as salt stress and soil-borne diseases. Therefore, it is imperative to develop sustainable and green agricultural systems that can synergistically boost crop productivity, reduce nutrient losses, promote carbon sequestration, improve soil health, and enhance resilience to climate change.

The *Research Topic, Microorganisms in sustainable and green agriculture: synergistic effect on carbon sequestration and crop productivity*, invited contributions in the following areas: (a) The composition and structure of the microbial community and its impact on plant nutrient uptake and soil organic carbon sequestration; (b) Mechanisms of plant-microbe interactions and their effects on nutrient cycling and organic matter turnover; (c) The influence of land use and management practices on the structure and function of soil microbiome and its impact on nutrient uptake and soil carbon storage; (d) The role of microbial inoculants and bio-stimulants in promoting plant nutrient uptake and soil carbon sequestration.

This Research Topic combined a total of nine articles, four of which provide insights into recent advances in soil microbiome response to different agricultural practices, such as the use of inorganic and organic fertilizers, crop rotation and quicklime application, in relation to crop productivity, nutrient uptake, and greenhouse gas emission. These studies covered a broad range of agroecosystems, including

cropping systems of maize, peanut, oilseed rape, and grassland. The remaining five articles present new findings in the isolation and functions of PGPB, highlighting that the potential of new isolated strains in *Serratia*, *Trichoderma, Bacillaceae, Pseudomonas* as beneficial and biocontrol agents in sustainable and green agriculture.

Yang et al. highlighted "*Multi-year crop rotation and quicklime application promote stable peanut yield and high nutrient-use efficiency by regulating soil nutrient availability and bacterial/fungal community*", wherein a multi-year field experiment was conducted to investigate the effects of crop rotation and quicklime application on peanut nutrient uptake, yield, soil chemical properties, the diversity and function of bacterial and fungal communities. The authors emphasized that wheat-maize-peanut rotation in combination with quicklime application effectively promoted the growth of peanut by improving soil fertility and establishing a healthy soil micro-ecology, thereby mitigating the negative effects of continuous peanut cropping.

Wang et al. investigated "*Synergistic effects of rhizosphere effect and combined organic and chemical fertilizers application on soil bacterial diversity and community structure in oilseed rape cultivation*", wherein they studied the impacts of different ratios of chemical and organic fertilizers on soil bacterial diversity and community structure, comparing rhizosphere and non-rhizosphere soil in oilseed rape cultivation. This study revealed that a fertilizer mix of 25% chemical and 75% organic significantly increased soil bacterial abundance, diversity, and ecological network complexity, as well as the aboveground biomass of oilseed rape.

Fudjoe et al. assessed "*The impact of fertilization on ammonia-oxidizing bacteria and comammox Nitrospira communities and the subsequent effect on N_2O emission and maize yield in a semi-arid region*". The findings revealed that fertilization treatments significantly influenced maize productivity, nitrogen use efficiency, and N_2O emissions. Notably, ammonia-oxidizing bacteria and comammox *Nitrospira* communities exhibited distinct keystone taxa, with both groups substantially contributing to maize productivity, NUE, and N_2O emissions. The study highlighted that the combined inorganic and organic fertilizer treatment holds considerable promise for reducing N_2O emissions while enhancing maize productivity.

King et al. compiled their research in a article titled "*Comparative analysis of the soil microbiome and carbohydrate content of Anthoxanthum nitens (Sweetgrass) and other Poaceae grass tissues and associated soils*", which focused on carbohydrate composition and content in plant tissues of greenhouse-grown Sweetgrass in comparison to other Poaceae grass in the field. They also studied the differences of soil microbial communities across sampling sites.

Furthermore, this Research Topic published five articles related to the isolation and/or functions of PGPB, which are instrumental in enhancing plant resilience and productivity under various stress conditions. Kulkova et al. mini-reviewed "*Serratia spp. as plant growth-promoting bacteria alleviating salinity, drought, and nutrient imbalance stresses*". These bacteria show promise in promoting plant growth by producing phytohormones, ACC deaminase, fixing nitrogen, solubilizing phosphorus and zinc, enhancing antioxidant properties, and modulating gene expression. This review suggested that further research is needed to understand the molecular mechanisms of *Serratia* spp. and their effects on soil and plant microbiota, utilizing omics techniques.

Liu et al. discussed "*Beneficial and biocontrol effects of Trichoderma atroviride, a dominant species in white birch rhizosphere soil*", wherein they reported 37 *Trichoderma* strains isolated from rhizosphere soils of White birch (*Betula platyphylla Suk.*), identifying *T. atroviride* as the dominant and most effective biocontrol species due to its stress tolerance and pathogen confrontation abilities. An *in vivo* experiment on Gynura cusimbua seedlings showed that *T. atroviride* enhanced seedling growth, soluble protein and sugar content, and catalase activity while reducing malonaldehyde levels. It also increased soil nitrogen and phosphorus availability and plant nutrient uptake. These traits suggest *T. atroviride*'s potential as a biocontrol agent in agriculture and forestry.

Bao et al. attempted to uncover "*Mechanism on the promotion of host growth and enhancement of salt tolerance by Bacillaceae isolated from the rhizosphere of Reaumuria soongorica*", wherein three Plant Growth-Promoting Rhizobacteria strains belonging to *Bacillaceae* were isolated from the rhizosphere of *Reaumuria soongorica*. These strains demonstrate tolerance to high salt levels and promoted plant growth by increasing height, biomass, and photosynthetic pigments while reducing stress markers. Strain S40, in particular, was found to reprogram plant metabolism, enhancing hormone signal transduction and promote plant growth under salt stress.

Sun et al. described "*Bacillus velezensis BVE7 as a promising agent for biocontrol of soybean root rot caused by Fusarium oxysporum*". This study found that *Bacillus velezensis* BVE7, isolated from soybean roots, exhibited broad-spectrum antifungal activity, significantly reducing pathogen growth and the incidence of soybean root rot. The authors emphasized that strain BVE7 enhanced enzymatic activities in soybean roots, boosting plant resistance and reducing disease severity. They highlighted the potential of *Bacillus velezensis* BVE7 as a viable option for soybean root rot management.

Wei et al. discussed "*Pseudomonas chlororaphis IRHB3 assemblies beneficial microbes and activates JA-mediated resistance to promote nutrient utilization and inhibit pathogen attack*", wherein they studied the effects of IRHB3 on the local rhizosphere microbiome, disease resistance, and soybean growth in a field pot experiment. The authors found that IRHB3 enriched the rhizosphere bacterial community and maintained its balance, even in the presence of *Fusarium oxysporum*. It activated JA-mediated resistance and nodulation genes, thereby enhancing nitrogen fixation and increasing soybean yield.

In conclusion, this Research Topic has provided valuable insights into the complex interactions between microorganisms, agricultural practices, and crop productivity, with a specific emphasis on the critical role of PGPB in sustainable agriculture. The findings from this Research Topic reinforce the importance of integrating microbial and agronomic strategies to develop sustainable and green agricultural systems. Future research should continue to explore these

interactions and leverage advanced omics technologies to further understand the molecular mechanisms underlying plant-microbe-soil interactions and their implications for agricultural management.

Author contributions

JF: Conceptualization, Writing – original draft, Writing – review & editing. YS: Writing – original draft, Writing – review & editing. YL: Writing – original draft, Writing – review & editing.

Funding

The author(s) declare financial support was received for the research, authorship, and/or publication of this article. This study was funded by Special Funds for Carbon Peak and Carbon Neutral Science and Technology Innovation of Jiangsu Province (grant number BE2022302).

Acknowledgments

We would like to express our profound thanks to all authors and reviewers for their valuable time and expertise.

Conflict of interest

The authors declare that the research was conducted in the absence of any commercial or financial relationships that could be construed as a potential conflict of interest.

Publisher's note

frontiers | Frontiers in Microbiology

TYPE Original Research
PUBLISHED 29 September 2023
DOI 10.3389/fmicb.2023.1249668

OPEN ACCESS

EDITED BY
Yichao Shi,
Agriculture and Agri-Food Canada (AAFC), Canada

REVIEWED BY
Jeanette M. Norton,
Utah State University, United States
Yongjie Yu,
Nanjing University of Information Science and Technology, China

*CORRESPONDENCE
Lingling Li
✉ lill@gsau.edu.cn

RECEIVED 29 June 2023
ACCEPTED 06 September 2023
PUBLISHED 29 September 2023

CITATION
Fudjoe SK, Li L, Anwar S, Shi S, Xie J, Yeboah FK and Wang L (2023) The impact of fertilization on ammonia-oxidizing bacteria and comammox *Nitrospira* communities and the subsequent effect on N_2O emission and maize yield in a semi-arid region. *Front. Microbiol.* 14:1249668. doi: 10.3389/fmicb.2023.1249668

The impact of fertilization on ammonia-oxidizing bacteria and comammox *Nitrospira* communities and the subsequent effect on N_2O emission and maize yield in a semi-arid region

Setor Kwami Fudjoe[1,2], Lingling Li[1,2]*, Sumera Anwar[3], Shangli Shi[4], Junhong Xie[1,2], Frederick Kwame Yeboah[5] and Linlin Wang[1,2]

[1]State Key Laboratory of Aridland Crop Science, Gansu Agricultural University, Lanzhou, China, [2]College of Agronomy, Gansu Agricultural University, Lanzhou, China, [3]Department of Botany, Government College Women University Faisalabad, Faisalabad, Pakistan, [4]College of Grassland Science, Gansu Agricultural University, Lanzhou, China, [5]State Key Joint Laboratory of Environment Simulation and Pollution Control, School of Environment, Beijing Normal University, Beijing, China

The control of nitrous oxide (N_2O) emissions through nitrification and the optimization of maize yield are important in agricultural systems. However, within the semi-arid region, the impact of fertilization on the function of nitrification communities and its connection with N_2O emissions in the rhizosphere soil is still unclear. Our study investigates the influence of fertilization treatments on the communities of ammonia-oxidizing bacteria (AOB) and the complete ammonia oxidizers of the *Nitrospira* known as comammox (CAOB) in a maize agroecosystem. Nitrous oxide production, potential nitrification activity (PNA), maize yield, and nitrogen use efficiency (NUE) were determined for the same samples. The fertilizer treatments included a control group without fertilization (NA), inorganic fertilizer (CF), organic fertilizer (SM), combined inorganic and organic fertilizer (SC), and maize straw (MS). The SC treatment indicated a lower cumulative N_2O emission than the CF treatment in the 2020 and 2021 cropping seasons. The AOB community under the CF, MS, and SM treatments was predominantly composed of *Nitrosospira* cluster 3b, while the SC treatment was associated with the comammox *Nitrospira* clade A.1 lineage, related to key species such as Ca. *Nitrospira inopinata* and Ca. *Nitrospira nitrificans*. Network analysis demonstrated a positive potential for competitive interaction between hub taxonomy and distinct keystone taxa among AOB and comammox *Nitrospira* nitrifiers. The structural equation model further revealed a significant positive association between AOB nitrifiers and N_2O emission, PNA, soil pH, SOC, NO_3^--N, and DON under organic fertilization. The keystone taxa in the comammox *Nitrospira* nitrifier and network Module II exhibited a positive correlation with maize productivity and NUE, likely due to their functional activities stimulated by the SC treatment. It is noteworthy that the AOB community played a more significant role in driving nitrification compared to the composition of comammox *Nitrospira*. Collectively, combined inorganic and organic fertilizer (SC) treatment exhibits high potential for reducing N_2O emissions, enhancing maize productivity,

increasing NUE, and increasing the sustainability of the nitrogen dynamics of maize agroecosystems in the semi-arid Loess Plateau.

KEYWORDS

nitrification communities, potential nitrification activity (PNA), keystone taxa, nitrogen use efficiency, competitive interaction

Introduction

Excessive fertilization has raised numerous environmental and ecological concerns, including soil acidification, increased nitrous oxide (N_2O) gas emissions, and water pollution (Hink et al., 2018; Fudjoe et al., 2021). N_2O is a potent greenhouse gas with a global warming potential of ∼300× that of carbon dioxide, which also poses a significant threat to the stratospheric ozone layer and overall climate stability (Schmidt et al., 2019; Chataut et al., 2023). Excessive nitrogen-based fertilization (NBF) continues to contribute to substantial levels of N_2O emissions from agroecosystems. In 2015, agricultural soils accounted for ∼55% of global N_2O emissions, a proportion projected to increase to 59% by 2030. Therefore, enhancing nitrogen use efficiency (NUE) in agriculture has become crucial for mitigating rising N_2O emissions (Cardenas et al., 2019; Govindasamy et al., 2023). Improving NUE can also lead to increased crop yields, reduced fertilizer costs, and improved soil health. To maximize efforts in mitigating N_2O emissions for sustainable soil ecosystems, the use of combined approaches such as the integration of inorganic and inorganic fertilizers has been recommended (Hink et al., 2018; Yang et al., 2018; Wang et al., 2019).

Nitrification is the key stage in the nitrogen cycle, converting ammonia (NH_3) into nitrite (NO_2^-) and then nitrate (NO_3^-), thus making nitrogen more mobile to plants and microbes. However, this process can lead to nitrogen loss through NO_3^- leaching, N_2O, and N_2 emissions (Yu et al., 2019; Wang et al., 2020; Sun et al., 2021). With the discovery of complete ammonia oxidizers of the *Nitrospira* known as comammox (CAOB), the traditional theory about the role of ammonia-oxidizing bacteria (AOB) and archaea as catalysts in the first step of nitrification no longer holds (Van Kessel et al., 2015; Yu et al., 2018; Osburn and Barrett, 2020). Moreover, the discovery of CAOB has complicated our understanding of nitrification, making it difficult to evaluate the roles of different nitrifiers, especially in soils with frequent N nutrient additions (Xia et al., 2018; Li et al., 2019; Xu et al., 2020). The comammox *Nitrospira* are indistinguishable from *Nitrospira* performing only nitrite oxidation by their ribosomal sequences, and the gene encoding ammonia monooxygenase subunit A (*amoA*) has been used to examine their phylogeny, abundance, and communities in environmental samples. The phylogeny of *amoA* divides CAOB into two distinct branches referred to as clades A and B. Clade A is more abundant in alkaline soil samples and nutrient-rich arable soil relative to clade B (Kits et al., 2017; Pjevac et al., 2017; Koch et al., 2019). CAOB has a high affinity for ammonia and is competitive in oligotrophic habitats. Studies by Hu and He (2017), Osburn and Barrett (2020), and Li et al. (2021) have documented that edaphic factors such as available nitrogen, pH, soil organic carbon, and carbon-to-nitrogen ratio influence the CAOB abundance, diversity, and composition in arable soils. Variations in soil conditions may have variable effects on nitrification communities and consequently impact their roles in N_2O emissions (Li et al., 2019; Schmidt et al., 2019). Researchers successfully isolated a culture of *Nitrospira inopinata*, a comammox bacterium, from a microbiological biofilm. This bacterium exhibited a strong affinity for ammonia, providing it with a competitive edge in environments with low nutrient levels. The comammox cultures, such as Ca. *Nitrospira nitrosa* and Ca. *Nitrospira nitrificans*, have been enriched from man-made systems and belong to clade A. The diversity of AOB and CAOB nitrifiers and their response to environmental factors and N fertilizer in soil ecosystems are essential in agricultural systems (Daims et al., 2015; Van Kessel et al., 2015; Koch et al., 2019). However, the role of AOB and CAOB communities within the semi-arid environs remains limited, hence the need for further research.

Maize is a widely cultivated crop in regions worldwide, including semi-arid areas such as the Loess Plateau. The semi-arid Loess Plateau (SALP), located in the northwestern region of China, is recognized as a highly vulnerable global agroecosystem due to its dependence on limited and unpredictable precipitation. To address this challenge, farmers often employ the plastic mulch technique to enhance maize yield. This technique elevates soil humidity and temperature and increases fertilizer usage. The increase in fertilizer usage enhances N_2O emissions within the maize field (Bu et al., 2014; Zhang F. et al., 2018; Govindasamy et al., 2023). The use of plastic mulch can reduce water evaporation and retain moisture to meet the needs of crops in their crucial growth stages, thereby increasing crop yield and water use efficiency (Lamptey et al., 2019; Fudjoe et al., 2021).

In the rhizosphere, microorganisms and plant roots interact, leading to enhanced microbial nitrogen conversion rates facilitated by the release of oxygen from the roots (Zhang B. et al., 2018; Lin et al., 2020). Understanding the collaborations between different taxa of AOB and CAOB is crucial for evaluating soil functions. Co-occurrence networks can help reveal their taxa's ecological and microbe-to-microbe associations. Additionally, these networks are capable of handling large datasets (Zhang B. et al., 2018; Fudjoe et al., 2021). However, it is essential to identify keystone taxa that maintain function and structure within soil microbial communities (Williams et al., 2014; Mamet et al., 2019). Despite ongoing research efforts, there is still limited knowledge regarding the co-occurrence of the canonical AOB and CAOB genes in the semi-arid Loess Plateau area. Existing studies have not sufficiently addressed this gap, and there remains a lack of understanding of how agricultural management practices influence these microbial communities. Hence, a detailed understanding is crucial. Considering this, this study aimed to: (1) examine how the diversity, and composition of AOB and CAOB communities are influenced by long-term inorganic and organic fertilization; (2) assess the impact of

inorganic and organic fertilizer on N_2O emissions, maize yield, and NUE; and (3) explore the niche differentiation and co-occurrence networks between AOB and CAOB communities regarding N_2O emissions, maize yield, and NUE. We hypothesized that AOB exhibited higher amoA gene transcriptional abundances and nitrification affinity activities under fertilization regimes (i.e., urea and organic nitrogen fertilizers) than CAOB due to their copiotrophic lifestyle and functional patterns.

Materials and methods

Field experimental description

The field study was conducted at the Rainfed Agricultural Experimental Station of Gansu Agricultural University, located in Gansu Province, NW China (35°28′N, 104°44′E, elevation: 1,971 m above sea level). The climate in this Loess Plateau area is semi-arid with 140 frost-free days annually. The region has steep terrain prone to erosion. The region's soil is aeolian, referred to as Huangmian, and has a sandy, loamy texture with at least 50% sand content. It is classified as Calcaric Cambisol according to the Food and Agriculture Organization (FAO) (1990) soil classification system. The other physiochemical properties of the soil measured before starting the experiment are shown in Supplementary Table S1. The average annual temperature and precipitation at the study site are recorded as 10.8°C and 400 mm, respectively. The yearly evaporation rate was 1,531 mm, and the average annual radiation was 5930 MJ m^{-2}. Between January and August, the temperature fluctuated between −23 and 37°C, and the average annual precipitation was 390.8 mm and 369.2 mm during the 2020 and 2021 cropping seasons.

The experiment followed a randomized complete block design with five treatments and three replicates per treatment. The five treatments were as follows: (i) no fertilizer (NA); (ii) inorganic fertilizer (CF) contained 200 kg N ha^{-1} of urea and 150 kg P_2O_5 ha^{-1} of triple superphosphate; (iii) inorganic fertilizer plus organic fertilizer (SC) contained 3.03 t ha^{-1} of organic fertilizer, 100 kg N ha^{-1} of urea, and 120 kg P_2O_5 ha^{-1} of triple superphosphate; (iv) organic fertilizer (SM) contained 6.06 t ha^{-1} of organic fertilizer and 90 kg P_2O_5 ha^{-1} of triple superphosphate; and (v) maize straw (MS) contained 28.5 t ha^{-1}, 100 kg N ha^{-1} of urea, and 36 kg P_2O_5 ha^{-1} of triple superphosphate. There were 15 plots, each measuring 3 m × 14.2 m. Treatments SC and MS were applied at the same N input rate. Urea, commercial organic fertilizer, and maize straw were broadcast and integrated into the top 20 cm soil layer.

The experiment was initiated in 2012, but this study reports data from the 2020 and 2021 cropping seasons. Before planting, the soil in the plots was manually inverted with shovels to a depth of 20 cm. Wide (0.7 m) and narrow (0.4 m) ridges were covered with colorless plastic film, and holes were made in the film over the furrows to collect precipitation. After placing the film over the soil, it was perforated using a handheld device (Lamptey et al., 2019). Maize seeds of the Pioneer 335 cultivar were sown in furrows (Supplementary Figure S1) at a density of 52,500 plants ha^{-1} in late April. Glyphosate (30%) was sprayed before planting to control weeds, and manual weeding was carried out when necessary, during the season. The maize grain was harvested in late September.

Soil sampling and property analysis

During the silking stage of the 2020 and 2021 cropping seasons, soil samples were gathered from the maize fields of the experiment. A total of 15 soil samples were randomly collected, with three replicates for each of the five treatments. The soil samples were specifically taken from the rhizosphere, which refers to the soil closely adhering to the root crowns, where the dense root system ensured that all the soil was influenced by the roots. The soil samples collected from each plot were sieved through a 2-mm sieve to eliminate any residues and then combined to create a collective sample. Immediately after collection, the soil samples were preserved on dry ice, transported to the laboratory, and preserved at −80°C for molecular analysis. A portion of the remaining subsample was kept at 4°C for microbial biomass C and N analyses, while the other soil samples were air-dried to facilitate subsequent chemical analysis.

To measure the soil pH, a deionized soil suspension was prepared with a soil-to-water ratio of 1:2.5 (mass to volume). A pH meter (Mettler Toledo FE20, Shanghai, China) was used for the pH measurement. Soil organic carbon (SOC) was determined using a modified Walkley-Black wet oxidation method, while total nitrogen (TN) was analyzed using the Kjeldahl method (Bao, 2000). Soil nitrate–nitrogen (NO_3^--N) and ammonium–nitrogen (NH_4^+-N) contents were extracted with 2 M KCl and determined using a flow injection auto-analyzer (FLA Star 5000 analyzers, Foss, Denmark) (Bremner, 1965). Soil dissolved organic N (DON) in H_2O (1:1) was analyzed using the Multi N/C® 2100 Analyzer (ANALYTIKJENA, Germany) (Ghani et al., 2003). Available phosphorus (AP) was measured using the molybdenum-blue method after extraction with sodium bicarbonate (Olsen et al., 1954). Soil water content (SWC) was measured by oven-drying the soil at 105°C for 24 h (Fudjoe et al., 2021).

Measurement of potential nitrification activity, maize productivity, and nitrogen use efficiency

To measure potential nitrification activity (PNA), the chlorate inhibition method was employed. In brief, 5 g of soil was weighed and placed in a 50-ml centrifuge tube, along with 20 ml of phosphate buffer solution (PBS) containing specific concentrations of NaCl (8.0 g/L), KCl (0.2 g/L), Na_2HPO_4 (1.44 g/L), and NaH_2PO_4 (0.2 g/L). Ammonium sulfate $(NH_4)_2SO_4$ was added to 1 mM concentration, and potassium chlorate ($KClO_3$) was added to inhibit nitrite oxidation (final concentration = 10 mM). The mixture was then incubated in the dark at a temperature of 25°C with shaking slurry at 180 r min^{-1} for 24 h. Following incubation, the inhibited nitrite was extracted by adding 5 ml of 2 M KCl solution, and its concentration was measured using a spectrophotometer at a wavelength of 540 nm with N-(1-naphthyl) ethylenediamine dihydrochloride (Kurola et al., 2005; Ullah et al., 2020).

The aboveground biomass and grain yield for the maize cropping seasons of 2020 and 2021 were determined by oven-drying at 105°C for 45 min and subsequently drying to constant

weight at 85°C. Grain and forage yields (kg ha^{-1}) were extrapolated (Alhassan et al., 2018). The NUE was calculated by subtracting the nitrogen uptake in the treatment without nitrogen fertilizer from the nitrogen buildup in the treatment with nitrogen fertilizer. This difference was then divided by the nitrogen application rate (Cardenas et al., 2019).

Collection and determination of N_2O emission samples

The gas samples were obtained using the static chamber technique, and the concentration of nitrous oxide (N_2O) was measured using gas chromatography (Agilent 7080B, Santa Clara, USA) at monthly or bi-monthly intervals throughout the maize cropping seasons of 2020 and 2021. Each sealed container (0.38 m × 0.35 m × 0.36 m) was constructed with an opaque outer lid covered with crenelated container foil to minimize the impact of thermal heat during gas sampling. Furthermore, two fans were installed inside the lid to ensure proper gas circulation prior to sampling. To minimize the impact of diurnal temperature variations, N_2O gas samples were collected using a 60-ml plastic gas-tight syringe within a specific time frame (within 9:00 and 11:00) during different sampling periods (0, 10, and 20 min after chamber closure). The collected gas samples were then stored in airtight aluminum bags (Dalian Delin Gas Packing, China). Gas chromatography (Agilent 7890A, United States) with an electron capture detector was utilized to analyze the gas samples.

(1) The N_2O fluxes (NF, mg m^{-2} h^{-1}) were calculated using Eq. (1) based on the procedure detailed by Huang et al. (2019);

$$NF = \frac{273}{273+T} \times \frac{44}{22.4} \times 60 \times 10^{-3} \times h \times \frac{dc}{dt} \quad (1)$$

In the equation, T (°C) represents the air temperature, 44 denotes the molecular weight of N_2O, 22.4 (L mol^{-1}) corresponds to the molecular volume at 101 kPa, 60×10^{-3} is a conversion factor, h represents the height of the chamber, and dc/dt represents the rate of change in N_2O concentration (c) per unit of time (t).

(2) N_2O cumulative emissions (NE, Kg ha^{-1}) were calculated using Eq. (2) based on Tao et al. (2018);

$$NE = \sum [\frac{NF_{i+1} + NF_i}{2} \times (t_{i+1} - t_i) \times 24 \times 10^{-2}] \quad (2)$$

where $i + 1$ and i are the last and current measurement dates, respectively, and t is the number of days after sowing.

Quantitative polymerase chain reaction of functional gene communities

The total genomic DNA was obtained from the rhizosphere soil (0.5 g dry weight) using the DNA Isolation Kit (MoBio, Carlsbad, CA, USA). Following the extraction, a Wizard DNA Clean-Up System (Axygen Bio, USA) was utilized to purify the extracted DNA. The DNA samples were then kept at −80°C until they were analyzed. The copy numbers of the amoA–AOB and comammox *Nitrospira* genes were determined using quantitative polymerase chain reaction (qPCR) with the specific primer set described in Supplementary Table S2. For qPCR, the 20 μl reaction mixture consisted of 7.2 μl of aseptic water, 0.4 μl of each primer (10 mM), 10 μl of GoTaq® qPCR Master Mix (Promega, USA), and 2 μl of template DNA. A calibration series (ranging from 10^2 to 10^8 copies) of plasmid DNA was employed to construct standard curves for quantifying the copy numbers of target genes (AOB and CAOB). All qPCR analyses were initiated with an initial denaturation stage at 95°C for 3 min, followed by 40 cycles (with plate-reading) consisting of 30 s at 95°C and 45 s at 60°C, subsequently concluding with a final melt curve step spanning 72 to 95°C. The qPCR process was performed three times, and high amplification efficiencies (>97%) were achieved, supported by standard curve r^2 values exceeding 0.99%.

High-throughput sequencing of functional gene amplicons

DNA sequencing was employed to investigate the relative abundance and composition of the *amoA*–AOB and comammox *Nitrospira* genes. For the forward primers, a 7-bp unique barcode sequence was appended, and the concentration of the refined PCR products was quantified using a TBS-380 fluorometer (Turner Biosystems, CA, United States). The PCR products were then diluted and subjected to paired-end sequencing on an Illumina MiSeq sequencer (Shanghai Personal Biotechnology, Co., Ltd., Shanghai, China). Detailed information regarding the primer pairs, reaction mixtures, and thermal cycling conditions employed to amplify fragments of all genes is shown in Supplementary Table S2. After the amplification step, the PCR products from the genes were retrieved from agarose gels and subjected to purification using a universal DNA Purification Kit (Tiangen Co., Beijing, China). To identify low-quality sequences, the raw sequences were screened for quality using Quantitative Insights Into Microbial Ecology (QIIME) (Caporaso et al., 2010). The Usearch tool was employed to screen for chimeric assembled sequences, while the FrameBot tool from the Ribosomal Database Project (RDP) was used (Edgar, 2013). The FunGene Pipeline was utilized to exclude sequences of low quality (Edgar and Flyvbjerg, 2015). Operational taxonomic units (OTUs) were defined using the CD-HIT approach within MOTHUR, with a 3% difference threshold in nucleotide sequences (Schloss et al., 2009). Homologs and the closest sequences in GenBank were identified using the MEGA software. Moreover, representative sequences from each OTU were aligned with the most closely related sequences and additional reference sequences that were retrieved using the MEGA software, as described by Tamura et al. (2013). The *amoA*–AOB and comammox *Nitrospira* gene sequences were deposited in the NCBI Sequence Read Archive (SRA) database under specific accession numbers, namely PRJNA722852 and PRJNA967803. A neighbor-joining tree was constructed in MEGA 6 using a Kimura 2-parameter distance and 1000 bootstrap replicates to classify *amoA*–AOB and comammox *Nitrospira* OTUs, following the nomenclature described by Wang et al. (2017) and Li et al. (2021), respectively.

Statistical analysis

Data analysis was performed using SPSS version 22 (IBM Corporation, Chicago, USA, 2013). A one-way analysis of variance (ANOVA) was utilized to examine the treatment means of the copy number of *amoA*–AOB and comammox *Nitrospira* genes, soil PNA, grain yield, and aboveground biomass. Duncan's multiple range tests (DMRTs) at a 95% confidence level ($p \leq 0.05$) were used to differentiate between the means. The alpha diversity indices (Shannon index, Simpson index, and Chao1 richness) of the functional genes were carried out using R software (version 3.5.3). The correlation analyses were performed to assess the connections between grain and biomass yield, soil water content, and soil chemical properties. Redundancy analysis (RDA) was implemented through the "vegan" package in R to utilize the impact of soil physiochemical properties on functional genes. Principal component analysis (PCA) was conducted using R statistical software to examine the variations among fertilization treatments.

Co-occurrence networks were employed to classify significant associations among taxa in the AOB and CAOB communities. A total of 15 soil fertilization treatment samples (consisting of three replications for each of the five treatments) were combined for analysis. The operational taxonomic units (OTUs) present in all treatment replicates were selected for network analysis. Pearson's correlation, Bray–Curtis, and Kullback–Leibler dissimilarities were employed in a collaborative approach. A true co-occurrence network was defined as a statistically significant association between species, indicated by a correlation coefficient (r) >0.8 or <-0.8 and a p-value of 0.01. To assess the reliability of the connections, permutation and bootstrap distributions were computed with 1,000 iterations. The network was visualized using the Fruchterman–Reingold algorithm in Gephi (version 0.9.2). Various topological properties of the network were calculated, such as the number of nodes and edges, average clustering coefficient, average degree, average path length, closeness centrality, network centrality, and modularity. Potential keystone taxa were identified as OTUs with higher degrees of centrality using the methodology outlined by Berry and Widder (2014).

To explore important predictors of the AOB and CAOB communities, maize productivity, and N_2O emissions, a random forest modeling approach was utilized. The analysis incorporated soil variables, and the forest package developed by Liaw and Wiener (2002) was utilized. The importance of analysis in the model was computed using the "A3R" package by Fortmannroe (2015), and the statistical significance of each forecaster was assessed using the "rfPermute" package developed by Archer (2020). The major forecasters obtained from the random forest analysis were utilized to investigate the direct and indirect effects of soil properties on abiotic and biotic variables, including physiochemical soil properties, biomass, network modules, soil AOB and CAOB communities, maize productivity, PNA, and N_2O. The analysis was performed using AMOS 21.0 in SPSS (SPSS, Inc., Chicago, IL). Before modeling, the normality of the data distribution was assessed. The structural equation model (SEM) was applied, and the model fitness was evaluated using the chi-square test (χ^2, $p > 0.05$), root mean square error of approximation (RMSEA), and goodness-of-fit index (GFI) following the methodology described by Sahoo (2019).

Results

Soil properties, maize productivity, and nitrogen use efficiency

The analysis of variance indicated significant differences among treatments for most soil indices (TN, NO_3^--N, AP, SOC, DON, and SWC) in the 2020 and 2021 cropping seasons, except for NH_4^+-N. The soil pH varied significantly across treatments, ranging from 8.10 to 8.80. However, no fertilizer (NA) treatment had a higher pH than the fertilization treatments (MS, SM, SC, and CF; Table 1). The SOC, NO_3^--N, AP, and DON tended to be higher in 2021 cropping season than in the 2020 cropping season, and they increased across fertilization treatments. Specifically, the MS, SM, and SC treatments increased SOC by 17.3%, 15.4%, and 15.1%, and increased DON by 69.7%, 63.3%, and 9.2% compared to NA, respectively. However, CF and MS significantly increased TN, while SM and SC treatments were high in AP compared to NA treatments in 2020 and 2021 cropping seasons. SWC exhibited a significant increase in SC, SM, and MS treatments compared to NA. There were significant differences ($p < 0.05$) observed in the NO_3^--N concentrations during the 2020 and 2021 cropping seasons in the CF treatment relative to the SC, SM, MS, and NA treatments (Table 1).

Fertilization treatments significantly ($p < 0.05$) enhanced maize productivity relative to no fertilizer (NA) treatment in the 2020 and 2021 cropping seasons (Supplementary Table S3). Grain yield during the 2020 and 2021 cropping seasons under CF and SC treatments increased by (61.99%, 58.24%) and (63.99%, 61.15%), respectively, compared to NA treatment. The CF treatment yielded the highest aboveground biomass, compared to the SC, MS, and SM treatments. In 2020, the CF, SC, MS, and SM treatments increased aboveground biomass by 2.8, 2.6, 1.7, and 1.4 times, respectively (Supplementary Table S3). In 2021, these treatments resulted in 2.2, 2.1, 1.4, and 1.3 times higher aboveground biomass. The NUE exhibited a similar pattern as maize productivity. In 2020, the CF, SC, and SM treatments enhanced NUE by 60%, 56%, and 24%, respectively compared to the MS treatment. In 2021, these treatments increased NUE by 56%, 53%, and 22%, respectively compared to the MS treatment (Supplementary Table S3).

Potential nitrification activity and N_2O emissions

The PNA index in the 2020 and 20221 cropping seasons increased significantly ($p < 0.05$) under CF (55.84%, 40.32%), SC (43.19%, 18.39%), SM (36.66%, 45.68%), and MS (30.07%, 23.36%) treatments relative to NA treatment, respectively (Figure 1).

The maximum peaks observed in N_2O flux emissions occurred in July, while the minimum levels were recorded in October and September through all fertilization treatments in the 2020 and 2021 cropping seasons of this study (Figure 2A). Furthermore, the release of N_2O flux emissions was significantly ($p < 0.05$) higher in the SM, MS, and CF treatments relative to SC and NA treatments in the growing seasons (Figure 2A). The highest N_2O emission flux

TABLE 1 Soil chemical characteristics under different fertilization treatments in the rhizosphere soil.

Year	Indices	NA	CF	SC	SM	MS
2020	pH	8.80a	8.43b	8.37b	8.19c	8.68ab
	TN (g kg^{-1})	0.85b	0.93a	0.94a	0.98a	0.99a
	SOC (g kg^{-1})	7.48c	7.93c	8.81b	8.84b	9.81a
	NO_3^--N (mg kg^{-1})	17.84c	30.81a	28.40ab	25.40b	21.93bc
	NH_4^+-N (mg kg^{-1})	15.33a	16.07a	14.87a	15.81a	16.53a
	AP (mg kg^{-1})	9.73c	16.70ab	18.32ab	19.81a	15.14b
	DON (mg kg^{-1})	10.89b	12.42b	11.89b	17.78a	18.48a
	SWC (%)	23.11b	28.21b	32.42a	31.93a	28.63b
2021	pH	8.66a	8.32c	8.44bc	8.45bc	8.54b
	TN (g kg^{-1})	0.80c	1.15ab	1.03b	1.07b	1.22a
	SOC (g kg^{-1})	7.84c	8.94bc	9.78b	9.96b	11.77a
	NO_3^--N (mg kg^{-1})	18.73c	32.48a	29.29b	26.08b	23.76bc
	NH_4^+-N (mg kg^{-1})	16.61a	17.82a	15.52a	17.08a	18.92a
	AP (mg kg^{-1})	10.69c	17.74b	20.77a	19.16ab	16.81bc
	DON (mg kg^{-1})	11.49c	19.91a	14.41b	17.97ab	12.55b
	SWC (%)	13.34c	23.39a	22.53ab	15.39bc	17.37b

Values are expressed as mean with letters indicating significant differences based on Duncan's HSD test ($p < 0.05$).
TN, total nitrogen; SOC, soil organic carbon; NO_3^--N, nitrate nitrogen; NH_4^+-N, ammonia nitrogen; AP, available phosphorus; DON, dissolved organic nitrogen; SWC, soil water content (0–20 cm); NA, no fertilization; CF, mineral fertilizer; SC, mineral fertilizer plus commercial organic fertilizer; SM, commercial organic fertilizer; MS, maize straw.

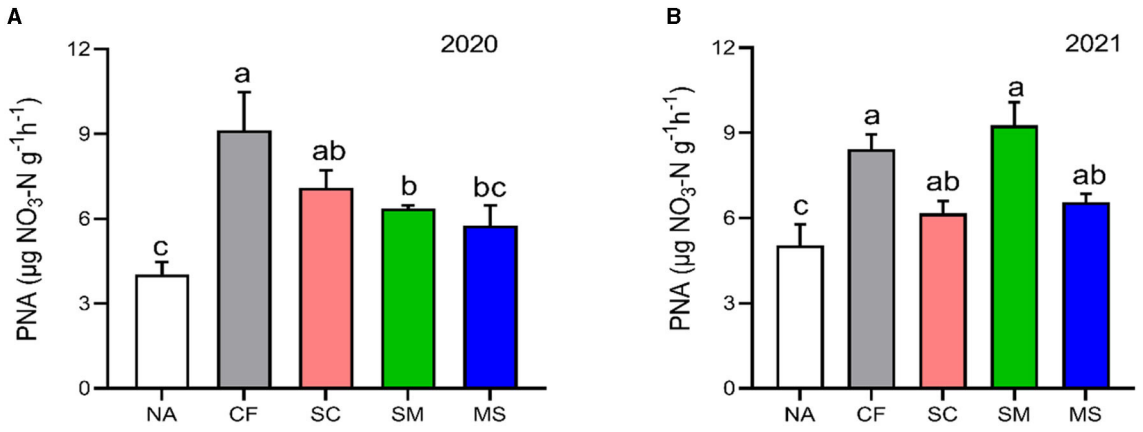

FIGURE 1
Potential nitrification activity (PNA) under different soil fertilization treatments in the **(A)** 2020 and **(B)** 2021 cropping seasons. Bars ($n = 3$) with different lowercase letters specify significant differences based on Duncan's HSD test ($p < 0.05$). NA, no fertilization; CF, inorganic fertilizer; SC, inorganic plus organic fertilizer; SM, organic fertilizer; MS, maize straw.

in the 2020 and 2021 cropping seasons was observed under SM, followed by MS treatment at (115.5 and 110 mg m^{-2} h^{-1}) and (98 and 80 mg m^{-2} h^{-1}), respectively, while the lowest was under NA treatment at 25 and 18 mg m^{-2} h^{-1}, respectively (Figures 2A, B). The cumulative N_2O emissions in 2020 cropping season were 45.7% greater with MS treatment relative to NA, while in the 2021 cropping season, they increased significantly under CF, SC, SM, and MS treatments at 31.5%, 23.3%, 44.3%, and 40.1%, respectively compared to NA treatment and were ranked as SM > MS > CF > SC ($p < 0.05$; Figures 3A, B). The SC treatment indicated a lower emissions rate and cumulative N_2O emissions than the CF treatment (Figures 3A, B).

Community structure of AOB and CAOB

The copy numbers of AOB were higher than CAOB across the 2020 and 2021 cropping seasons. The AOB abundance under SM, CF, SC, and MS treatments increased significantly by 12.77%, 6.9%, 5.36%, and 2.23%, respectively compared with the NA in the

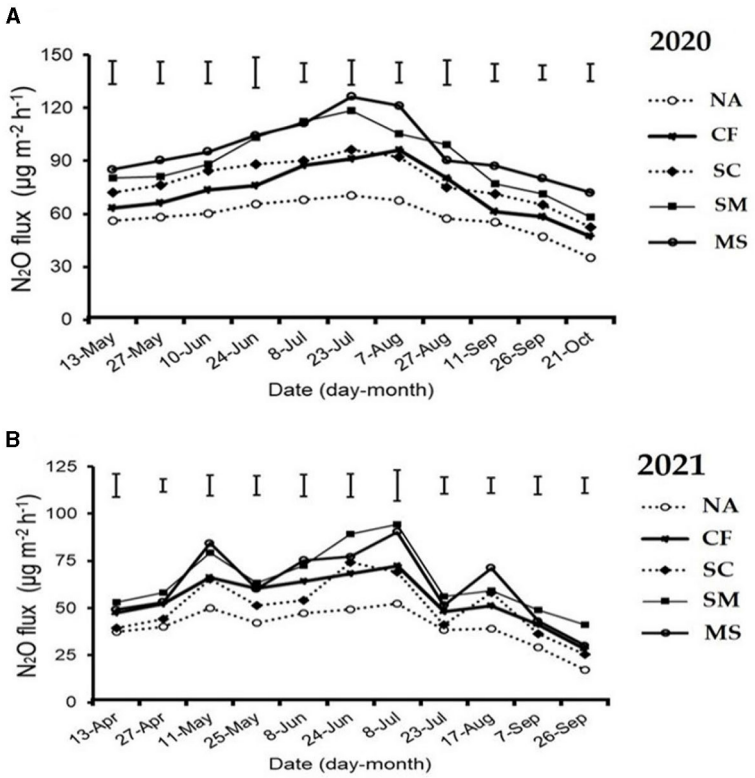

FIGURE 2
Seasonal variations of N_2O flux emissions; **(A)** in 2020 and **(B)** in 2021 as influenced by fertilization treatments. The vertical bars represent the least significant difference (LSD) at a p-value of < 0.05. Bars ($n = 3$). NA, no fertilization; CF, inorganic fertilizer; SC, inorganic plus organic fertilizer; SM, organic fertilizer; MS, maize straw.

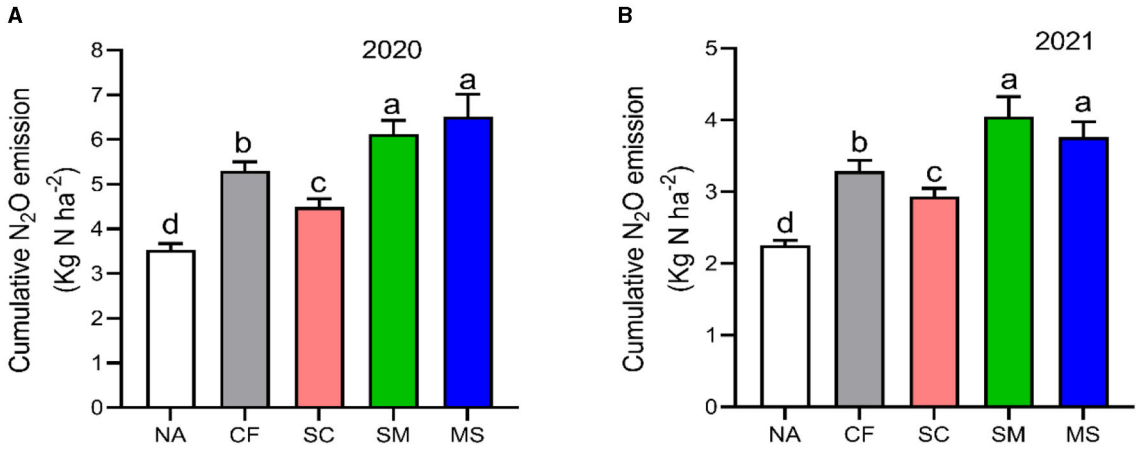

FIGURE 3
Seasonal variations of N_2O cumulative emissions; **(A)** in 2020 and **(B)** in 2021 as influenced by fertilization treatments. The vertical bars represent the least significant difference (LSD) at a p-value of < 0.05. Bars ($n = 3$) with different lowercase letters indicate significant differences based on Duncan's HSD test ($p < 0.05$). NA, no fertilization; CF, inorganic fertilizer; SC, inorganic plus organic fertilizer; SM, organic fertilizer; MS, maize straw.

2020 cropping season (Figure 4A). In the 2021 cropping season, the abundance of AOB was considerably greater ($p < 0.05$) under the CF, SC, and SM treatments compared to the NA and MS treatments (Figure 4C). Compared to the NA treatment, CF, SC, MS, and SM increased significantly by 15.48%, 8.65%, 8.03%, and 5.01%, respectively, under the CAOB abundance ($p < 0.05$, Figure 4B) in the 2020 cropping season, whereas in 2021, the growing season had no significant effect among the treatments ($p > 0.05$, Figure 4D).

The diversity index of AOB and CAOB OTUs was significantly higher under SM and SC treatments relative to NA treatment (Table 2). The CF and SM treatments were significantly higher in

10.3389/fmicb.2023.1249668

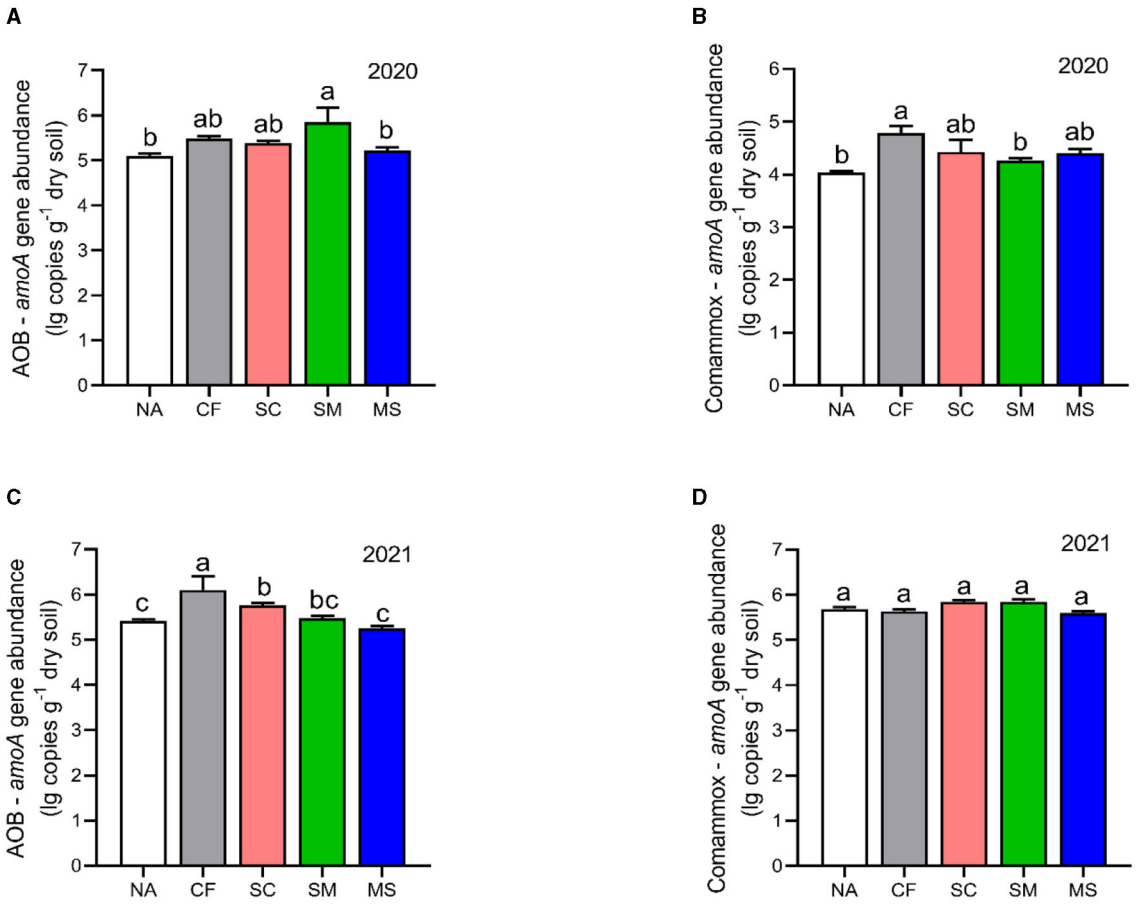

FIGURE 4
Gene copy numbers of **(A–C)** *amoA*-AOB and **(B–D)** comammox *Nitrospira* (CAOB) genes as influenced by fertilization treatments. Values are mean ± standard error ($n = 3$), with different lowercase letters indicating significant differences based on Duncan's HSD test ($p < 0.05$). NA, No fertilization; CF, inorganic fertilizer; SC, inorganic plus organic fertilizer; SM, organic fertilizer; MS, maize straw.

TABLE 2 Alpha diversity indices of *amoA*–AOB and comammox *Nitrospira* (CAOB) at the similarity level of 97% under the influence of fertilization treatments in the rhizosphere soil.

Nitrifiers	Treatments	OTUs	Chao1	Shannon
AOB nitrifiers	NA	$1{,}796.3 \pm 85.2^{c}$	$2{,}143 \pm 56.6^{c}$	5.1 ± 0.24^{c}
	CF	$2{,}472.6 \pm 47.1^{ab}$	$3{,}442 \pm 14.3^{a}$	5.75 ± 0.16^{ab}
	SC	$1{,}859 \pm 55.6^{bc}$	$2{,}177 \pm 9.8^{bc}$	5.73 ± 0.29^{ab}
	SM	$2{,}604 \pm 94.3^{a}$	$2{,}991 \pm 29.6^{ab}$	5.47 ± 0.38^{abc}
	MS	$2{,}062 \pm 76.5^{b}$	$2{,}429 \pm 20.5^{b}$	6.14 ± 0.15^{a}
	p-value	< 0.012	0.001	0.004
CAOB nitrifiers	NA	$1{,}145 \pm 63.1^{c}$	$1{,}440 \pm 44.5^{b}$	6.50 ± 0.18^{c}
	CF	$1{,}410 \pm 47.1^{b}$	$1{,}701 \pm 11.3^{a}$	6.75 ± 0.19^{b}
	SC	$1{,}953 \pm 55.6^{a}$	$1{,}468 \pm 29.6^{b}$	6.81 ± 0.21^{ab}
	SM	$1{,}208 \pm 83.1^{bc}$	$1{,}667 \pm 18.4^{a}$	6.88 ± 0.38^{a}
	MS	$1{,}839 \pm 65.5^{a}$	$1{,}697 \pm 23.6^{a}$	6.78 ± 0.17^{b}
	p-value	<0.002	0.001	0.036

The data include the mean with standard error. Values with the same alphabet are not statistically different, but values with different letters indicate a statistically significant difference between fertilization treatments at Duncan's HSD test ($p < 0.05$).
NA, no fertilization; CF, inorganic fertilizer; SC, inorganic plus organic fertilizer; SM, organic fertilizer; MS, maize straw.

the diversity indices of AOB of Chao1 richness and Shannon index ($p < 0.05$) compared to the NA treatment (Table 2). Similarly, for the comammox *Nitrospira* region, the Chao1 richness and Shannon indices under CF, SC, SM, and MS increased by 1.18-, 1.01-, 1.16-, and 1.17-fold and by 1.03-, 1.05-, 1.06-, and 1.04-fold relative to NA treatments (Table 2).

Using the 50 most prevalent OTUs across all treatments, a phylogenetic tree was created to examine the community composition of the AOB and CAOB populations (Figures 5A, B). Among the AOB community, 50 dominant OTUs are seen in Figure 5A. Five clustered lineages of *Nitrosospira*: 7, 3c, 3a, 3b, and 4 were identified. Fertilization significantly increased across seven AOB OTUs (ANOVA, $p < 0.05$; Figure 5A and Supplementary Figure S2A). AOB38, AOB10, AOB49, and AOB47 were significantly higher in CF, SC, MS, and SM than the no fertilizer treatments (NA) affiliated with *Nitrosospira* Cluster 7, 3c, and 3a, respectively (Figure 4A and Supplementary Figure S2A). AOB7 was significantly higher in MS relative to other N fertilization treatments and NA (Figure 5A and Supplementary Figure S2A). In *Nitrosospira* 3b, both AOB18 and AOB26 were associated with *Nitrosospira briensis*, which was significantly higher in SC and CF than in the NA treatment (Figure 5A and Supplementary Figure S2A). The fertilization materials affected eight of the most abundant OTUs in the CAOB (ANOVA, $p < 0.05$). In the *Nitrospira* clade A.1, CAOB7 was associated with Ca. *N. inopinata*, Ca. *N. nitrosa*, and Ca. *N. nitrificans* and was significantly higher in SC than in NA treatment (Figure 5B and Supplementary Figure S2B). The primary descriptive sequences of the CAOB OTU were associated with the *Nitrospira* clade A.2.1 lineage (Figure 5B). CAOB21 and CAOB8 were high under organic and inorganic fertilizer materials (CF and SC) and no fertilizer treatment (NA), (which was related to *Nitrospira* sp. SG). At the same time, CAOB18 was significantly higher in SC and SM compared to NA treatment, respectively (Figure 5B and Supplementary Figure S2B). CAOB2 and CAOB23 were closely related to uncultured *Nitrospira* bacterium within *Nitrospira* Clade A.2.2 and A.3, and their contents were substantially greater in MS and CF compared to the NA treatments. CAOB46 was also greater in the NA group relative to the N fertilizer treatments and was affiliated with *Nitrospira* Clade B (Figure 5B and Supplementary Figure S2B).

Furthermore, the relative abundance of AOB by real-time PCR showed positive correlations to SOC ($r = 0.51$, $p < 0.05$), NO_3^--N ($r = 0.75$, $p < 0.01$), PNA ($r = 0.79$, $p < 0.01$), N_2O emission ($r = 0.62$, $p < 0.05$), and yield ($r = 0.54$, $p < 0.05$), but was negatively associated with pH ($r = 0.63$, $p < 0.05$; Table 3). The CAOB abundance by real-time PCR indicated a negative correlation with pH ($r = -0.67$, $p < 0.05$), TN ($r = -0.72$, $p < 0.01$), and N_2O emission ($r = -0.52$, $p < 0.05$), while being positively associated with AP ($r = 0.55$, $p < 0.05$), NO_3^--N ($r = 0.61$, $p < 0.05$), SWC ($r = 0.55$, $p < 0.05$), PNA ($r = 0.84$, $p < 0.01$), and yield ($r = 0.68$, $p < 0.05$; Table 3). However, the AOB diversity showed OTU, Shannon, and Simpson indices correlated positively with pH ($r = 0.63$, $p < 0.05$), SOC ($r = 0.52$, $p < 0.05$), and N_2O emission ($r = 0.78$, $p < 0.05$), respectively. The Chao and Shannon indices correlated negatively with PNA ($r = -0.52$, $p < 0.05$) and DON ($r = -0.66$, $p < 0.05$), respectively (Supplementary Figure S3). Among the comammox *Nitrospira* diversity, the Chao, Shannon, and Simpson indices correlated positively with pH ($r = 0.61$, $p < 0.05$), NO_3^--N ($r = 0.74$, $p < 0.05$), and SWC ($r = 0.52$, $p < 0.05$), respectively. The Simpson index was negatively associated with yield ($r = -0.57$, $p < 0.01$; Supplementary Figure S3).

Co-occurrence networks and prediction analysis

Distinct topological characteristics were observed in the AOB and CAOB populations based on the treatment's relative abundance. The AOB network community exhibited variations through Module I (28 nodes with 206 edges), Module II (21 nodes with 107 edges), Module III (37 nodes with 186 edges), and Module IV (41 nodes with 98 edges; Supplementary Table S4). On the other hand, the CAOB network community was Module I (23 nodes with 73 edges), Module II (20 nodes with 52 edges), and Module III (53 nodes with 153 edges), respectively (Supplementary Table S4).

Furthermore, the AOB and CAOB network communities exhibited a superior number of positive associations (411 and 197 edges) than negative associations (186 and 81 edges), respectively (Figures 6A–D). Modules I and III displayed more positive associations (126 and 138 edges) than negative correlations (60 and 67 edges) in the AOB network community (Figures 6A, B). However, the CAOB network community, Modules I and II, expressed a more positive relationship (107 and 51 edges) than a negative relationship (46 and 22 edges) compared to Modules II and IV (Figures 6C, D). Furthermore, key taxonomic groups were identified by assessing the network centrality and closeness centrality across the OTU modules. The AOB community was primarily composed of the genera *Nitrosospira* and *Nitrosomonas,* whereas the CAOB network *community*, genera Ca. *N. inopinata*, Ca. *N. nitrificans* and Ca. *N. nitrosa* (Figures 6B, D).

In the AOB network, Module I had a negative association with SOC ($r = -0.62$, $p < 0.05$), DON ($r = -0.78$, $p < 0.01$), and N_2O emissions ($r = -0.55$, $p < 0.05$; Figure 7). Module II was positively correlated with pH ($r = 0.66$, $p < 0.01$) and abundance ($r = 0.74$, $p < 0.01$) but negatively associated with NO_3^--N ($r = -0.76$, $p < 0.01$), AP ($r = -0.57$, $p < 0.05$), SWC ($r = -0.73$, $p < 0.01$), PNA ($r = -0.86$, $p < 0.01$), and yield ($r = -0.69$, $p < 0.01$; Figure 7). Module III was positively correlated with SOC ($r = 0.52$, $p < 0.05$), AP ($r = 0.59$, $p < 0.05$), DON ($r = 0.76$, $p < 0.01$), diversity ($r = 0.64$, $p < 0.05$), and N_2O emissions ($r = 0.75$, $p < 0.01$; Figure 7). In the CAOB network, Module II showed a positive correlation to SWC ($r = 0.52$, $p < 0.05$), while it displayed a negative relation with PNA ($r = -0.53$, $p < 0.05$; Figure 7). Module III exhibited a positive association with SOC ($r = 0.57$, $p < 0.05$), AP ($r = 0.59$, $p < 0.05$), DON ($r = 0.71$, $p < 0.01$), abundance ($r = 0.53$, $p < 0.05$), and diversity ($r = 0.64$, $p < 0.05$), but was negatively correlated with pH ($r = -0.78$, $p < 0.01$) and N_2O emissions ($r = -0.67$, $p < 0.01$; Figure 7).

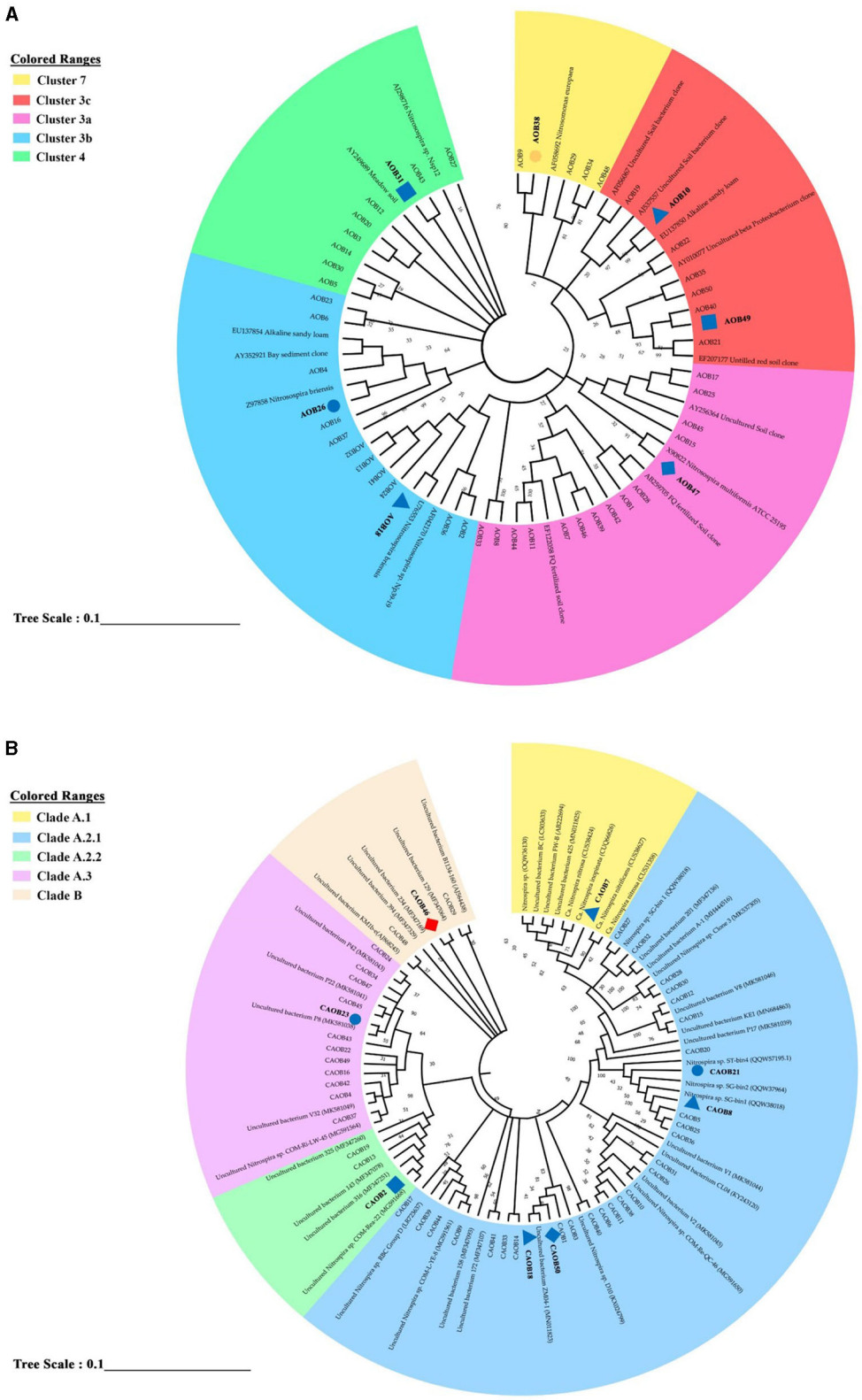

FIGURE 5
Phylogenetic neighbor-joining tree based on the genus level of **(A)** *amoA*–AOB genes and **(B)** comammox *Nitrospira* (CAOB) genes. The study provided information on the top 50 most prevalent sample sequences and their closest matches in the custom FunGene amoA sequence database. Additionally, the NCBI taxonomic classification of the database entries was included. The results also show the percentage of clone trees in which related taxa were grouped in the bootstrap test. A bootstrap value exceeding 50% is indicated next to the branches. Different shapes and colors were used to represent significant differences between the study's various fertilizer treatments and no fertilization. A circle represented a significant difference between inorganic fertilizer (CF) and no fertilization (NA). In contrast, a triangle shape represented a significant difference between inorganic plus organic fertilizer (SC) and no fertilization (NA). A rectangle shape was used to represent a significant difference between organic
(Continued)

FIGURE 5 (Continued)
fertilizer (SM) and no fertilization (NA), and a diamond shape represented a significant difference between maize straw only (MS) and no fertilization (NA). Blue indicated a significantly higher abundance than the control treatment, while red indicated a significantly lower abundance than no fertilization (NA).

TABLE 3 Pearson's correlation between gene copies of the ammonia-oxidizing bacteria (AOB), and comammox *Nitrospira* (CAOB) abundance, soil properties, PNA, N_2O, and yield.

	pH	TN	SOC	AP	NO_3^--N	NH_4^+-N	DON	SWC	PNA	N_2O	Yield
AOB	−0.63*	0.04	0.51*	0.44	0.75**	−0.19	−0.27	0.42	0.79**	0.62*	0.54*
CAOB	−0.67*	−0.72*	−0.37	0.55*	0.61*	0.32	−0.22	0.55*	0.84**	−0.52*	0.68*

pH; TN, total nitrogen; SOC, soil organic carbon; NO_3^--N, nitrate nitrogen; NH_4^+-N, ammonia nitrogen; AP, available phosphorous; DON, dissolved organic nitrogen; SWC, soil water content; PNA, soil potential nitrification activity; N_2O, cumulative nitrous oxide emission; yield, sum of grain and biomass.
*Significant correlations are indicated at a p-value of < 0.05.
**Suggesting significant correlations at a p-value of < 0.01.

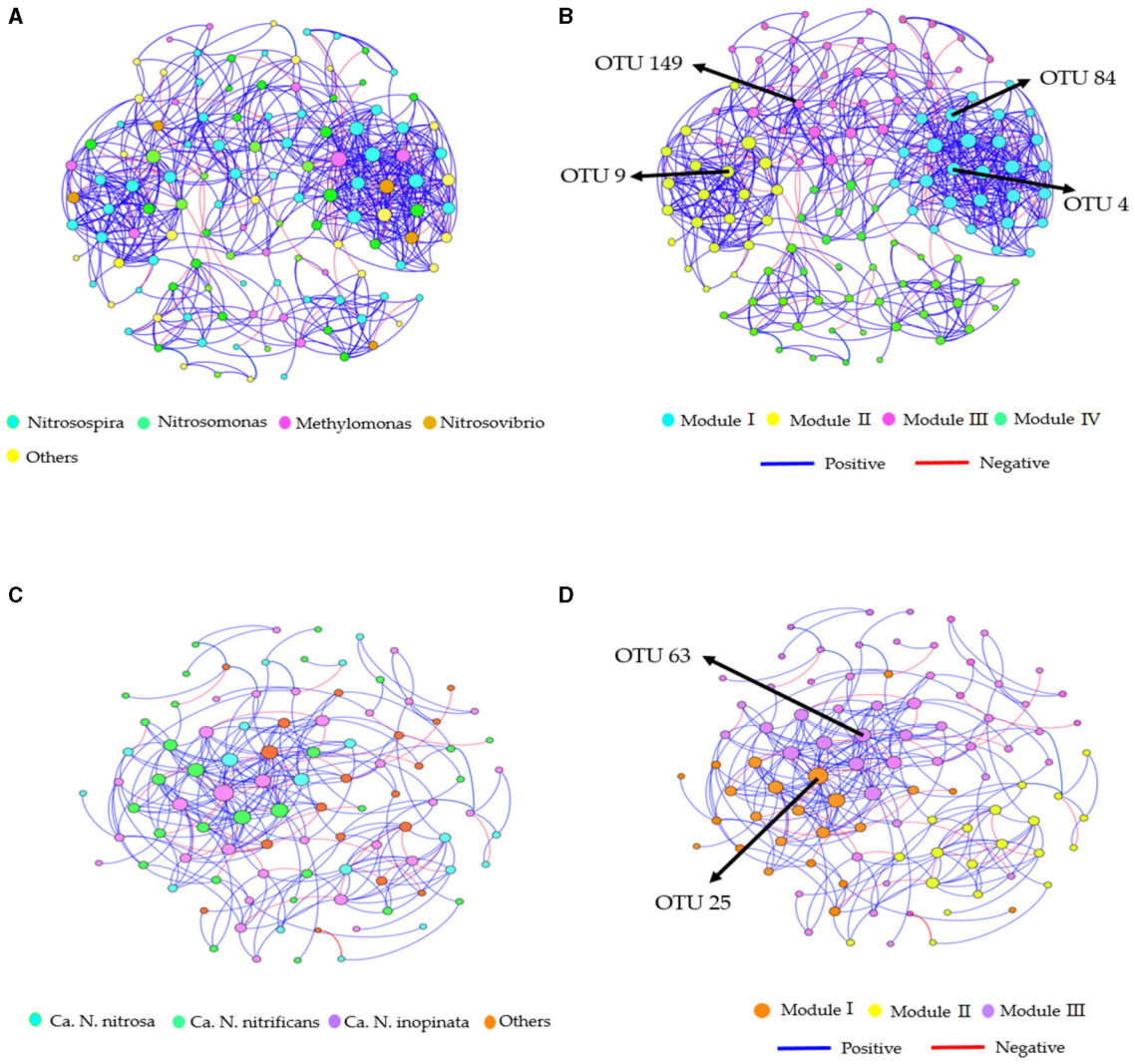

FIGURE 6
Co-occurrence network analysis of soil nitrification communities at the genus level. **(A, B)** *amoA*–AOB network OTU taxa and modules in the rhizosphere soil; **(C, D)** comammox *Nitrospira* (CAOB) network OTU taxa and modules in the rhizosphere soil. Modules consist of clusters of closely interconnected nodes. The size of the OTU nodes indicates their degrees, and they are colored based on their genus-level classification. Numbers identified in the modules indicate the Keystone taxa. Blue edges represent positive associations, while red edges represent negative associations.

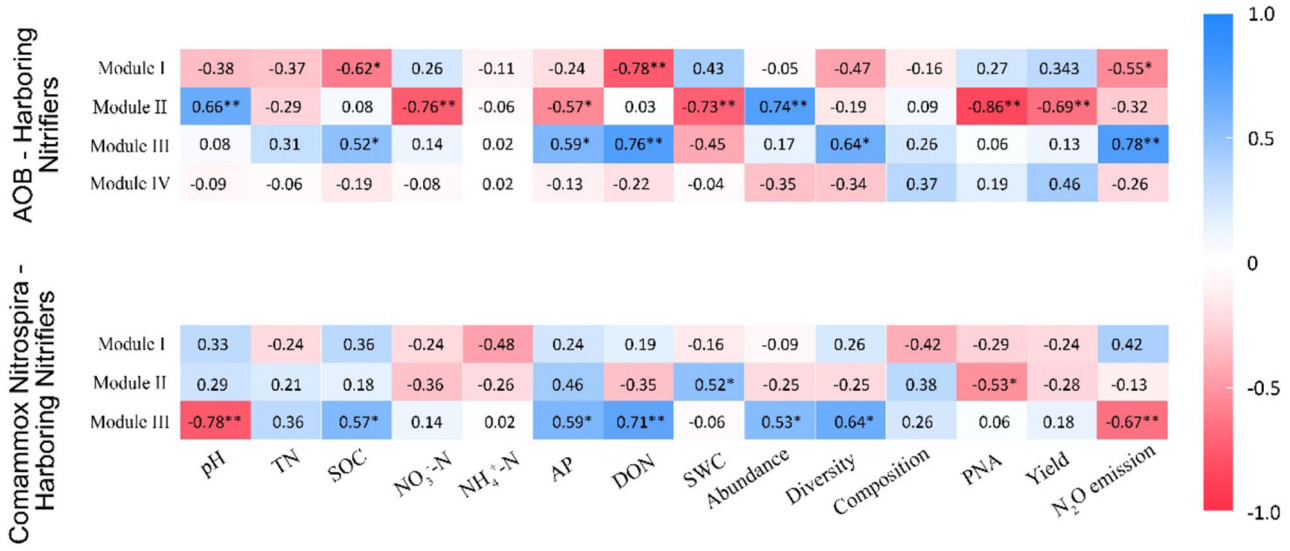

FIGURE 7
Correlation coefficients between major modules and soil parameters on the *amoA*–AOB and comammox *Nitrospira* (CAOB) nitrifier genes. Red represents positive correlation, and blue represents a negative correlation. The asterisk symbol represents the statistical significance, where *stands for $p < 0.05$ and **for a p-value of <0.01. TN, total nitrogen; SWC, soil water content; SOC, soil organic carbon; NO_3^--N, nitrate nitrogen; NH_4^+-N, ammonia nitrogen; AP, available phosphorus; DON, dissolved organic nitrogen, PNA, potential nitrification activity; yield, sum of grain and biomass and N_2O emission. The nitrification communities are represented by abundance (the copy numbers of genes), diversity (Chao1 richness), and composition (first principal coordinates, PC1).

Soil properties, AOB, and CAOB communities affected maize productivity, NUE, and N_2O emission

The study utilized random forest modeling to ascertain potential N_2O emissions, maize productivity, and NUE predictors, including soil properties and the AOB and CAOB populations. Random forest modeling revealed that pH (7.1%, $p < 0.05$ and 9.0%, $p < 0.05$), SOC (9.5%, $p < 0.01$ and 5.3%, $p > 0.01$), TN (8.2%, $p < 0.05$ and 8.7%, $p < 0.01$), and NO_3^--N (8.1%, $p < 0.05$ and 9.8%, $p < 0.01$) were identified as the crucial indicators of abiotic variables on the N_2O emission and maize productivity, respectively (Figures 8A, B). Furthermore, the abundance (5.0%−7.8%, $p < 0.05$ and 6.5%−7.0%, $p < 0.05$), composition (6.7%−8.9%, $p < 0.01$ and −1.1%−5.1%, 6.5%, $p > 0.05$), Module I (5.1%−7.1%, $p < 0.05$ and 3.6%−3.9%, $p < 0.05$), and Module II (6.2%−7.2%, $p < 0.05$; and 5.0%−6.9%, $p < 0.05$) were identified as the biotic drivers of the N_2O emission and maize yield in the AOB and CAOB nitrifiers, respectively (Figures 8A, B).

Structural equation modeling was constructed to further interconnect the prospective predictor's influences of AOB and CAOB nitrifier communities (i.e., composition, abundance, diversity, and network modules) and the abiotic drivers (i.e., soil properties) and their impacts on potential nitrification activity (PNA), the N_2O emission, maize productivity, and NUE. The physiochemical soil properties (i.e., SOC, pH, TN, and NO_3^--N) showed significant positive effects on the soil AOB community through abundance, composition, Module I, and Module II ($r = 0.53$, $p < 0.05$), as well as the CAOB community through abundance and Module II ($r = 0.57$, $p < 0.05$) and maize productivity ($r = 0.49$, $p < 0.05$), but expressed a significant negative effect on the PNA ($r = -0.36$, $p < 0.05$; Figure 9).

The AOB community exhibited a significant positive effect on the PNA ($r = 0.68$, $p < 0.05$) and maize productivity ($r = 0.58$, $p < 0.05$) through abundance, composition, Module I, and Module II. On the other hand, the CAOB community, through abundance and Module II, displayed a significant positive effect on maize productivity ($r = 0.72$, $p < 0.01$) but expressed a significantly negative influence with potential nitrification activity (PNA; $r = -0.60$, $p < 0.05$). PNA showed a significant positive association with N_2O emission ($r = 0.51$, $p < 0.05$). However, maize productivity ($r = 0.69$, $p < 0.01$) exhibited a positive correlation with NUE ($r = 0.53$, $p < 0.05$; Figure 9). The result points to the fact that AOB nitrifiers link positively to PNA activity, which contributes significantly to N_2O emissions compared to CAOB nitrifier communities. However, soil microbiome diversity and abiotic factors might influence the positive association between maize productivity and NUE.

Discussion

Fertilization impacts maize productivity, nitrogen use efficiency, and N_2O emissions

The application of inorganic fertilizer (CF) and the combined use of inorganic and organic fertilizer (SC) treatments exerted a significant positive influence on maize yield and NUE when compared to alternative treatments. These findings emphasize the pivotal role of appropriate fertilizer management

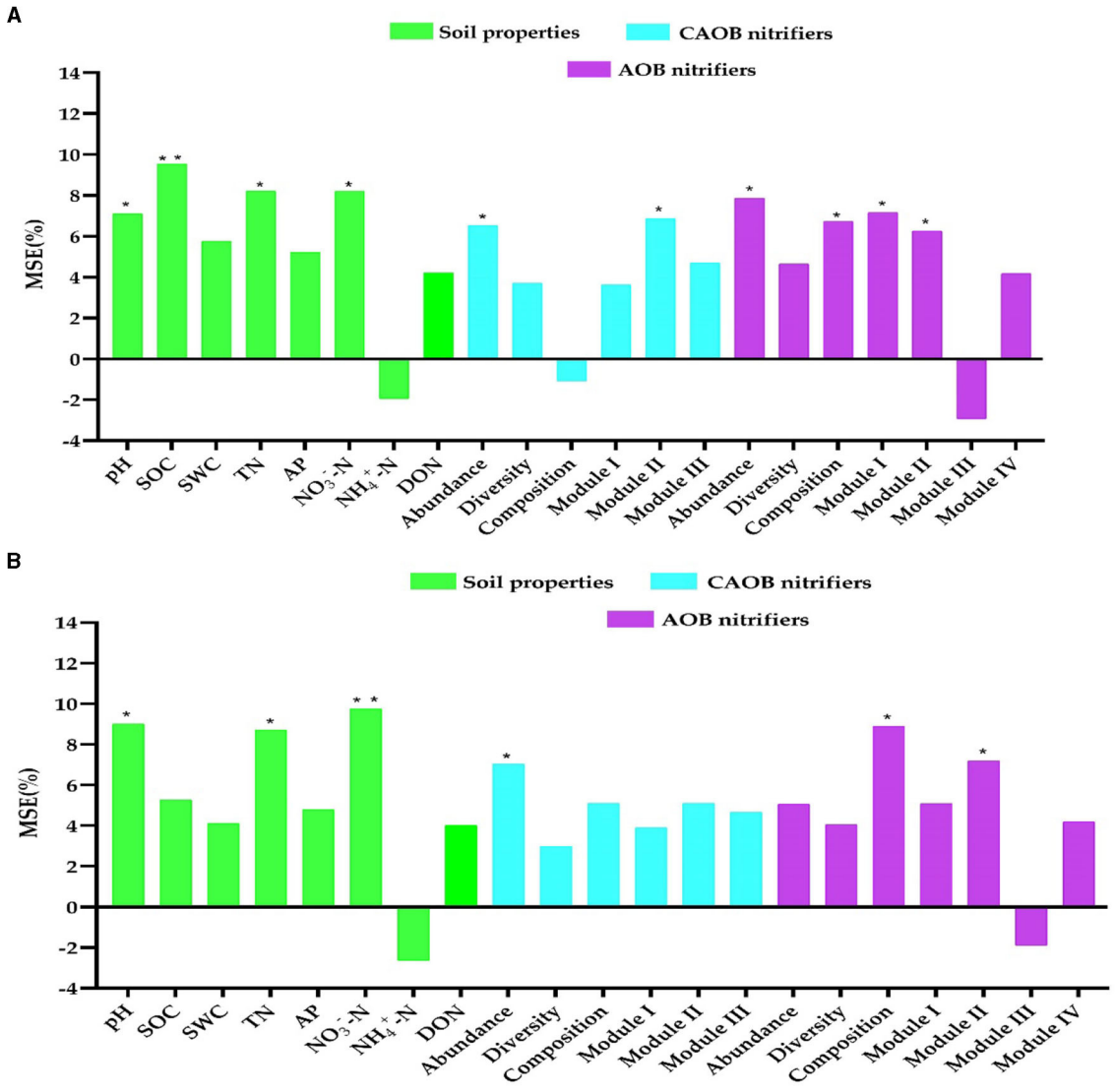

FIGURE 8
Random forest modeling was performed to evaluate the contributions of soil physiochemical properties and soil nitrification community variables to N_2O emission and maize productivity. **(A)** N_2O emission and **(B)** maize productivity in the *amoA*–AOB and comammox *Nitrospira* (CAOB) nitrifiers in the rhizosphere soil. Random forest modeling was performed based on 15 samples (5 treatments × 3 replicates). Soil properties include pH, total nitrogen (TN), soil organic carbon (SOC), available phosphorus (AP), nitrate nitrogen (NO_3^--N), ammonium nitrogen (NH_4^+-N), and dissolved organic nitrogen (DON). The soil nitrifying community includes diversity (Shannon index), composition (first principal coordinates, PC1), and three module eigengenes in the trophic co-occurrence network. $^*p < 0.05$; $^{**}p < 0.01$.

strategies in optimizing agricultural productivity and nutrient utilization (Ouyang et al., 2018; Cardenas et al., 2019). The utilization of inorganic fertilizer (CF) and the combined application of inorganic and organic fertilizer (SC) ensure a continuous supply of nitrogen derived from organic matter. This improved synchronization between the rate of nitrogen uptake by crops and its availability in the soil environment, resulting in enhanced yields and a moderate level of nitrogen use efficiency (Lin et al., 2020; Wang et al., 2020; Govindasamy et al., 2023).

In our study, N_2O emissions were higher in soils treated with organic fertilizer (MS and SM), with the highest levels observed between June and July. N_2O emissions are comparatively lower in processed organic fertilizers than in raw organic fertilizers. Additionally, prevailing climatic conditions play a vital role in N_2O emission rates, as evidenced in the current study. The use of plastic mulch led to an increase in soil moisture and temperature (21–31°C), causing fluctuations in drying and wetting cycles during the same period (June and July). These fluctuations are known to influence N_2O emissions by altering the populations of nitrifiers (Ouyang et al., 2018; Wang et al., 2020; Chataut et al., 2023). Some studies argue that severe soil water stress conditions can hinder the positive impacts of temperature on nutrient supply to microbes (Prosser and Nicol, 2012; Fowler

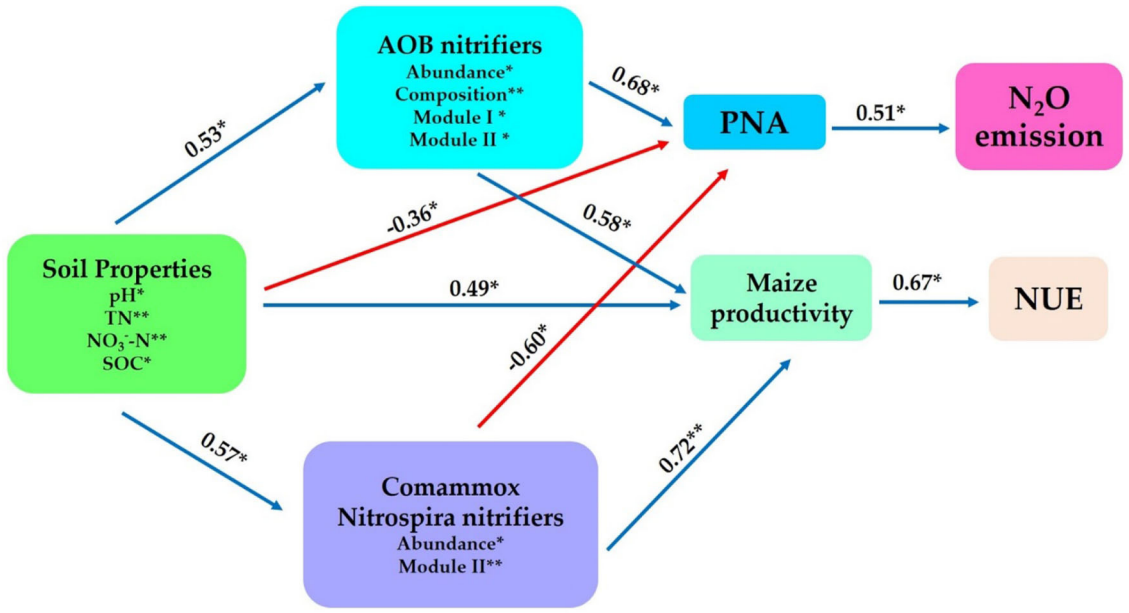

FIGURE 9
Structural equation modeling was performed to indicate the direct and indirect significant effects of soil physiochemical properties and soil nitrification communities (*amoA*–AOB and comammox *Nitrospira* (CAOB) nitrifiers) on N_2O emission, maize productivity, and NUE. In rhizosphere soil. Soil properties include pH, total nitrogen (TN), soil organic carbon (SOC), available phosphorus (AP), nitrate nitrogen (NO_3^--N), ammonium nitrogen (NH_4^+-N), and dissolved organic nitrogen (DON). The soil nitrifying community includes diversity (Shannon index), composition (first principal coordinates, PC1), and three module eigengenes in the trophic co-occurrence network. *$p < 0.05$; **$p < 0.01$.

et al., 2013). The sole application of organic fertilizer treatment significantly increased organic C and improved N_2O emissions. Existing studies have demonstrated that microorganisms adjust their carbon allocation between cell growth and stress tolerance, impacting their involvement in nutrient cycling (Hink et al., 2018; Lin et al., 2020). The addition of organic fertilizer (SM) and maize straw (MS) creates a conducive environment for nitrifiers due to the high levels of organic carbon and nitrogen compounds. This can enhance soil bacterial functioning and contribute to the production of PNA and nitrous oxide emissions (Shi et al., 2019; Ullah et al., 2020). The CF and SM treatments had a positive effect on the potential nitrification activity (PNA) process relative to the NA treatment. This might be due to the favorable conditions created by inorganic and organic fertilizers for microbial activities in the soil ecosystem (Domeignoz-Horta et al., 2018; Yang et al., 2018; Ullah et al., 2020). The unique niche interactions induced by root exudates promote nitrification processes in alkaline soils within semi-arid regions (Schmidt et al., 2019; Wang et al., 2019). Our research revealed the relationship between higher soil organic carbon (SOC) levels, PNA, and N_2O emissions when using organic fertilizer. The SC treatment increased soil water-holding capacity, which improved soil aeration (Cui et al., 2016; He et al., 2017). The SC treatment did not significantly affect soil N_2O emissions relative to solely using inorganic fertilizer (CF). However, the hydrolysis of urea provided highly oxidized nitrate substrates (NO_3^--N) that increased N_2O emissions (Tao et al., 2017; Ouyang et al., 2018; Fudjoe et al., 2021).

The AOB community was more active than the CAOB community in response to fertilization

Fluctuations in the abundance and diversity of the soil nitrification community pose a potential threat to the microbiome's function and the long-term sustainability of the soil agroecosystem (Kong et al., 2019; Lin et al., 2020). In our previous study, we found that the AOB, when compared to the abundance and diversity of the AOA, tends not to be sensitive to changes in fertilization regimes (i.e., urea and organic nitrogen fertilizers) and environmental conditions in the semi-arid Loess Plateau. This phenomenon is likely attributed to the mixotrophic lifestyle of AOA (Fudjoe et al., 2021). However, our findings provide compelling evidence that fertilization practices have a substantial impact on the abundance and diversity of the AOB and CAOB communities in the soil. The AOB nitrifiers had a relatively higher influence than CAOB nitrifiers, which can be attributed to their inherent physiological response or a major difference in substrate affinity (Pjevac et al., 2017; Xu et al., 2020).

The AOB were more abundant in the organic (SM) and organic and inorganic (SC) treatments, while the CAOB were higher in the inorganic-treated (CF) soils. Such variations have been linked to the soil's carbon and nitrogen availability (He et al., 2017; Schmidt et al., 2019). Despite the substantial presence of CAOB in all fertilizer treatments, its function and impact on ammonia oxidation were significantly less than those of AOB abundance. This distinction can be attributed to the ecosystem's alkaline soil (Li et al., 2019;

Wang et al., 2021). Some studies have traced the reaction to the oligotrophic lifestyle of CAOB, which could make them more sensitive to soils with low levels of nitrogen fertilization (Hu and He, 2017; Kits et al., 2017). Furthermore, these findings validate previous studies indicating that nitrifiers containing AOB are more pivotal in ammonia oxidation and nitrogen cycling within alkaline soils compared to nitrifiers containing CAOB (Hu and He, 2017; Li et al., 2021).

The phylogenetic analysis provides a categorized clustering technique by classifying microbes based on transcription factor lineages and ecological functioning. The *Nitrosospira* cluster was functionally active in the genus AOB community (Hu and He, 2017; Pjevac et al., 2017; Lin et al., 2020). Most of the sequences were associated with *Nitrosospira* cluster 3b, which is affiliated with *N. briensis,* which might be due to the significant nitrogen in alkaline calcareous soils (Wang et al., 2017; Fudjoe et al., 2021). The application of combined inorganic and organic (SC) and sole application of organic (SM and MS) fertilizer relative to no fertilization (NA) might have caused the dominance of *Nitrosospira* Cluster 3b in arable soils due to their nitrification activity (Kong et al., 2019; Wang et al., 2019). Within the genera comammox *Nitrospira*, based on phylogenetic analysis, Clades A.2.1 and A.3 formed the majority of clusters in our analysis, accounting for 89.9% of all sequences relative to *Nitrospira* clade A.1, which accounted for 5.8% of the sequence. In the *Nitrospira* clade A.1, CAOB7 was associated with three key species: Ca. *N. inopinata*, Ca. *N. nitrosa*, and Ca. *N. nitrificans* were significantly higher in the combination of organic and inorganic fertilizer (SC) than the no fertilizer (NA) treatment. The findings of this study are consistent with previous phylogenetic analyses, which have indicated that the majority of comammox *Nitrospira* clade A.1 sequences originate from aquatic or artificial environments, while clades A.2.1 and A.3 are predominantly found in terrestrial ecosystems (Li et al., 2019; Xu et al., 2020). Previous research by Hu and He (2017) reveals that the physiological adaptability and ecological niche differentiation of clades A and B comammox *Nitrospira* can be attributed to the distinct transport proteins and physiological characteristics in each subgroup (He et al., 2017; Pjevac et al., 2017).

Interactions in the nitrification communities contributed to maize productivity, NUE, and N_2O emissions

Nitrifying bacteria play a crucial role in regulating nitrogen fixation, N_2O emissions, and maize productivity in soil. Fertilization practices have a significant impact on the composition and functional diversity of microbial communities involved in decomposition, mineralization, and nitrification processes. Consequently, these modifications in microbial populations influence N_2O emissions in agricultural fields (Hu and He, 2017; Ouyang et al., 2018). The AOB and CAOB nitrifier communities indicated both positive and significant negative effects on maize productivity, NUE, PNA, and N_2O emissions, respectively. The current study showed a positive association between AOB and soil property dynamics (soil pH, TN, NO_3^--N, and SOC), PNA, and N_2O emission due to potential competitive interactions and functional diversity activities (Lin et al., 2020; Fudjoe et al., 2021; Zheng et al., 2022). On the other hand, the CAOB nitrifier community was negatively correlated with PNA and indirectly with N_2O emissions but positively associated with maize productivity, NUE, and soil properties (soil pH, TN, NO_3^--N, and SOC). The positive relationship between the CAOB community and maize NUE might be due to the synergistic effects of nitrogen cycling and nutrient dynamics in the soil ecosystem (Kits et al., 2017; Pjevac et al., 2017). The soil pH, carbon, and nitrogen properties were essential to calcareous soils' microbial cell growth and metabolic activities (Ouyang et al., 2018; Li et al., 2019). The key soil properties are crucial in determining habitat selection and niche differentiation between AOB and CAOB nitrifier communities (Hu and He, 2017; Osburn and Barrett, 2020).

The findings of Berry and Widder (2014) and Mamet et al. (2019) emphasize the significant effect of environmental changes and external factors on the relationships between nitrifying microbes in a community and their ecological functions. The network composition of the AOB and CAOB communities was characterized by more positive correlations between microbes compared to negative correlations (Lin et al., 2020; Fudjoe et al., 2021). The nitrification community's network edges have a high percentage of beneficial interactions compared to adverse connections, which shows that taxonomic competition has increased and enhanced the network structure (Osburn and Barrett, 2020; Zheng et al., 2022). However, the AOB community modules were closely linked to abiotic and biotic variables, unlike the CAOB network populations. The network centrality modules among the different operational taxonomic units (OTUs) demonstrated the importance of interactions and identifying potential keystone taxa (Wang et al., 2020; Li et al., 2021). Keystone taxa are crucial in enhancing competition and maintaining the microbiomes and their functions. Specific keystone taxa and biodiversity adaptability sustained the high diversity of the AOB (*Nitrosospira*) and comammox *Nitrospira* (Ca. *N. inopinata*) communities in response to organic-rich additions (Pjevac et al., 2017; Hink et al., 2018). The soil pH, SOC, NO_3^--N, and DON sources impacted the keystone taxa of AOB and CAOB nitrifier communities by promoting microbial diversity, community structural integrity, and network stability (Williams et al., 2014; Hu and He, 2017; Lin et al., 2020). Our study further found that the difference in habitat preferences between AOB and CAOB composition was largely due to variations in their cell affinities, mediated keystone taxa performance on nitrogen cycling, and diversity–functioning relationships (Xu et al., 2020; Zheng et al., 2022). Furthermore, discretion is required when concluding on the underlying effect of organic–inorganic fertilization on keystone taxa's considerable impact on nitrification communities (Kong et al., 2019; Li et al., 2019; Schmidt et al., 2019). Additional investigation using stable isotope techniques and empirical data are required to support the current conclusions on the prospective keystone species' contribution to the network system.

Conclusion

The application of inorganic fertilizer (CF) and the combined use of inorganic and organic fertilizer (SC) resulted in significant improvements in maize productivity and nitrogen use efficiency (NUE) compared to no fertilizer (NA). The SC treatment

exhibited lower rates of N_2O emissions and cumulative N_2O emissions compared to the CF treatment. This is because SC treatment increased the abundance of comammox *Nitrospira* (CAOB), particularly the clade A.1 lineage group, including Ca. *N. inopinata*, Ca. *N. nitrosa*, and Ca. *N. nitrificans*, compared to the NA treatment. The keystone taxa of the CAOB community showed positive correlations with maize productivity and NUE, likely due to their stimulated functional activities under the SC treatment. Among the AOB community, *Nitrosospira* was the dominant genus at the cluster level; specifically, *N. briensis* species were observed under the CF and SM treatments. The AOB community exhibited a significant positive association with N_2O emissions and potential nitrification activity (PNA), showing a prominent role in nitrification. Overall, these findings suggest that the SC treatment effectively improves maize yield and nitrogen use efficiency while mitigating N_2O emissions and promoting a sustainable agroecosystem in the study area.

Data availability statement

The datasets presented in this study can be found in online repositories. The names of the repository/repositories and accession number(s) can be found at: https://www.ncbi.nlm.nih.gov/genbank/, PRJNA813620 and PRJNA813629.

Author contributions

SF and LL: conceptualization and methodology. SF: validation, writing—original draft preparation, and visualization. JX and LW: resources. SF: data curation. FY, SA, and LL: writing—review and editing. LL and SS: supervision. JX: project administration. All authors have read and approved the content of the manuscript and agreed to the published version of the manuscript.

Funding

The research was supported by the National Key R&D Program of China (2022YFD1900300), the National Natural Science Foundation of China (32260549), and the State Key Laboratory of Aridland Crop Science, Gansu Agricultural University (GSCS-2022-Z02).

Conflict of interest

The authors declare that the research was conducted in the absence of any commercial or financial relationships that could be construed as a potential conflict of interest.

Publisher's note

All claims expressed in this article are solely those of the authors and do not necessarily represent those of their affiliated organizations, or those of the publisher, the editors and the reviewers. Any product that may be evaluated in this article, or claim that may be made by its manufacturer, is not guaranteed or endorsed by the publisher.

Supplementary material

The Supplementary Material for this article can be found online at: https://www.frontiersin.org/articles/10.3389/fmicb.2023.1249668/full#supplementary-material

References

Alhassan, A. M., Ma, W., Li, G., Jiang, Z., Wu, J., Chen, G., et al. (2018). Response of soil organic carbon to vegetation degradation along a moisture gradient in a wet meadow on the Qinghai–Tibet Plateau. *Ecol. Evol.* 10999–12010. doi: 10.1002/ece3.4656

Archer, E. (2020). *rfpermute: Estimate Permutation p-Values for Important Metrics*. R package version 2.1–5.

Bao, S. (2000). *Soil Agrochemical Analysis*, 3rd ed. Beijing: China Agricultural Press, 265–267.

Berry, D., and Widder, S. (2014). Deciphering microbial interactions and detecting keystone species with co-occurrence networks. *Front. Microbiol.* 5, 101–219. doi: 10.3389/fmicb.2014.00219

Bremner, J. M. (1965). "Chemical and microbiological properties," in *Methods of Soil Analysis,* ed. C. A. Black (Madison, WI: American Society of Agronomy), 1085–1121.

Bu, L. D., Liu, J. L., Zhu, L., Luo, S. S., Chen, X. P., Li, S. Q., et al. (2014). Attainable yield achieved for plastic film-mulched maize in response to nitrogen deficit. *Eur. J. Agron.* 55, 53–62. doi: 10.1016/j.eja.2014.01.002

Caporaso, J. G., Kuczynski, J., Stombaugh, J., Bittinger, K., Bushman, F. D., Costello, E. K., et al. (2010). QIIME allows the analysis of high-throughput community sequencing data. *Nat. Methods* 7, 335–336. doi: 10.1038/nmeth.f.303

Cardenas, L. M., Bhogal, A., Chadwick, D. R., McGeough, K., Misselbrook, T., Rees, R. M., et al. (2019). Nitrogen use efficiency and nitrous oxide emissions from five UK fertilised grasslands. *Sci. Total Environ.* 661, 696–710. doi: 10.1016/j.scitotenv.2019.01.082

Chataut, G., Bhatta, B., Joshi, D., Subedi, K., and Kafle, K. (2023). Greenhouse gases emission from agricultural soil: a review. *J. Agric. Food Res.* 11, 100533. doi: 10.1016/j.jafr.2023.100533

Cui, P., Fan, F., Yin, C., Song, A., Huang, P., Tang, Y., et al. (2016). Long-term organic and inorganic fertilization alters temperature sensitivity of potential N_2O emissions and associated microbes. *Soil Biol. Biochem.* 93, 131–141. doi: 10.1016/j.soilbio.2015.11.005

Daims, H., Lebedeva, E. V., Pjevac, P., Han, P., Herbold, C., Albertsen, M., et al. (2015). Complete nitrification by *Nitrospira* bacteria. *Nature* 528, 504–509. doi: 10.1038/nature16461

Domeignoz-Horta, L. A., Philippot, L., Peyrard, C., Bru, D., Breuil, M., Bizouard, F., et al. (2018). Peaks of in situ N_2O emissions are influenced by N_2O-producing and reducing microbial communities across arable soils. *Glob. Change Biol.* 24, 360–370. doi: 10.1111/gcb.13853

Edgar, R. C. (2013). UPARSE: highly accurate OTU sequences from microbial amplicon reads. *Bioinformatics* 27, 2194–2200. doi: 10.1093/bioinformatics/btr381

Edgar, R. C., and Flyvbjerg, H. (2015). Error filtering, pair assembly and error correction for next-generation sequencing reads. *Bioinformatics* 31, 3476–3482. doi: 10.1093/bioinformatics/btv401

Food and Agriculture Organization (FAO) (1990). *Soil Map of the World: Revised Legend; World Soil Resources Report 60*. Rome: Food and Agriculture Organization of the United Nations.

Fortmannroe, S. (2015). *A3: Accurate, Adaptable, and Accessible Error metrics for Predictive Models*. R package version 1.0.0.

Fowler, D., Coyle, M., Skiba, U., Sutton, M. A., Cape, J. N., Reis, S., et al. (2013). The global nitrogen cycle in the twenty-first century. *Philos. Trans. R. Soc. Biol. Sci.* 368, 201–301. doi: 10.1098/rstb.2013.0164

Fudjoe, S. K., Jiang, Y., Li, L., Karikari, B., Xie, J., Wang, L., et al. (2021). Soil amendments alter ammonia-oxidizing archaea and bacteria communities in rain-fed maize field in semi-arid Loess Plateau. *Land* 10, 10–39. doi: 10.3390/land10101 01039

Ghani, A., Dexter, M., and Perrott, K. W. (2003). Hot-water extractable carbon in soils: a sensitive measurement for determining impacts of fertilization, grazing, and cultivation. *Soil Biol. Biochem*. 35, 1231–1243. doi: 10.1016/S0038-0717(03)00186-X

Govindasamy, P., Muthusamy, S. K., Bagavathiannan, M., Mowrer, J., Jagannadham, P. T. K., Maity, A., et al. (2023). Nitrogen use efficiency-a key to enhance crop productivity under a changing climate. *Front. Plant Sci.* 14, 1121073. doi: 10.3389/fpls.2023.1121073

He, Y., Hu, W. G., Ma, D. C., Lan, H. Z., Yang, Y., Gao, Y., et al. (2017). Abundance and diversity of ammonia-oxidizing archaea and bacteria in the rhizosphere soil of three plants in the Ebinur Lake wetland. *Can. J. Microbiol.* 63, 573–582. doi: 10.1139/cjm-2016-0492

Hink, L., Gubry-Rangin, C., Nicol, G. W., and Prosser, J. I. (2018). The consequences of niche and physiological differentiation of archaeal and bacterial ammonia oxidizers for nitrous oxide emissions. *ISME J.* 12, 1084–1093. doi: 10.1038/s41396-017-0025-5

Hu, H. W., and He, J. Z. (2017). Comammox-A newly discovered nitrification process in the terrestrial nitrogen cycle. *J. Soils Sediments* 17, 2709–2717. doi: 10.1007/s11368-017-1851-9

Huang, R., Wang, Y., Liu, J., Li, J., Xu, G., Luo, M., et al. (2019). Variation in N_2O emission and N_2O related microbial functional genes in straw- and biochar-amended and non-amended soils. *Appl. Soil Ecol.* 137, 57–68. doi: 10.1016/j.apsoil.2019.01.010

Kits, K. D., Sedlacek, C. J., Lebedeva, E. V., Han, P., Bulaev, A., Pjevac, P., et al. (2017). Kinetic analysis of a complete nitrifier reveals an oligotrophic lifestyle. *Nature* 549, 269–272. doi: 10.1038/nature23679

Koch, H., van Kessel, M., and Lucker, S. (2019). Complete nitrification: insights into the ecophysiology of comammox *Nitrospira*. *Appl. Microbiol. Biotechnol.* 103, 177–189. doi: 10.1007/s00253-018-9486-3

Kong, Y., Ling, N., Xue, C., Chen, H., Ruan, Y., Guo, J., et al. (2019). Long-term fertilization regimes change soil nitrification potential by impacting active autotrophic ammonia oxidizers and nitrite oxidizers as assessed by DNA stable isotope probing. *Environ. Microbiol.* 21, 1224–1240. doi: 10.1111/1462-2920.14553

Kurola, J., Salkinoja-Salonen, M., Aarnio, T., Hultman, J., and Romantschuk, M. (2005). Activity, diversity and population size of ammonia-oxidizing bacteria in oil-contaminated land farming soil. *FEMS Microbiol. J.* 25, 33–98. doi: 10.1016/j.femsle.2005.06.057

Lamptey, S., Nartey, E., and Kwapong, P. K. (2019). Influence of organic amendment on soil respiration and maize productivity in a semi-arid environment. *Agronomy* 9, 97–128. doi: 10.3390/agronomy9100611

Li, C., Hu, H. W., Chen, Q. L., Chen, D., and He, J. Z. (2019). Comammox *Nitrospira* play an active role in nitrification of agricultural soils amended with nitrogen fertilizers. *Soil Biol. Biochem.* 38, 107–609. doi: 10.1016/j.soilbio.2019.107609

Li, C., Hu, H. W., Chen, Q. L., Yan, Z. Z., Nguyen, B. T., Chen, D., et al. (2021). Niche specialization of comammox *Nitrospira* clade A in terrestrial ecosystems. *Soil Biol. Biochem*. 56, 108–231. doi: 10.1016/j.soilbio.2021.108231

Liaw, A., and Wiener, M. (2002). Classification and regression by random forest. *R News* 2, 18–22.

Lin, Y., Ye, G., Ding, W., Hu, H., Zheng, Y., Fan, J., et al. (2020). Niche differentiation of comammox *Nitrospira* and canonical ammonia oxidizers in soil aggregate fractions following 27-year fertilizations. *Agric. Ecosyst. Environ*. 304, 107147. doi: 10.1016/j.agee.2020.107147

Mamet, S. D., Redlick, E., Brabant, M., Lamb, E. G., Helgason, B. L., Stanley, K., et al. (2019). Structural equation modeling of a winnowed soil microbiome identifies how invasive plants re-structure microbial networks. *ISME J.* 13, 1988–1996. doi: 10.1038/s41396-019-0407-y

Olsen, S. R., Cole, C., Watanabe, F. S., and Dean, L. (1954). *Estimation of Available Phosphorus in Soils by Extraction with Sodium Bicarbonate. Circular (No. 939)*. Washington DC: USDA Press, 1–19.

Osburn, E. D., and Barrett, J. E. (2020). Abundance and functional importance of complete ammonia-oxidizing bacteria (comammox) versus canonical nitrifiers in temperate forest soils. *Soil Biol. Biochem.* 145, 107–801. doi: 10.1016/j.soilbio.2020.107801

Ouyang, Y., Evans, S. E., Friesen, M. L., and Tiemann, L. K. (2018). Effect of nitrogen fertilization on the abundance of nitrogen cycling genes in agricultural soils: a meta-analysis of field studies. *Soil Biol. Biochem*. 127, 71–78. doi: 10.1016/j.soilbio.2018.08.024

Pjevac, P., Schauberger, C., Poghosyan, L., Herbold, C. W., van Kessel, J., Daebeler, A., et al. (2017). AmoA-targeted polymerase chain reaction primers for the specific detection and quantification of comammox *Nitrospira* in the environment. *Front. Microbiol*. 8, 1508. doi: 10.3389/fmicb.2017.01508

Prosser, J. I., and Nicol, G. W. (2012). Archaeal and bacterial ammonia-oxidizers in soil: the quest for niche specialization and differentiation. *Trends Microbiol.* 20, 523–531. doi: 10.1016/j.tim.2012.08.001

Sahoo, M. (2019). "Structural equation modeling: threshold criteria for assessing model fit," in *Methodological Issues in Management Research: Advances, Challenges, and the Way Ahead*, ed R. N. Subudhi, and S. Mishra (Bingley: Emerald Publishing Limited), 269–276. doi: 10.1108/978-1-78973-973-220191016

Schloss, P. D., Westcott, S. L., Ryabin, T., Hall, J. R., Hartmann, M., Hollister, E. B., et al. (2009). Introducing mothur: open-source, platform-independent, community-supported software for describing and comparing microbial communities. *Appl. Environ. Microbiol.* 75, 7537–7541. doi: 10.1128/AEM.01541-09

Schmidt, J. E., Kent, A. D., Brisson, V. L., and Gaudin, A. C..M (2019). Agricultural management and plant selection interactively affect rhizosphere microbial community structure and nitrogen cycling. *Microbiome* 7, 146–200. doi: 10.1186/s40168-019-0756-9

Shi, Y. L., Liu, X. R., and Zhang, Q. W. (2019). Effects of combined biochar and organic fertilizer on nitrous oxide fluxes and the related nitrifier and denitrifier communities in a saline-alkali soil. *Sci. Total Environ.* 686, 199–211. doi: 10.1016/j.scitotenv.2019.05.394

Sun, P. Zhao. Z, Fan, P., Chen, W., Ruan, Y., Wang, Q. (2021). Ammonia- and nitrite-oxidizing bacteria are dominant in nitrification of maize rhizosphere soil following combined application of biochar and chemical fertilizer. *Front. Microbiol.* 12, 715070. doi: 10.3389/fmicb.2021.715070

Tamura, K., Stecher, G., Peterson, D., Filipski, A., and Kumar, S. (2013). MEGA6: molecular evolutionary genetics analysis version 6. 0. *Mol. Biol. Evol.* 30, 2725–2729. doi: 10.1093/molbev/mst197

Tao, R., Steven, A. W., Liang, Y. C., and Chu, G. X. (2017). Response of ammonia-oxidizing archaea and bacteria in calcareous soil to mineral and organic fertilizer application and their relative contribution to nitrification. *Soil Boil Biochem*. 114, 20–30. doi: 10.1016/j.soilbio.2017.06.027

Tao, R., Wakelin, S. A., Liang, Y., Hu, B., and Chu, G. (2018). Nitrous oxide emission and denitrifier communities in drip-irrigated calcareous soil as affected by chemical and organic fertilizers. *Sci. Total Environ.* 612, 739–749. doi: 10.1016/j.scitotenv.2017.08.258

Ullah, S., Ai, C., Huang, S., Song, D., Abbas, T., Zhang, J., et al. (2020). Substituting ecological intensification of agriculture for conventional agricultural practices increased yield and decreased nitrogen losses in North China. *Appl. Soil Ecol.* 147, 103–395. doi: 10.1016/j.apsoil.2019.103395

Van Kessel, M. A., Speth, D. R., Albertsen, M., Nielsen, P. H., Op den Camp, H. J., and Kartal, B. (2015). Complete nitrification by a single microorganism. *Nature* 58, 555–559. doi: 10.1038/nature16459

Wang, J., Ni, L., Song, Y., Rhodes, G., Li, J., Huang, Q., et al. (2017). Dynamic response of ammonia-oxidizers to four fertilization regimes across a wheat-rice rotation system. *Front. Microbiol*. 8, 630. doi: 10.3389/fmicb.2017.00630

Wang, J. C., Wang, J. L., Rhodes, G., He, J. Z., and Ge, Y. (2019). Adaptive responses of comammox *Nitrospira* and canonical ammonia oxidizers to long-term fertilizations: implications for the relative contributions of different ammonia oxidizers to soil nitrogen cycling. *Sci. Total Environ.* 168, 224–233. doi: 10.1016/j.scitotenv.2019.02.427

Wang, X., Lu, L., Zhou, X., Tang, X., Kuang, L., Chen, J., et al. (2021). Niche differentiation of comammox *Nitrospira* in the mudflat and reclaimed agricultural soils along the north branch of Yangtze River Estuary. *Front. Microbiol*. 11, 618287. doi: 10.3389/fmicb.2020.618287

Wang, X., Wang, S., Jiang, Y., Zhou, J., Han, C., Zhu, G., et al. (2020). Comammox bacterial abundance, activity, and contribution in agricultural rhizosphere soils. *Sci. Total Environ.* 727, 138563. doi: 10.1016/j.scitotenv.2020.138563

Williams, R. J., Howe, A., and Hofmockel, K. S. (2014). Demonstrating microbial co-occurrence pattern analyses within and between ecosystems. *Front. Microbiol*. 5, 358. doi: 10.3389/fmicb.2014.00358

Xia, F., Wang, J. G., Zhu, T., Zou, B., Rhee, S. K., Quan, Z. X., et al. (2018). Ubiquity and diversity of complete ammonia oxidizers (comammox). *Appl. Environ. Microbiol.* 14, 53–90. doi: 10.1128/AEM.01390-18

Xu, S., Wang, B., Li, Y., Jiang, D., Zhou, Y., Ding, A., et al. (2020). Ubiquity, diversity, and activity of comammox *Nitrospira* in agricultural soils. *Sci. Total Environ.* 76, 135–684. doi: 10.1016/j.scitotenv.2019.135684

Yang, Y. D., Ren, Y. F., Wang, X. Q., Hu, Y. G., Wang, Z. M., Zemg, Z. H., et al. (2018). Ammonia-oxidizing archaea and bacteria responding differently to fertilizer type and irrigation frequency as revealed by Illumina Miseq sequencing. *J. Soils Sediments* 58, 1029–1040. doi: 10.1007/s11368-017-1792-3

Yu, C., Hou, L., Zheng, Y., Liu, M., Yin, G., Gao, J., et al. (2018). Evidence for complete nitrification in enrichment culture of tidal sediments and diversity analysis of clade a comammox *Nitrospira* in natural environments. *Appl. Microbiol. Biotechnol. 102:9363–9377*, 9274–0. doi: 10.1007/s00253-018-9274-0

Yu, L., Homyak, P. M., Kang, X. X., Brookes, P. C., Ye, Y. K., Lin, Y. N., et al. (2019). Changes in abundance and composition of nitrifying communities in barley (Hordeum vulgare L.) rhizosphere and bulk soils over the growth period following combined biochar and urea amendment. *Biol. Fertil. Soils* 56, 169–183. doi: 10.1007/s00374-019-01410-6

Zhang, B., Zhang, J., Liu, Y., Shi, P., and Wei, G. (2018). Co-occurrence patterns of soybean rhizosphere microbiome at a continental scale. *Soil Biol. Biochem.* 38, 178–186. doi: 10.1016/j.soilbio.2017.12.011

Zhang, F., Zhang, W., Qi, J., and Li, F. M. (2018). A regional evaluation of plastic film mulching for improving crop yields on the Loess Plateau of China. *Agric. For. Meteorol.* 28, 458–468. doi: 10.1016/j.agrformet.2017.10.030

Zheng, J., Tao, L., Dini-Andreote, F., Luan, L., Kong, P., Xue, J., et al. (2022). Dynamic responses of ammonia-oxidizing archaea and bacteria populations to organic material amendments affect soil nitrification and nitrogen use efficiency. *Front. Microbiol.* 13, 911799. doi: 10.3389/fmicb.2022.911799

frontiers | Frontiers in Microbiology

TYPE Original Research
PUBLISHED 20 October 2023
DOI 10.3389/fmicb.2023.1275986

OPEN ACCESS

EDITED BY
Jianling Fan,
Nanjing University of Information Science and Technology, China

REVIEWED BY
Osama Abdalla Abdelshafy Mohamad,
Chinese Academy of Sciences (CAS), China
Xiaoyulong Chen,
Guizhou University, China

*CORRESPONDENCE
Yonggang Li
✉ neaulyg@126.com

RECEIVED 11 August 2023
ACCEPTED 26 September 2023
PUBLISHED 20 October 2023

CITATION
Sun L, Wang W, Zhang X, Gao Z, Cai S, Wang S and Li Y (2023) *Bacillus velezensis* BVE7 as a promising agent for biocontrol of soybean root rot caused by *Fusarium oxysporum*. *Front. Microbiol.* 14:1275986. doi: 10.3389/fmicb.2023.1275986

Bacillus velezensis BVE7 as a promising agent for biocontrol of soybean root rot caused by *Fusarium oxysporum*

Lei Sun[1], Wei Wang[1], Xue Zhang[2], Zhongchao Gao[1], Shanshan Cai[1], Shuang Wang[1] and Yonggang Li[2]*

[1]Heilongjiang Academy of Black Soil Conservation & Utilization, Harbin, China, [2]College of Plant Protection, Northeast Agricultural University, Harbin, Heilongjiang, China

Introduction: Soybean root rot (SRR), caused by *Fusarium oxysporum*, is a severe soil-borne disease in soybean production worldwide, which adversely impacts the yield and quality of soybean. The most effective method for managing crop soil-borne diseases and decreasing reliance on chemical fungicides, such as *Bacillus* spp., is via microbial biocontrol agents.

Methods and Results: In this study, a soil-isolated strain BVE7 was identified as *B. velezensis*, exhibiting broad-spectrum activity against various pathogens causing soybean root rot. BVE7 sterile filtrate, at a concentration of 10%, demonstrated significant antifungal activity by inhibiting the conidial germination, production, and mycelial growth of *F. oxysporum* by 61.11%, 73.44%, and 85.42%, respectively, causing hyphal malformations. The antifungal compound produced by BVE7 demonstrated adaptability to a standard environment. The pot experiment showed that BVE7 suspension could effectively control soybean root rot, with the highest control efficiency of 75.13%. Furthermore, it considerably enhanced the activity of catalase, phenylalanine ammonia lyase, superoxide dismutase, and peroxidase in soybean roots, while also preventing an increase in malondialdehyde activity. By improving the host resistance towards pathogens, the damage caused by fungi and the severity of soybean root rot have been reduced.

Discussion: This study presents the innovative utilization of *B. velezensis*, isolated from soybean roots in cold conditions, for effectively controlling soybean root rot caused by *F. oxysporum*. The findings highlight the remarkable regional and adaptive characteristics of this strain, making it an excellent candidate for combating soybean root rot in diverse environments. In conclusion, *B. velezensis* BVE7 demonstrated potential in effectively reducing SRR incidence and can be considered as a viable option for SRR management.

KEYWORDS

soybean root rot, *Bacillus velezensis*, antifungal activities, biological control, growth-promoting effects

1. Introduction

Soybean is a significant food crop that provides a sustainable source of protein, oil, vitamins, and other essential nutrients for human consumption globally (Hu et al., 2016; Yang et al., 2023). As the primary soybean-producing region in China, Northeast China accounts for 50% of the country's total soybean production (source: China National Data, https://data.stats.gov.cn/). It is crucial to reduce disease damage during soybean planting to

enhance yields (Dorrance et al., 2003). In the early spring, when soybean seeding occurs, the damp environment is conducive to pathogen invasion, which can cause soybean root rot at different temperatures (Zitnick-Anderson and Nelson, 2015). *Fusarium* spp. including *F. redolens* in Minnesota (Bienapfl et al., 2010), *F. oxysporum*, *F. graminearum, F. solani*, *F. avenaceum*, *F. tricinctum*, *F. sporotrichioides*, *F. equiseti*, and *F. poae*in and *F. proliferatum* Ontario, Canada (Zhang et al., 2009, 2013; Chang et al., 2015), *F. commune*, *F. solani*, *F. tricinctum* and *F. fujikuroi* in the United States (Ellis et al., 2013; Detranaltes et al., 2021; Yan and Nelson, 2021), *F. oxysporum, F. brachygibbosum* and *F. fujikuroi* in China (Li et al., 2018; Zhao et al., 2020; Wang et al., 2021), cause soybean root rot (SRR), a soil-borne disease with a high risk of infection, significantly impacting soybean emergence, seedling growth, plant vigor, and yield losses (Nelson et al., 1999; Han et al., 2021). *F. oxysporum* is the dominant strain reported in the United States (Nelson et al., 1999; Cruz Jimenez et al., 2018), Northeast China (Li et al., 2018), and Ontario, Canada (Wang et al., 2004; Zhang et al., 2013).

SRR, caused by *F. oxysporum*, is a common soil-borne disease. Conventional methods for controlling root rot, such as seed dressing and leaf-spraying with chemical fungicides in the field, have been utilized to manage some Fusarium diseases (Zhang et al., 2000). However, given the impact of chemical fungicides on the ecological environment, human health, and pathogen resistance, there has been increased attention on the limitations of chemical control. Crop rotation with non-host plants is an effective measure for controlling SRR. Buhre and Kluth (2009) employed crop rotation of maize and beet to manage the incidence of beet root rot. Nonetheless, there are few land resources and accumulated temperatures in Northeast China, this measure may not be applicable in areas with continuous soybean cropping due to specific climatic conditions and economic considerations (Li et al., 2010). Therefore, there is an urgent need to identify a harmless and feasible strategy for suppressing the development of Fusarium root rot on soybean.

Soil is a living natural resource on which the sustainability of agricultural systems depends. Soil quality is attributed to multiple interactions between physical, chemical, and biological components, with microbial communities playing a crucial role in soil functionality (Janvier et al., 2007). In addition, the complexity of ecosystems is directly involved in the performance of soil system functions, determining its quality (Vezzani and Mielniczuk, 2009). Biological control of plant diseases using plant-associated bacteria or natural compounds of biological origin is now recognized as one of the most promising alternatives to the use of chemical fungicides (Etesami et al., 2023). Employing beneficial microorganisms for biological control is a noteworthy strategy that has significant potential for managing Fusarium root rot on soybean. Currently, chemical control remains the main approach for preventing and treating crop root rot. Yuan et al. (2011) effectively managed wheat root rot using difenoconazole. Tanni et al. (2016) successfully controlled the root rot of chickpea through the use of Bavistin 70 WP. Naqvi (2005) controlled root rot (*Phytophthora nicotianae*) in citrus soils with foselyl-Al and Metalaxyl. However, chemical control methods have negative impacts on ecological environment and human health, and are not conducive to the sustainability of agriculture. In comparison to the application of chemical agents, biological control measures can be both cost-effective and environmentally friendly, and can significantly inhibit the activity of soil-borne pathogens and induce plant resistance due to the natural and pathogenic origins of their biological control agents (BCAs) (Zhang et al., 2009; Amin et al., 2015; Raza et al., 2019). Furthermore, biological control provides long-lasting and sustainable effects in reducing the incidence and severity of root rot, ensuring the healthy growth of current and subsequent crops. Huang et al. (2013) found that the rhizosphere soil of healthy plants that survive in plots infected by plant pathogens is a good source for the isolation of BCAs. In recent years, numerous BCAs have been successfully isolated from rhizosphere soil, including *Bacillus* spp. (Xu et al., 2020), *Pseudomonas* spp. (Liu et al., 2019), *Trichoderma* spp. (Saravanakumar et al., 2017), and *Streptomyces* spp. (Faheem et al., 2015). Among these promising BCAs, *Bacillus* spp. produces stress-resistant spores and exhibits resistance to extreme conditions, fast reproduction, and strong colonization ability. It is amenable to artificial large-scale fermentation and cultivation, making it an ideal candidate for use as a biocontrol bacterium (Santoyo et al., 2012; Shafi et al., 2017; Fira et al., 2018). *Bacillus* spp., among the various biotic components, is a predominant bacterial genus with tremendous metabolic and genetic diversity, which enables it to play a crucial role in the soil ecosystem. Many *Bacillus* species have been found in different ecological niches. Globally developed and distributed commercial *Bacillus*-based preparations contain *B. amyloliquefaciens*, *B. cereus*, *B. licheniformis*, *B. megaterium*, *B. pumilus*, *B. subtilis*, *B. thuringiensis*, and *B. velezensis* species (Mazzola and Freilich, 2017; Etesami et al., 2023). *Bacillus* spp. populations can coexist with other bacterial populations in the soil and rhizosphere without any negative effects (Vardharajula et al., 2011; Radhakrishnan et al., 2017). Zhang et al. (2009) utilized *Bacillus subtilis* strains through seed and soil treatments to manage soybean root rot induced by *F. oxysporum* and *F. graminearum*. Therefore, *Bacillus* species were chosen as an alternative biocontrol factor for preventing and managing SRR caused by *F. oxysporumin* in this paper.

The research aimed to achieve the following objectives: (i) to screen and identify biocontrol bacteria for the management of SRR, (ii) to analyze the antifungal mechanisms of *B. velezensis*, a potential biological control bacterium, (iii) to investigate the impact of biocontrol bacteria on defense-related enzymes in soybean, and (iv) to evaluate the efficacy of employing biocontrol bacteria in the management of SRR.

2. Materials and methods

2.1. Isolation of bacterial strains

Three hundred and twenty-four bacterial strains were isolated from the rhizosphere soil of soybean fields located in Harbin (126.93° E, 45.77° N), China, using the soil dilution method (Li et al., 2020). Following a 72-h incubation period at 28°C, a single bacterial colony was selected and purified via repeated streaking on beef extract peptone medium (BPM) (Beijing Aoboxing Biology Technology Co., Ltd.) plates.

2.2. Screening of biological control bacteria against SRR

The targeted pathogen, *Fusarium oxysporum* isolate BLD3, was isolated and preserved by our team and eventually emerged as the primary population of SRR-causing pathogens in Northeast China, emerging as the predominant pathogen responsible for SRR in the area. Initial screening of antagonistic bacteria was accomplished using the confrontational approach (Birber et al., 1998). After incubating the bacterial strains on a nutrient agar medium (NA) plate for 48 h at a temperature of 28°C, a center of a potato dextrose agar (PDA) plate with a diameter of 9 cm was inoculated using the parallel streak method positioned at a distance of 3 cm. Following this, a disk of *F. oxysporum* with a diameter of 0.7 cm was inserted in the center of the PDA plate. Cultivating for 5 days at a temperature of 26°C with three replicates, measurements were taken for the maximum and minimum radii of *F. oxysporum* colonies to determine the antagonistic activity of the tested bacterial strains (Wang et al., 2020). Strains that displayed the most significant ratio of the longest-to-shortest radius were selected for further in-depth study.

2.3. Identification of biocontrol bacterium BVE7

The morphological features of BVE7 were observed on nutrient agar (NA), while the physiological and biochemical characteristics were measured based on standard protocols by Schaad et al. (2001), Buchanan (1984), and Dong and Cai (2001). Based on the aforementioned references, we had chosen these physiological and biochemical parameters to assist in the identification of the genus and species of biocontrol bacteria, including tests for gram stain, lactose utilization, catalase activity, sucrose utilization, aerobism, mannitol fermentation, glucose fermentation, V.P. test, fructose fermentation, gelatin liquefaction, arabinose utilization, mannose fermentation, xylose utilization, casein hydrolysis, sorbitol utilization, phaseomannite utilization, starch hydrolysis, malonate utilization, cellobiose fermentation, rhamnose utilization, M.R. test, maltose fermentation, galactose fermentation, and nitrate reduction using commercially available physiological and biochemical test kits (Guangdong Huankai Microbial Sci.&Tech. Co., Ltd., Guangdong, China).

To identify BVE7, genomic DNA was extracted using a Tiangen Genome Extraction Kit (Tiangen Biotech, Beijing, China). Bacterial universal primers, 27F (5′-AGAGTTGATCCTGGCTCAG-3′) and 1492R (5′-GGTTACCTTGTTACGACTT-3′), were employed to amplify partial sequences of the 16S rRNA gene. The genomic template was amplified by PCR in a 50-μl reaction volume consisting of 25-μl PCR Master Mix (2X) (Invitrogen, Carlsbad, CA, United States), 2.0 μL of 10 mM forward primer, 2.0 μL of 10 mM reverse primer, 2 μL of template DNA, and 19 μL of nuclease-free water. The PCR program consisted of an initial denaturation at 94°C for 5 min, followed by 36 cycles of denaturation at 94°C for 1 min, annealing at 58°C for 1 min, and extension at 72°C for 1.5 min; and a final extension at 72°C for 10 min. The amplified product was sequenced by Shanghai Biological Engineering Co., Ltd. (Shanghai, China). Phylogenetic trees of BVE7 were constructed using Mega 6.0 software (Mega Limited, Auckland, New Zealand) based on the neighbour-joining (NJ) method (Nei and Kumar, 2000).

2.4. Antifungal spectrum

Using the described confrontation technique, the antifungal efficacy of BVE7 against 10 strains of SRR-causing pathogenic fungi, including *F. tricinctum*, *Diaporthe longicolla*, *F. acuminatum*, *Bipolaris zeicola*, *Chaetomium globosum*, *F. verticillioides*, *Botrytis cinerea*, *F. solani*, *Clonostachys rosea*, *F. chlamydosporum*, was assessed. These pathogenic fungi were obtained from the plant pathology laboratory of Northeast Agricultural University in China. The measurement and evaluation techniques were identical to those outlined in Section 2.2.

2.5. Determination of antagonistic mechanism of BVE7

BVE7 was activated at 28°C for 24 h with agitation at 180 rpm and subsequently inoculated into Luria-Bertani (LB) liquid medium with a liquid loading of 200 mL·L − 1 in a 500-mL Erlenmeyer flask under identical conditions for six days. The aseptic filtrate of BVE7 was obtained through an aseptically sterilized bacterial filter with a pore size of 0.22 μm (YY3014236, Millipore, United States) (Li et al., 2020).

An aseptically filtered solution of BVE7 was added to Potato Dextrose Agar (PDA) medium at final concentrations of 1, 5, and 10%, with three replicates each. An equivalent volume of liquid Luria-Bertani (LB) medium was added as a control. This experiment was conducted twice. A 7 mm diameter disc of *F. oxysporum* mycelium grown on PDA medium for 120 h was transferred to the center of the PDA plate and incubated for another 120 h at 26°C. The diameter of *F. oxysporum* colonies was measured to evaluate the inhibitory effect of BVE7 on its growth.

Fusarium oxysporum was cultivated on PDA plates at 26°C until the colony reached a diameter of 4 cm. The medium without hyphae was discarded, and then 20 mL of aseptic BVE7 filtrate was added to the PDA plates with the colony at concentrations of 1, 5, and 10%. 20 mL of LB liquid medium was used as a control with three replicates. After a 20-min incubation period, the mycelium was carefully removed. Following 72 h of incubation at 26°C, 20 mL of sterile water was poured into the plates to wash the conidia, and conidia concentration was recorded using a haemocytometer (Li et al., 2020). The experiments were repeated twice to ensure accuracy.

Fusarium oxysporum was cultivated on PDA media at 26°C for 5 days followed by washing with sterile distilled water (SDW) to obtain conidia. A haemocytometer was used to adjust the conidial suspension to 1×10^8 conidia/mL. BVE7 filtrate was then added to the conidial suspension at concentrations of 1, 5, and 10%, which was prepared using the same method as described earlier. For the control, conidial suspension amended with an equal volume of LB liquid medium was used. Each treatment was subjected to three replicates. The conidial suspensions were incubated at 25°C. Conidia germination (100 spores per treatment) was counted when the control's conidial germination rate exceeded 60%.

Fusarium oxysporum was inoculated onto PDA plates and incubated at 26°C for 12 h. Fresh hyphae were then scraped and immersed in aseptic BVE7 filtrate at concentrations of 1, 5, and 10%. After 24 h, the morphology of the hyphae was observed under an optical microscope (Nikon 90i, Japan) in order to obtain precise results.

2.6. Stability of antifungal substances

Aseptic filtrates of BVE7, obtained through procedures outlined in section 2.5, were subjected to incubation in a water bath at temperatures of 20, 40, 60, 80, and 100°C, and 121°C. The effects of aseptic filtrates treated at varying temperatures were evaluated on the mycelial growth of F. oxysporum at a concentration of 5%.

The pH of the aseptic BVE7 filtrate was adjusted in increments of 1 unit from 3.0 to 12.0 using 0.1 M HCl or NaOH. The impacts of different pH treatments on BVE7 were determined by using the mycelial growth rate method.

The aseptic BVE7 filtrate was exposed to UV light at a distance of 1 cm and at a wavelength of 100 W/cm^2 for 30, 60, and 90 min. The effects of the UV light exposure on BVE7 were evaluated utilizing the aforementioned method.

2.7. Evaluation of biological control efficacy of BVE7 under pot conditions

The specific procedures were carried out as follows: the biocontrol bacteria BVE7 were cultured in liquid LB medium for 48 h and subsequently diluted to a concentration of 1×10^8 CFU/mL (where an OD of 0.1 at 600 nm is equivalent to 10^8 CFU/mL) using 0.9% normal saline solution as a diluent for storage. Inoculum of *F. oxysporum* was prepared by inoculating sorghum seeds following the protocol described in our previous research (Li et al., 2018). The study included six treatments, each with three replicates. i was the control group with no treatment. Iiwas only inoculated with *F. oxysporum* iii involved irrigating 0.5 mL of bacterial suspension to the roots and *F. oxysporum* on the day of planting and 7 days later. iv used 1 mL of bacterial suspension per plant and *F. oxysporum*, while v used 1.5 mL per plantand *F. oxysporum*. vi involved spraying seeds with 43% tebuconazole at 0.14 mg/mL. The pots were placed in a greenhouse with a temperature of 23 ± 3°C. A total of fifty plants were inoculated with three repetitions, and after inoculation, conventional methods were utilized in managing the seeds (cv. Dongnong 52). The occurrence of SRR was then evaluated after 20 days.

The severity of the disease was evaluated by assessing the growth status of soybean roots using a scale ranging from 0 to 9 (Li et al., 2018): Where 0 = no symptoms; 1 = slightly darkening fibrous root, the aboveground portion grew well; 3 = slightly darkening taproot, the aboveground portion grew well; 5 = severe darkening taproot or hypocotyls erosion, the aboveground portion grew poorly; and 7 = root necrotized and infected plant dead. The experiment was conducted twice under identical conditions. Disease index (DI) for SRR was calculated, as follows:

$$DI = \sum(\text{number of diseased plants at each level} \times \text{number of relative ratings}) / (\text{total number of surveyed plants} \times \text{highest number of diseased levels}) \times 100.$$

2.8. Analysis of defense-related enzymes in soybean seedlings treated by the biocontrol bacterial strain BVE7

Soybean seedlings (10 plants per pot) grown for 15 days were inoculated with a suspension of BVE7 spores at a concentration of 1×10^8 cfu/mL by root irrigation, with 1.5 mL per plant, while an equal amount of sterile water was used as a blank control. Each treatment was replicated three times. The treated plants were placed in a constant-temperature incubator maintained at 25°C, with a light/dark regime of 12/12 h and 85–95% relative humidity (RH). After 0, 12, 24, 48, 72 and 96 h of incubation, root tissues from the treated soybean were collected and analyzed for defense-related enzyme activity. The enzyme activities of catalase (CAT), malondialdehyde (MDA), phenylalanine ammonia-lyase (PAL), peroxidase (POD), and superoxide dismutase (SOD) were determined using appropriate kits (Suzhou Grace Biotechnology Co., Ltd., Suzhou, China) and calculated according to the fresh weight of the sample in units per kilogram (U kg-1).

2.9. Data analysis

All experiments were replicated twice under identical conditions. Statistical analysis was performed using SPSS Statistics 19.0 software (IBM Corporation, Armonk, NY, United States), and results were evaluated using ANOVA. Subsequently, statistically significant differences were observed between the means of the treatments using Duncan's multiple range test ($p < 0.05$).

3. Results

3.1. Isolation and screening of biological control bacteria

A total of 324 strains extracted from the rhizosphere soil of soybean plants were screened for their antagonistic activity against *F. oxysporum*, the causal agent of SRR. Out of all the tested strains, a total of 24 demonstrated superior antagonistic activity in comparison to the remaining strains, with the BVE7 strain exhibiting the most prominent effect (Table 1) and was identified as a potential biocontrol agent with an average ratio of 2.50. Further evaluation of BVE7 in potted soybean plants demonstrated its excellent control efficacy against SRR. Accordingly, BVE7 was selected for subsequent experiments. Additionally, BVE7 displayed remarkable antagonistic activity against various pathogenic fungi causing SRR (Table 2 and Figure 1), including *Diaporthe longicolla*, *Clonostachys rosea*, *Bipolaris zeicola, Chaetomium globosum*, *F. solani*, *F. tricinctum*, and *F. verticillioides*.

3.2. Identification of isolate BVE7

BVE7 was a gram-positive, rod-shaped bacterium, measuring 0.4 to 0.8 μm in diameter and 1.5 to 3.4 μm in length, with round cell ends (Figure 2) and usually no fold and forms milky-white colonies on LB agar plates. With aging, the colony margins of BVE7 exhibited a folded morphology with a depressed surface. It was aerobic, and could produce nitrate reductase and hydrolyze starch and casein. M.R.,

TABLE 1 Twenty-four bacterial strains screened for their strong antagonistic effects against *Fusarium oxysporum* causing root rot in soybeans.

Antagonistic Strains No.	Maximum/Minimum radius[a]	Antagonistic Strains No.	Maximum/Minimum radius[a]
BVE7	2.50	B-13	2.01
F3	2.47	12–2	2.01
107	2.47	24	2.00
H-18	2.41	A27	1.99
B6	2.35	26	1.97
21	2.35	22	1.97
18	2.35	23	1.94
F5	2.13	25	1.76
19	2.09	94	1.76
30	2.07	S2	1.75
91	2.06	12	1.67
13	2.04	11	1.54

[a]Values in the column indicate mean of the maximum/ minimum radius of the pathogens.

TABLE 2 Determination of antagonistic fungal spectrum suppressed by biological bacteria BVE7 *in vitro*.

Strains No.	Mean ± SE[a]	Strains No.	Mean ± SE[a]
Diaporthe longicolla	2.67 ± 0.08a	*Fusarium acuminatum*	1.47 ± 0.09 g
Clonostachys rosea	2.18 ± 0.11bcd	*F. solani*	2.10 ± 0.04cde
Bipolaris zeicola	2.00 ± 0.10de	*F. tricinctum*	2.31 ± 0.05b
Chaetomium globosum	2.01 ± 0.13de	*F. chlamydosporum*	1.93 ± 0.12ef
Botrytis cinerea	1.82 ± 0.09f	*F. verticillioides*	2.31 ± 0.05b

[a]Values in the column indicate mean ± standard error (SE) of the maximum/ minimum radius of the pathogens on the fifth day after inoculation.
Values followed by different letters are significantly different according to Duncan's multiple range tests ($p < 0.05$).

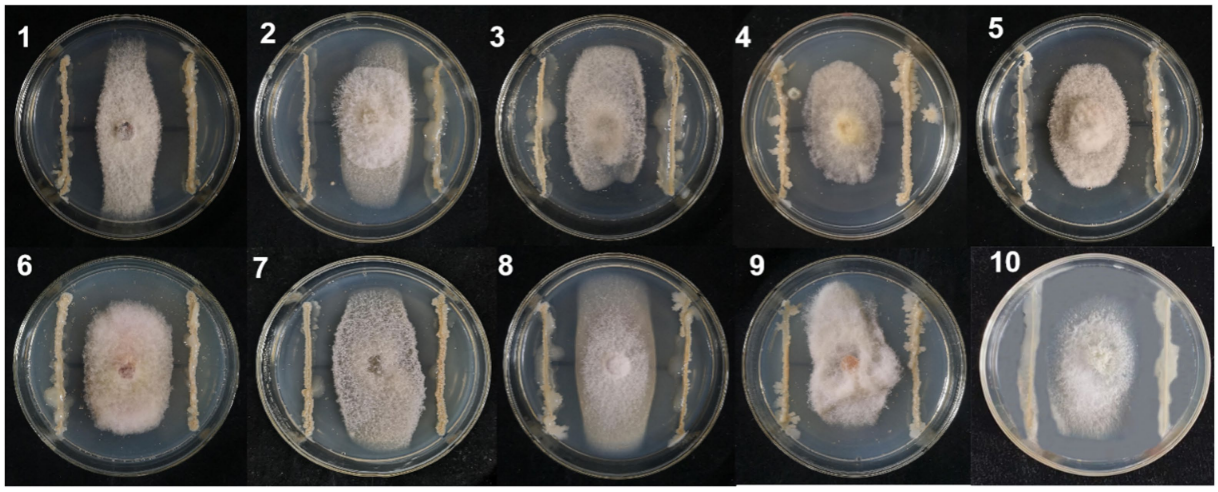

FIGURE 1
Antagonistic effect of biological bacteria BVE7 on the mycelial growth of pathogenic fungi on the fifth day after inoculation. 1. *Diaporthe longicolla*; 2. *Clonostachys rosea*; 3. *Bipolaris zeicola*; 4. *Chaetomium globosum*; 5. *Botrytis cinerea*; 6. *Fusarium acuminatum*; 7. *F. Solani*; 8. *F. tricinctum*; 9. *F. chlamydosporum*; 10. *F. verticillioides*.

amylum hydrolase and V-P tests were positive. BVE7 could utilize a variety of sugars, including sucrose, glucose, arabinose, mannitol, seminose lactose, xylose, phaseomannite, galactose, maltose, rhamnose, cellobiose and fructose, but not malonate. The bacterium did not produce hydrogen sulfide and catalase. The 16 s rRNA gene sequence of BVE7 showed 99.9% similarity to *B. velezensis* strain Bv-HR6-1 (accession no. MF192765.1) and was deposited in GenBank (accession no. OP905633.1). A phylogenetic tree based on the 16 s

rRNA gene sequence comparison indicated that BVE7 belonged to the *B. velezensis* (Figure 3).

3.3. Effect of BVE7 on hyphal and conidia of *Fusarium oxysporum*

The antagonistic active components of BVE7, administered at varied concentrations, significantly inhibited the conidial production, germination, and hyphal growth of *F.* oxysporum (Figures 4, 5). At a concentration of 10%, BVE7 demonstrated a 61.1% inhibition rate on spore germination, 73.4% on spore production, and 85.42% on hyphal growth. Additionally, treatment with the BVE7 filtrate resulted in protoplasmic aggregation, swelling deformation, and folding of the *F. oxysporum* mycelium (Figure 6). As the concentration of BVE7 filtrate increased, these effects became more prominent.

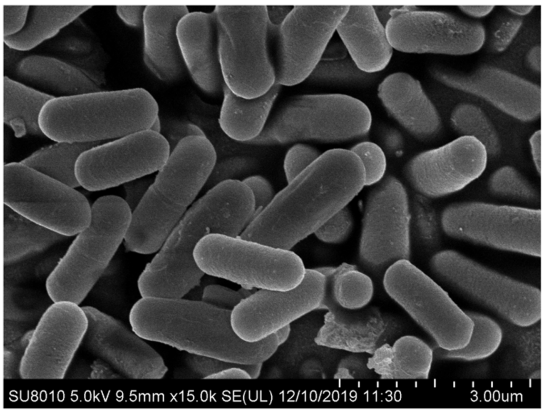

FIGURE 2
Scanning electron micrograph depicting the cellular morphology of *Bacillus velezensis* BVE7 cultivated for 24h at 30°C on nutrient agar medium.

3.4. Stability of the antifungal substances of BVE7

The antifungal substances in BVE7 were found to be unaffected by temperatures up to 60°C, but were significantly weakened at temperatures exceeding 80°C, though some antifungal activity persisted (Figure 7A). The antifungal substances were also observed to be pH-sensitive, with maximal activity at a pH of 7.0 (Figure 7B). Prolonged exposure to UV radiation was observed to enhance the antagonistic effect (Figure 7C).

3.5. Reduction SRR following application of BVE7

As shown in Table 3, the disease index of SRR when inoculated solely with *F. oxysporum* was around 70. When applied to a bacterial suspension of 1 mL per plant and 0.5 mL per plant, the control efficacy of SRR surpassed 65%. However, when treated with BVE7 at a bacterial suspension of 1.5 mL/plant, the control efficacy of SRR exceeded 75% when compared to the control group, which was equivalent to that of chemical fungicides.

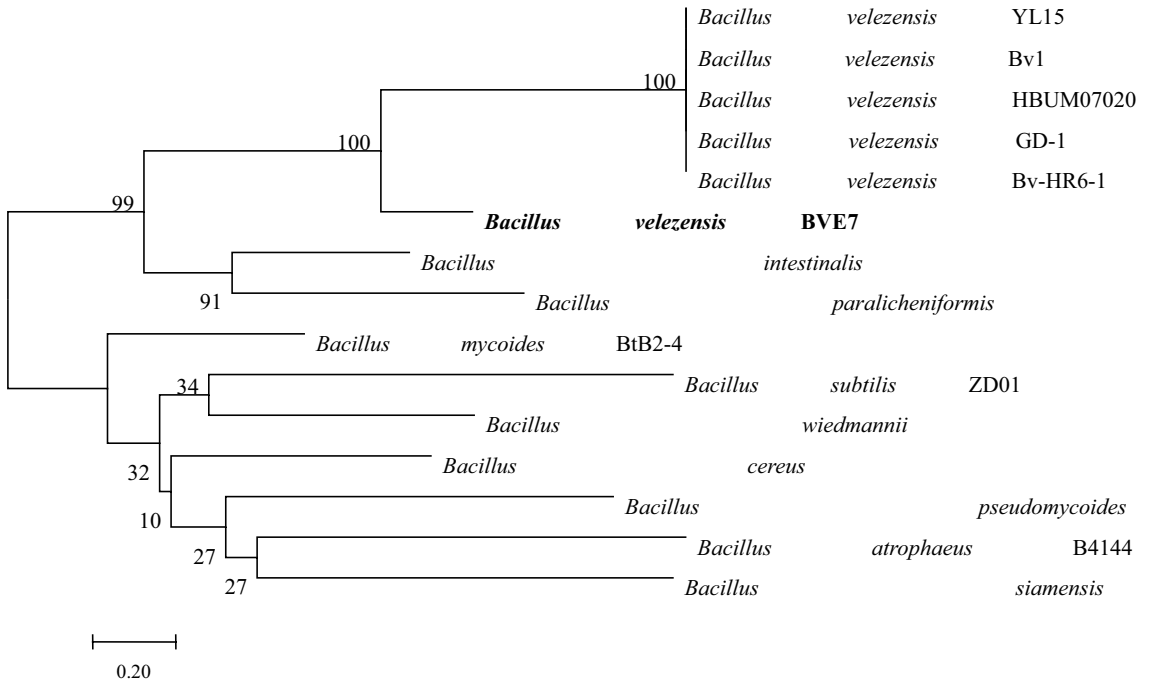

FIGURE 3
Phylogenetic tree depicting the identification of *Bacillus velezensis* isolate BVE7 based on 16S rRNA gene sequencing. The bootstrap values on the branching nodes were calculated on 1,000 replications.

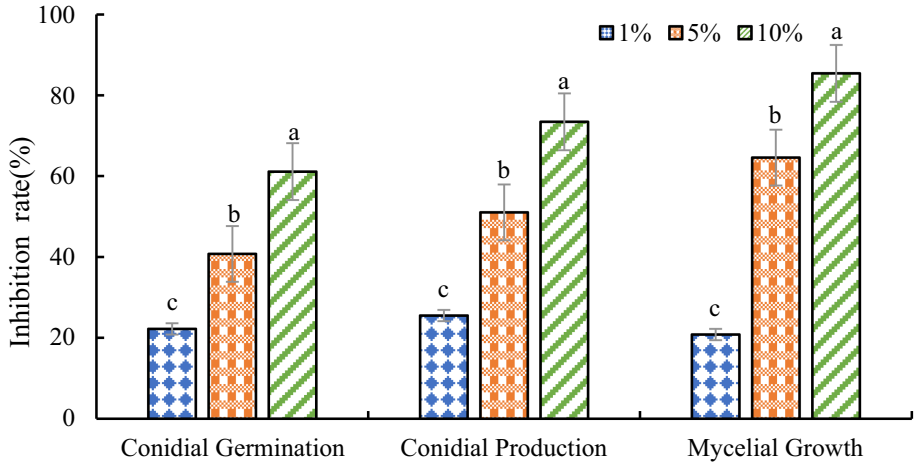

FIGURE 4
Effect of BVE7 filtrate on conidial germination, production and mycelial growth of *Fusarium oxysporum*. BVE7 filtrate was applied at concentrations of 1, 5, and 10%. Error bars indicate standard errors of the mean of two repeated experiments. Different letters above the bars indicate a significant difference within each group (i.e., conidial germination, conidial production, and mycelial growth) as determined by Duncan's multiple range test ($p < 0.05$).

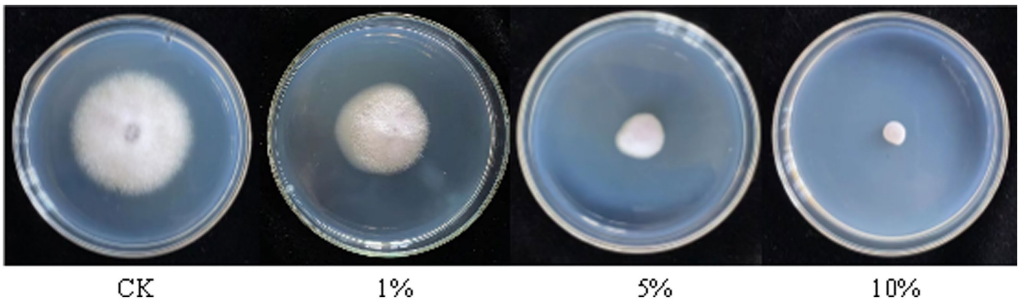

FIGURE 5
Effect of sterile fermented broth from BVE7 on *Fusarium oxysporum* mycelial growth on the fifth day after inoculation.

3.6. Effects of BVE7 treatment on the activities of defense enzymes in soybean root tissues

The efficacy of five major defense-associated enzymes in soybean roots treated with BVE7 was evaluated. The results showed that that CAT, SOD, and PAL activities exhibited an initial increase within 24 to 48 h, followed by a subsequent decline. Notably, treatment with BVE7 resulted in significantly higher activity levels than those observed in the control group (Figures 8A–C). Within 96 h, POD demonstrated a consistent upward trend, surpassing that of the control group by a significant margin (Figure 8D). MDA demonstrated slight fluctuations over a span of 96 h, yet remained significantly lower than the control group (Figure 8E).

In conclusion, soybean root treated by BVE7 activated the defense enzyme system to improve the disease-resistance.

4. Discussion

SRR, caused by *Fusarium oxysporum*, is the most important soil-borne disease in various soybean growing regions around the world, seriously affecting the yield and quality of soybeans. The Northeast Black Soil Region in China is one of the "Four Great Black Soil Regions of the World" and the "Three Great Cold Region Black Soil Regions." The climate characteristics of this region are also one of the important reasons for the serious occurrence of SRR. At the same time, the cold environment results in significant differences in microbial species and biological control compared to other regions. Therefore, this study, based on isolation and application under cold conditions, has greater practical value for the prevention and control of SRR in the northern cold regions.

Biological control has attracted extensive attention due to its safety, environmental friendliness, and sustainability (Wei et al., 2023). Most of the *Bacillus* spp. reported as effective biocontrol agents have been isolated from the rhizosphere, and occasionally from the phyllosphere, and are classified as members of the *B. subtilis* complex (Cawoy et al., 2011), which form populations on plant tissues and can colonize roots of different monocot and dicot plant species (Fan et al., 2011). Therefore, this study obtained a soil-isolated strain *B. velezensis* BVE7, which a good antagonistic effect on the dominant strain *F. oxysporum* causing SRR and also had a good broad-spectrum against various pathogens causing SRR. *B. velezensis* has been widely

10.3389/fmicb.2023.1275986

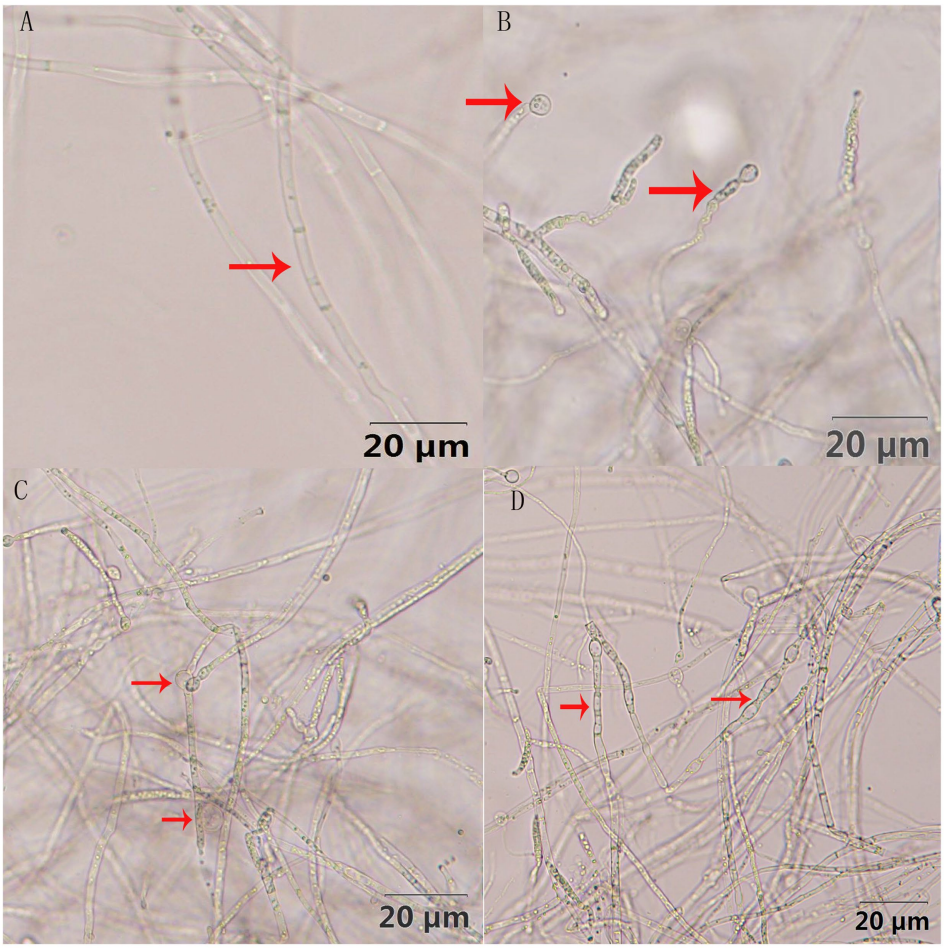

FIGURE 6
Effect of BVE7 filtrate on the mycelial morphology of *Fusarium oxysporum* (at a magnification of 400x). **(A)**, Non-treated control; **(B–D)** denote different concentrations (1, 5 and 10%, respectively) of treatment.

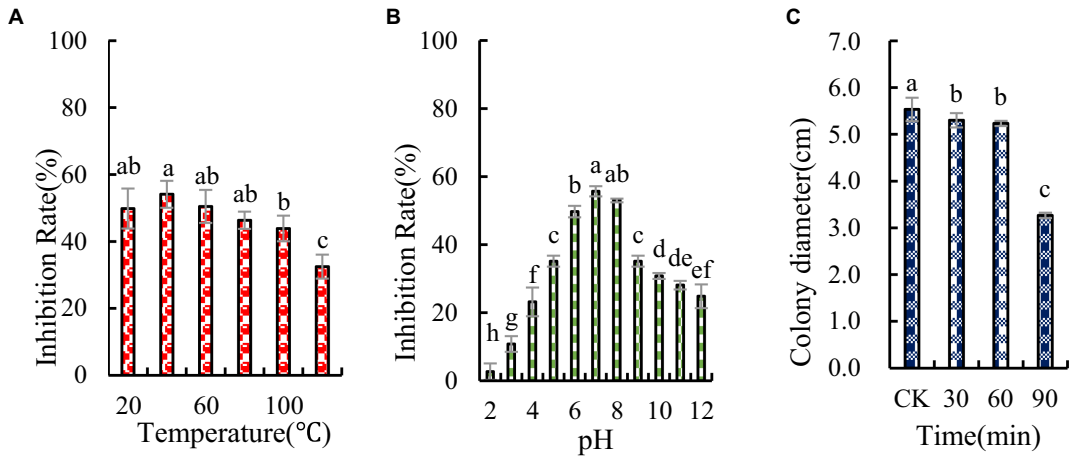

FIGURE 7
Stability of antifungal compounds in BVE7 under varied temperature regimes **(A)**, pH values **(B)**, and durations of ultraviolet exposure **(C)**. Error bars indicate standard errors of the means of two repeated experiments. CK was not exposed to UV. Different letters above the bars indicate significant difference within each treatment group (i.e., temperature, pH value, and ultraviolet treatment time) according to Duncan's multiple range test ($p < 0.05$).

TABLE 3 Evaluation of the efficacy of biological bacteria BVE7 suspension preventing soybean root rot caused by *Fusarium oxysporum* in pot experiments.

No.		Treatment	Disease index (%)[a]	Disease reduction (%)
1	i	Ck	0.0 ± 0.0e	–
	ii	*F. oxysporum* only	70.8 ± 2.9a	–
	iii	BVE7 suspension (0.5 mL/plant)	22.2 ± 1.2 b	68.3
	iv	BVE7 suspension (1 mL/plant)	20.1 ± 1.0c	71.2
	v	BVE7 suspension (1.5 mL/plant)	17.4 ± 1.3d	75.1
	vi	43% prochloraz(0.14 mg/mL)	18.2 ± 1.1d	74.0
2	i	Ck	0.0 ± 0.0e	–
	ii	*F. oxysporum* only	68.9 ± 1.8a	–
	iii	BVE7 suspension (0.5 mL/plant)	21.6 ± 0.9b	68.7
	iv	BVE7 suspension (1 mL/plant)	18.4 ± 1.1c	73.3
	v	BVE7 suspension (1.5 mL/plant)	16.2 ± 0.9d	76.5
	vi	43% prochloraz(0.14 mg/mL)	16.8 ± 1.2d	75.6

[a]Values in the column indicate Mean ± standard error (SE).
Values followed by different letters were significantly different according to Duncan's multiple range tests ($p < 0.05$).

used in the prevention and control of soil borne diseases in crops, including *B. velezensis* against *F. oxysporum* causing *Panax ginseng* root rot (Wei et al., 2023), *F. oxysproum* caused strawberry fusarium wilt (Hong et al., 2022), *F. oxysproum* caused root rot in *Polygonatum cyrtonema* (Chi et al., 2019), late blight of potato caused by *Phytophthora infestans* (Mahendra et al., 2022). Therefore, the application value of *B. velezensis* BVE7 in controlling soil-borne SRR is significant.

In this study, we discovered that the BVE7 sterile filtrate at a 10% concentration effectively inhibited the spore germination, production, and mycelial growth of *F. oxysporum*, with rates of 61.11, 73.44, and 85.42%, respectively, while also inducing hyphal malformations.

Cuellar-Gaviria et al. (2021) demonstrated that *B. tequilensis* EA-CB0015 had the capacity to colonize banana leaf surfaces and produce lipopeptides that could significantly reduce the severity of black sigatoka disease. Wu et al. (2014) determined that both the fermentation broth and cell suspension of *B. amyloliquefaciens* NJZJSB3 were capable of fully protecting detached leaves of canola (*Brassica napus* L.) from *Sclerotinia sclerotiorum* infection, while also exhibiting effective antifugal properties through their toluene, phenol, and benzothiazole volatiles. Wei et al. (2023) inferred that *B. velezensis* YW17 inhibited *F. oxysporum* by secreting antifungal lipopeptides, proteins, and volatile substances, thereby indirectly protecting ginseng from pathogenic fungal infections. Furthermore, *B. amyloliquefaciens* FZB42, reclassified as *B. velezensis*, produced surfactin, fengycin, and bacillomycin D in the lettuce rhizosphere, enhancing the lettuce's defense response against fungal pathogens (Chowdhury et al., 2015). Tahir et al. (2017) found that the volatile organic compounds (VOCs) produced by *B. subtilis* SYST2 significantly inhibited the growth and spore germination of plant fungal pathogens. Myo et al. (2019) found that *B. velezensis* NKG-2 produced VOCs that negatively impacted the growth of several plant fungal pathogens, including *Fusarium* spp., *Botrytis cinerea*, and *Alternaria alternata*. Some VOCs produced by BCAs could also promote plant growth and induce plant systemic resistance (Gao et al., 2017; Wu et al., 2019). *B. amyloliquefaciens* FZB42 exhibited antagonistic interactions with *F. graminearum*, a plant-pathogenic fungus that threatened the production and quality of wheat and barley globally (Gu et al., 2017). Among these, bacillomycin-D and fengycin were found to effectively inhibit the growth of *F. oxysporum* (Koumoutsi et al., 2004) and induce morphological changes in the plasma membranes and cell walls of *F. graminearum* hyphae and conidia (Gu et al., 2017). Culture filtrates from two strains of *B. velezensis* CE 100 not only induced abnormal mycelial development with reduction in pigment, but also caused hyphal deformations with swelling and bulging of the fungal pathogen. In addition, an antifungal dipeptide [cyclo(prolyl-valyl)], isolated from the culture of CE 100, exhibited concentration-dependent inhibition of conidial germination in *F. oxysporum* f. sp. *Lycopersici* and prolonged incubation periods, which resulted in irregular hyphal morphologies with swollen septa and disorganized cell contents in treatments with the dipeptide (Hwang et al., 2022). These findings are consistent with our research outcomes and indicate the need for future isolation and identification of antifungal compounds. Additionally, we will conduct further analysis on the fungicidal agents found in BVE7. The results of this study will provide a theoretical foundation for the development of more efficient, safe, and reliable biological agents.

Bacteria inhabiting the rhizosphere, which can colonize plant roots and confer advantageous outcomes on plant growth, are known as plant growth-promoting rhizobacteria (PGPR) (Karthikeyan et al., 2010). The colonization of the rhizosphere by PGPR enhances their ability to promote plant growth and health. PGPR possess the potential to promote plant growth, enhance legume plant nodulation with *Rhizobium* spp., and inhibit the growth of plant pathogens. Rhizobial inoculants have been utilized for disease management in peanut caused by *A. flavus* or *A. niger* (Ahmad et al., 2008; Moretti et al., 2008). These PGPR have the ability to synthesize a diverse array of antibiotics which are commonly linked to their efficacy in inhibiting the growth of plant pathogens. Meanwhile, a number of PGPRs are capable of producing enzymes, including chitinases, cellulases, glucanases, proteases, and lipases, which can hydrolyze portions of the cell walls of various pathogenic fungi (Remans et al., 2008; Majeed et al., 2015). Within the rhizosphere microbial communities, the predominant PGPR

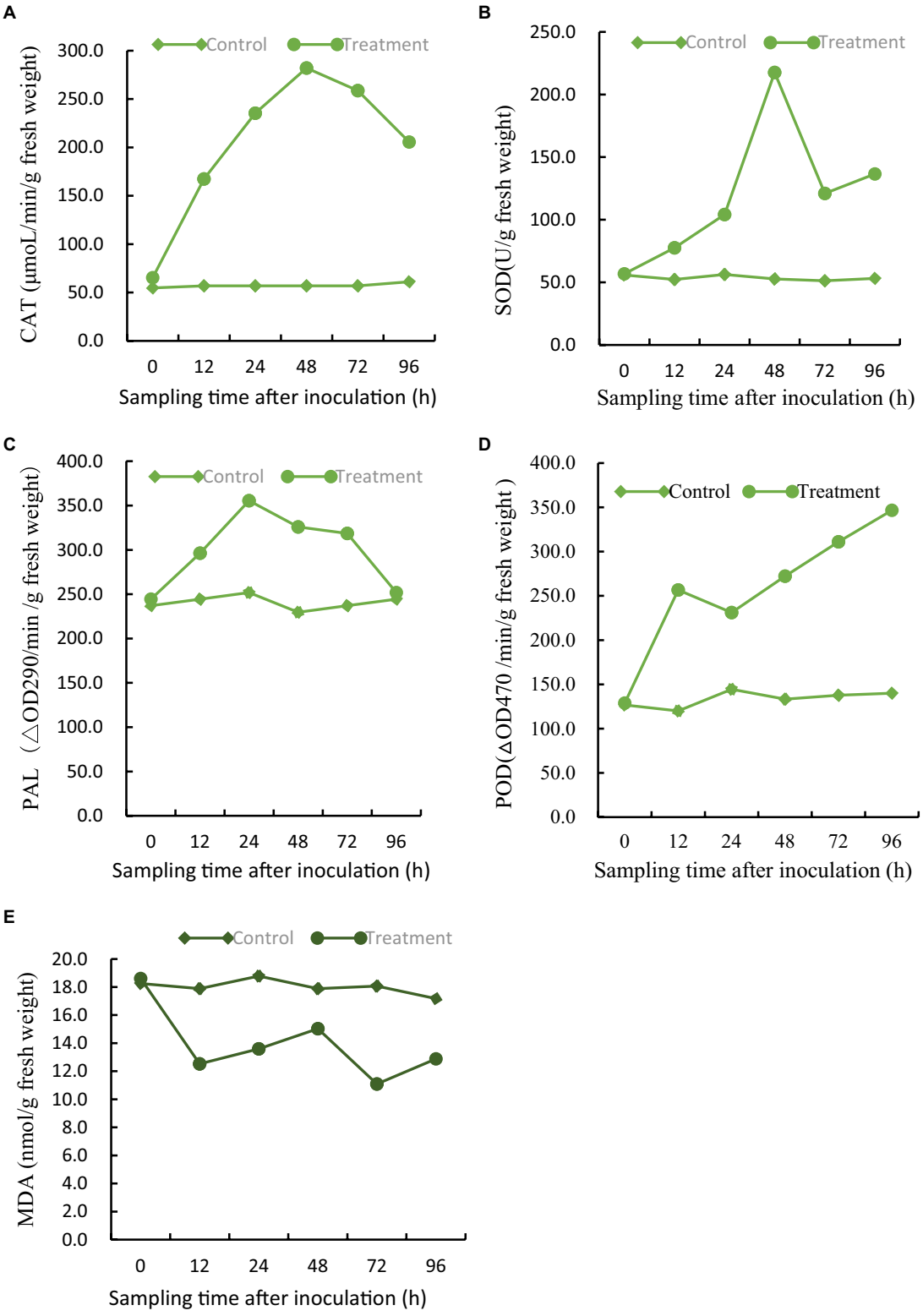

FIGURE 8
Effect of BVE7 on **(A)**, catalase (CAT), **(B)**, superoxide dismutase (SOD), **(C)**, phenylalanine ammonia-lyase (PAL), **(D),** peroxidase (POD), **(E)**, malondialdehyde (MDA). Two treatments with 3 replicates were included: **i**, 3mL of sterile water as a control; **ii**, 1.5mL suspension ($1x10^8$ CFU/mL) of BVE7/each plant. Error bars indicate standard errors of the means of two repeated experiments. Different letters above the bars indicate significant differences (p <0.05).

strains require investigation to determine their mechanisms for promoting growth, which can subsequently be utilized to develop and enhance related agricultural products (Wang et al., 2022). *B. velezensis* L-1 caused abnormal growth of the *Botryosphaeria berengeriana* mycelium, inciting defense-related enzyme expression in pears. Its inhibitory percentage of pear ring rot was observed to

be 76.55% after 11 days post inoculation (Sun et al., 2017). Gao et al. (2017) found that *B. velezensis* provided protection to tomato plants against fungal pathogens, such as *Alternaria solani* and *Botrytis cinerea*. The study showed that BVE7 significantly reduced the disease index of SRR, exhibiting a control efficacy of over 75% at a bacterial suspension of 1.5 mL/plant in the pot experiments. Moreover, BVE7 aided in improving the activities of CAT, PAL, POD, and SOD while concurrently reducing MDA activity. Multiple studies have demonstrated that elevated levels of ROS-scavenging enzymes, antioxidant enzymes, and defense enzymes are indicative of increased disease resistance (Warabieda et al., 2020). Augmented levels of POD and PALserve to protect plant cells against pathogenic infection (Zhang et al., 2016; Zhu et al., 2021). CAT is considered an important antioxidant enzyme that prevents cellular damage by the action of free radicals(Gebicka and Krych-Madej, 2019). SOD is a crucial cellular antioxidant enzyme that converts superoxide free radicals into oxygen and hydrogen peroxide (H_2O_2), thereby protecting cells from oxidative damage (Singh, 2022). Meanwhile, MDA, a widely-used indicator of oxidative stress, provides insights into the degree of lipid peroxidation in plant membranes. Therefore, the BVE7 is able to effectively enhance the level of defense enzymes in soybean roots, resisting the invasion of Fusarium oxysporum to protect the roots and mitigate the severity of root rot.

Therefore, we conducted a thorough assessment of BVE7's efficacy in managing SRR, indicating its potential utility as a means of controlling SRR in soybean cultivation.

5. Conclusion

In this study, a soil-isolated strain BVE7 was identified as *B. velezensis*, which exhibited broad-spectrum activity against various pathogens responsible for SRR. The BVE7 sterile filtrate, at a concentration of 10%, demonstrated significant antifungal activity, effectively inhibiting the conidial germination, production, and mycelial growth of *F. oxysporum* by 61.11, 73.44, and 85.42%, respectively, leading to hyphal malformations. The antifungal compound produced by BVE7 showed adaptability to a normal environment. In a pot experiment, the BVE7 suspension effectively controlled SRR, with the highest control efficiency of 75.13%. Furthermore, BVE7 can effectively stimulate the activation of soybean root's plant protection defense enzymes to reduce the damage caused by fungi and the severity of SRR. In the next step, we will conduct in-depth research on the antimicrobial substances in BVE7 and longer growth stage test instead of just the seedling stage, aiming to provide materials for the development of new biocontrol agents against fungi causing SRR and strengthen applied research.

Data availability statement

The datasets presented in this study can be found in online repositories. The names of the repository/repositories and accession number(s) can be found in the article/supplementary material.

Author contributions

LS: Writing – original draft, Resources, Validation. WW: Writing – original draft, Data curation, Formal analysis, Investigation. XZ: Formal analysis, Writing – original draft, Methodology, Software. ZG: Formal analysis, Writing – original draft, Supervision, Validation. SC: Writing – original draft, Data curation, Investigation, Methodology. SW: Writing – original draft, Formal analysis, Funding acquisition, Resources. YL: Writing – original draft, Writing – review & editing.

Funding

The author(s) declare financial support was received for the research, authorship, and/or publication of this article. This study was supported by China Agriculture Research System of MOF and MARA (CARS04), National Key R&D Program of China MOST (2021YFD1500300), Key Scientific and Technological Project of Heilongjiang Province of China (2021ZXJ05B011), Water Resources Management Program for Cooperation between China and the United Nations Development Programme-Demonstration Project for Promoting Water Resources Protection and Sustainable Agricultural Development in Black Soil Areas (CPR/21/401), Heilongjiang Provincial Natural Science Foundation of China (ZD2023C001).

Conflict of interest

The authors declare that the research was conducted in the absence of any commercial or financial relationships that could be construed as a potential conflict of interest.

Publisher's note

References

Ahmad, R., Arshad, M., Khalid, A., and Zahir, Z. A. (2008). Effectiveness of organic-/bio-fertilizer supplemented with chemical fertilizers for improving soil water retention, aggregate stability, growth and nutrient uptake of maize (*Zea mays* L.). *J. Sustain. Agr.* 31, 57–77. doi: 10.1300/J064v31n04_05

Amin, M., Rakhisi, Z., and Ahmady, A. Z. (2015). Isolation and identification of bacillus species from soil and evaluation of their antibacterial properties. *Avicenna J. Clin. Microbiol. Infect.* 2:23233. doi: 10.17795/ajcmi-23233

Bienapfl, J. C., Malvick, D. K., and Percich, J. A. (2010). First report of fusarium redolens causing root rot of soybean in Minnesota. *Plant Dis.* 94:1069. doi: 10.1094/PDIS-94-8-1069B

Birber, B., Nueske, J., Ritzau, M., and Grafe, U. (1998). Alnumycin, a new naphthoquinone antibiotic produced by an endophytic Streptomyces sp. *J. Antibiot.* 51, 381–382. doi: 10.7164/antibiotics.51.381

Buchanan, R. E. (1984). *Berger bacterial identification manual. 8th* ed. Beijing: Science Press.

Buhre, C., and Kluth, C. (2009). Integrated control of root and crown rot in sugar beet: combined effects of cultivar, crop rotation, and soil tillage. *Plant Dis.* 93, 155–161. doi: 10.1094/PDIS-93-2-0155

Cawoy, H., Bettiol, W., Fickers, P., and Ongena, M. (2011). Pesticides in the modern world: bacillus-based biological control of plant diseases. *Frbsf Econ. Lett.* 2, 140–158. doi: 10.1177/2158244012441940

Chang, K. F., Hwang, S. F., Conner, R. L., Ahmed, H. U., Zhou, Q., Turnbull, G. D., et al. (2015). First report of fusarium proliferatum causing root rot in soybean (*Glycine max* L.) in Canada. *Crop Prot.* 67, 52–58. doi: 10.1016/j.cropro.2014.09.020

Chi, H. R., Zhang, Y. H., and Zeng, X. (2019). Isolation and identification of antagonistic endophytic *Bacillus velezensis* from Polygonatumcyrtonema Hua and analysis of its antimicrobial and growth-promoting activity. *Plant Prot.* 45, 122–131. doi: 10.16688/j.zwbh.2018337

Chowdhury, S. P., Uhl, J., Grosch, R., Alquéres, S., Pittroff, S., Dietel, K., et al. (2015). Cyclic lipopeptides of *Bacillus amyloliquefaciens* subsp. plantarum colonizing the lettuce rhizosphere enhance plant defense responses toward the bottom rot pathogen Rhizoctonia solani. *Mol. Plant Microbe. Interact.* 28, 984–995. doi: 10.1094/MPMI-03-15-0066-R

Cruz Jimenez, D. R., Ellis, M. L., Munkvold, G. P., and Leandro, L. F. S. (2018). Isolate–cultivar interactions, in vitro growth, and fungicide sensitivity ofFusarium oxysporumIsolates causing seedling disease on soybean. *Plant Dis.* 102, 1928–1937. doi: 10.1094/PDIS-03-17-0380-RE

Cuellar-Gaviria, T. Z., González-Jaramillo, L. M., and Villegas-Escobar, V. (2021). Role of *Bacillus tequilensis* EA-CB0015 cells and lipopeptides in the biological control of black Sigatoka disease. *Biol. Control* 155:104523. doi: 10.1016/j.biocontrol.2020.104523

Detranaltes, C., Jones, C. R., and Cai, G. (2021). First report of fusarium fujikuroi causing root rot and seedling elongation of soybean in Indiana. *Plant Dis.* 105:3762. doi: 10.1094/PDIS-03-21-0570-PDN

Dong, X. Z., and Cai, M. Y. (2001). *Handbook of systematic identification of common bacteria*. Beijing: Science Press.

Dorrance, A., McClure, S., and Martin, S. (2003). Effect of partial resistance on Phytophthora stem rot incidence and yield of soybean in Ohio. *Plant Dis.* 87, 308–312. doi: 10.1094/PDIS.2003.87.3.308

Ellis, M., Díaz Arias, M. M., Jimenez, D. R. C., Munkvold, G. P., and Leandro, L. F. (2013). First report of fusarium commune causing damping-off, seed rot, and seedling root rot on soybean (*Glycine max*) in the United States. *Plant Dis.* 97:284. doi: 10.1094/PDIS-07-12-0644-PDN

Etesami, H., Jeong, B. R., and Glick, B. R. (2023). Biocontrol of plant diseases by bacillus spp. *Physiol. Mol. Plant Pathol.* 126:102048. doi: 10.1016/j.pmpp.2023.102048

Faheem, M., Raza, W., Zhong, W., Nan, Z., Shen, Q., and Xu, Y. (2015). Evaluation of the biocontrol potential of *Streptomyces goshikiensis* YCXU against fusarium oxysporum f. sp. niveum. *Biol. Control* 81, 101–110. doi: 10.1016/j.biocontrol.2014.11.012

Fan, B., Chen, X. H., Budiharjo, A., Bleiss, W., Vater, J., and Borriss, R. (2011). Efficient colonization of plant roots by the plant growth promoting bacterium *Bacillus amyloliquefaciens* FZB42, engineered to express green fluorescent protein. *J. Biotechnol.* 151, 303–311. doi: 10.1016/j.jbiotec.2010.12.022

Fira, D., Dimkić, I., Berić, T., Lozo, J., and Stanković, S. (2018). Biological control of plant pathogens by bacillus species. *J. Biotechnol.* 285, 44–55. doi: 10.1016/j.jbiotec.2018.07.044

Gao, Z., Zhang, B., Liu, H., Han, J., and Zhang, Y. (2017). Identification of endophytic *Bacillus velezensis* ZSY-1 strain and antifungal activity of its volatile compounds against Alternaria solani and Botrytis cinerea. *Biol. Control* 105, 27–39. doi: 10.1016/j.biocontrol.2016.11.007

Gebicka, L., and Krych-Madej, J. (2019). The role of catalases in the prevention/promotion of oxidative stress. *J. Inorg. Biochem.* 197:110699. doi: 10.1016/j.jinorgbio.2019.110699

Gu, Q., Yang, Y., Yuan, Q., Shi, G., Wu, L., Lou, Z., et al. (2017). Bacillomycin D produced by *Bacillus amyloliquefaciens* is involved in the antagonistic interaction with the plant-pathogenic fungus fusarium graminearum. *Appl. Environ. Microbiol.* 83, 1–17. doi: 10.1128/AEM.01075-17

Han, S., Chen, J., Zhao, Y., Cai, H., and Guo, C. (2021). *Bacillus subtilis* HSY21 can reduce soybean root rot and inhibit the expression of genes related to the pathogenicity of fusarium oxysporum. *Pestic. Biochem. Physiol.* 178:104916. doi: 10.1016/j.pestbp.2021.104916

Hong, S., Kim, T. Y., Won, S. J., Moon, J. H., Ajuna, H. B., Kim, K. Y., et al. (2022). Control of fungal diseases and fruit yield improvement of strawberry using *Bacillus velezensis* CE 100. *Microorganisms* 10:365. doi: 10.3390/microorganisms10020365

Hu, Y. F., You, J., Li, C. J., Williamson, V. M., and Wang, C. L. (2016). Ethylene response pathway modulates attractiveness of plant roots to soybean cyst nematode *Heterodera glycines*. *Sci. Rep.* 7:41282. doi: 10.1038/srep41282

Huang, J., Wei, Z., Tan, S., Mei, X., Yin, S., Shen, Q., et al. (2013). The rhizosphere soil of diseased tomato plants as a source for novel microorganisms to control bacterial wilt. *Appl. Soil Ecol.* 72, 79–84. doi: 10.1016/j.apsoil.2013.05.017

Hwang, S. H., Chaw, E. H. M., Jun, S. N., Woon, S. B., Jeong-Yong, C., and Kil, Y. K. (2022). Efficiency and mechanisms of action of pelletized compost loaded with *Bacillus velezensis* CE 100 for controlling tomato fusarium wilt. *Biol. Control* 176:105088. doi: 10.1016/j.biocontrol.2022.105088

Janvier, C., Villeneuve, F., Alabouvette, C., Edel-Hermann, C., Mateille, T., and Steinberg, C. (2007). Soil health through soil disease suppression: which strategy from descriptors to indicators? *Soil biol. Biochemist* 39, 1–23. doi: 10.1016/j.soilbio.2006.07.001

Karthikeyan, B., Joe, M. M., Jaleel, M. M., and Deiveekasundaram, M. (2010). Effect of root inoculation with plant growth promoting rhizobacteria (PGPR) on plant growth, alkaloid content and nutrient control of *Catharanthus roseus* (L.) G. Don. *Natura Croat.* 19, 205–212.

Koumoutsi, A., Chen, X. H., Henne, A., Liesegang, H., Hitzeroth, G., Franke, P., et al. (2004). Structural and functional characterization of gene clusters directing nonribosomal synthesis of bioactive cyclic lipopeptides in *Bacillus amyloliquefaciens* strain FZB42. *J. Bacteriol.* 186, 1084–1096. doi: 10.1128/JB.186.4.1084-1096.2004

Li, Y. G., Cai, Y. N., Liang, Y. B., Ji, P. S., and Xu, L. K. (2020). Assessment of antifungal activities of a biocontrol bacterium BA17 for managing postharvest gray mold of green bean caused by Botrytis cinerea. *Postharvest Biol. Technol.* 161:111086. doi: 10.1016/j.postharvbio.2019.111086

Li, C. G., Li, X. M., Kong, W. D., Wu, Y., and Wang, J. G. (2010). Effect of monoculture soybean on soil microbial community in the Northeast China. *Plant Soil* 330, 423–433. doi: 10.1007/s11104-009-0216-6

Li, Y. G., Zhao, T. X., HoangHua, G. K., Xu, L. K., Liu, J. X., Li, S. X., et al. (2018). Pathogenicity and genetic diversity of fusarium oxysporum causing soybean root rot in Northeast China. *J. Agric. Sci.* 10, 13–23. doi: 10.5539/jas.v10n5p13

Liu, X., Jiang, X., He, X., Zhao, W., Cao, Y., Guo, T., et al. (2019). Phosphate-solubilizing pseudomonas sp. strain P34-L promotes wheat growth by colonizing the wheat rhizosphere and improving the wheat root system and soil phosphorus nutritional status. *J. Plant Growth Regul.* 38, 1314–1324. doi: 10.1007/s00344-019-09935-8

Mahendra, K., Nakkeeran, S., Saranya, N., Janani, R., Malathi, V. G., Saleh, A., et al. (2022). Pan-genome analysis and molecular docking unveil the biocontrol potential of *Bacillus velezensis* VB7 against *Phytophthora infestans*. *Microbiol. Res.* 268:127277. doi: 10.1016/j.micres.2022.127277

Majeed, A., Abbasi, M. K., Hameed, S., Imran, A., and Rahim, N. (2015). Isolation and char-acterization of plant growth-promoting rhizobacteria from wheat rhizosphere and their effect on plant growth promotion. *Front. Microbiol.* 6:198. doi: 10.3389/fmicb.2015.00198

Mazzola, M., and Freilich, S. (2017). Prospects for biological soil borne disease control: application of indigenous versus synthetic microbiomes. *Phytopathology* 107, 256–263. doi: 10.1094/PHYTO-09-16-0330-RVW

Moretti, G., Pasquini, M., Mandarelli, G., Tarsitani, L., and Biondi, M. (2008). What every psychiatrist should know about PANDAS: a review. *Clin. Pract. Epidemiol. Ment. Health*, 18495013. doi: 10.1186/1745-0179-4-13

Myo, E. M., Liu, B., Ma, J., Shi, L., Jiang, M., Zhang, K., et al. (2019). Evaluation of *Bacillus velezensis* NKG-2 for bio-control activities against fungal diseases and potential plant growth promotion. *Biol. Control* 134, 23–31. doi: 10.1016/j.biocontrol.2019.03.017

Naqvi, S. A. M. H. (2005). Efficacy and mobility of fungicides used to manage root rot (Phytophthora nicotianae) in citrus soils. *J. Mycol. Plant Pathol.* 35, 295–297.

Nei, M., and Kumar, S. (2000). *Molecular evolution and Phylogenetics*. Oxford University Press, Oxford, UK. pp, 333.

Nelson, B. D., Hartman, G. L., Sinclair, J. B., and Rupe, J. C. (1999). "Fusarium blight or wilt, root rot, and pod and collar rot" in *Compendium of soybean diseases*. *4th* ed (St. Paul, MN: APS Press), 35–36.

Radhakrishnan, R., Hashem, A., and Abd Allah, E. F. (2017). Bacillus, a biological tool for crop improvement through bio-molecular changes in adverse environments. *Front. Physiol.* 8:667. doi: 10.3389/fphys.2017.00667

Raza, W., Wei, Z., Ling, N., Huang, Q. W., and Shen, Q. R. (2019). Effect of organic fertilizers prepared from organic waste materials on the production of antibacterial volatile organic compounds by two biocontrol Bacillus amyloliquefaciens strains. *J. Biotechnol.* 227, 43–53. doi: 10.1016/j.jbiotec.2016.04.014

Remans, R., Beebe, S., Blair, M., Manrique, G., Tovar, E., Rao, I., et al. (2008). Physiological and genetic analysis of root responsiveness to auxin-producing plant growth-promoting bacteria in common bean (*Phaseolus vulgaris* L.). *Plant Soil* 302, 149–161. doi: 10.1007/s11104-007-9462-7

Santoyo, G., Orozco-Mosqueda, M. D. C., and Govindappa, M. (2012). Mechanisms of biocontrol and plant growth-promoting activity in soil bacterial species of bacillus and pseudomonas: a review. *Biocontrol Sci. Tech.* 22, 855–872. doi: 10.1080/09583157.2012.694413

Saravanakumar, K., Li, Y., Yu, C., Wang, Q. Q., Wang, M., Sun, J., et al. (2017). Effect of Trichoderma harzianum on maize rhizosphere microbiome and biocontrol of fusarium stalk rot. *Sci. Rep.* 7, 1–13. doi: 10.1038/s41598-017-01680-w

Schaad, N. W., Jones, J. B., and Chun, W. (2001). *Laboratory guide for identification of plant pathogenic bacteria*, *3rd* American Phytopathological Society Press. St. Paul, MN, USA.

Shafi, J., Tian, H., and Ji, M. (2017). Bacillus species as versatile weapons for plant pathogens: a review. *Biotechnol. Biotechnol. Equip.* 31, 446–459. doi: 10.1080/13102818.2017.1286950

Singh, D. (2022). Juggling with reactive oxygen species and antioxidant defense system – a coping mechanism under salt stress. *Plant Stress* 5:100093. doi: 10.1016/j.stress.2022.100093

Sun, P. P., Cui, J. C., Jia, X. H., and Wang, W. H. (2017). Isolation and characterization of *Bacillus amyloliquefaciens* L-1 for biocontrol of pear ring rot. *Hortic. Plant J.* 3, 183–189. doi: 10.1016/j.hpj.2017.10.004

Tahir, H. A., Gu, Q., Wu, H., Raza, W., Hanif, A., Wu, L., et al. (2017). Plant growth promotion by volatile organic compounds produced by *Bacillus subtilis* SYST2. *Front. Microbiol.* 8:171. doi: 10.3389/fmicb.2017.00171

Tanni, T., Datta, J., Hasan, R., Hossain, A., and Haque, M. (2016). Evaluation of botanical and chemical fungicides to control foot and root rot of chickpea. *Int. J. Plant Sci.* 12, 1–7. doi: 10.9734/IJPSS/2016/27918

Vardharajula, S., Zulfikar, A. S., Grover, M., Reddy, G., and Bandi, V. (2011). Drought-tolerant plant growth promoting bacillus spp.: effect on growth, osmolytes, and antioxidant status of maize under drought stress. *J. Plant Interact.* 6, 1–14. doi: 10.1080/17429145.2010.535178

Vezzani, F. M., and Mielniczuk, J. (2009). Uma visão sobre qualidade do solo. *Rev. Brasileira de Ciência do Solo* 33, 743–755. doi: 10.1590/S0100-06832009000400001

Wang, X. Q., Bi, X. F., Xie, X. F., Xing, Y. G., and Li, M. Y. (2020). Antibacterial effect of iturin a on strawberry spoilage mold. *Nat. Prod. Res.* 32, 1889–1895. doi: 10.16333/j.1001-6880.2020.11.012

Wang, D., Kurle, J. E., Estevez de Jensen, C., and Percich, J. A. (2004). Radiometric assessment of tillage and seed treatment effect on soybean root rot caused by fusarium spp. in central Minnesota. *Plant Soil* 258, 319–331. doi: 10.1023/B:PLSO.0000016561.58742.93

Wang, S., Li, X., Liu, C., Liu, L., Yang, F., Guo, Y., et al. (2021). First report of fusarium brachygibbosum causing root rot on soybean in Northeastern China. *Plant Dis.* 105:1560. doi: 10.1094/PDIS-05-20-0941-PDN

Wang, J. Z., Qu, F., Liang, J. Y., Yang, M. F., and Hu, X. H. (2022). *Bacillus velezensis* SX13 promoted cucumber growth and production by accelerating the absorption of nutrients and increasing plant photosynthetic metabolism. *Sci. Hortic.* 301:111151. doi: 10.1016/j.scienta.2022.111151

Warabieda, W., Markiewicz, M., and Wojcik, D. (2020). Mutual relations between jasmonicacid and acibenzolar-S-methyl in the induction of resistance to the two-spottedspider mite (Tetranychus urticae) in apple trees. *Exp. Appl. Acarol.* 82, 59–79. doi: 10.1007/s10493-020-00539-6

Wei, J. B., Zhao, J., Suo, M., Wu, H., Zhao, M., and Yang, H. Y. (2023). Biocontrol mechanisms of *Bacillus velezensis* against fusarium oxysporum from *Panax ginseng*. *Biol. Control* 182:105222. doi: 10.1016/j.biocontrol.2023.105222

Wu, Y., Yuan, J., Raza, W., Shen, Q., and Huang, Q. (2014). Biocontrol traits and antagonistic potential of *Bacillus amyloliquefaciens* strain NJZJSB3 against Sclerotinia sclerotiorum, a causal agent of canola stem rot. *J. Microbiol. Biotechnol.* 24, 1327–1336. doi: 10.4014/jmb.1402.02061

Wu, Y., Zhou, J., Li, C., and Ma, Y. (2019). Antifungal and plant growth promotion activity of volatile organic compounds produced by *Bacillus amyloliquefaciens*. *Microbiology* 8:e00813. doi: 10.1002/mbo3.813

Xu, F., Chen, Y., Cai, Y., Gu, F., and An, K. (2020). Distinct roles for bacterial and fungal communities during the curing of vanilla. *Front. Microbiol.* 11:2342. doi: 10.3389/fmicb.2020.552388

Yan, H., and Nelson, B. (2021). Effects of spore density and interaction with *Heterodera glycines* on soybean root rot caused by fusarium solani and F. tricinctum. *Plant Dis.* 105, 2426–2434. doi: 10.1094/PDIS-09-20-1944-RE

Yang, Z. H., Wu, X., Yang, Y. M., Qu, Y. W., Xu, J. R., Wu, D. P., et al. (2023). Identification of QTNs, QEIs interactions and genes for isoflavones in soybean seeds. *Ind. Crop. Prod.* 197:116631. doi: 10.1016/j.indcrop.2023.116631

Yuan, S. L., Liu, F., and Zhang, N. (2011). Toxicity assay of several chemical fungicides against pathogen of wheat root rot. *Chinese Agri. Sci. Bull.* 27, 273–276.

Zhang, S., Gao, Z., and Liu, H. (2000). Continuous cropping obstacle and rhizospheric microecology. III. Soil phenolic acids and their biological effect. *Chinese. J. Appl. Ecol.* 11, 741–744.

Zhang, J. X., Xue, A. G., Cober, E. R., Morr-son, M. J., Zhang, H. J., Zhang, S. Z., et al. (2013). Prevalence, pathogenicity and cultivar resistance of fusarium and Rhizoctonia species causing soybean root rot. *Can. J. Plant Sci.* 93, 221–236. doi: 10.4141/cjps2012-223

Zhang, J. X., Xue, A. G., and Tambong, J. T. (2009). Evaluation of seed and soil treatments with novel *Bacillus subtilis* strains for control of soybean root rot caused by fusarium oxysporum and F. graminearum. *Plant Dis.* 93, 1317–1323. doi: 10.1094/PDIS-93-12-1317

Zhang, Q., Yong, D., Zhang, Y., Shi, X., Li, B., Li, G., et al. (2016). *Streptomyces rochei* A-1 induces resistance and defense-related responses against Botryosphaeria dothidea in apple fruit during storage. *Postharvest Biol. Technol.* 115, 30–37. doi: 10.1016/j.postharvbio.2015.12.013

Zhao, W., Chi, Y. K., Cao, S., Wang, T., Zhang, L. Y., Ye, M. D., et al. (2020). Occurrence of root rot caused by fusarium fujikuroi on soybean (*Glycine max*) in the central eastern regions. *China. Plant Dis.* 104:981. doi: 10.1094/PDIS-03-19-0615-PDN

Zhu, Y., Wang, Q., Wang, Y., Xu, Y., Li, J., Zhao, S., et al. (2021). Combined transcriptomic and metabolomic analysis reveals the role of phenylpropanoid biosynthesis pathway in the salt tolerance process of Sophora alopecuroides. *Int. J. Mol. Sci.* 22:2399. doi: 10.3390/ijms22052399

Zitnick-Anderson, K., and Nelson, B. (2015). Identification and pathogenicity of Pythium on soybean in North Dakota. *Plant Dis.* 99, 31–38. doi: 10.1094/PDIS-02-14-0161-RE

frontiers | Frontiers in Microbiology

TYPE Original Research
PUBLISHED 30 October 2023
DOI 10.3389/fmicb.2023.1265435

OPEN ACCESS

EDITED BY
Yichao Shi,
Agriculture and Agri-Food Canada (AAFC), Canada

REVIEWED BY
Abdul Gafur,
SMF Corporate R&D Advisory Board, Indonesia
Diana Elena Aguirre,
Autonomous University of Nuevo León, Mexico

*CORRESPONDENCE
Ze-Yang Yu
✉ yzynxu@126.com

†These authors have contributed equally to this work and share first authorship

RECEIVED 22 July 2023
ACCEPTED 06 October 2023
PUBLISHED 30 October 2023

CITATION
Liu K, Zhang Y-Z, Du H-Y, Wang Z-Y, Gu P-W, Liu Z-H and Yu Z-Y (2023) Beneficial and biocontrol effects of *Trichoderma atroviride*, a dominant species in white birch rhizosphere soil.
Front. Microbiol. 14:1265435.
doi: 10.3389/fmicb.2023.1265435

Beneficial and biocontrol effects of *Trichoderma atroviride*, a dominant species in white birch rhizosphere soil

Kuo Liu[1†], Yu-Zhou Zhang[2†], Hua-Ying Du[1†], Zhi-Ying Wang[3], Pei-Wen Gu[1], Zhi-Hua Liu[3,4] and Ze-Yang Yu[1,3*]

[1]School of Agriculture, Ningxia University, Yinchuan, Ningxia, China, [2]Ningxia Forest Disease and Pest Control and Quarantine Station, Yinchuan, Ningxia, China, [3]School of Forestry, Northeast Forestry University, Harbin, Heilongjiang, China, [4]College of Forestry, Shenyang Agricultural University, Shenyang, Liaoning, China

White birch (*Betula platyphylla* Suk.) is a typical pioneer tree species that is important in forest restoration in northern China, Japan, and Korea. In the present study, 37 isolates were obtained from *B. platyphylla* rhizosphere soils in Heilongjiang Province; they were identified as *T. pleuroticola* (3 isolates), *T. virens* (2 isolates), *T. hamatum* (8 isolates), *T. atroviride* (21 isolates, dominant species) and *T. asperelloides* (3 isolates). Stress tolerance tests (salt, alkali, and nutritional stress that simulated saline alkali or barren soil) and confrontation assays (with four pathogens) were performed to determine which isolates had good biocontrol ability in barren soil; the results show that *T. atroviride* was outstanding. Then, in order to determine the effect of *T. atroviride* on plants and soil, *Gynura cusimbua* seeds were sown and treated with a *T. atroviride* spore suspension, as was unsown soil. The seedlings treated using *T. atroviride* had significantly greater height, stem diameter, soluble protein content, soluble sugar content, and malonaldehyde (MDA) content and their catalase (CAT) activity was also significantly increased. In addition, when the plants were inoculated with *Alternaria alternata*, the plants treated using *T. atroviride* had stronger CAT activity, significantly higher soluble protein content and soluble sugar content, and significantly lower MDA content, which indicates stronger resistance and less injury caused by the pathogen. In addition, *T. atroviride* not only increased the content of available nitrogen and available phosphorus in the soil, but also promoted *G. cusimbua* seedlings' absorption of available nitrogen and available phosphorus. Thus, the characteristics of *T. atroviride* may make it the main factor that helps *B. platyphylla* colonise cut-over lands. *T. atroviride*, a promising biocontrol candidate, can be used in agriculture and forestry.

KEYWORDS

***Trichoderma* identification, resistance induction, pioneer tree species, growth promotion, soil improvement**

1. Introduction

Trichoderma spp. are important biocontrol agents worldwide because they can inhibit the growth of pathogens, promote plant growth, and induce plant resistance (Poveda, 2021). The pathogen inhibition mechanisms of *Trichoderma* were found to be competition, antibiotism, and mycoparasitism, while the plant benefit mechanisms of *Trichoderma* were found to

be growth promotion and plant defence response induction (Poveda, 2021). Much research has reported the biocontrol functions of *Trichoderma*; one study found that *T. harzianum* and *T. viride* could suppress 15 strains of *Alternaria alternata* (Uniyal and Singh, 2017). *T. atroviride* isolated from wheat straw can effectively inhibit *Fusarium graminearum* and can produce xylanases linked to the colonisation of *F. graminearum* (Cabrera et al., 2020). In addition, potatoes treated with *T. asperellum* TaspHu1 grew better and had stronger resistance to *A. alternata* (Yu et al., 2021b). *T. virens* and *T. atroviride* promoted the formation of lateral roots in *Arabidopsis*, which resulted in improved nutrient uptake capacity and an increase in the biomass of the roots and shoots (López-Bucio et al., 2015). *T. atroviride* enhanced the resistance of *Populus*, as the leaves inoculated with pathogens showed smaller specks (Raghavendra and Newcombe, 2013).

However, the effect of biopesticides made from *Trichoderma* spp. is influenced by complicated environments, and efficiency loss caused by location, temperature, humidity, or nutrients is a common problem with biocontrol agents (Mukherjee et al., 2012). A good way to solve this problem is by continuously collecting and filtering robust *Trichoderma*, which may rely on natural mutation and natural selection. The collection of *Trichoderma* is performed globally, and 320 *Trichoderma* strains were isolated in fields and identified across 71 species (Braithwaite et al., 2017). Ten *Trichoderma* strains were isolated in *Juglans mandshurica* rhizosphere soil and identified as four species, out of which *T. asperellum* TaspHu1 showed outstanding biocontrol potential (Yu et al., 2021b).

Betula platyphylla, a typical pioneer tree species, is often the first to colonise cut-over lands and lands affected by forest fire or typhoon damage and forms its population below the layer of the coniferous belt in the forest vertical distribution. It is thought that this species plays an important role in the secondary succession process (Wu et al., 2002), which is also important in forest restoration. As one species of mycorrhizal fungi, *Trichoderma* may play an important role in protecting or promoting the growth of *B. platyphylla*, and when we need to plant white birch for forest restoration, the addition of some *Trichoderma* may significantly increase plant survival rates. Therefore, the investigation and collection of *Trichoderma* in *B. platyphylla* rhizosphere soil is necessary and useful for application in forest restoration or incult soil. In the present study, *Trichodema* strains were isolated from 13 *B. platyphylla* rhizosphere soil samples and identified. The biocontrol potential of these *Trichoderma* isolates was measured, including stress resistance, pathogen inhibition, growth promotion, and effect on soil. Based on these measurements, the *Trichoderma* distribution in *B. platyphylla* was roughly revealed, and the relevant strains for future use in forestry restoration were evaluated.

2. Materials and methods

2.1. Isolation of *Trichoderma*

Trichoderma fungi were isolated from 13 soil samples (each sample was approximately 100 g) of white birch rhizosphere soil (at a depth of 5–15 cm). Of these soil samples, 10 were collected from planted forest at the forest farm of Northeast Forestry University and three were collected from the natural forest of Maoer Mountain (126.63°E, 45.72°N). From these soil samples, five 5 g subsamples of each sample were dissolved in 100 mL of sterile water, shaken well using a muddler, and made into stock solution, which was diluted to four concentrations (1/10, 1/100, 1/1000, and 1/1000). Each concentration of the solution (200 μL) was plated onto potato dextrose agar medium (PDA medium) in a 9 cm Petri dish and cultured at 28°C for 24–96 h. During this period, the Petri dishes were observed every 24 h, and the *Trichoderma* colonies were transferred to a new PDA medium for purification culture (Zhou et al., 2019).

2.2. Morphological and molecular identification of *Trichoderma*

The purified *Trichoderma* were inoculated on a PDA plate medium and cultured in the dark for 7 days at 28°C to observe their macroscopic morphology; images of the colonies were obtained. Some PDA medium blocks (their length, width, and height were approximately 0.5 cm × 0.5 cm × 0.1 cm) were prepared using a sterile blade and placed on a glass slide under aseptic conditions. Then, the *Trichoderma* spores were inoculated on the PDA medium block and the aseptic coverslip was covered to make hyphae grow on the coverslip. The *Trichoderma* fungi were cultured in the dark at 28°C for 48–72 h, and the relative humidity was 60%. The hyphae were stained with a blue dye (biohao Biotechnology Co., Ltd., Beijing, China, Catalog No. C0710) to observe and record their morphology and that of their spores under a microscope (Leica DM750, Wetzlar, Germany). Morphological identification relied on the descriptions found in previous research (Yang, 2009, in Chinese).

One isolate in each species identified by morphology was randomly chosen for molecular identification. The purified *Trichoderma* was inoculated in potato dextrose (PD) liquid medium and shaken at 28°C at 180 rpm for 48 h. The mycelia were filtered and collected using eight layers of gauze for DNA extraction using a DNA extraction kit (OMEGA Biotek, Beijing, China). Then, the extracted DNA were used as a template to amplify the ITS (internal transcribed spacer) region and *tef1-α* (translation elongation factor-1α) region; the primers were designed with reference to previous studies (Dou et al., 2019), The PCR products were purified using a gel extraction kit (Promega, Madison, WI, USA, Kit No. A9281) and subjected to direct automated sequencing using fluorescent terminators using an ABI 377 Prism Sequencer (Sangon Biotech, Shanghai, China). The sequencing results were compared and identified using the website of the Center for Culture Collection of *Trichoderma* (CCTC), Shanghai Jiaotong University.[1] Other recommended reference *Trichoderma* gene sequences were selected from the database (Dou et al., 2019), and a phylogenetic tree was constructed using the maximum likelihood (ML) method, with 1,000 bootstrap replications in the MEGA 7.0 (Kumar et al., 2016) package. After identification, the sequences were submitted to Genbank.[2] The *Trichoderma* isolates that underwent molecular identification were subjected to further analyses.

2.3. Stress resistance and confrontation assay of *Trichoderma*

To investigate the tolerance of the *Trichoderma* isolates to a harsh environment (saline alkali soil or barren soil), a culture medium

1 http://mmit.china-cctc.org/action1.php
2 https://www.ncbi.nlm.nih.gov/genbank/

simulating a harsh environment was established. Salt stress, alkali stress, and nutrition stress experiments were created using a diluted PDA medium (diluted to 1/2, 1/4, 3/4, 1/8, 1/16, or zero, only made up of agar and water), a concentrated PDA medium (concentrated to 2-fold or 4-fold), a PDA medium to which was added NaCl (to generate final concentrations of 2, 4, 6, 8, and 10%, w/v, g/mL), or a PDA medium to which was added $NaHCO_3$ (to generate final concentrations of 0.1, 0.4, 0.7, 1, and 1.3%, w/v, g/mL). Then, 3 μL of spore suspension (10^6 spores/mL) was pipetted out and inoculated into the salt stress, alkali stress, and nutrition stress media, after which the Petri dishes were left to stand for 5–10 min and then sealed using parawax film. The *Trichoderma* were cultured at 28°C and the colony radii was measured using a ruler at 48 h.

In order to analyse the antagonism of the *Trichoderma* isolates, dual culture was performed between *Trichoderma* and phytopathogens on a PDA medium. Purified cultured *Trichoderma* and *Cytospora chrysosperma*, *Botrytis cinerea*, *A. alternata*, and *Fusarium oxysporum* were prepared as inocula. A 5 mm diameter mycelial disc of each *Trichoderma* isolate was added to the periphery of a new aseptic Petri dish; opposite this placement, a 5 mm diameter mycelial disc of the phytopathogen was positioned. Each dual culture was set up with three replicates. The plates were cultured for 12 days, and a modified resistance evaluation was performed based on a previously described protocol (Popiel et al., 2008), which used the following scoring system: +8 meant the antagonist had fully grown on the plate, completely covering the plate and the phytopathogen; +6 meant the antagonist occupied 85% of the plate's surface area; +4 meant the antagonist occupied 70% of the plate's surface area; and 0 meant the antagonist occupied 50% of the plate's surface area.

2.4. Influence of *Trichoderma atroviride* on *Gynura cusimbua*

A spore suspension of *T. atroviride* was prepared to a concentration of 10^7 spores/mL. Twenty seeds of *Gynura cusimbua* (bought from the Taobao online shopping platform[3]) were planted in each pot (size: L × W × H = 40 cm × 28 cm × 6 cm); for the treatment group, 800 mL of spore suspension was evenly poured into the soil before planting, while for the control group, 800 mL of water was evenly poured into the soil before planting. Three replicates were performed. The seedlings were cultivated under a 16 h light/8 h dark photoperiod (under a daylight lamp) and 40% relative humidity and watered every 10 days with 500 mL of additional water. The germination rates and germination times of the plants were recorded. At 30 days after seed sowing, the stem height and stem diameter were recorded, and the leaves of three randomly chosen seedlings were harvested and stored at −80°C for malondialdehyde (MDA), catalase (CAT) activity, soluble sugar content, and soluble protein content analyses (Jiancheng Bioengineering Institute, Nanjing, Jiangsu, China, Kit A003-1-2, Kit A00-1-1, Kit A145-1-1 and Kit A045-2-2).

Then, the 6–10 randomly chosen leaves of other plants in the control group and treatment group were pierced (4 times on each leaf) and inoculated with *A. alternata*, marked as C + A (control + *A. alternata*) and T + A (treatment + *A. alternata*). After 12 days, the morbidity was observed, and the MDA, CAT activity, soluble sugar content, and soluble protein content were also analysed.

Approximately 200 g of soil samples in the control group and treatment group were collected, marked as the P group (the soil in which *G. cusimbua* was planted) and T + P group (the soil watered with the spore suspension of *T. atroviride* in which *G. cusimbua* was planted), and stored at −20°C for further analysis.

2.5. Influence of *Trichoderma atroviride* on soil nutrition

Six pots (size: L × W × H = 40 cm × 28 cm × 6 cm) containing the same soil as that in the experiment above were prepared; for three of these, 800 mL of spore suspension of *T. atroviride* was evenly poured into the soil, while for the other three, 800 mL of water was evenly poured. The pots were placed under a 16 h light/8 h dark photoperiod (under a daylight lamp) and 40% relative humidity and watered every 10 d with 500 mL of additional water for 30 days (three times). Then, the soil samples (approximately 200 g) were collected, marked as the T group (the soil watered with the spore suspension of *T. atroviride*) and the CK group (the soil watered with water) and stored at −20°C for further analysis. The available nitrogen and available phosphorus of the soil in the P, T + P, T, and CK groups were analysed according to previous research (Bardgett et al., 2007; Zhou et al., 2020).

2.6. Statistical analysis

All experimental data were subjected to an analysis of variance (ANOVA) using SPSS software v19.0 (IBM Corp., Armonk, NY, USA). The statistical significance of the differences between the means was determined using Duncan's multiple-range tests and an independent-sample T test ($p < 0.05$).

3. Results

3.1. Morphological and molecular identification of *Trichoderma*

In total, 37 *Trichoderma* isolates were obtained from 13 soil samples, and 5 species were identified based on morphological comparison (Figure 1): *T. pleuroticola* (3 isolates), *T. virens* (2 isolates), *T. hamatum* (8 isolates), *T. atroviride* (21 isolates), and *T. asperellum* (3 isolates). One isolate was randomly selected from each *Trichoderma* species for further molecular identification. The ITS regions and *tef1-α* regions of these five *Trichoderma* isolates were amplified and sequenced. The sequences were by consulting the Center for Culture Collection of *Trichoderma* (CCTC), Shanghai Jiaotong University (see footnote 1). The alignment results show that most morphological identification was accurate, except for the *T. asperellum* sample, which was identified as *T. asperelloides* based on molecular characteristics. Phylogenetic trees were also constructed using the reference sequences recommended by the CCTC database (Figure 2); the results accompany the alignment results. Based on the above results, five species of *Trichoderma* were obtained: *T. pleuroticola*, *T. virens*,

3 https://www.taobao.com/

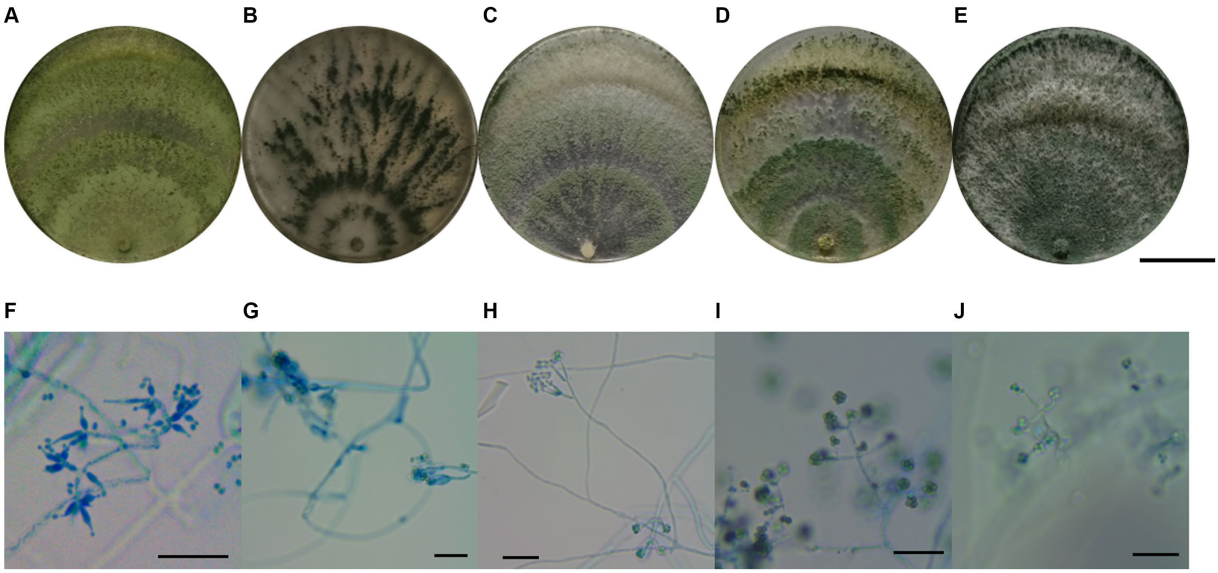

FIGURE 1
Morphology of *Trichoderma*. **(A)** Macro-morphology of *T. pleuroticola*. **(B)** Macro-morphology of *T. virens*. **(C)** Macro-morphology of *T. hamatum*. **(D)** Macro-morphology of *T. atroviride*. **(E)** Macro-morphology of *T. asperelloides*. **(F)** Micro-morphology of *T. pleuroticola*. **(G)** Micro-morphology of *T. virens*. **(H)** Micro-morphology of *T. hamatum*. **(I)** Micro-morphology of *T. atroviride*. **(J)** Micro-morphology of *T. asperelloides*. Ruler in **(A–E)** = 3 cm, ruler in **(F–J)** = 50 μm.

T. hamatum, *T. atroviride*, and *T. asperelloides*. The sequenced ITS and *tef1-α* sequences of the five *Trichoderma* isolates were submitted to Genbank (see footnote 2), and the accession numbers of these ITS sequences are MK377309 (*T. pleuroticola*), MK377310 (*T. virens*), MK377311 (*T. hamatum*), MK377312 (*T. atroviride*), and MK377313 (*T. asperelloides*). The accession numbers of the *tef1-α* sequences are OL547398 (*T. pleuroticola*), OL547399 (*T. virens*), OL547400 (*T. hamatum*), OL547401 (*T. atroviride*), and OL547402 (*T. asperelloides*). Among these isolated *Trichoderma*, the number of isolates of *T. atroviride* was the highest (21 isolates), accounting for 57% of the total isolated *Trichoderma*. *T. hamatum* followed with 8 isolates, accounting for 22% of the total. *T. asperelloides* and *T. pleuroticola* both had three isolates, accounting for 8% of the total. There were the least *T. virens* isolates, with two strains, accounting for 5% of the total (Figure 3).

3.2. Stress tolerance and pathogen inhibition of *Trichoderma* isolates

In this study, all five *Trichoderma* candidate strains for which molecular identification was performed could grow in the five concentrations of the salt stress medium, among which *T. asperelloides* grew better and had stronger salt stress adaptability, followed by *T. hamatum*, which also had relatively good salt stress tolerance. In the alkaline stress medium, *T. atroviride* could not grow when the alkali concentration reached 0.7% (weight/volume, g/mL), while *T. virens* grew slowly when the alkali concentration reached 1.3% (weight/volume, g/mL). *T. virens* and *T. pleuroticola* have better adaptability to alkali stress. In the media with different nutrient concentrations, *T. pleuroticola*, *T. virens*, and *T. asperelloides* grew better (Figure 4).

The confrontation assay shows that the five *Trichoderma* isolates spread in the Petri dish rapidly reacted to and had varying degrees of antagonistic responses against *F. oxysporum*, *A. alternata*, *B. cinerea*, and *C. chrysosperma* (Figure 5). Among them, *T. asperelloides* could not only inhibit the growth of the four pathogens, but also parasitised the tested pathogens, occupying the entire plate; thus, it had the highest evaluation score (Figure 5B). With the exception of *F. oxysporum*, the other three pathogens were also parasitised by *T. atroviride*, *T. pleuroticola*, and *T. virens* (Figure 5A); thus, those species also have relatively high evaluation scores. *T. hamatum* could only parasitise *C. chrysosperma* but could not parasitise the other three pathogens (Figure 5A).

3.3. Influences of *Trichoderma atroviride* on *Gynura cusimbua*

In the treatment group (T), the seed germination rate of the treatment group was 90% and the average germination time was 102.3 h, while in the control group, the germination rate was 80% and the average germination time was 105.2 h; this difference was not significant (Table 1). Thirty days later, we found that the seedlings in the treatment group had better growth than those in the control group (Figure 6). The average plant height of the plants in the treatment group was 4.60 cm, significantly higher than that (4.12 cm) of the control group ($p < 0.05$). Similarly, the average stem diameter of the plants in the treatment group (5.98 mm) was also significantly higher than that (5.04 mm) of the control group ($p < 0.05$, Table 1). After inoculation with *A. alternata*, the height and stem diameter of plants did not significantly change in the treatment group (T + A) and control group (C + A).

Further, some physiological indices were measured. For the treatment group, the MDA was 31.709 μmol/100 g, significantly higher than the MDA of the control group (16.13 μmol/100 g, $p < 0.05$). The soluble protein for the treatment group was 1,555.458 μg/g,

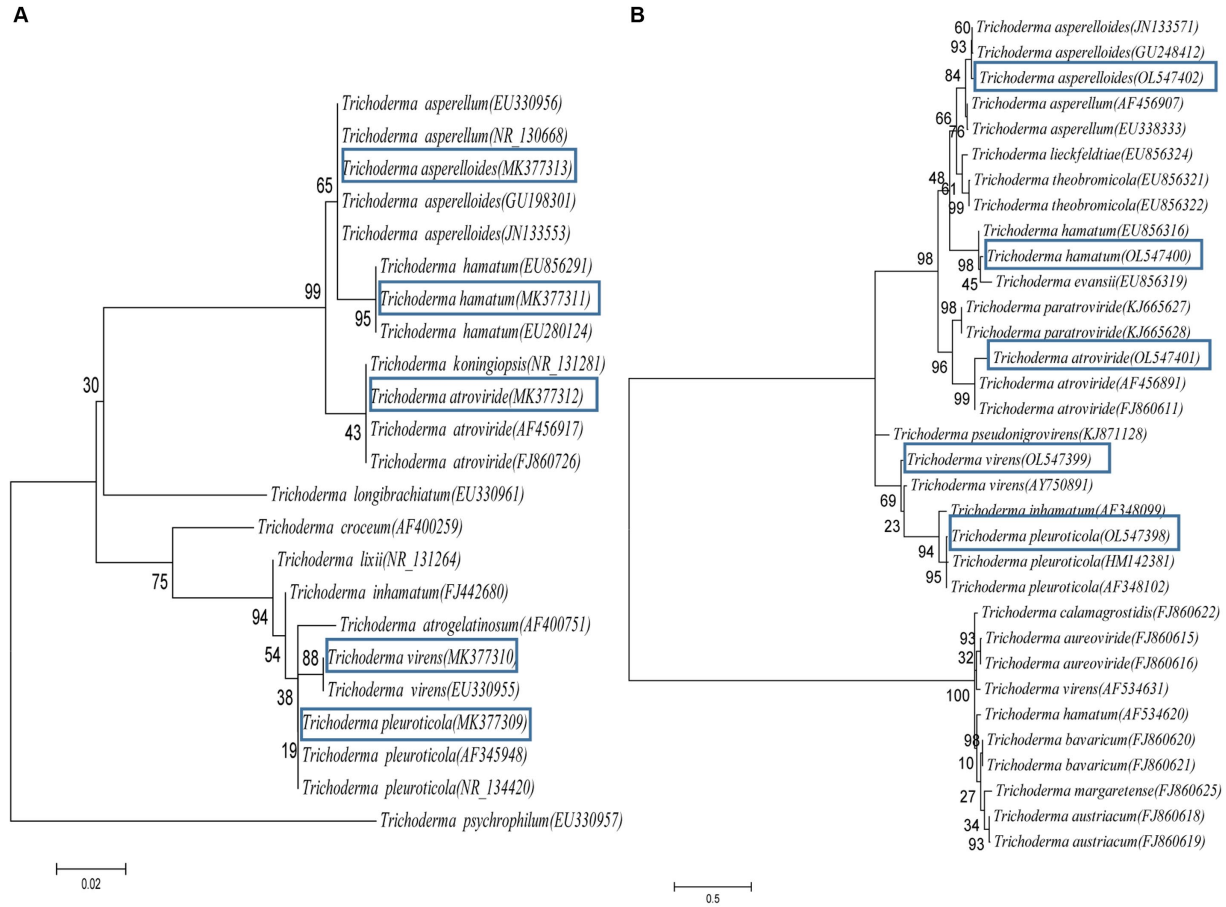

FIGURE 2
Phylogenetic analysis based on ITS and *tef1-α* sequences of *Trichoderma* strains. **(A)** Phylogenetic tree constructed using ITS sequences. **(B)** Phylogenetic tree constructed using *tef1-α* sequences. The accession numbers of the sequences are provided in brackets.

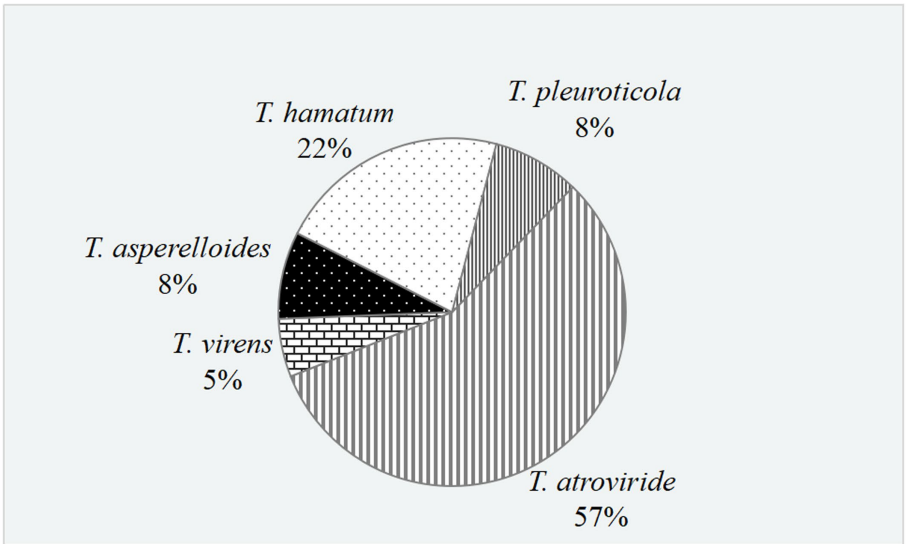

FIGURE 3
Proportion of *Trichoderma* in the rhizosphere soil of white birch.

significantly higher than that of the control group (1,161.634 μg/g); the soluble sugar of the treatment group was 1.5362 mg/g, significantly higher than that of the control group (1.3238 mg/g, $p < 0.05$). The catalase activity showed similar results, with the activity in the treatment group (1,053.63 nmol/min g) significantly higher than that in the control group (256.95 nmol/min g, $p < 0.05$).

10.3389/fmicb.2023.1265435

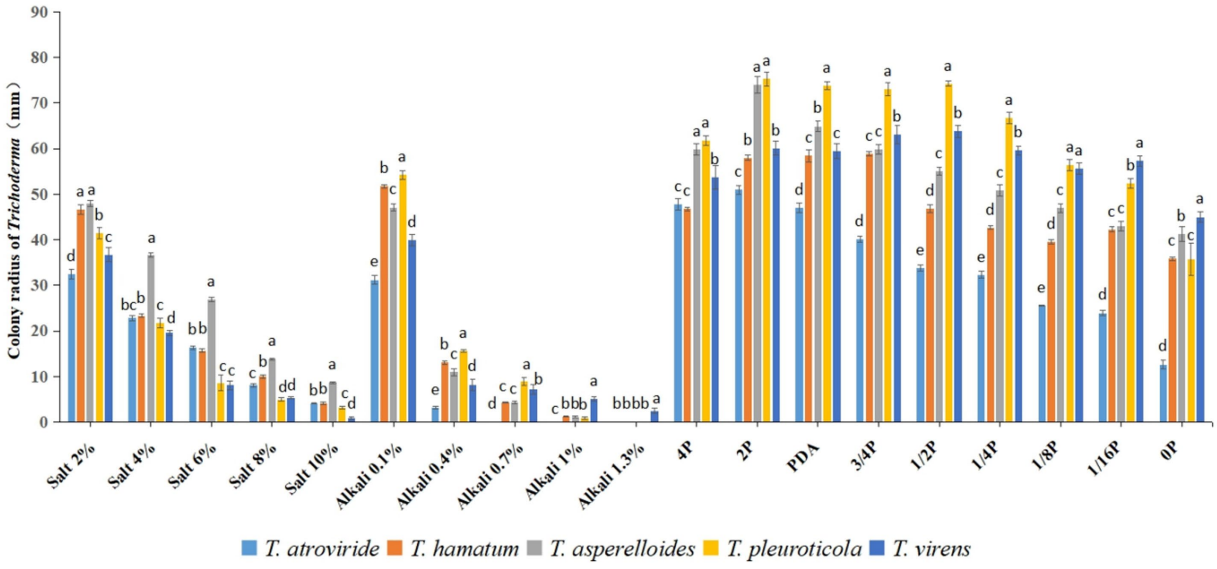

FIGURE 4
Radius of *Trichoderma* colonies in different conditions. All values represent the mean of three replicates ± standard error; in each condition, different letters denote a statistically significant difference according to a one-way ANOVA test ($p < 0.05$).

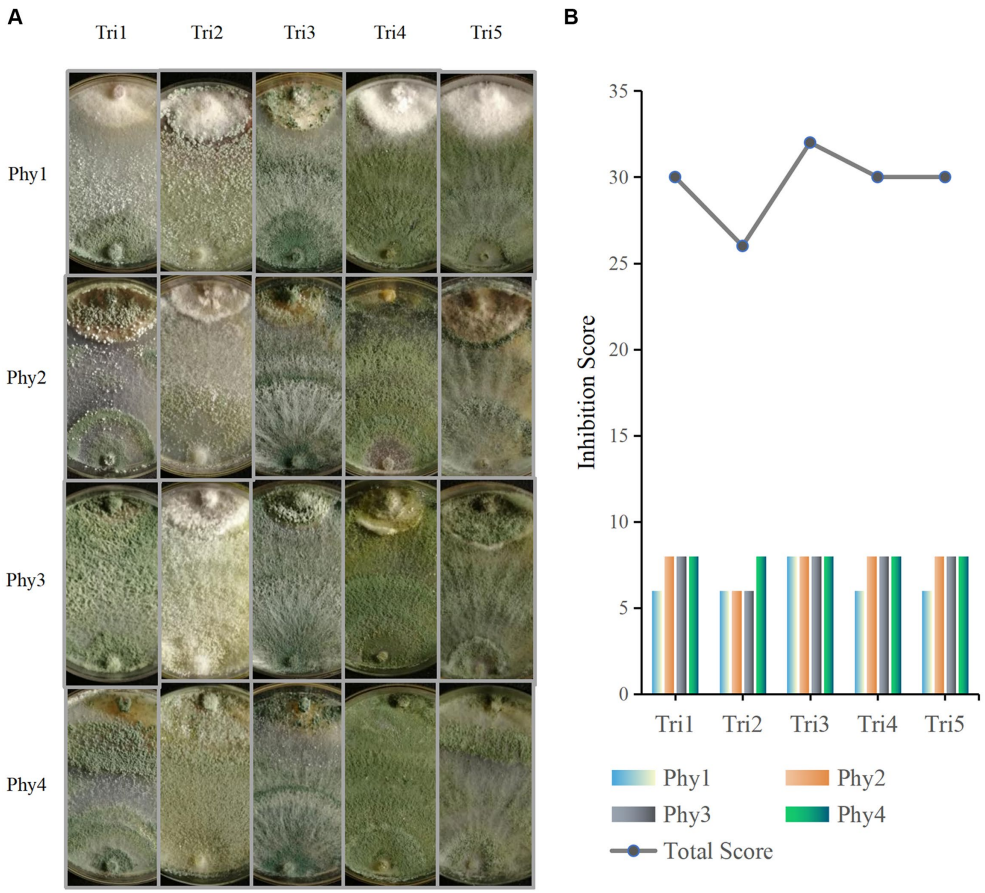

FIGURE 5
Phytopathogen inhibition ability of *Trichoderma* isolates. **(A)** Confrontation assay between *Trichoderma* (Tri) and phytopathogens (Phy); in the picture, *Trichoderma* are at the bottom and phytopathogens are at the top. **(B)** Pathogen inhibition ability evaluation. Tri1: *T. atroviride*; Tri2: *T. hamatum*; Tri3: *T. asperelloides*; Tri4: *T. pleuroticola*; Tri5: *T. virens*; Phy1: *F. oxysporum*; Phy2: *A. alternata*; Phy3: *B. cinerea*; Phy4: *C. chrysosperma*. Each dual culture was set up with three replicates.

10.3389/fmicb.2023.1265435

TABLE 1 Physiological index of *Gynura cusimbua*.

	Malonaldehyde (μmol/100 g)	Soluble protein (μg/g)	Soluble sugar (mg/g)	Catalase activity (nmol/min/g)	Height (cm)	Stem diameter (mm)	Germination rate (%)	Mean germination time (h)
T	31.709 ± 0.542^{c}	1555.458 ± 27.984^{b}	1.5362 ± 0.050^{b}	1053.63 ± 45.147^{b}	4.60 ± 0.235^{ab}	5.98 ± 0.20^{a}	90	102.3 ± 19.8
Control	16.13 ± 0.418^{d}	1161.634 ± 31.607^{d}	1.3238 ± 0.045^{c}	256.95 ± 37.86^{d}	4.120 ± 0.149^{b}	5.04 ± 0.15^{b}	80	105.3 ± 21.9
T + A	35.797 ± 1.469^{b}	1694.710 ± 15.204^{a}	1.7677 ± 0.040^{a}	1773.78 ± 97.064^{a}	4.72 ± 0.217^{a}	6.04 ± 0.16^{a}		
C + A	39.077 ± 0.446^{a}	1397.893 ± 12.891^{c}	1.664 ± 0.037^{a}	735.70 ± 40.554^{c}	4.22 ± 0.140^{b}	5.12 ± 0.18^{b}		

All values represent the mean of three replicates ± standard error. T represents *G. cusimbua* watered with a spore suspension of *T. atroviride*; Control represents *G. cusimbua* watered with water; T + A represents *G. cusimbua* watered with a spore suspension of *T. atroviride*, then inoculated with *Alternaria alternata*; and Control + A represents *G. cusimbua* watered with water, then inoculated with *A. alternata*. Different letters denote statistically significant differences according to a one-way ANOVA test ($p < 0.05$).

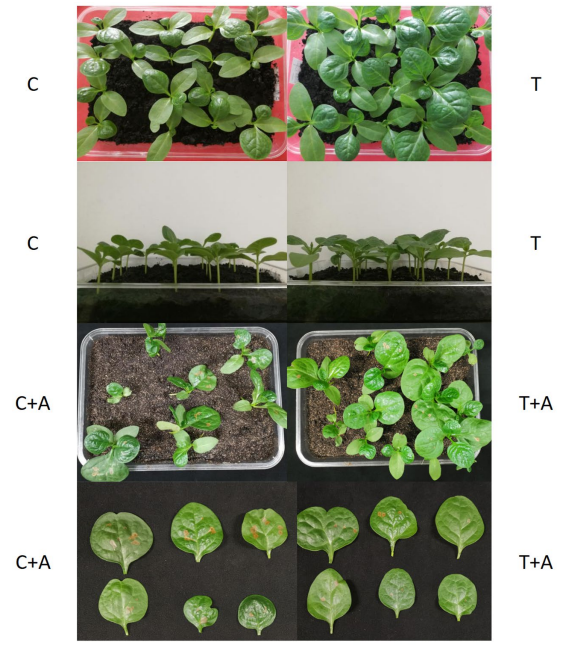

FIGURE 6
Growth of *G. cusimbua* at 30 days (left: control; right: treatment) and test of pathogen resistance ability. T represents *G. cusimbua* watered with a spore suspension of *T. atroviride*; C represents *G. cusimbua* watered with water; T + A represents *G. cusimbua* watered with a spore suspension of *T. atroviride*, then inoculated with *Alternaria alternata*; and C + A represents *G. cusimbua* watered with water, then inoculated with *A. alternata*.

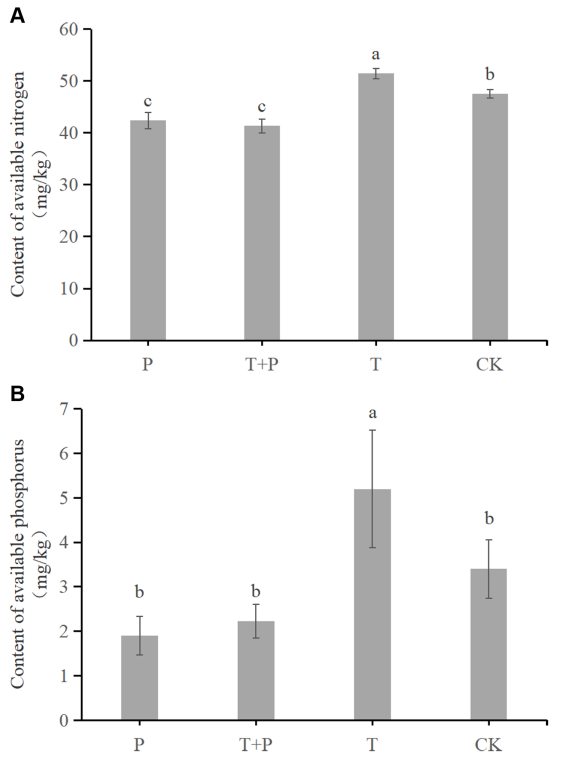

FIGURE 7
The influence on soil nutrients of *T. atroviride* and *G. cusimbua*. **(A)** Content of available nitrogen; **(B)** Content of available phosphorus. P: the soil in which *G. cusimbua* was planted; T+P: the soil watered with spore suspension of *T. atroviride*, in which *G. cusimbua* was planted; T: the soil watered with spore suspension of *T. atroviride*; CK: the soil watered with water. All values are the mean of three replicates ± standard error. Different letters denote statistically significant differences according to a one-way ANOVA test ($p < 0.05$).

After inoculation with *A. alternata*, the MDA values in both T + A and C + A were increased, but the MDA in C + A increased more dramatically (from 16.13 μmol/100 g to 39.077 μmol/100 g) and was significantly higher than the MDA of the plants in T + A (35.797 μmol/100 g, $p < 0.05$). The soluble protein of the plants increased in both groups, its value in T + A (1,694.710 μg/g) being still significantly higher than that in C + A (1,397.893 μg/g, $p < 0.05$). The soluble sugar of the plants also increased in both groups, and its value in T + A (1.7677 mg/g) was also still significantly higher than that in C + A (1.664 mg/g, $p < 0.05$). The CAT activity in plants of both groups was increased, and its value in T + A (1,773.78 nmol/min g) was significantly higher than that in C + A (735.70 nmol/min g, $p < 0.05$). Meanwhile, the plants in the T + A group grew better and had less or smaller disease spots compared to the plants in C + A group, which indicates that *T. atroviride* improves the disease resistance of *G. cusimbua*.

3.4. Beneficial effects of *Trichoderma atroviride* on soil nutrients

The contents of available nitrogen and available phosphorus in the four groups were measured (Figure 7). The available nitrogen in the P group, T + P group, T group, and CK group was 38.7 mg/kg, 41.33 mg/kg, 51.43 mg/kg, and 47.5 mg/kg, respectively (Figure 7A). The available phosphorus in the P group, T + P group, T group, and CK group was 1.9 mg/kg, 2.33 mg/kg, 5.2 mg/kg and 3.4 mg/kg, respectively (Figure 7B). The results show that the use of *T. atroviride*

significantly improves the content of available nitrogen and available phosphorus in soil. Meanwhile, compared with the soil in which *G. cusimbua* was not planted, the soil in which *G. cusimbua* was planted had significantly lower available nitrogen content ($p < 0.05$, Figure 7A) and lower available phosphorus (Figure 7B). Furthermore, the decrease in available nitrogen from T to T + P (10.1 mg/kg) was more than the decrease from CK to P (8.8 mg/kg); the decrease in available phosphorus from T to T + P (2.87 mg/kg) was more than the decrease from CK to P (1.5 mg/kg), which indirectly shows that *T. atroviride* promotes the absorption of available nitrogen and available phosphorus in *G. cusimbua*.

4. Discussion

Trichoderma spp. have been widely used in agriculture and forestry as biocontrol agents due to their good biocontrol ability (Gafur, 2023; Gafur et al., 2023). The collection and identification of *Trichoderma* resources has also become an important way to continuously explore high-quality *Trichoderma* in terms of biocontrol (Błaszczyk et al., 2011; Yu et al., 2021a,b). Dou et al. isolated 3,999 *Trichoderma* strains from four ecosystems (forest, grassland, wetland, and agro-ecosystem) in 28 provinces of China, and they were identified as 50 species. In Heilongjiang Province, they isolated 472 *Trichoderma* isolates and identified 23 species, of which *T. harzianum* was the main species, followed by *T. hamatum* and *T. atroviride* (Dou et al., 2019). In this study, among the *Trichoderma* isolated from the rhizosphere soil of *B. platyphylla* in Harbin, *T. atroviride* was the main species, accounting for 57% of the total number, followed by *T. hamatum*; *T. harzianum* was not isolated (Figure 3). The results are similar to those in previous research, where *T. atroviride* was the dominant species isolated from the rhizosphere soil of *J. mandshurica*, *Acer saccharum*, *Populus simonii*, and *Ulmus pumila* forests in Heilongjiang Province (Zhou et al., 2019). The similarity or difference in *Trichoderma* distribution may be caused by the differences in the rhizosphere environment, nutrition, and secondary metabolites of different plant species.

The identification methods in this study were combined morphological identification and molecular identification (Figures 1, 2). Most of the *Trichoderma* isolated in this study were correctly identified via careful morphological identification and consistent with the molecular identification results, except one: *T. asperelloides* was wrongly identified as *T. asperellum*. The main reason for this is that the book we referenced was published in 2009 (Yang, 2009, in Chinese), but *T. asperelloides* was reported in 2010 (Samuels et al., 2010); in addition, Samuels (Samuels et al., 2010) reported that *T. asperellum* is morphologically indistinguishable from *T. asperelloides*. This indicates that morphological identification is insufficient for *Trichoderma* identification. In our opinion, morphological identification is an important skill for taxonomists; we do not suggest that researchers should abandon this skill, nor do we advise that molecular identification is the only way to identify *Trichoderma*. Furthermore, even though the cost of molecular identification has decreased, it is still costly to sequence each isolate for some researchers who are short of funds, which may limit the development of taxonomy. In addition, taxonomy is not an exact science: it is the classification of species based on characteristics, similarities, evolutionary history, and even particular lifestyles (Garnett et al., 2020; Lücking et al., 2020); therefore, we should carefully evaluate the decision to base classification solely on tiny differences in gene loci.

In order to filter potential biocontrol agents, resilience experiments and confrontation assays were performed (Figures 4, 5). After comprehensively evaluating our five *Trichoderma* isolates for resilience and pathogen-inhibiting ability, *T. asperelloides* was outstanding above the other four *Trichoderma* isolates; this result is consistent with Ramírez-Cariño's research that reported that *T. asperelloides* was able to exert an outstanding mycoparasitic effect on *A. alternata* and *F. oxysporum* in a dual confrontation assay by hyphal strangulation and penetration (Ramírez-Cario et al., 2020). Similar results have also been found for its sibling species, *T. asperellum*; TaspHu1 showed better biocontrol ability compared to other isolates (Yu et al., 2021b). However, inconsistent results in the laboratory and field have also been reported (Mukherjee et al., 2012; López-Quintero et al., 2013). Additionally, *T. atroviride* also has relatively good adaption to different conditions and good inhibition ability; *T. atroviride* grew fast and effectively inhibited the growth of the four tested phytopathogens and could also mycoparasitise three of the four phytopathogens, except for *F. oxysporum*. This result is similar to that of a previous study, in which *T. atroviride* isolated from organic composts was reported to successfully control the disease of *Clarireedia* spp., *Rhizoctonia solani*, and *Sclerotium rolfsii*, which showed 53.5, 69.3, and 43.5% less affected area, respectively, on *Agrotis stolonifera* compared to the control (Coelho et al., 2021). The number of *T. atroviride* isolates was the greatest and accounted for 57% of the total number, while the number of isolated *T. asperelloides* accounted for only 8%. Therefore, considering that *T. atroviride* is widely distributed in rhizosphere soils of *B. platyphylla*, it may have good ability in the field; thus, *T. atroviride* was further analysed. As an additional consideration, trees grow slowly and we did not have the ability to plant white birch, so we decided to plant vegetables to verify *Trichoderma*'s plant-promoting abilities.

That *Trichoderma* can promote plant growth has been widely reported; for example, in tomatoes treated using *T. atroviride* MUCL45632, the shoot height significantly increased from 46.8 cm to 48.5 cm and the root dry weight significantly increased from 1.3 g to 2.7 g (Colla et al., 2015). In our study, *T. atroviride* significantly increased the stem diameter from 5.04 mm to 5.98 mm and the shoot height also increased from 4.12 cm to 4.60 cm. MDA reflects the degree of cell damage. Ji et al. found that *Trichoderma* induced the expression of the MsERF105 gene of *Malus sieversii,* which led to a significant decrease in MDA after 72 h (Ji et al., 2021). Rawat et al. also found lower MDA accumulation in *Trichoderma*-treated plants, which might be the reason that the plants endured salt stress (Rawat et al., 2016). In our study, a similar result also appeared; *T. atroviride* reduced the content of MDA when *G. cusimbua* was inoculated with *A. alternata*. However, treatment using *T. atroviride* alone still significantly increased the content of MDA, which indicates that *T. atroviride* also slightly injures plants, which may trigger their defence response.

Soluble protein and soluble sugar play important roles in the response to stress as osmotic balancers (Hoekstra et al., 2001; Afzal et al., 2021). In poplars treated using *T. asperellum* T-Pa2, the contents of soluble protein and soluble sugar were significantly increased (Yu et al., 2021a). The contents of soluble protein and proline in tomatoes increased significantly, by 32.08 and 26.7%, respectively, after induction with *T. harzianum*, which enhanced the stress tolerance of the tomatoes. In our study, after treatment using *T. atroviride*, the

content of soluble protein and soluble sugar in *G. cusimbua* were also significantly increased; meanwhile, after inoculating with *A. alternata*, *G. cusimbua* treated using *T. atroviride* expressed higher contents of soluble sugar and soluble protein compared to the control. Reactive oxygen species (ROS) increase when plants are under stress, and ROS damage the cell and its DNA (Zhao et al., 2019). Enzymes such as catalase (CAT) and superoxide dismutase (SOD) can "clear out" ROS; therefore, their enzyme activity reflects the ability to counter and eliminate ROS and also reflects the ability to adapt to stress (Zhao et al., 2019). *T. afroharzianum* T52 induced a 7.4-fold increase in CAT activity in *Syringa oblata*, while the H_2O_2 content decreased significantly to 0.82 μmol/g relative to 4.03 μmol/g in the control (Liu et al., 2020). In addition, poplars treated using *T. asperellum* T-Pa2 led to CAT significantly increasing to 3618.2 nmol/min/g compared to 2,926.62 nmol/min/g in the control (Yu et al., 2021a). In the present study, the plants treated with *T. atroviride* alone (T) or *A. alternata* alone (C + A) both improved in terms of CAT activity; however, the CAT activity of plants in T (1,053.63 nmol/min/g) was significantly higher than that of plants in C + A (735.70 nmol/min/g). Further, the plants treated using *T. atroviride* were more sensitive to *A. alternata* and had stronger responses to *A. alternata*, and the CAT activity in T + A (1,773.78 nmol/min/g) was significantly higher than in T or C + A. Therefore, we speculate that one of the reasons for the successful infection of pathogens is the failure to provoke sufficiently fast and strong defence responses in plants.

Strain *T. atroviride* MUCL45632 increased the nutrient levels of the plants, which caused increases in root and shoot weights (Colla et al., 2015). *T. asperellum* TaspHu1 promoted the absorption of available nitrogen in tomatoes, which caused increases in tomato growth; however, the strain did not influence the soil nitrogen content (Yu et al., 2021b). In the present study, *T. atroviride* significantly increased the content of available nitrogen and available phosphorus in the soil and also promoted the absorption of nutrients by *G. cusimbua*.

In conclusion, *T. atroviride* was found to be the leading species in *B. platyphylla* rhizosphere soil. It has a good effect on pathogen inhibition, plant growth promotion, plant resistance induction, and soil nutrient improvement, demonstrating potential for further applications in agriculture and forestry.

Data availability statement

The datasets presented in this study can be found in online repositories. The names of the repository/repositories and accession number(s) can be found in the article/supplementary material.

Author contributions

KL: Investigation, Methodology, Writing – original draft. Y-ZZ: Writing – review & editing, Formal analysis, Writing – original draft. H-YD: Formal analysis, Writing – original draft, Investigation, Methodology, Validation. Z-YW: Funding acquisition, Resources, Supervision, Writing – review & editing. P-WG: Funding acquisition, Supervision, Writing – review & editing. Z-HL: Funding acquisition, Resources, Supervision, Writing – review & editing. Z-YY: Funding acquisition, Methodology, Project administration, Writing – review & editing.

Funding

The author(s) declare financial support was received for the research, authorship, and/or publication of this article. This work is supported by grants from the National Natural Science Foundation of China (NSFC: 31870627), the Key Research and Development Project of Ningxia Hui Autonomous Region (grant number: 2023BCF01026-04), and the High Level Teachers Troop Construction of Ningxia University.

Acknowledgments

The authors thank for Jian Diao and Mingxiu Ju for providing advice on this article, as well as the peer reviewers for their helpful comments on the manuscript.

Conflict of interest

The authors declare that the research was conducted in the absence of any commercial or financial relationships that could be construed as a potential conflict of interest.

Publisher's note

References

Afzal, S., Chaudhary, N., and Singh, N. K. (2021) in *Role of soluble sugars in metabolism and sensing under abiotic stress, in plant growth regulators: Signalling under stress conditions*. eds. T. Aftab and K. R. Hakeem (Switzerland: Springer International Publishing AG), 305–334.

Bardgett, R. D., Wal, R. V. D., Jónsdóttir, I. S., Quirk, H., and Dutton, S. (2007). Temporal variability in plant and soil nitrogen pools in a high-Arctic ecosystem. *Soil Biol. Biochem.* 39, 2129–2137. doi: 10.1016/j.soilbio.2007.03.016

Błaszczyk, L., Popiel, D., Chełkowski, J., Koczyk, G., Samuels, G. J., Sobieralski, K., et al. (2011). Species diversity of *Trichoderma* in Poland. *J. Appl. Genet.* 52, 233–243. doi: 10.1007/s13353-011-0039-z

Braithwaite, M., Johnston, P. R., Ball, S. L., Nourozi, F., Hay, A. J., Shoukouhi, P., et al. (2017). *Trichoderma* down under: species diversity and occurrence of *Trichoderma* in New Zealand. *Australas Plant Path* 46, 11–30. doi: 10.1007/s13313-016-0457-9

Cabrera, M., Garmendia, G., Rufo, C., Pereyra, S. A., and Silvana, V. (2020). *Trichoderma atroviride* as a biocontrol agent of *fusarium* head blight by reducing the inoculum of the pathogen in wheat straw. *Terra Latinoamerican* 38, 629–651. doi: 10.28940/terra.v38i3.664

Coelho, L., Reis, M., Guerrero, C., and Dionísio, L. (2021). Biological control of turfgrass diseases with organic composts enriched with *Trichoderma atroviride*. *Biol. Control* 159:104620. doi: 10.1016/j.biocontrol.2021.104620

Colla, G., Rouphael, Y., Mattia, E. D., El-Nakhel, C., and Cardarelli, M. (2015). Co-inoculation of *Glomus intraradices* and *Trichoderma atroviride* acts as a biostimulant to promote growth, yield and nutrient uptake of vegetable crops. *J. Sci. Food Agr.* 95, 1706–1715. doi: 10.1002/jsfa.6875

Dou, K., Gao, J., Zhang, C., Yang, H., Jiang, X., Li, J., et al. (2019). *Trichoderma* biodiversity in major ecological systems of China. *J. Microbiol.* 57, 668–675. doi: 10.1007/s12275-019-8357-7

Gafur, A. (2023). "Red root rot disease of tropical estate forests: pathogen identification, dispersal and management" in *Detection, diagnosis and management of soil-borne phytopathogens*. eds. U. B. Singh, R. Kumar and H. B. Singh (Singapore: Springer Press)

Gafur, A., Naz, R., Nosheen, A., and Sayyed, R. Z. (2023). "Role of plant growth promoting microbes in managing soil-borne pathogens in forestry" in *Plant growth promoting microorganisms of arid region*. eds. R. Mawar, R. Z. Sayyed, S. K. Sharma and K. S. Sattiraju (Singapore: Springer Press)

Garnett, S. T., Christidis, L., Conix, S., Costello, M. J., and Frank, K. R. (2020). Principles for creating a single authoritative list of the world's species. *PLoS Biol.* 18:e3000736. doi: 10.1371/journal.pbio.3000736

Hoekstra, F. A., Golovina, E. A., and Buitink, J. (2001). Mechanisms of plant desiccation tolerance. *Trends Plant Sci.* 6, 431–438. doi: 10.1016/S1360-1385(01)02052-0

Ji, S., Liu, Z., and Wang, Y. (2021). *Trichoderma*-induced ethylene responsive factor MsERF105 mediates defense responses in *Malus sieversii*. *Front. Plant Sci.* 12:708010. doi: 10.3389/fpls.2021.708010

Kumar, S., Stecher, G., and Tamura, K. (2016). MEGA7: molecular evolutionary genetics analysis version 7.0 for bigger datasets. *Mol. Biol. Evol.* 33, 1870–1874. doi: 10.1093/molbev/msw054

Liu, B., Ji, S., Zhang, H., Wang, Y., and Liu, Z. (2020). Isolation of *Trichoderma* in the rhizosphere soil of *Syringa oblata* from Harbin and their biocontrol and growth promotion function. *Microbiol. Res.* 235:126445. doi: 10.1016/j.micres.2020.126445

López-Bucio, J., Pelagio-Flores, R., and Herrera-Estrella, A. (2015). *Trichoderma* as biostimulant: exploiting the multilevel properties of a plant beneficial fungus. *Sci. Hortic.* 196, 109–123. doi: 10.1016/j.scienta.2015.08.043

López-Quintero, C. A., Atanasova, L., Franco-Molano, A. E., Gams, W., Komon-Zelazowska, M., Theelen, B., et al. (2013). DNA barcoding survey of *Trichoderma* diversity in soil and litter of the Colombian lowland Amazonian rainforest reveals *Trichoderma strigosellum* sp. nov. and other species. *Anton Leeuw. Int. J. G.* 104, 657–674. doi: 10.1007/s10482-013-9975-4

Lücking, R., Aime, M. C., Robbertse, B., Miller, A. N., Ariyawansa, H. A., Schoch, C. L., et al. (2020). Unambiguous identification of fungi: where do we stand and how accurate and precise is fungal DNA barcoding? *IMA Fungus* 11:14. doi: 10.1186/s43008-020-00033-z

Mukherjee, M., Mukherjee, P. K., Horwitz, B. A., Zachow, C., Berg, G., and Zeilinger, S. (2012). *Trichoderma*-plant-pathogen interactions: advances in genetics of biological control. *Indian J. Microbiol.* 52, 522–529. doi: 10.1007/s12088-012-0308-5

Popiel, D., Kwaśna, H., Chełkowski, J., Stępień, Ł., and Laskowska, M. (2008). Impact of selected antagonistic fungi on *Fusarium* species – toxigenic cereal pathogens. *Acta Mycol* 43, 29–40. doi: 10.5586/am.2008.004

Poveda, J. (2021). Glucosinolates profile of *Arabidopsis thaliana* modified root colonization of *Trichoderma* species. *Biol. Control* 155:104522. doi: 10.1016/j.biocontrol.2020.104522

Raghavendra, A. K. H., and Newcombe, G. (2013). The contribution of foliar endophytes to quantitative resistance to *Melampsora* rust. *New Phytol.* 197, 909–918. doi: 10.1111/nph.12066

Ramírez-Cario, H. F., Guadarrama-Mendoza, P. C., Sánchez-López, V., Cuervo-Parra, J. A., Ramírez-Reyes, T., Dunlap, C. A., et al. (2020). Biocontrol of *Alternaria alternata* and *Fusarium oxysporum* by *Trichoderma asperelloides* and *Bacillus paralicheniformis* in tomato plants. *Antonie Van Leeuwenhoek* 113, 1247–1261. doi: 10.1007/s10482-020-01433-2

Rawat, L., Bisht, T. S., Upadhayay, R. G., and Kukreti, A. (2016). *Trichoderma harzianum* enhancing plant growth parameters and reducing deleterious effects of natural saline-sodic soil in rice. *Int. J. Trop. Agric.* 34, 1855–1867.

Samuels, G. J., Ismaiel, A., Bon, M. C., Respinis, S. D., and Petrini, O. (2010). *Trichoderma asperellum* sensu lato consists of two cryptic species. *Mycologia* 102, 944–966. doi: 10.3852/09-243

Uniyal, K., and Singh, Y. P. (2017). Evaluation of antagonist activity of *Trichoderma* species against *Alternaria alternata* isolated from *Populus deltoides*. *Int. J. Sci. Res.* 3, 1070–1074. doi: 10.21276/ijlssr.2017.3.3.18

Wu, B., Lian, C., and Hogetsu, T. (2002). Development of microsatellite markers in white birch (*Betula platyphylla var. japonica*). *Mol. Ecol. Resour.* 2, 413–415. doi: 10.1046/j.1471-8286.2002.00260.x

Yang, H. (2009). *Classification and identification of Trichoderma*. Beijing: China Land Press (in Chinese).

Yu, Z., Liu, Z., Zhang, Y., and Wang, Z. (2021a). The disease resistance potential of *Trichoderma asperellum* T-Pa2 isolated from *Phellodendron amurense* rhizosphere soil. *J. Forestry Res.* 33, 321–331. doi: 10.1007/s11676-021-01332-w

Yu, Z., Wang, Z., Zhang, Y., Wang, Y., and Liu, Z. (2021b). Biocontrol and growth-promoting effect of *Trichoderma asperellum* TaspHu1 isolate from *Juglans mandshurica* rhizosphere soil. *Microbiol. Res.* 242:126596. doi: 10.1016/j.micres.2020.126596

Zhao, M., Wen, J. L., Wang, L., Wang, X. P., and Chen, T. S. (2019). Intracellular catalase activity instead of glutathione level dominates the resistance of cells to reactive oxygen species. *Cell Stress Chaperon* 24, 609–619. doi: 10.1007/s12192-019-00993-1

Zhou, L., Dong, H., Huang, D., Fan, H., and Jia, Y. (2020). Responses of available phosphorus in different slope aspects to seasonal freeze-thaw cycles in Northeast China. *Soil Tillage Res.* 203:104706. doi: 10.1016/j.still.2020.104706

Zhou, C., Guo, R., Ji, S., Fan, H., and Liu, Z. (2019). Isolation of *Trichoderma* from forestry model base and the antifungal properties of isolate TpsT17 toward *Fusarium oxysporum*. *Microbiol. Res.* 231:126371. doi: 10.1016/j.micres.2019.126371

frontiers | Frontiers in Microbiology

TYPE Original Research
PUBLISHED 06 February 2024
DOI 10.3389/fmicb.2024.1328863

OPEN ACCESS

EDITED BY
Jianling Fan,
Nanjing University of Information Science and Technology, China

REVIEWED BY
Muhammad Ibrahim,
Sindh Agriculture University, Pakistan
Xin Guan,
Southwest University, China

*CORRESPONDENCE
Xiaoli Chang
✉ xl_chang14042@sicau.edu.cn

†These authors have contributed equally to this work

RECEIVED 27 October 2023
ACCEPTED 11 January 2024
PUBLISHED 06 February 2024

CITATION
Wei D, Zhu D, Zhang Y, Yang Z, Hu Y, Song C, Yang W and Chang X (2024) *Pseudomonas chlororaphis* IRHB3 assemblies beneficial microbes and activates JA-mediated resistance to promote nutrient utilization and inhibit pathogen attack.
Front. Microbiol. 15:1328863.
doi: 10.3389/fmicb.2024.1328863

Pseudomonas chlororaphis IRHB3 assemblies beneficial microbes and activates JA-mediated resistance to promote nutrient utilization and inhibit pathogen attack

Dengqin Wei†, Dan Zhu†, Yunfeng Zhang, Zheng Yang, Yu Hu, Chun Song, Wenyu Yang and Xiaoli Chang*

College of Agronomy, Sichuan Engineering Research Center for Crop Strip Intercropping System, Sichuan Agricultural University, Chengdu, Sichuan, China

Introduction: The rhizosphere microbiome is critical to plant health and resistance. PGPR are well known as plant-beneficial bacteria and generally regulate nutrient utilization as well as plant responses to environmental stimuli. In our previous work, one typical PGPR strain, *Pseudomonas chlororaphis* IRHB3, isolated from the soybean rhizosphere, had positive impacts on soil-borne disease suppression and growth promotion in the greenhouse, but its biocontrol mechanism and application in the field are not unclear.

Methods: In the current study, IRHB3 was introduced into field soil, and its effects on the local rhizosphere microbiome, disease resistance, and soybean growth were comprehensively analyzed through high-throughput sequencing and physiological and molecular methods.

Results and discussion: We found that IRHB3 significantly increased the richness of the bacterial community but not the structure of the soybean rhizosphere. Functional bacteria related to phosphorus solubilization and nitrogen fixation, such as *Geobacter*, *Geomonas*, *Candidatus Solibacter*, *Occallatibacter*, and *Candidatus Koribacter*, were recruited in rich abundance by IRHB3 to the soybean rhizosphere as compared to those without IRHB3. In addition, the IRHB3 supplement obviously maintained the homeostasis of the rhizosphere microbiome that was disturbed by *F. oxysporum*, resulting in a lower disease index of root rot when compared with *F. oxysporum*. Furthermore, JA-mediated induced resistance was rapidly activated by IRHB3 following *PDF1.2* and *LOX2* expression, and meanwhile, a set of nodulation genes, *GmENOD40b*, *GmNIN-2b*, and *GmRIC1*, were also considerably induced by IRHB3 to improve nitrogen fixation ability and promote soybean yield, even when plants were infected by *F. oxysporum*. Thus, IRHB3 tends to synergistically interact with local rhizosphere microbes to promote host growth and induce host resistance in the field.

KEYWORDS

***Pseudomonas chlororaphis*, *Fusarium* root rot, rhizosphere microbiome, induced systemic resistance (ISR), root nodules**

1 Introduction

Soybean [*Glycine max* (L.) Merri.] is one of the most significant oilseed crops and also the main source of plant proteins for human and animal health in the world (Liu et al., 2020). Soybean root rot is one type of soil-borne disease caused by *Fusarium* spp., *Rhizoctonia solani*, *Phytophthora* sp., etc. (Ajayi-Oyetunde and Bradley, 2017; Chang et al., 2018) and often results in root and stem rot, seedlings yellowing and dwarfing, root hypoplasia, and nodule reduction (Tyler, 2007; Lin et al., 2012). This disease is typically characterized by wide distribution, serious damage, and difficult control, and therefore it has become the major cropping obstacle to soybean production worldwide (Chang et al., 2018; Cruz et al., 2020; Xu and Wei, 2020). In the last decades, several methods, including disease-resistant varieties, agricultural practices, and chemical seed coating, have been widely applied in disease control, but the yield losses are still estimated at 10–30% annually (Casida and Durkin, 2017; Cao et al., 2018; Zhang et al., 2020). Recently, biological control has received more attention because of its characteristics of being environment-friendly, pollution-free, requiring less reliance on chemical products, and having no resistance problem (Abdelaziz et al., 2023). Currently, some valuable biocontrol microbial agents have been constantly explored in different environmental samples and applied to the control of soybean root rot (Chang et al., 2022; Xu et al., 2022). Especially some beneficial bacteria or fungi isolated from the *in situ* rhizosphere of host plants have obvious advantages for disease control efficiency and display good potential for exploration (Xu et al., 2022; Wei et al., 2023).

The rhizosphere microbiome plays a vital role in maintaining the homeostasis of the rhizosphere microenvironment and ensuring plant health (Eisenhauer et al., 2010; Berendsen et al., 2012). Some beneficial rhizosphere microbes are responsible for nutrient uptake and substance conversion, while others have certain functions in biofilm formation, environmental communication, microorganism recognition, etc. This kind of diverse function among the rhizosphere microbiome helps host plants well adapt to or cope with complicated environmental stimuli, directly or indirectly (Compant et al., 2019; Arif et al., 2020). To be worthwhile, some rhizosphere beneficial microbes like plant growth-promoting rhizobacteria (PGPR) and fungi (PGPF) often trend to improve the diversity and structure of the rhizosphere microbiome in a conductive way to plant growth and health (Lugtenberg and Kamilova, 2009; Santoyo, 2022). For example, pre-inoculation of PGPR *Bacillus velezensis* NJAU-Z9 in seedlings changed the rhizosphere microbial structure of pepper in the field and especially increased the relative abundance of beneficial bacterial genera, including *Pseudomonas*, *Rhizomicrobium*, *Streptomyces*, *Lysobacter*, and the fungal genera, including *Cladorrhinum*, *Cladosporium*, and *Aspergillus*, which are positively associated with yield increase (Zhang et al., 2019). Using *Bacillus amyloliquefaciens* B1408 isolated from cucumber rhizosphere soil to control cucumber *Fusarium* wilt also remarkably increased the relative abundance of rhizosphere microbes, including *Streptomyces*, *Rhizobium*, *Acidovorax*, *Rhodanobacter*, *Mesorhizobium*, *Asticcacaulis*, and *Rhizoscyphus*, which were negatively correlated with the disease index of *Fusarium* wilt (Han et al., 2019).

In addition to the above, when host plants suffer from pathogen invasion, on the one hand, some rhizosphere PGPR act as strong competitors for space and nutrients or produce antibiotics to directly suppress, antagonistize, or kill pathogens (Cao et al., 2018; Abdelaziz et al., 2023). On the other hand, they can also induce host resistance, typically as induced systemic resistance (ISR) (Pieterse et al., 2014), which is distinguished from systemic acquired resistance (SAR) triggered by plant pathogens (Durrant and Dong, 2004). Furthermore, induced resistance is often regulated by a network of interconnected signaling pathways in which plant hormones play a major regulatory role (Pieterse et al., 2009). Generally, SAR is characterized by increased levels of salicylic acid (SA), which activates the expression of a large set of pathogenesis-related (PR) genes involved in defense responses (Durrant and Dong, 2004; Liu et al., 2016). In contrast, ISR is usually mediated by the jasmonic acid (JA) and ethylene (ET)-dependent pathways (Choudhary et al., 2007), which usually induce the expression of *PDF*, *LOX*, *PAL*, *ERF*, etc. (Bukhat et al., 2020; Abdelaziz et al., 2023). In some specific cases, ISR and SAR can share some components (Alizadeh et al., 2013). Some PGPG, like *Pseudomonas*, have been reported to induce host ISR in rice, grapes, tobacco, and *Arabidopsis*, significantly improve plant resistance, and effectively limit pathogen invasion (Pathak et al., 2004; Choudhary et al., 2007; Verhagen et al., 2010). In addition, the signaling pathways involved in the induction of ISR can be different depending on the microbial species and plant species (Alizadeh et al., 2013). So far, the mechanism of beneficial rhizosphere microbes-triggered ISR is still not clearly understood.

In general, the regulation mechanisms of PGPR in plant health are complex and diverse. In a previous study, we demonstrated that *Pseudomonas chlororaphis* IRHB3 had big potential for the control of soybean root rot and displayed good adaptation to environmental stresses through greenhouse experiments (Chang et al., 2022; Wei et al., 2023), but it is unclear about the biocontrol mechanism and efficacy of IRHB3 when applied in the field. Thus, we further introduced IRHB3 into the field soil to make it clear as follows: (i) whether IRHB3 as one kind of PGPR can play a role in promoting growth and disease resistance when applied in the field; and (ii) how IRHB3 regulates the rhizosphere microbiome and host resistance to impact soybean health.

2 Materials and methods

2.1 Field pot experiment design

Field soil was collected from a 5-year continuous cropping field in May 2022 at Qingpu Farm (103°88 N, 30°72 E). A 20-cm depth of farmland soil was shoveled up and mixed thoroughly. The soil had a pH of 5.02, a total N content of 1.99 g·kg^{-1}, a total P content of 1.021 g·kg^{-1}, an available N content of 254.68 mg·kg^{-1}, and an available P content of 83.80 mg·kg^{-1}, respectively.

Four treatments were designed in the field pot experiment, as follows: (i) Con, blank field soil; (ii) IRHB3, soil irrigated with biocontrol strain *Pseudomonas chlororaphis* IRHB3; (iii) Fo, soil inoculated by pathogenic *Fusarium oxysporum* B3S1 of soybean root rot; and (iv) IRHB3_Fo, soil co-treated with IRHB3 and B3S1. The cultivar Nandou12, moderately susceptible to *F. oxysporum*, was selected for pot experiments. Soybean seeds of Nandou12 were sequentially surface-disinfected with 30% H_2O_2 (V/V) for 10 min and washed three times with sterile water. Sterilized seeds were then transferred into a sterile budding box and cultured for 4 days at 28°C with 16 h of light and 8 h of darkness. Three healthy soybean seedlings

with consistent growth were transplanted into plastic pots for four different treatments, as shown above.

For *F. oxysporum* inoculation (Fo), the pathogen *F. oxysproum* B3S1 was inoculated using the sorghum grain method as described by Chang et al. (2022). In short, sorghum grains were inoculated with B3S1 and cultured for 7–10 days at 25°C in the dark. Successfully infected sorghum was then dried at 25°C and ground into powder, and the abundance of B3S1 was approximately 2×10^7 ppg per gram of sorghum powder. About 5 kg of field soil with 10% moisture content were mixed with 25 g of infected sorghum powder in one polypropylene pot (29 cm in diameter × 26 cm in height), which was covered about 6 cm above the un-infected soil layer above. Field soil without pathogen inoculation was used as the blank control (Con).

For IRHB3 treatment, the bacterium strain was inoculated through the bacterial suspension irrigation method. IRHB3 was cultured in LB liquid medium at 28°C, 150 rpm·min^{-1} for 24 h. After being centrifuged at 6,000 rpm·min^{-1} for 12 min, the bacterial pellets were collected and re-suspended using ddH_2O to obtain the OD_{600} value of 0.5. About 1,000 mL aliquots of bacterial suspension were irrigated into each pot to ensure that per gram of soil contained approximately 107 cfu of IRHB3 as the treatment of IRHB3. The equal volume of IRHB3 bacterial suspension to irrigate the soybean seedlings grown in the *F. oxysporum*-inoculated soil was used as the treatment of IRHB3_Fo. Each treatment contained 15 replicative pots, and each pot contained three seedlings. All pots were placed in a randomized complete block design in the field. The detailed methods were described as shown in Supplementary Figure S1.

2.2 Sampling and analysis of roots and rhizosphere soils

Rhizosphere soil and plant roots from the four treatments (Con, IRHB3, Fo, and IRHB3_Fo) described above were sampled at the growth period (V5), flowering period (R2), and harvest period (R8) of soybeans, respectively. For plant sampling, a total of 15 plants per treatment were dug up during the corresponding period. After being watered with tap water, the disease symptom of root rot was observed, and the disease occurrence rate as well as the disease index (DI) were calculated as described by Chang et al. (2018). Plant roots were then scanned and analyzed using the LD-WinRHIZO Plant Root System Analyzer (RHIZO 2009, Quebec, Canada), and growth parameters, including the shoot dry weight, root dry weight, nodule fresh weight, and seed fresh weight per plant, were measured. For quantitative real-time PCR (qRT-PCR) analysis, parts of root tissues were randomly cut into small pieces, thoroughly mixed, frozen in liquid nitrogen for 30 min, and finally stored at −80°C.

For soil samples, rhizosphere soil was carefully collected by shaking off the soil blocks from the plants and then brushing the soil tightly attached to the root surface using a hairbrush. Samples from the same treatment were mixed, thoroughly homogenized, and then divided into two parts. One part of the rhizosphere soil was air-dried for the analysis of soil characteristics according to the method established by Xiong et al. (2015), whereas the other part was stored at −80°C for high-throughput sequencing analysis.

2.3 Genome DNA extraction and high-throughput sequencing of rhizosphere soil bacterial community

For each soil sample (20 in total: four treatments × five replicates), genomic DNA was extracted from 0.5 g of rhizosphere soil using the E.Z.N.A.® Soil DNA Kit (Omega Bio-tek, Norcross, GA, USA) according to the manufacturer's protocols. DNA concentration and purity were determined using a NanoDrop ND-2000 spectrophotometer (NanoDrop Technologies, Wilmington, DE, USA). The V1-V9 region of the bacteria *16S rRNA* gene was amplified using primers 27F and 1492R (Supplementary Table S1) in a 20-μL PCR reaction system, which contained 4 μL of 5× FastPfu Buffer, 2 μL of 2.5 mM dNTPs, 0.8 μL of each primer (5 μM), 0.4 μL of FastPfu Polymerase, and 10 ng of template DNA. PCR was performed at 95°C for 2 min, followed by 27 cycles at 95°C for 30 s, 55°C for 30 s, and 72°C for 60 s, and a final extension at 72°C for 5 min. Amplicons were examined by 2% agarose gels and purified using the AxyPrep DNA Gel Extraction Kit (Axygen Biosciences, Union, CA, USA) according to the manufacturer's instructions.

The sequencing of purified SMRTbell libraries generated from the Zymo and HMP mock communities was conducted on dedicated PacBio Sequel II 8 M cells using the Sequencing Kit 2.0 chemistry, while purified SMRTbell libraries generated from the pooled and barcoded samples were sequenced on a single PacBio Sequel II cell. All amplicons were sequenced by Shanghai Biozeron Biotechnology Co. Ltd. (Shanghai, China). The SMRT Link Analysis software version 9.0 was employed to process PacBio raw reads to obtain demultiplexed circular consensus sequence (CCS) reads with the minimum number of passes = 3 and minimum predicted accuracy = 0.99, respectively. Raw reads were processed using the SMRT Portal to ensure sequence length (<800 or > 2,500 bp) and quality. After that, sequences containing 10 consecutive identical bases were further filtered to remove barcodes, primer sequences, primers, and other sequences. OTUs were clustered with 98.65% similarity cut-off using UPARSE 7.1,[1] and chimeric sequences were identified and removed using UCHIME. The phylogenetic analysis of each *16S rRNA* gene sequence was conducted through the RDP Classifier[2] against the silva (SSU132) *16S rRNA* database using a confidence threshold of 70% (Amato et al., 2013).

2.4 Bioinformatics analysis for high-throughput sequencing

The rarefaction analysis was performed using Mothur v.1.21.1 (Schloss et al., 2009) to disclose the diversity indices, including the Chao, Shannon, and Evenness diversity indices. The beta diversity analysis, including the values of PCOA and NMDS, was conducted through UniFrac (Lozupone et al., 2011). The Spearman's correlation coefficients were assessed to determine the relationships between bacteria and soil physicochemical factors. Correlation was considered to be significant when the absolute value of Spearman's rank

1 http://drive5.com/uparse/

2 http://rdp.cme.msu.edu/

correlation coefficient (Spearman's r) was >0.6 and statistically significant at the value of $p < 0.05$. All statistical analysis was performed by the R *stats* package. The R (*pheatmap* package) and Cytoscape[3] were used to evaluate the relationships through correlation heatmaps and network diagrams, respectively. Venn diagrams were prepared by Draw Venn Diagram[4] to analyze overlapped and unique OTUs. One-way permutation analysis of variance (PERMANOVA) was conducted using the R vegan package to assess the statistically significant impacts of treatment processes on bacterial communities.

2.5 Quantification of *Pseudomonas chlororaphis* IRHB3 and *Fusarium oxysporum* B3S1 in rhizosphere soil samples

Quantitative real-time PCR (qRT-PCR) was used to determine the abundance of *P. chlororaphis* IRHB3 and *F. oxysporum* B3S1 in soybean rhizosphere soil from different treatments, and the specific fragments of *gryB* and *rDNA ITS* genes were amplified using primer pairs PC03F/PC03R and FOF/FOR1 (Jiménez-Fernández et al., 2010) for the quantification of IRHB3 and B3S1, respectively (Supplementary Table S1). Briefly, total DNA was extracted from 0.5 g of rhizosphere soil using the DNasy Power Soil Pro Kit (Qiagen, Stuttgart, Germany) according to the manufacturer's protocols. Then, qRT-PCR was performed on the Chromo4 Real-Time PCR System (Bio-Rad, Hercules, CA, USA) in a 10-μL reaction mixture containing 5 μL of the SYBR qPCR Mix (2×) (Vazyme-Bio, Shanghai, China), 1 μL of each primer (10 mM), 1 μL of template DNA (10 ng), and 2 μL of ddH_2O. The PCR thermal cycling conditions were set as follows: 3 min at 95°C for heat activation, 40 cycles of 10 s at 95°C, 30 s at annealing temperature (Supplementary Table S1) for amplification, 15 s at 95°C, 1 min at 60°C, and 15 s at 95°C for melting curve analysis. The *16S rRNA* for *P. chlororaphis* and the *ITS* for *F. oxysporum* were used as the reference genes. Gene expression values were calculated as Log10 values (target copy number per gram soil) prior to further statistical analysis. This experiment for each sample included four technical replicates and three biological replicates.

2.6 Expression analysis of defense and nodulation signaling genes in soybean root

The total RNA of soybean roots harvested from four treatments in the field was extracted using the Fast Pure® Universal Plant Total RNA Isolation Kit (Vazyme-Bio, Chengdu, China). The RNA concentration was quantified using the NanoDrop fluorometer (Thermo Fisher Scientific, Stuttgart, Germany). The first-strand cDNA was synthesized using 2.5 μg of RNA in a 20-μL reaction volume according to the instructions of the BeyoRT™ II First Strand cDNA Synthesis Kit (Beyotime-Bio, China). Four genes, including *PR1*, *PR5*, *PDF1.2*, and *LOX2*, were selected to examine JA or SA signaling-related resistance (Lenis et al., 2010), whereas three genes, *GmENOD40b*, *GmNIN-2b*, and *GmRIC1*, were amplified to analyze the nodulation formation (Hayashi et al., 2012). Specific primer pairs used in this study are listed in Supplementary Table S1. qRT-PCR was performed in 10-μL reaction mixtures containing 5 μL of the SYBR Qpcr Mix (2×), 1 μL of 10 mM of each primer (Supplementary Table S1), 1 μL of cDNA templates (diluted five times from the original cDNA synthesis reaction), and 2 μL of ddH_2O. The PCR thermal cycling conditions were the same as in Section 2.5. Gene relative expression was investigated using the $2^{-\Delta\Delta Ct}$ method (Livak and Schmittgen, 2001), with the *GmActin* gene as an endogenous reference for normalization. There were three biological replicates and four technical replicates.

2.7 Statistical analyses

High-throughput sequencing statistical analyses and data visualization were performed by R 4.3.1 (R software, Auckland, New Zealand). qRT-PCR raw data were analyzed using Excel 2010 (Microsoft Excel software, Washington, USA) by the $2^{-\Delta\Delta Ct}$ method. Differential analysis and visualization of soybean field agronomic traits, soil chemistry, and gene relative expression were conducted using SPSS 24 software (SPSS Software Inc., Chicago, IL, USA) and GraphPad Prism 10 (GraphPad Software Inc., San Diego, CA, USA), respectively. One-way analyses of variance (ANOVA) with the Duncan's multiple range test were performed for multiple comparisons.

3 Results

3.1 IRHB3 promotes soybean growth and suppresses root rot in the field

As shown in Figure 1A, soybean seedlings grown in the IRHB3-supplemented soils (IRHB3 and IRHB3_Fo) were the most robust, with the highest and strongest stems and lush green leaves at the R2 growth stage. Specifically, plant roots were obviously well developed after IRHB treatment (IRHB3), which were characterized by strong taproots, abundant lateral roots, and increased root nodules. Compared with those in the blank soil (Con), the dry weight of plant stems and roots after IRHB3 treatment was increased by 54.35 and 64.87%, respectively (Figure 1B), and meanwhile, the nodule fresh weight also sharply rose up by 132.55% and went up to 1658.96 mg per plant (Figure 1C). Furthermore, seed fresh weight reached 5.86 g per plant in the IRHB3-treated soil as compared to 4.20 g in the blank soil, which increased by 39.60% (Figure 1D). Interestingly, IRHB3 has similar effects on soybean growth at the R2 period to those at the V5 and R8 periods, and the detailed data are listed in Supplementary Figure S2.

To evaluate the IRHB3 impacts on root rot disease, we found that *F. oxysporum* inoculation (Fo) had negative impacts on plant growth and root development, whereas the IRHB3 supplement (IRHB3_Fo) largely alleviated these negative effects caused by *F. oxysporum* (Figure 1A). The dry weight of shoots and roots after IRHB3 addition reached 59.94 and 64.20%, respectively, which was remarkably higher

3 http://www.cytoscape.org

4 http://bioinformatics.psb.ugent.be/webtools/Venn

10.3389/fmicb.2024.1328863

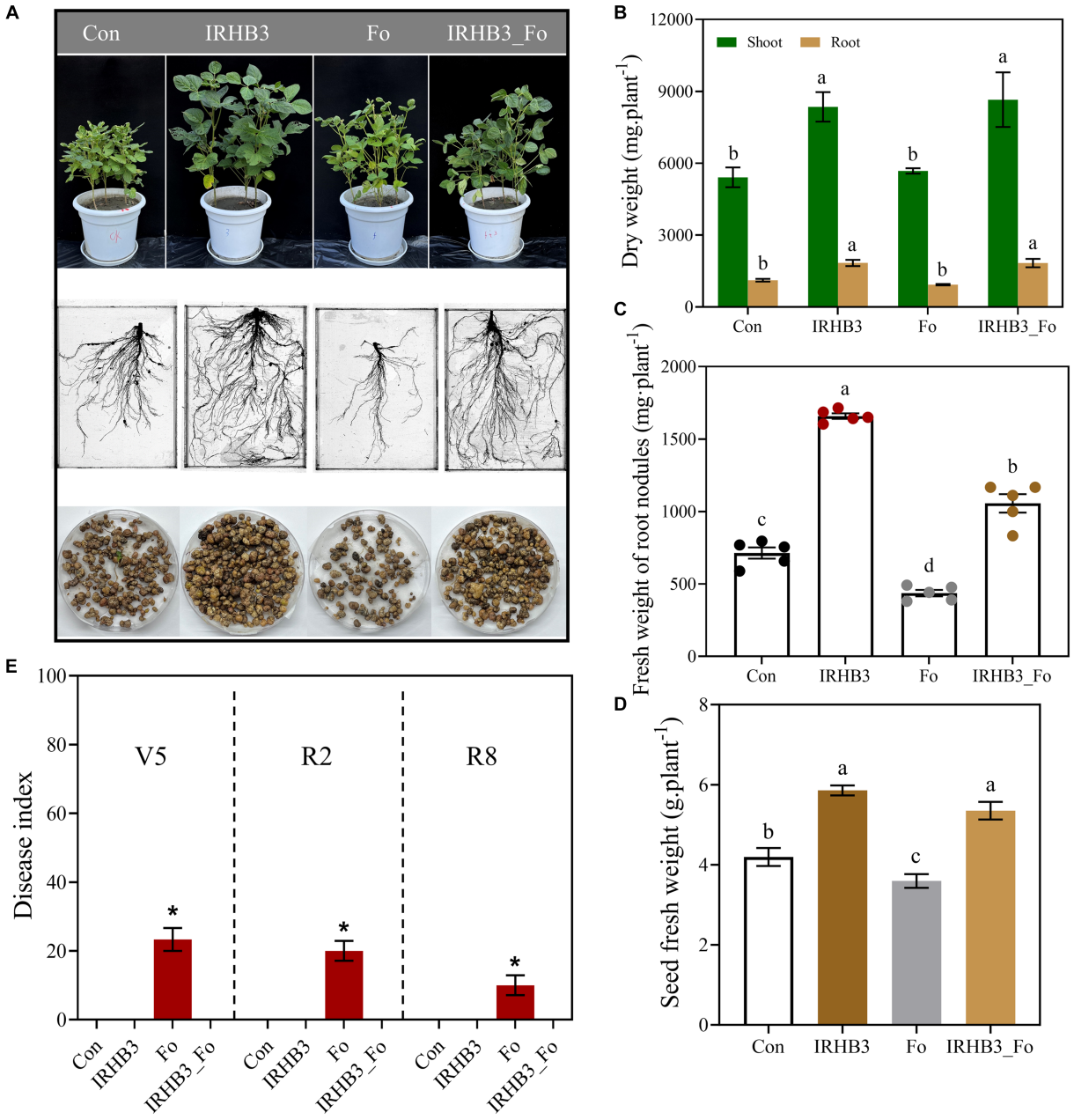

FIGURE 1
Effects of IRHB3 on soybean growth, *Fusarium* root rot, and soybean yield. **(A)** Effects of different treatments on shoot growth (upper), root development (middle), and nodule formation (lower) of soybeans at R2 period. **(B)** Dry weight of shoots and roots of soybeans at the R2 period. **(C)** Nodule fresh weight of soybean at R2 period. **(D)** Seeds fresh weight of soybean at R8 period. **(E)** Disease index of *Fusarium* root rot at V5, R2, and R8 periods. The data represent the mean ± SEM. Con, blank field soil; IRHB3, soil irrigated with biocontrol strain *Pseudomonas chlororaphis* IRHB3; Fo, soil inoculated by pathogenic *Fusarium oxysporum* B3S1 of soybean root rot; and IRHB3_Fo, soil co-treated with IRHB3 and B3S1. Asterisks or different lowercase letters indicate significant differences ($p < 0.05$) according to Duncan's multiple range test, similarly hereinafter.

than those in the treatments of *F. oxysporum* (Fo) and even control (Con) (Figure 1C). In addition, pathogen inoculation seriously decreased soybean nodule formation, and the abundance of root nodules was 38.83% less than those in the control (Con). Interestingly, the nodulation ability in the combined treatment of *F. oxysporum* and IRHB3 (IRHB3_Fo) was no longer restricted by pathogens, and instead, the nodule fresh weight significantly rose by 141.92 and 47.99% as compared to *F. oxysporum* and control, respectively. Meanwhile, seed fresh weight affected by *F. oxysporum* had also dramatically recovered and even increased by 27.52% as compared to control (Figure 1D). At all three growth periods, *F. oxyporum* inoculation caused the highest disease index and accounted for 23.33% (V5), 20% (R2), and 10% (R8), respectively (Figure 1E), whereas almost no root rot symptoms were observed in the combined treatments of IRHB3 and *F. oxysporum* (IRHB3_Fo). Thus, IRHB3 has positive effects on soybean growth and root rot suppression.

3.2 IRHB3 promotes soybean uptake of available nitrogen and phosphorus from soil

In order to evaluate the effects of four treatments on soil physicochemical properties, several parameters, including total phosphorus (TP), total nitrogen (TN), available phosphorus (AP), alkaline nitrogen (AN), and pH, were examined at the R2 stage. As shown in Table 1, three parameters, including TP, TN, and pH, of the rhizosphere soil were not affected by all treatments, but the contents of AP and AN were obviously distinct. The contents of AP varied from 84.19 to 8.65 mg·kg^{-1} with the trend of IRHB3 > Con > IRHB3_Fo > Fo. Compared with control, both treatments of IRHB3 and IRHB3_Fo increased AP by 5.31 mg·kg^{-1} and 5.45 mg·kg^{-1}, respectively. The contents of AN ranged from 236.11 to 284.67 mg·kg^{-1} with the trend of IRHB3 > IRHB3_Fo > Con > Fo, and comparison of IRHB3 vs. Con and IRH3_Fo vs. Fo showed AN contents were increased by 41.316 mg·kg^{-1} and 32.23 mg·kg^{-1}, respectively. Thus, IRHB3 has positive impacts on the increase of AN and AP, and also partially recovers the ability of AN and AP utilization.

3.3 Dynamic tracking and correlation analysis of IRHB3 and *Fusarium oxysporum* in soybean rhizosphere

Since most exogenously applied microorganisms are relatively difficult to survive and colonize in the complicated field environment, their work amounts generally need to account for 10^5 cfu·g^{-1} (Pieterse et al., 2014; Liu et al., 2021). In this study, copies of *gyrB* and *ITS* fragments were examined by qRT-PCR to record the survival abundance and dynamics of *P. chlororaphis* IRHB3 and *F. oxysporum* B3S1 in soybean rhizosphere soil. As shown in Figure 2, both *P. chlororaphis* and *F. oxysporum* copies in rhizosphere soil gradually decreased from V5 to R8 stages, but the overall survival ability remained relatively strong. Specifically, *F. oxysporum* gene copies were recorded as 10^7, 10^6, and 10^5 cfu·g^{-1} and 10^6, 10^5, and 10^4 cfu·g^{-1} at V5, R2, and R8 stages of soybean growth in the treatments of Fo and IRHB3_Fo, respectively (Figure 2A), whereas *P. chlororaphis* copies accounted for 10^6, 10^4, and 10^3 cfu·g^{-1} and 10^5, 10^3, 10^3 cfu·g^{-1} in the corresponding treatments of IRHB3 and IRHB3_Fo at three stages in sequence (Figure 2B). There was a significant positive correlation between

TABLE 1 Rhizosphere soil physicochemical properties of different treatments examined in this study.

Treatment	TP (g·kg^{-1})	TN (g·kg^{-1})	AP (mg·kg^{-1})	AN (mg·kg^{-1})	pH
Con	1.09 ± 0.03a	1.90 ± 0.01a	93.33 ± 0.30b	243.36 ± 0.43c	5.04 ± 0.01a
IRHB3	1.04 ± 0.01a	1.95 ± 0.03a	98.65 ± 0.64a	284.67 ± 0.78a	5.05 ± 0.01a
Fo	1.04 ± 0.02a	1.89 ± 0.03ab	84.19 ± 0.03d	236.11 ± 0.99d	5.08 ± 0.01a
IRHB3 + Fo	1.04 ± 0.01a	1.94 ± 0.03a	89.64 ± 0.24c	268.35 ± 0.67b	5.07 ± 0.03a

TP, total phosphorus; TN, total nitrogen; AP, available phosphorus; AN, alkaline nitrogen. Data are means ± SEM. Different lowercase letters in the same row mean significant differences ($p < 0.05$) according to Duncan's *multiple range* test, similarly hereinafter.

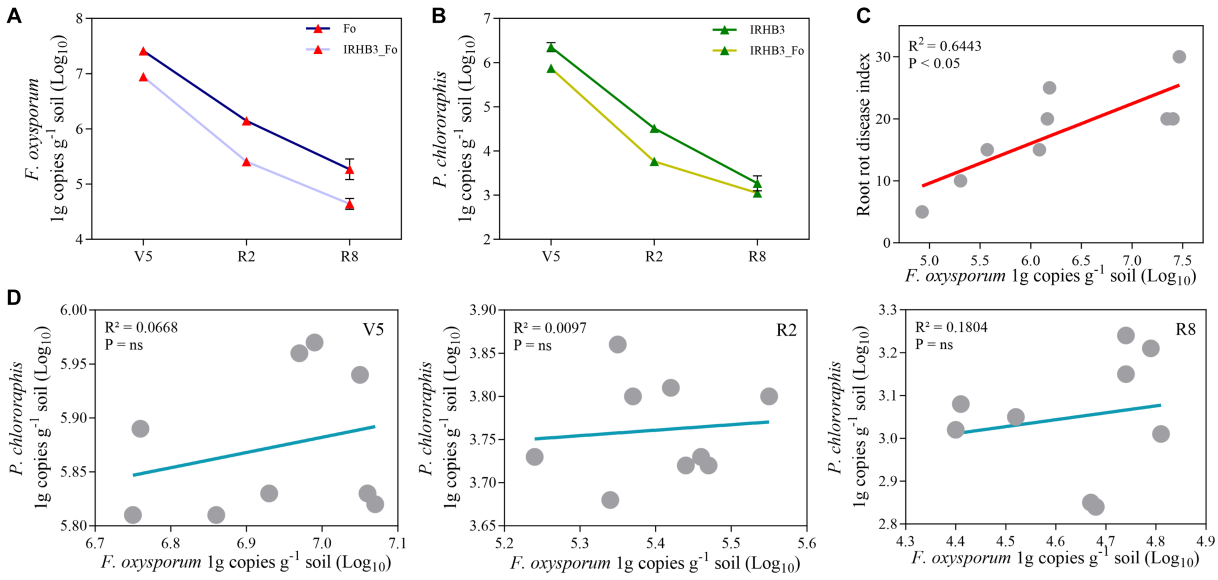

FIGURE 2
Survival dynamic tracking and correlation analysis of beneficial IRHB3 and pathogen *F. oxysporum* in rhizosphere soils. **(A)** *F. oxysporum* and **(B)** *P. chlororaphis* copies in soybean rhizosphere soil. **(C)** Correlation analysis of *F. oxysporum* abundance and disease index of soybean root rot. **(D)** Correlation analysis of the abundance of *F. oxysporum* and *P. chlororaphis* IRHB3 at V5, R2, and R8 periods. R2 represents the correlation coefficient. $p < 0.05$ and p = ns indicate a significant difference and no difference, respectively.

the disease index of root rot and *F. oxysporum* copies ($R^2 = 0.6443$, $p < 0.05$) (Figure 2C), indicating that the more abundant *F. oxysporum*, the more serious root rot disease. Furthermore, the correlation coefficients R2 of *P. chlororaphis* and *F. oxysporum* copies were 0.0668, 0.0097, and 0.1804 at the V5, R2, and R8 stages, respectively (Figure 2D), demonstrating that there was no close correlation (P = ns) between *P. chlororaphis* and *F. oxysporum*.

Although the abundance of *F. oxysporum* gradually decreased with soybean growth, its concentration remained as high as 10^5 cfu·g^{-1} in *F. oxysporum*-treated rhizosphere soil, which is still enough to exert pathogenic functions. In addition, *F. oxysporum* abundance in IRHB3_Fo treatment reached the working concentration in both V5 (10^6 cfu·g^{-1}) and R2 (10^5 cfu·g^{-1}) periods, but the occurrence of root rot disease was never observed. For the biocontrol bacterium, IRHB3 only reached the working concentration (10^6 cfu·g^{-1} in IRHB3 treatment, 10^5 cfu·g^{-1} in IRHB3_Fo treatment) at V5 period, and after that, it was always lower than 10^5 cfu·g^{-1}, indicating that IRHB3 might not individually service host to confront pathogen attack.

3.4 IRHB3 increases soybean rhizosphere bacterial diversity but does not alter the structure

To investigate the impacts of different treatments on the local bacterial community in the field, the diversity and structure of the rhizosphere bacterial community were analyzed and compared through *16S rRNA* high-throughput sequencing. Alpha diversity analysis showed that IRHB3 treatment (IRHB3) improved the richness (Chao index), diversity (Shannon index), and evenness (Evenness index) of soybean root bacteria ($p < 0.05$) when compared with control (Con) (Figure 3A). As expected, *F. oxysporum* inoculation (Fo) also significantly changed the bacterial community abundance, but IRHB3 supplement (IRHB3_Fo) partially returned the bacterial species diversity and evenness. To compare the numbers of OTUs, we found that the numbers of unique bacterial OTUs were 5,558 for Con, 5,709 for IRHB3, 6,464 for Fo, and 3,412 for IRHB3_Fo, respectively. There were the most shared OTUs between IRHB3_Fo and Fo treatments (2460) and the lowest shared OTUs between IRHB3 and Fo treatments (2116) (Figure 3B), which indicates the more similar bacterial community diversity in the corresponding comparison group.

Beta diversity analysis was conducted through PCOA and NMDS analyses based on Weighted UniFrac distance (Figures 3C, D). PCOA analysis showed that except for *F. oxysporum*, the other three treatments had a relatively close relationship and clustered together in the second principal component (PC2) (Figure 3C). NMDS analysis had the same trend as PCOA analysis, and the treatments of IRHB3 and IRHB3_Fo had partial overlap with the healthy control (Con), implying the same structure of the bacterial community. In contrast, the treatment of IRHB3_Fo was totally separated from *F. oxysporum*, indicating the bacterial structure was clearly altered because of the IRHB3 supplement (Figure 3D). Overall, IRHB3 could improve the abundance of the rhizosphere bacterial community but not the structure, especially since this strain displays good impacts on

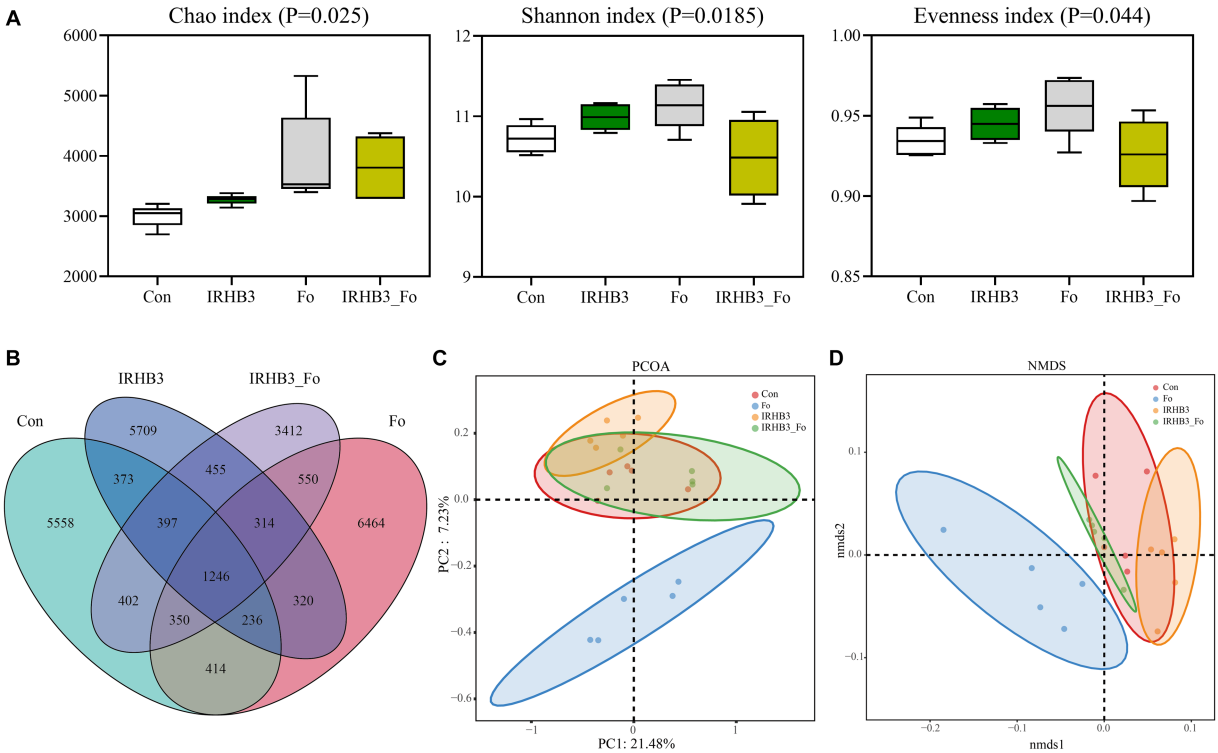

FIGURE 3
The diversity, structure, and abundance of the rhizosphere bacteria were community affected by four different treatments. **(A)** Alpha diversity analysis. **(B)** Venn diagram of rhizosphere bacterial OUTs. **(C)** PCOA principal component analysis. **(D)** NMDS structure analysis.

recovering the bacterial diversity and structure affected by *F. oxysporum*.

3.5 IRHB3 does not directly recruit beneficial biological microbes in soybean rhizosphere

Previous studies demonstrated that *Pseudomonas*, *Bacillus*, *Streptomyces*, *Flavobacterium*, *Rhizobia*, and *Microbacterium* were common beneficial microorganisms in the soil. Therefore, we compared the relative abundance of these bacterial genera in rhizosphere soil from four treatments. As shown in Figure 4, there were no significant differences in the abundance of rhizosphere *Pseudomonas*, *Bacillus*, *Streptomyces*, and *Microbacterium* among the four treatments. In contrast, *Flavobacterium* was considerably recruited by both *F. oxysporum* and IRHB3 as compared to the control, whereas *Rhizobium* was preferably accumulated by *F. oxysporum* rather than IRHB3. These results demonstrate that neither IRHB3 nor *F. oxysprum* have any direct impacts on *Pseudomonas*, *Bacillus*, *Streptomyces*, or *Microbacterium*, but they might have certain competition on the activation or re-activation of *Flavobacterium* and *Rhizobium*.

3.6 IRHB3 recruits functional bacteria related to phosphorus and nitrogen utilization for rhizosphere colonization

Nitrogen and phosphorus, as essential nutrients for plant growth and development, have an influence on the structure of the rhizosphere microbial community. In return, some soil microbes have the ability to activate or convert unusable nitrogen and phosphorus into usable forms to meet the nutrient demands of plants (Agren et al., 2012). In the current study, 12 bacterial genera, including *Tengunoibacter*, *Dictyobacter*, *Methylovirgula*, *Terracidiphilus*, *Candidatus dormibacter*, *Acidobacteriaceae*, *Conexibacter*, *Methylobacillus*, *Geobacter*, *Geomonas*, *Candidatus solibacter*, *Occallatibacter*, and *Candidatus koribacter*, were positively correlated with soil available phosphorus (AP), alkaline nitrogen (AN), and total nitrogen (TN). In addition, 17 genera of bacteria, like *Frateuria*, *Phycisphaera*, *Nodosilinea*, *Cupriavidus*, *Paraflavitalea*, *Achromobacter*, *Geoalkalibacter*, *Niabella*, *Schlesneria*, *Terrimonas*, *Pirellula*, *Gemmatimonas*, *Rhodocyclus*, *Bellilinea*, *Rhodanobacter*, *Pyrinomonas*, and *Luteitalea*, were negatively correlated with AP, AN, and TN, implying their negative effects on the nutrient uptake of soybean (Figure 5A).

To further uncover whether these functional bacteria related to nitrogen and phosphorate uptake and utilization can be affected by the biocontrol strain IRHB3 or the pathogen *F. oxysporum*, the relative abundance of these genera in rhizosphere soil was compared among four different treatments. As shown in Figure 5B, except for *Conexibacter*, *Acidobacteriaceae*, and *Tengunoibacter*, IRHB3 effectively increased the relative abundance of 10 potential phosphorus-solubilizing and nitrogen-fixing function bacteria in the soybean rhizosphere as compared to the control. *F. oxysporum* inoculation had almost no impact on the relative abundance of these functional bacteria; however, once IRHB3 was added to the *F. oxysporum*-inoculated soil, it largely decreased the abundance of seven functional bacteria, including *Candidatus Koribacter*, *Occallatibacter*, *Geomonas*, *Geobacter*, *Methylobacillus*, *Candidatus Dormibacter*, and *Terracidiphilus*, which obviously were increased by IRHB3, indicating that *F. oxysporum* abolished the positive effects of IRHB3 on phosphorus and nitrogen utilization (Figure 5B).

Moreover, the annotation data based on high-throughput sequencing showed that five functional bacteria, such as *Geobacter*, *Geomonas*, *Candidatus solibacter*, *Occallatibacter*, and *Candidatus koribacter*, belonged to core bacteria in the rhizosphere soil of soybean, as shown in Figure 6, and meanwhile, compared with the control, IRHB3 administration increased the relative abundance of these five functional bacteria. Compared with *F. oxysporum*, the addition of IRHB3 to *F. oxysporum*-treated soil recovered the relative abundance of *Candidatus koribacter*, *Occallatibacter*,

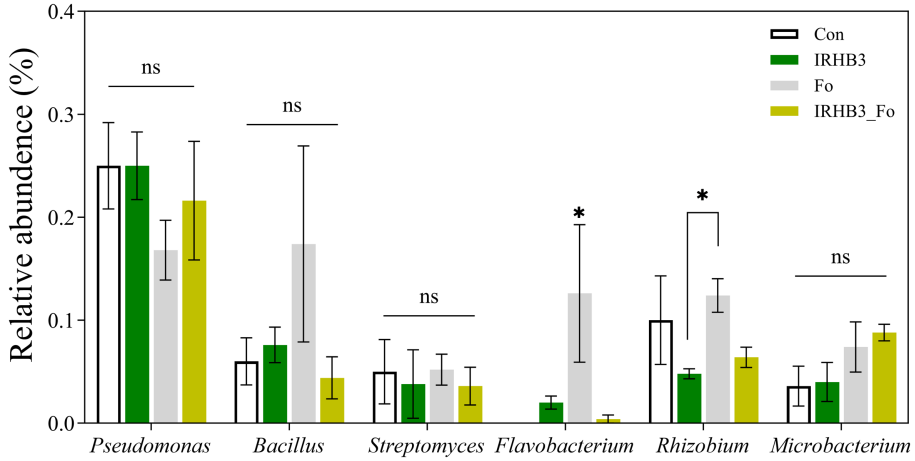

FIGURE 4
Relative abundance of six species of beneficial bacteria. ns represents no significant difference, whereas asterisks indicate significant differences ($p < 0.05$) according to Duncan's multiple range test.

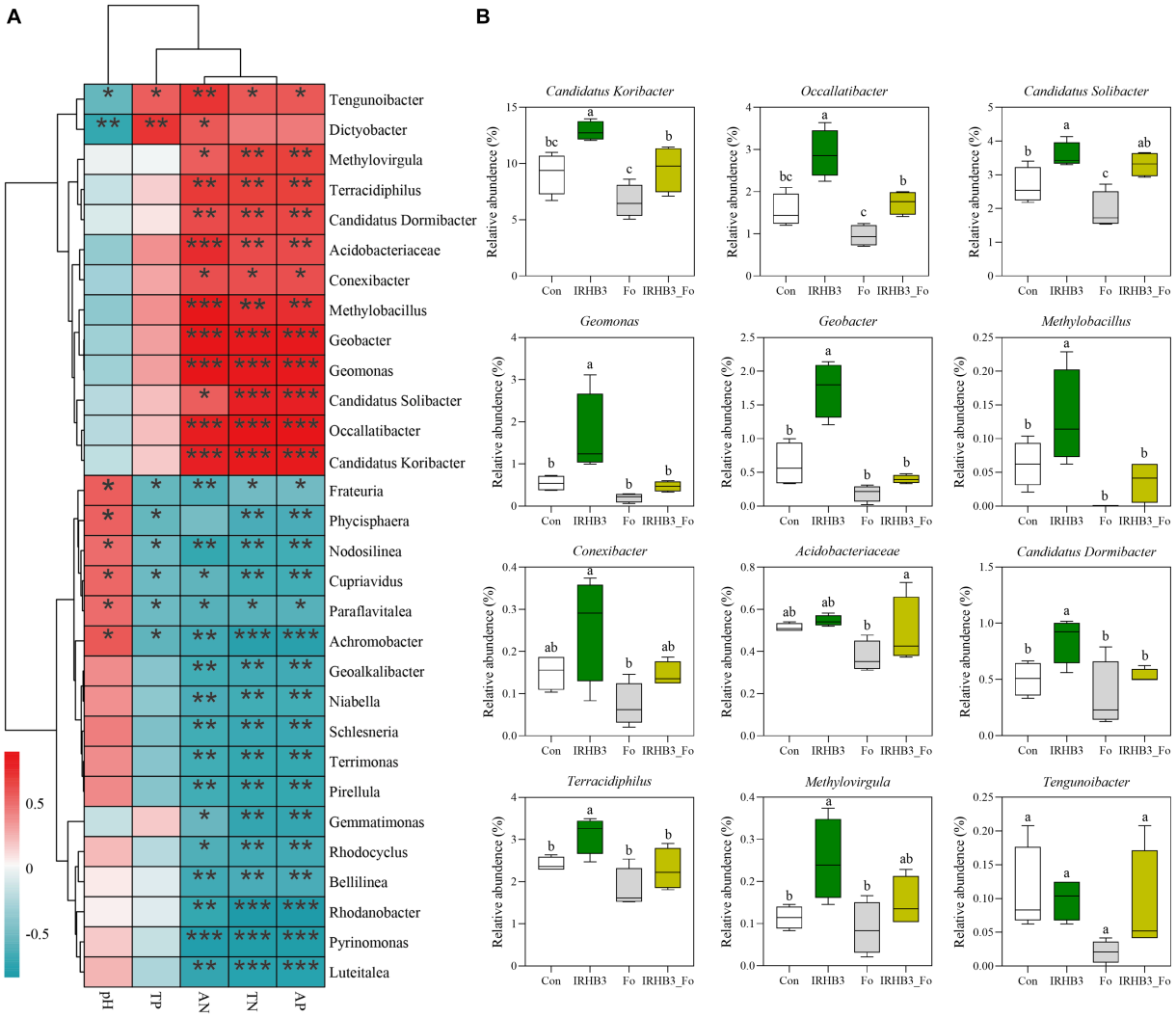

FIGURE 5
Function-based bacterial analysis related to phosphorus solution and nitrogen fixation among different treatments. **(A)** Correlation analysis of soil chemistry and bacterial communities. Red represents a positive correlation; blue represents a negative correlation. *$p < 0.05$; **$p < 0.01$; ***$p < 0.001$. **(B)** Relative abundance of phosphorus solution and nitrogen fixation functional bacteria.

Candidatus solibacter, and *Terracidiphilus* to some extent. Furthermore, *Methylobacillus* was the unique functional bacterium recruited by IRHB3 but was not detected in *F. oxysporum*-inoculated treatment.

3.7 IRHB3 depends on the JA signaling pathway to induce systemic resistance

To find out whether IRHB3 was able to induce host resistance, both *PR1* and *PR5* were selected as the markers for SA signaling-mediated SAR, whereas *PDF1.2* and *LOX2* were used as the detection for JA signaling-mediated ISR. Relative gene expression was examined from soybean roots at V5 and R2 growth stages from four different treatments. As shown in Figure 7A, compared with the control, *PR1* was remarkably induced by *F. oxysporum* at the V5 stage, but it decreased after IRHB3 addition. Although IRHB3 had no significant effect on *PR1* expression, it significantly reduced *PR1* expression levels induced by *F. oxysporum* (Figure 7A). At the R2 stage, *F. oxysporum* did not alter *PR1* expression as compared to the control, but the IRHB3 supplement induced a lower expression level of *PR1* as compared to *F. oxysporum*. For the *PR5* gene, there were similar trends of gene expression activation at the V5 and R2 stages. Interestingly, all three treatments of IRHB3, *F. oxysporum*, and IRHB3_Fo significantly decreased *PR5* expression as compared to the control, when IRHB3 addition had almost no impact on *PR5* expression, which was downregulated by *F. oxysporum*. Therefore, neither IRHB3 nor *F. oxysporum* could induce *PR5*-dependent soybean resistance. Thus, IRHB3 and *F. oxysporum* have distinct impacts on *PR1* and *PR5* expression. *F. oxysporum* inoculation trends to activate *PR1*-mediated SA signaling, whereas IRHB3-triggered resistance might not or at least not totally depend upon this pathway.

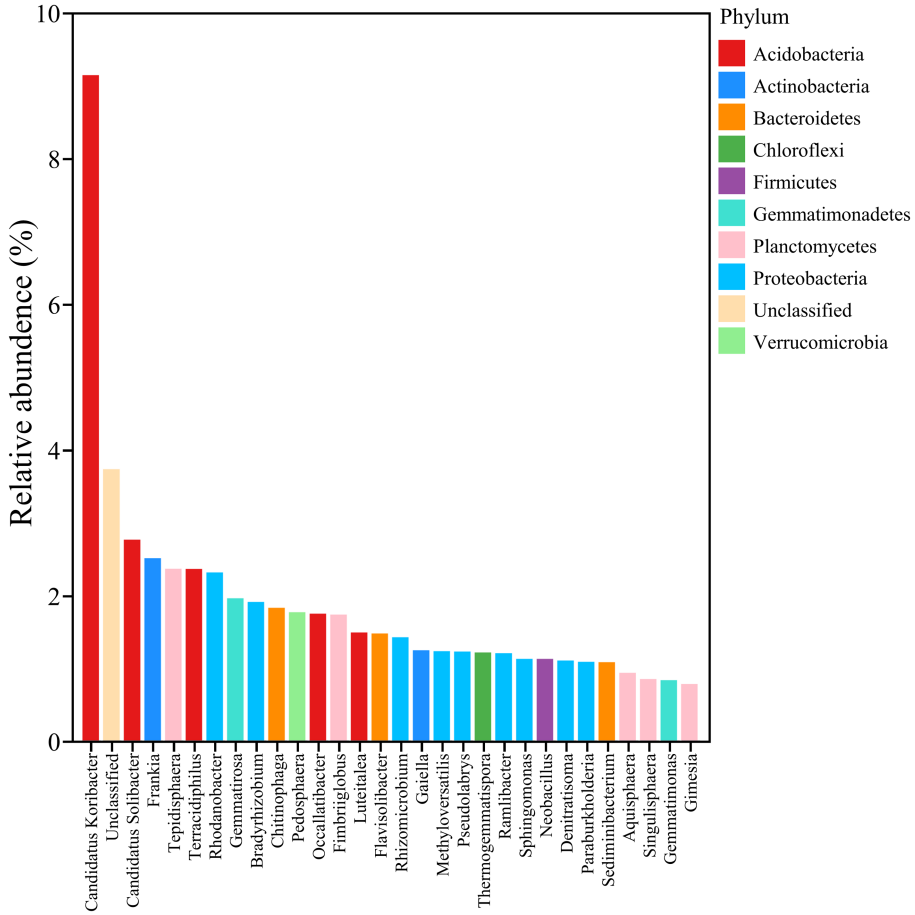

FIGURE 6
Core bacteria in rhizosphere soil (top 30).

JA signaling is often activated by wounding or necrotrophic pathogen attacks and is often related to induced systemic resistance (ISR). In this study, as shown in Figure 7B, we found that IRHB3 dramatically induced *PDF1.2* and *LOX2* gene expression as compared to the control at the V5 growth stage of soybean, but IRHB3 addition to the soil did not affect the expression of both *PDF1.2* and *LOX2*, which were not triggered by *F. oxysporum* inoculation. At the R2 stage, although IRHB3 continuously triggered *PDF1.2* expression and even enhanced *PDF1.2* expression when co-treated with *F. oxysporum*, it failed to activate *LOX2* expression. In general, IRHB3 prefers to activate JA-mediated ISR rather than SA-dependent SAR to confront pathogen attacks in the soybean rhizosphere.

3.8 IRHB3 induces expression of nodulation genes to promote symbiotic nitrogen fixation

As shown in Figure 7C, IRHB3 observably increased the expression level of nodulation-related genes *GmENOD40b* and *GmRIC1* of soybean roots rather than control, but it had almost no statistically significant influences on *GmNIN-2b* expression at V5 stages. In comparison, *F. oxysporum* remarkably suppressed the expression of *GmENOD40b* and *GmRIC1*, but IRHB3 addition into *F. oxysporum*-infected soil (IRHB3_Fo) effectively re-activated *GmENOD40b* and also weakly affected the other two genes. Surprisingly, IRHB3 induced much higher expression of *GmENOD40b*, *GmNIN-2b*, and *GmNIN-2b* at the R2 stage as compared to control, and meanwhile, even IRHB3 co-inoculation with *F. oxysproum* (IRHB3_Fo) did not decrease the high expression level of three genes. In particular, *GmNIN-2b* had an even higher level than that in IRHB3-treated roots. Thus, IRHB3 could activate nodulation gene expression to promote root nodule formation, which is rarely affected by pathogen attacks.

4 Discussion

The rhizosphere is the core area of the plant–microbe–pathogen interaction that determines the occurrence of soil-borne diseases (Raaijmakers et al., 2008). The rhizosphere microbiome has recently been recognized as the first defense line to limit pathogen invasion and maintain plant health (Eisenhauer et al., 2010; Berendsen et al., 2012). In particular, beneficial rhizosphere microbes play an important role in plant health and defenses, and

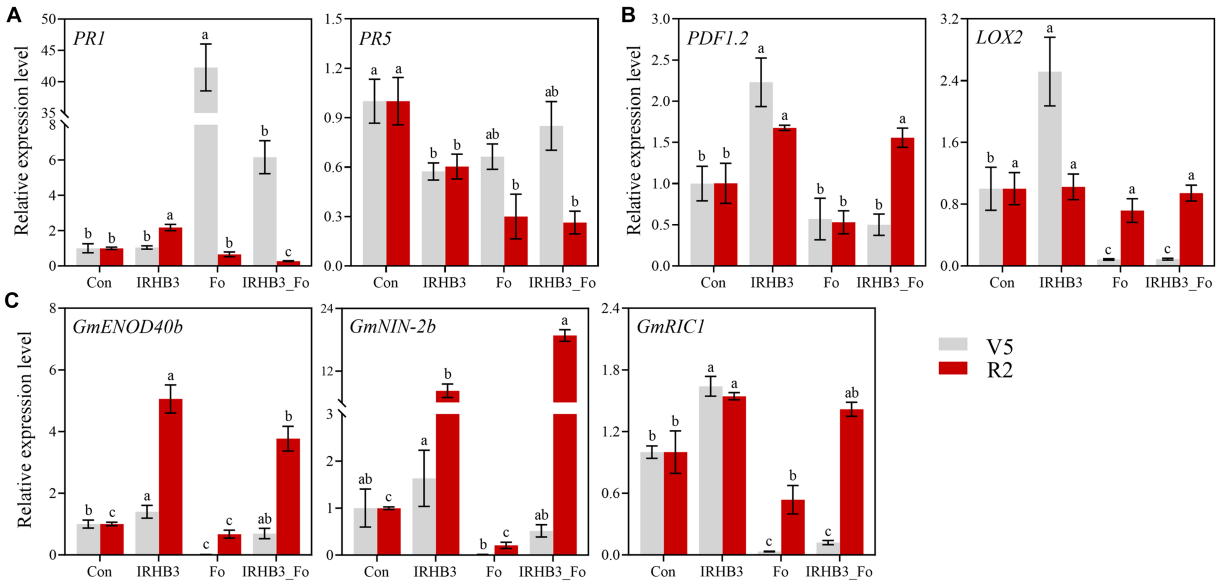

FIGURE 7
Expression analysis of defense and nodulation signaling marker genes in soybean root. **(A)** Relative expression levels of *PR1* and *PR5* related to SA signaling. **(B)** Relative expression levels of *PDF1.2* and *LOX2* related to JA signaling. **(C)** Relative expression levels of *GmENOD40b*, *GmNIN-2b*, and *GmRIC1* related to nodulation signaling Gene relative expression was calculated using the $2^{-\Delta\Delta Ct}$ method with the *GmActin* gene as a reference for normalization. The gray and red bars represent the relative expression levels of marker genes at the V5 and R2 periods, respectively. Different lowercase letters in the same color bar indicate significant differences ($p < 0.05$) according to Duncan's multiple range test.

some of them have also been widely applied as biocontrol agents for soil-borne disease control. IRHB3 was screened from the intercropped soybean rhizosphere, and it not only displayed good antagonistic effects on the main *Fusarium* species of soybean root rot as well as several agricultural fungi but also exhibited certain growth promotion (Chang et al., 2022; Wei et al., 2023). Here, we further find out the disease biocontrol and growth-promoting mechanisms of *P. chlororaphis* IRHB3 when introduced into field soil. We found that IRHB3 significantly improved root development and increased root nodules. In particular, when supplemented with *F. oxysporum*-inoculated soil, IRHB3 nearly suppressed root rot, alleviated the negative effects caused by *F. oxysporum*, and rescued the root nodulation ability. These results are consistent with those previously examined in the greenhouse (Wei et al., 2023).

The diversity and structure of the rhizosphere microbiome play an important role in the homeostasis of rhizosphere microecology (Eisenhauer et al., 2010). A higher microbial diversity and suitable combination are more conducive to hosts when coped with environmental stimuli (Garbeva et al., 2004; Wei et al., 2015). Our previous studies found that the rhizosphere microorganisms of strip intercropped soybeans had a higher diversity and attracted more beneficial microorganisms as compared to those under soybean monoculture, ultimately resulting in stronger resistance to root rot (Chang et al., 2022; Xu et al., 2022). In the current study, IRHB3 application improved the diversity of the rhizosphere bacterial community, and IRHB3 also had remarkable advantages in recovering the rhizosphere bacterial diversity that was altered by the pathogen *F. oxysporum*, thus maintaining the homeostasis of the healthy rhizosphere microbiome in plant hosts.

In addition, Xiong et al. (2017) and Tao et al. (2020) found that the application of bio-fertilizer *Bacillus* in field soil recruited more PGPR *Pseudomonas* sp., *Bacillus* sp., etc. for colonization in the host rhizosphere. Chihaoui et al. (2015) reported that inoculation of nodule-endophyte *Agrobacterium* sp. 10C2 altered the abundance and structure of rhizosphere bacteria and increased the relative abundance of PGPR *B. licheniformis*, *B. pumilus*, *B. senegalis*, etc., thereby promoting root nodulation and growth. Previous studies have shown that maize–soybean strip intercropping is capable of recruiting much richer and more diverse species of *Pseudomonas*, *Bacillus*, *Streptomyces*, and *Microbacterium* in the soybean rhizosphere when compared with monoculture (Chang et al., 2022). However, as one representative beneficial bacterial strain, IRHB3 addition in field soil did not significantly recruit *Pseudomonas*, *Bacillus*, *Streptomyces*, and *Microbacterium* for colonization in the soybean rhizosphere as compared to *F. oxysporum* and the blank control. In contrast, the pathogen *F. oxysporum* inoculation attracted some beneficial genera like *Flavobacterium* and *Rhizobium*. This can be explained by the "Cry help" of host plants, which tends to recruit beneficial microbiome colonization to build an alliance to resist pathogen infection (Liu et al., 2021). Similarly, Yin et al. (2021) found that successive monocultures and pathogen *Rhizoctonia solani* AG8 infection could stimulate wheat to regulate rhizosphere microbiome structure and specifically accumulate a group of beneficial microbiomes, such as *Chitinophaga*, *Pseudomonas*, *Chryseobacterium*, *Flavobacterium*, and *Rhizobium*, to inhibit fungal pathogens. Wen et al. (2020) study showed that the host root could actively secrete long-chain fatty acids, amino acids, etc. to recruit specific beneficial bacteria, *Pseudomonas* sp., to help the host alleviate the damage caused by shoot pathogen infection.

Thus, IRHB3 suppression of root rot might not depend on its attraction to other biocontrol bacteria.

Nitrogen (N) and phosphorus (P) are the essential macronutrients for plant growth and development (Pradhan et al., 2015). Unfortunately, most of the N and P in the soil cannot be directly utilized by plants due to their mineralization (Agren et al., 2012; Alori et al., 2017). However, some microbes related to P solubilization and N fixation can effectively improve the uptake and utilization of soil nutrients (Rodríguez and Fraga, 1999). Song et al. (2022) reported nine species of P-solubilizing bacteria (PSBs) from the rhizosphere soil of intercropped soybean, and these functional bacteria increased the solubilization of unavailable P and improved soil P availability through secreting organic acids to promote maize seed germination and seedling growth. Zhang et al. (2022) showed that *Curtobacterium citreum* A02, as a nitrogen-fixing bacterium, promoted cassava growth through nitrogen fixation, P dissolution, and IAA secretion. In this study, we found that IRHB addition increased the contents of available N and P nutrients in soybean rhizosphere soil, and the same effects had also been observed in the co-treatment of IRHB3 and *F. oxysporum*. Analysis of the rhizosphere microbiome demonstrated that a total of 12 bacterial genera were closely related to P solubilization and N fixation, and among them, five genera, including *Geobacter*, *Geomonas*, *Candidatus solibacter*, *Occallatibacter*, and *Candidatus Koribacter,* were the most abundant and core bacteria in field soil. Interestingly, both IRHB3 and IRHB3_Fo treatments could significantly attract those P solubilization and N fixation bacteria for colonization in the soybean rhizosphere. Furthermore, since *GmENOD40b*, *GmNIN-2b*, and *GmRIC1* are early nodulation genes in soybean (Hayashi et al., 2012; Lin et al., 2012), we found that IRHB3 activated expression of these three nodulation genes in the early stages (V5), whereas *F. oxysporum* significantly inhibited the expression of these genes. This supports that IRHB3 promotes root development and increases root nodules rather than *F. oxysporum*, which is also consistent with previous research (Tyler, 2007; Lin et al., 2012). Based on these results, we can predict that IRHB3 cooperates with local functional bacteria responsible for nutrient availability to improve root development and nodule formation, eventually contributing to growth promotion.

When faced with the complex composition of a field ecosystem, most externally applied beneficial microbes struggle to survive because of poor competition, low colonization, weak environmental adaptation, and other factors (Jez et al., 2016; Zhang et al., 2020). Some researchers pointed out that the abundance of single-species microorganisms in soil needs to account for 10^5 cfu·g^{-1} at least to perform individual function (Pieterse et al., 2014; Liu et al., 2021). In the current study, the abundance of IRHB3 and *F. oxsporum* was gradually decreased in soybean rhizosphere soil during the growth period through monitoring relative gene copies using RT-qPCR. The amounts of the pathogen *F. oxyporum* were more than 10^5 cfu·g^{-1} in the whole life of soybean growth to continuously infect soybean, and it had a close correlation with the disease index of root rot. In contrast, IRHB3 in the soybean rhizosphere only maintained a high abundance at the V5 stage, and after that, IRHB3 still survived, but its overall population was probably not enough to provide specific help for the host in an individual way. Moreover, correlation analysis shows that there was no significant correlation between *P. chlororaphis* and *F. oxysporum* in soil. This indicates that IRHB3 does not directly defend against *F. oxysporum* to suppress root rot. Furthermore, beneficial microbes often induce host resistance to cope with pathogen invasion. Yang et al. (2023) reported that the application of *B. proteolyticus* OSUB18 activated ISR through upregulating expression levels of genes *PDF1.2*, *LOX3*, etc. In this study, although IRHB3 did not significantly recruit a set of other beneficial biocontrol microbes in the rhizosphere, its addition dramatically activated high-level expression of *PDF1.2* and *LOX2*, which are responsible for JA-mediated ISR, rather than *PR1*, which is related to SA-mediated SAR. Thus, IRHB3 might trigger JA-mediated ISR to confront *F. oxysporum* infection.

Above all, we depicted one simple work model of IRHB3 when applied to field soil and interacted with the pathogen *F. oxysporum*, as shown in Figure 8. As the pathogen microbe of root rot, *F. oxysporum* inoculation changes the diversity of the rhizosphere microbial community, especially reducing some species related to P and N utilization, inhibiting the expression of nodulation genes, and thus severely affecting plant root development, nodule formation, and soybean yield. On the plant side, to ensure survival, the "Cry help" strategy in soybeans is rapidly activated. Typically, a high abundance of beneficial microbes like *Flavobacterium* are rapidly recruited in the soybean rhizosphere, and plant SAR is activated to fight with or suppress pathogen infection while plant-promoting microbes like *Rhizobium* partially maintain plant growth. In contrast, *P. chlororaphis* IRHB3 is one typical PGPR beneficial to soybeans. When added to field soil, it significantly optimizes the diversity of the soybean rhizosphere microbiome, recruits more microbes responsible for P and N utilization, and activates a set of nodulation gene expression that contribute to root development and the increase in root nodules and soybean yield. In addition, JA-mediated ISR can also be induced to enhance plant adaptation to external stimuli. Due to the IRHB3 biocontrol function, the application of IRHB3 into *F. oxysporum*-inoculated soil effectively improves root development and nodulation ability and alleviates the symptoms of root rot.

5 Conclusion

This study demonstrates that the application of IRHB3 in the field could increase bacteria diversity and recruit more P solubilization and N fixation functional bacteria for colonization in the soybean rhizosphere. IRHB3 also enhanced host symbiotic nitrogen fixation efficiency by activating nodule-related gene expression to promote plant growth. When plants were faced with rhizosphere microstructure changes caused by the pathogen *F. oxysporum*, IRHB3 could effectively alleviate this stress by maintaining the healthy homeostasis of rhizosphere bacteria. Moreover, IRHB3 and their microbiome could trigger ISR, depending on the JA signaling pathway, to improve host disease resistance. Due to the growth promotion and disease resistance characteristics of IRHB3 in collaboration with the local microbiome, the soybean seed harvest was significantly increased upon IRHB3 treatment and even when combined with *F. oxysporum* inoculation.

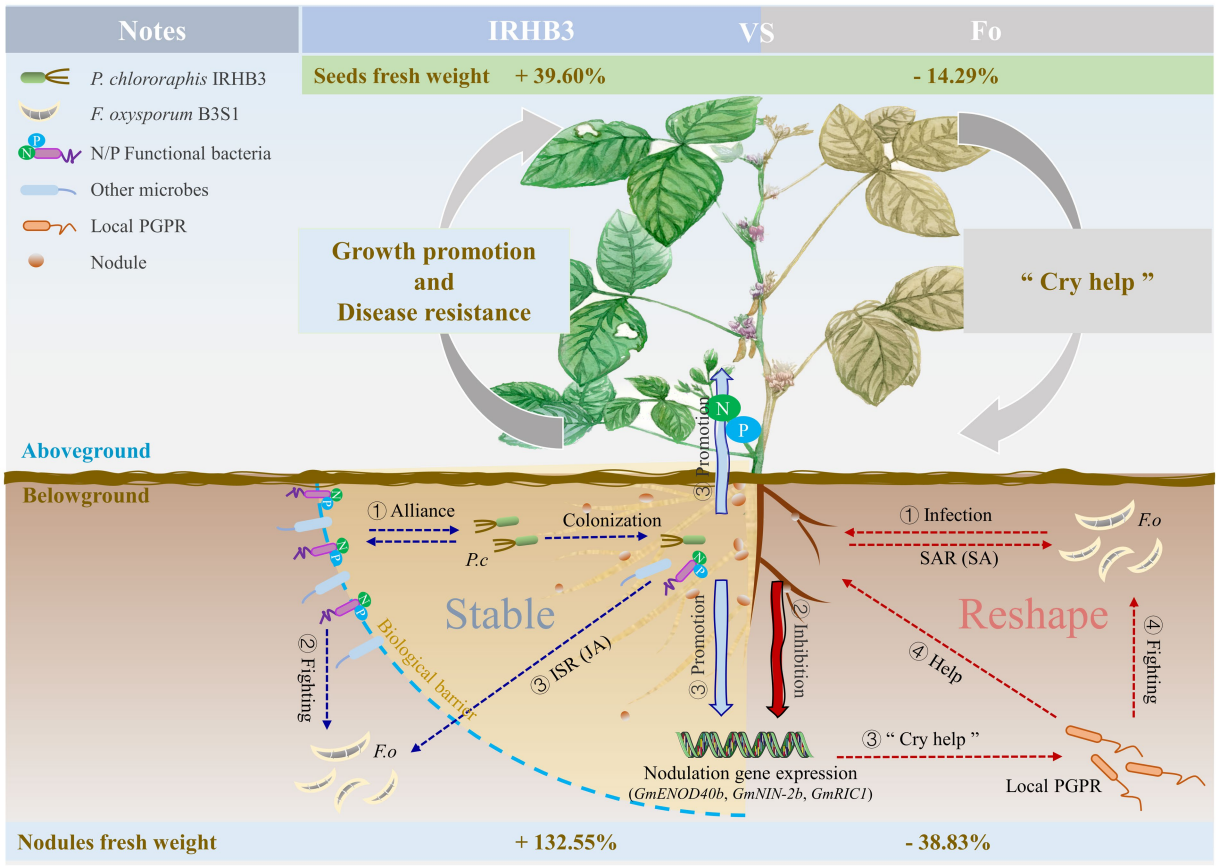

FIGURE 8
Schematic diagram of the mechanism of soybean growth promotion and disease suppression in the field for IRHB3.

Data availability statement

The original contributions presented in the study are included in the article/Supplementary material, further inquiries can be directed to the corresponding author.

Author contributions

DW: Data curation, Methodology, Software, Visualization, Writing – original draft, Validation, Writing – review & editing. DZ: Validation, Visualization, Writing – original draft. YZ: Data curation, Writing – original draft, Software. ZY: Software, Writing – original draft. YH: Software, Writing – original draft. CS: Funding acquisition, Writing – review & editing. WY: Funding acquisition, Writing – review & editing. XC: Funding acquisition, Writing – review & editing, Project administration.

Funding

The author(s) declare financial support was received for the research, authorship, and/or publication of this article. This work was supported by the Natural Science Foundation of Sichuan Province (2022NSFSC0173), the Project of Sichuan Innovation Team of the National Modern Agricultural Industry Technology System (Sccxtd-2023-20), and the Key Research and Development Plan of Sichuan Province (2023YFN0018).

Conflict of interest

The authors declare that the research was conducted in the absence of any commercial or financial relationships that could be construed as a potential conflict of interest.

Publisher's note

All claims expressed in this article are solely those of the authors and do not necessarily represent those of their affiliated organizations, or those of the publisher, the editors and the reviewers. Any product that may be evaluated in this article, or claim that may be made by its manufacturer, is not guaranteed or endorsed by the publisher.

Supplementary material

The Supplementary material for this article can be found online at: https://www.frontiersin.org/articles/10.3389/fmicb.2024.1328863/full#supplementary-material

References

Abdelaziz, A. M., Hashem, A. H., El-Sayyad, G. S., El-Wakil, D. A., Selim, S., Alkhalifah, D. H. M., et al. (2023). Biocontrol of soil borne diseases by plant growth promoting rhizobacteria. *Trop. Plant Pathol.* 48, 105–127. doi: 10.1007/s40858-022-00544-7

Agren, G. I., Wetterstedt, J. A. M., and Billberger, M. F. K. (2012). Nutrient limitation on terrestrial plant growth--modeling the interaction between nitrogen and phosphorus. *New Phytol.* 194, 953–960. doi: 10.1111/j.1469-8137.2012.04116.x

Ajayi-Oyetunde, O., and Bradley, C. (2017). Identification and characterization of rhizoctonia species associated with soybean seedling disease. *Plant Dis.* 101, 520–533. doi: 10.1094/PDIS-06-16-0810-RE

Alizadeh, H., Behboudi, K., Ahmadzadeh, M., Javan-Nikkhah, M., Zamioudis, C., Pieterse, C. M. J., et al. (2013). Induced systemic resistance in cucumber and *Arabidopsis thaliana* by the combination of *Trichoderma harzianum* Tr6 and *Pseudomonas* sp. Ps14. *Biol. Control* 65, 14–23. doi: 10.1016/j.biocontrol.2013.01.009

Alori, E. T., Glick, B. R., and Babalola, O. O. (2017). Microbial phosphorus solubilization and its potential for use in sustainable agriculture. *Front. Microbiol.* 8:971. doi: 10.3389/fmicb.2017.00971

Amato, K. R., Yeoman, C. J., Kent, A., Righini, N., Carbonero, F., Estrada, A., et al. (2013). Habitat degradation impacts black howler monkey (*Alouatta pigra*) gastrointestinal microbiomes. *ISME J.* 7, 1344–1353. doi: 10.1038/ismej.2013.16

Arif, I., Batool, M., and Schenk, P. M. (2020). Plant microbiome engineering: expected benefits for improved crop growth and resilience. *Trends Biotechnol.* 38, 1385–1396. doi: 10.1016/j.tibtech.2020.04.015

Berendsen, R. L., Pieterse, C. M., and Bakker, P. A. (2012). The rhizosphere microbiome and plant health. *Trends Plant Sci.* 17, 478–486. doi: 10.1016/j.tplants.2012.04.001

Bukhat, S., Imran, A., Javaid, S., Shahid, M., Majeed, A., and Naqqash, T. (2020). Communication of plants with microbial world: exploring the regulatory networks for PGPR mediated defense signaling. *Microbiol. Res.* 238:126486. doi: 10.1016/j.micres.2020.126486

Cao, Y., Pi, H., Chandrangsu, P., Li, Y., Wang, Y., Zhou, H., et al. (2018). Antagonism of two plant-growth promoting *Bacillus velezensis* isolates against *Ralstonia solanacearum* and *Fusarium oxysporum*. *Sci. Rep.* 8:4360. doi: 10.1038/s41598-018-22782-z

Casida, J. E., and Durkin, K. A. (2017). Pesticide chemical research in toxicology: lessons from nature. *Chem. Res. Toxicol.* 30, 94–104. doi: 10.1021/acs.chemrestox.6b00303

Chang, X., Dai, H., Wang, D., Zhou, H., He, W., Fu, Y., et al. (2018). Identification of *fusarium* species associated with soybean root rot in Sichuan Province, China. *Eur. J. Plant Pathol.* 151, 563–577. doi: 10.1007/s10658-017-1410-7

Chang, X., Wei, D., Zeng, Y., Zhao, X., Hu, Y., Wu, X., et al. (2022). Maize-soybean relay strip intercropping reshapes the rhizosphere bacterial community and recruits beneficial bacteria to suppress *Fusarium* root rot of soybean. *Front. Microbiol.* 13:1009689. doi: 10.3389/fmicb.2022.1009689

Chihaoui, S. A., Trabelsi, D., Jdey, A., Mhadhbi, H., and Mhamdi, R. (2015). Inoculation of *Phaseolus vulgaris* with the nodule-endophyte *Agrobacterium* sp. 10C2 affects richness and structure of rhizosphere bacterial communities and enhances nodulation and growth. *Arch. Microbiol.* 197, 805–813. doi: 10.1007/s00203-015-1118-z

Choudhary, D. K., Prakash, A., and Johri, B. N. (2007). Induced systemic resistance (ISR) in plants: mechanism of action. *Indian J. Microbiol.* 47, 289–297. doi: 10.1007/s12088-007-0054-2

Compant, S., Samad, A., Faist, H., and Sessitsch, A. (2019). A review on the plant microbiome: ecology, functions, and emerging trends in microbial application. *J. Adv. Res.* 19, 29–37. doi: 10.1016/j.jare.2019.03.004

Cruz, D. R., Leandro, L. F. S., Mayfield, D. A., Meng, Y., and Munkvold, G. P. (2020). Effects of soil conditions on root rot of soybean caused by *Fusarium graminearum*. *Phytopathology* 110, 1693–1703. doi: 10.1094/PHYTO-02-20-0052-R

Durrant, W. E., and Dong, X. (2004). Systemic acquired resistance. *Annu. Rev. Phytopathol.* 42, 185–209. doi: 10.1146/annurev.phyto.42.040803.140421

Eisenhauer, N., Beßler, H., Engels, C., Gleixner, G., Habekost, M., Milcu, A., et al. (2010). Plant diversity effects on soil microorganisms support the singular hypothesis. *Ecology* 91, 485–496. doi: 10.1890/08-2338.1

Garbeva, P., van Veen, J. A., and van Elsas, J. D. (2004). Microbial diversity in soil: selection microbial populations by plant and soil type and implications for disease suppressiveness. *Annu. Rev. Phytopathol.* 42, 243–270. doi: 10.1146/annurev.phyto.42.012604.135455

Han, L., Wang, Z., Li, N., Wang, Y., Feng, J., and Zhang, X. (2019). *Bacillus amyloliquefaciens* B1408 suppresses *Fusarium* wilt in cucumber by regulating the rhizosphere microbial community. *Appl. Soil Ecol.* 136, 55–66. doi: 10.1016/j.apsoil.2018.12.011

Hayashi, S., Reid, D. E., Lorenc, M. T., Stiller, J., Edwards, D., Gresshoff, P. M., et al. (2012). Transient nod factor-dependent gene expression in the nodulation-competent zone of soybean (*Glycine max* [L.] Merr.) roots. *Plant Biotechnol. J.* 10, 995–1010. doi: 10.1111/j.1467-7652.2012.00729.x

Jez, J. M., Lee, S. G., and Sherp, A. M. (2016). The next green movement: plant biology for the environment and sustainability. *Science* 353, 1241–1244. doi: 10.1126/science.aag1698

Jiménez-Fernández, D., Montes-Borrego, M., Navas-Cortés, J. A., Jiménez-Díaz, R. M., and Landa, B. B. (2010). Identification and quantification of *Fusarium oxysporum* in planta and soil by means of an improved specific and quantitative PCR assay. *Appl. Soil Ecol.* 46, 372–382. doi: 10.1016/j.apsoil.2010.10.001

Lenis, J. M., Gillman, J. D., Lee, J. D., Shannon, J. G., and Bilyeu, K. D. (2010). Soybean seed lipoxygenase genes: molecular characterization and development of molecular marker assays. *Theor. Appl. Genet.* 120, 1139–1149. doi: 10.1007/s00122-009-1241-9

Lin, M. H., Gresshoff, P. M., and Ferguson, B. J. (2012). Systemic regulation of soybean nodulation by acidic growth conditions. *Plant Physiol.* 160, 2028–2039. doi: 10.1104/pp.112.204149

Liu, H., Carvalhais, L. C., Kazan, K., and Schenk, P. M. (2016). Development of marker genes for jasmonic acid signaling in shoots and roots of wheat. *Plant Signal. Behav.* 11:e1176654. doi: 10.1080/15592324.2016.1176654

Liu, H., Li, J., Carvalhais, L. C., Percy, C. D., Prakash Verma, J., Schenk, P. M., et al. (2021). Evidence for the plant recruitment of beneficial microbes to suppress soil-borne pathogens. *New Phytol.* 229, 2873–2885. doi: 10.1111/nph.17057

Liu, S., Zhang, M., Feng, F., and Tian, Z. (2020). Toward a "green revolution" for soybean. *Mol. Plant* 13, 688–697. doi: 10.1016/j.molp.2020.03.002

Livak, K. J., and Schmittgen, T. D. (2001). Analysis of relative gene expression data using real-time quantitative PCR and the 2(-Delta Delta C(T)) method. *Methods* 25, 402–408. doi: 10.1006/meth.2001.1262

Lozupone, C., Lladser, M. E., Knights, D., Stombaugh, J., and Knight, R. (2011). UniFrac: an effective distance metric for microbial community comparison. *ISME J.* 5, 169–172. doi: 10.1038/ismej.2010.133

Lugtenberg, B., and Kamilova, F. (2009). Plant-growth-promoting rhizobacteria. *Annu. Rev. Plant Biol.* 63, 541–556. doi: 10.1146/annurev.micro.62.081307.162918

Pathak, A., Sharma, A., and Johri, B. N. (2004). *Pseudomonas* strain GRP3 induces systemic resistance to sheath blight in rice. *Int. Rice Res. Notes* 29, 35–36.

Pieterse, C. M., Leon-Reyes, A., Van der Ent, S., and Van Wees, S. C. (2009). Networking by small-molecule hormones in plant immunity. *Nat. Chem. Biol.* 5, 308–316. doi: 10.1038/nchembio.164

Pieterse, C. M., Zamioudis, C., Berendsen, R. L., Weller, D. M., Van Wees, S., and Bakker, P. A. (2014). Induced systemic resistance by beneficial microbes. *Annu. Rev. Phytopathol.* 52, 347–375. doi: 10.1146/annurev-phyto-082712-102340

Pradhan, P., Fischer, G., Van Velthuizen, H., Reusser, D. E., and Kropp, J. P. (2015). Closing yield gaps: how sustainable can we be? *PLoS One* 10:e0129487. doi: 10.1371/journal.pone.0129487

Raaijmakers, J. M., Paulitz, T. C., Steinberg, C., Alabouvette, C., and Moënne-Loccoz, Y. (2008). The rhizosphere: a playground and battlefield for soilborne pathogens and beneficial microorganisms. *Plant Soil* 321, 341–361. doi: 10.1007/s11104-008-9568-6

Rodríguez, H., and Fraga, R. (1999). Phosphate solubilizing bacteria and their role in plant growth promotion. *Biotechnol. Adv.* 17, 319–339. doi: 10.1016/s0734-9750(99)00014-2

Santoyo, G. (2022). How plants recruit their microbiome? New insights into beneficial interactions. *J. Adv. Res.* 40, 45–58. doi: 10.1016/j.jare.2021.11.020

Schloss, P. D., Westcott, S. L., Ryabin, T., Hall, J. R., Hartmann, M., Hollister, E. B., et al. (2009). Introducing mothur: open-source, platform-independent, community-supported software for describing and comparing microbial communities. *Appl. Environ. Microbiol.* 75, 7537–7541. doi: 10.1128/AEM.01541-09

Song, C., Wang, W., Gan, Y., Wang, L., Chang, X., Wang, Y., et al. (2022). Growth promotion ability of phosphate-solubilizing bacteria from the soybean rhizosphere under maize-soybean intercropping systems. *J. Sci. Food Agric.* 102, 1430–1442. doi: 10.1002/jsfa.11477

Tao, C., Li, R., Xiong, W., Shen, Z., Liu, S., Wang, B., et al. (2020). Bio-organic fertilizers stimulate indigenous soil *Pseudomonas* populations to enhance plant disease suppression. *Microbiome* 8, 137–114. doi: 10.1186/s40168-020-00892-z

Tyler, B. M. (2007). Phytophthora sojae: root rot pathogen of soybean and model oomycete. *Mol. Plant Pathol.* 8, 1–8. doi: 10.1111/j.1364-3703.2006.00373.x

Verhagen, B. W., Trotel-Aziz, P., Couderchet, M., Höfte, M., and Aziz, A. (2010). *Pseudomonas* spp. induced systemic resistance to *Botrytis cinerea* is associated with induction and priming of defence responses in grapevine. *J. Exp. Bot.* 61, 249–260. doi: 10.1093/jxb/erp295

Wei, Z., Yang, T., Friman, V. P., Xu, Y., Shen, Q., and Jousset, A. (2015). Trophic network architecture of root-associated bacterial communities determines pathogen invasion and plant health. *Nat. Commun.* 6, 8413–8419. doi: 10.1038/ncomms9413

Wei, D., Zhu, D., Zhang, Y., Yang, Z., Wu, X., Shang, J., et al. (2023). Characterization of rhizosphere *Pseudomonas chlororaphis* IRHB3 in the reduction of *Fusarium* root rot and promotion of soybean growth. *Biol. Control* 186:105349. doi: 10.1016/j.biocontrol.2023.105349

Wen, T., Zhao, M., Yuan, J., Kowalchuk, G. A., and Shen, Q. (2020). Root exudates mediate plant defense against foliar pathogens by recruiting beneficial microbes. *Soil Ecol. Lett.* 3, 42–51. doi: 10.1007/s42832-020-0057-z

Xiong, W., Guo, S., Jousset, A., Zhao, Q., Wu, H., Li, R., et al. (2017). Bio-fertilizer application induces soil suppressiveness against *Fusarium wilt* disease by reshaping the soil microbiome. *Soil Biol. Biochem.* 114, 238–247. doi: 10.1016/j.soilbio.2017.07.016

Xiong, W., Li, Z., Liu, H., Xue, C., Zhang, R., Wu, H., et al. (2015). The effect of long-term continuous cropping of black pepper on soil bacterial communities as determined by 454 pyrosequencing. *PLoS One* 10:e0136946. doi: 10.1371/journal.pone.0136946

Xu, Y. L., and Wei, W. (2020). Research progress of *Fusarium* species and soybean root rot. *J. Northeast. Agric. Univ.* 3, 87–96. doi: 10.19720/j.cnki.issn.1005-9369.2020.03.0011

Xu, H., Yan, L., Zhang, M., Chang, X., Zhu, D., Wei, D., et al. (2022). Changes in the density and composition of rhizosphere pathogenic *Fusarium* and beneficial *Trichoderma* contributing to reduced root rot of intercropped soybean. *Pathogens* 11:478. doi: 10.3390/pathogens11040478

Yang, P., Zhao, Z., Fan, J., Liang, Y., Bernier, M. C., Gao, Y., et al. (2023). *Bacillus proteolyticus* OSUB18 triggers induced systemic resistance against bacterial and fungal pathogens in *Arabidopsis*. *Front. Plant Sci.* 14:1078100. doi: 10.3389/fpls.2023.1078100

Yin, C., Casa Vargas, J. M., Schlatter, D. C., Hagerty, C. H., Hulbert, S. H., and Paulitz, T. C. (2021). Rhizosphere community selection reveals bacteria associated with reduced root disease. *Microbiome* 9, 86–18. doi: 10.1186/s40168-020-00997-5

Zhang, Y., Gao, X., Shen, Z., Zhu, C., Jiao, Z., Li, R., et al. (2019). Pre-colonization of PGPR triggers rhizosphere microbiota succession associated with crop yield enhancement. *Plant Soil* 439, 553–567. doi: 10.1007/s11104-019-04055-4

Zhang, H., Godana, E. A., Sui, Y., Yang, Q., Zhang, X., and Zhao, L. (2020). Biological control as an alternative to synthetic fungicides for the management of grey and blue mould diseases of table grapes: a review. *Crit. Rev. Microbiol.* 46, 450–462. doi: 10.1080/1040841X.2020.1794793

Zhang, X., Tong, J., Dong, M., Akhta, R. K., and He, B. (2022). Isolation, identification and characterization of nitrogen fixing endophytic bacteria and their effects on cassava production. *Peer J.* 10:e12677. doi: 10.7717/peerj.12677

frontiers | Frontiers in Microbiology

TYPE Original Research
PUBLISHED 14 March 2024
DOI 10.3389/fmicb.2024.1374199

OPEN ACCESS

EDITED BY
Jianling Fan,
Nanjing University of Information Science and Technology, China

REVIEWED BY
Yongxin Lin,
Fujian Normal University, China
Jiangbing Xu,
Nanjing University of Information Science and Technology, China

*CORRESPONDENCE
Junjiang Long
✉ long0109_agro@163.com
Baoli Zhu
✉ baoli.zhu@isa.ac.cn

RECEIVED 21 January 2024
ACCEPTED 04 March 2024
PUBLISHED 14 March 2024

CITATION
Wang J, Qin H, Zhang L, Tang Y, Long J, Xu H and Zhu B (2024) Synergistic effects of rhizosphere effect and combined organic and chemical fertilizers application on soil bacterial diversity and community structure in oilseed rape cultivation.
Front. Microbiol. 15:1374199.
doi: 10.3389/fmicb.2024.1374199

Synergistic effects of rhizosphere effect and combined organic and chemical fertilizers application on soil bacterial diversity and community structure in oilseed rape cultivation

Jingyuan Wang[1,2], Hongling Qin[2], Leyan Zhang[1,2], Yafang Tang[3], Junjiang Long[1]*, Huaqin Xu[1] and Baoli Zhu[2]*

[1]College of Environment and Ecology of Hunan Agricultural University, Changsha, China, [2]Key Laboratory of Agro-ecological Processes in Subtropical Region, Institute of Subtropical Agriculture, Chinese Academy of Sciences, Changsha, China, [3]Hubei Key Laboratory of Quality Control of Characteristic Fruits and Vegetables, College of Life Science and Technology, Hubei Engineering University, Xiaogan, China

The combined application of chemical and organic fertilizers has been recognized to enhance soil fertility and foster the soil microbial ecosystem. However, the optimal ratio of chemical and organic fertilizers in oilseed rape cultivation is still uncertain, and the role of rhizosphere effect is still unclear. Thus, this study aimed to elucidate the impacts of varying ratios of chemical and organic fertilizers on the structure and potential functionalities of rhizosphere and non-rhizosphere soil microbial communities. The interplay of microbial communities with soil properties and oilseed rape root exudates was investigated in controlled pot cultivations receiving varying ratios of chemical and organic fertilizers. Results indicated clear segregation in the soil bacterial community, influenced by both fertilization treatments and rhizosphere effects. The bacterial community structure significantly correlated with nitrate nitrogen, organic acids, and dissolved organic carbon (DOC) content. Rhizosphere effects led to increased bacteria abundance, reduced diversity, and decreased network stability. Notably, F3 treatment receiving 25% chemical and 75% organic fertilizers showed a significantly higher abundance at 1.43×10^{11} copies g^{-1} dry soil, accompanied by increased species and genetic diversity, and ecological network complexity. This treatment also yielded the highest aboveground biomass of oilseed rape. However, the application of organic fertilizers also increased the risk of plant pathogenicity. This study reveals the impact of fertilizers and rhizosphere effects on soil microbial community structure and function, shedding light on the establishment of more effective fertilization schemes for oilseed rape agriculture.

KEYWORDS

oilseed rape, organic fertilizer, chemical fertilizer, rhizosphere effect, root exudates

1 Introduction

In agriculture, the augmentation of soil fertility usually involves substantial fertilizer applications to bolster crop yields (Brtnicky et al., 2023). However, the excessive reliance on chemical fertilizers has led to a range of environmental concerns, including biodiversity loss, soil acidification and degradation, greenhouse emissions, and contamination of ground and surface water systems (Searchinger et al., 2018; Yu et al., 2020; Kanthilanka et al., 2023). To mitigate the adverse repercussions of chemical fertilizer application, organic fertilizers have emerged as a potential alternative strategy (Chen et al., 2020; Kumari et al., 2024). Numerous studies have underscored the capacity of organic fertilizers to improve soil fertility and promote crop growth (Cui et al., 2018; Maltas et al., 2018; Wu et al., 2018; He et al., 2022; Li et al., 2024). However, organic fertilizer also has limitations, such as the nutrient release rate is often slow (Garzón et al., 2011; Zhang et al., 2024). Combined application of organic and chemical fertilizers has positive effects on soil fertility and microbial properties compared to application of single type of fertilizers (Qaswar et al., 2020; Kumari et al., 2024). Studies suggest prolonged application of mixed organic and chemical fertilizers improves crop growth, nutrient utilization, and yield stability across various crops, including wheat, apple, rice, and other crops (Wang et al., 2023; Zhao et al., 2023; Lu et al., 2024). This practice also nurtures bacterial resilience to environmental changes, promoting soil carbon and nitrogen cycling (Chen W. et al., 2023). Fertilizer application strategy and rates affect soil fertility, microorganisms, and crop growth (Li D. et al., 2023), reducing the amount of chemical fertilizers and determining the optimal ratio of organic fertilizers to chemical fertilizers are key measures to achieve sustainable agricultural development.

Soil microbial communities are integral to an array of soil- and plant-related processes and play a pivotal role in regulating plant health (Fahey et al., 2020). Microbial communities are fundamental in maintaining agricultural sustainability and the overall functioning of soil ecosystems (Trivedi et al., 2016; Manoharan et al., 2017; Vezzani et al., 2018). In recent years, the rhizosphere microbiota has received much attention due to the important role of beneficial interactions between roots and rhizosphere microorganisms in fostering plant growth (Zheng et al., 2017). Notably, rhizosphere microorganisms are regarded as the second genome of plants (Deng et al., 2021). These microorganisms can enhance nutrient availability, promote plant growth, and confer resilience on plants against various abiotic and biotic stresses (Zheng et al., 2018; Ali and Khan, 2021). Recent evidence suggests that an increase in endospheric microorganisms diversity and abundance under stress conditions might contribute to plant survival, suggesting a significant role of microbes in improving plant health (Yuan et al., 2018).

Soil microorganisms are sensitive to environmental changes, and fertilization often exerts a significant influence on microbial activity (Francioli et al., 2016). Studies have shown that moderate organic fertilizer applications increase bacterial abundance and diversity (Liu et al., 2021, 2023). For example, rhizosphere microbial biomass increased and endosphere microbial community composition changed significantly after the application of organic fertilizer (Peng et al., 2016); the combination of organic fertilizer and chemical fertilizer improved the soil quality of maize arable land, increased the diversity of bacterial communities, and led to a more stable bacterial network and an increase in the complexity of potential microbial metabolites (Lu et al., 2024). In addition, bacterial community composition varies depending on the proportion of organic fertilizer applied. For example, manure treatment enriched bacterial taxa involved in phosphorus transformation (Zhang et al., 2023). Thus, the blending of organic and chemical fertilizers emerges as a promising avenue to regulate soil health and enhance the microecological environment by modulating the soil bacterial community. However, there remains a dearth of research on the effects of organic-chemical fertilizer combinations on rhizosphere processes mediated by microbes and the intricate relationship between microbial diversity, soil properties, and crop root systems, particularly under diverse fertilization conditions (Pang et al., 2021).

Oilseed rape is a major cash crop in China and serves as a vital feedstock for biofuel production. While previous studies have demonstrated significant soil quality and yield improvements with the combined application of organic and chemical fertilizers, the specific impacts of chemical-organic fertilizer dosing on soil microbiology in oilseed rape cultivation remain nebulous. Therefore, this study aims to investigate the effects of chemical and organic fertilizer allocation alongside rhizosphere effects on the structure and potential functionalities of microbial communities in oilseed rape soils, and to determine the optimal chemical and organic fertilizer ratio for reducing chemical fertilizer usage while promoting oilseed rape growth, laying a theoretical foundation for the eco-efficient management of oilseed rape cultivation.

2 Materials and methods

2.1 Test materials and site selection

The experiment was conducted in a well-lit and ventilated greenhouse at the Institute of Subtropical Agriculture, Chinese Academy of Sciences (118°05′E, 28°12′N). The oilseed rape cultivar was Xiangmai Oil No. 6. The test soil was collected from 0 to 20 cm of dryland soil at the Taoyuan Agricultural Ecology Experimental Station of the Chinese Academy of Sciences (111°26′E, 28°55′N, 92.2 m above sea level). The soil used was typical red soil in subtropical regions (derived from Quaternary red clay), with a pH of 4.5, organic matter of 13.81 g kg^{-1}, total nitrogen 0.84 g kg^{-1}, total phosphorus 0.38 g kg^{-1}, total potassium 12.33 g kg^{-1}, alkaline dissolved nitrogen 77.81 g kg^{-1}, effective phosphorus 6.05 g kg^{-1}, and quick-acting potassium 103.40 g kg^{-1}.

2.2 Experimental design

The soil used for cultivation was air-dried and crushed, then passed through a 2-mm sieve, and after removing residues and impurities, the soil was mixed with fertilizers of different organic and chemical fertilizer ratios. Five fertilization treatments were set up, each receiving the same amount of total N, i.e., F0: application of chemical fertilizer alone (CK) was used as the control; F1: 25% organic fertilizer and 75% chemical fertilizer (1:3); F2: 50% organic fertilizer and 50% chemical fertilizer (1:1); F3: 75% organic fertilizer and 25% chemical fertilizer (3:1); and F4: only organic fertilizer was applied. Each treatment contained four replicates. Fertilizers with different ratios of chemical fertilizers were mixed well, considering the amount of

fertilizers applied in the field (Nitrogen fertilizers: 105–225 kg N ha^{-1}, Phosphorus fertilizers: 45–78 kg P ha^{-1}, Potassium fertilizers: 78–137 kg K ha^{-1}), so that the content of the fertilizers added to the potting soil eventually reached 200 mg kg^{-1} of N. Nitrogen, Phosphorus, and potassium fertilizers were added in the form of urea, calcium superphosphate, and potassium chloride, respectively, and organic fertilizers used were fermented and then air-dried cow dung, with nutrient contents of total N 1.09 g kg^{-1}, total P (as P_2O_5) 4.39 g kg^{-1} and total K (as K_2O) 18.46 g kg^{-1}.

PVC pots, 20 cm high and 16 cm in diameter, were used for cultivation experiments. Each pot was filled with 3.5 kg of mixed fertilizer soil, and the water content was adjusted to 75% of the soil water holding capacity. Then, three 2-week-old rapeseed seedlings in uniform growth were transplanted. After 15 days, the seedlings were planted. On day 58, when the rapeseed reached the budding stage, samples of rhizosphere soil (collected using the root shaking method) and non-rhizosphere soil were obtained. A portion of these soil samples was preserved in a refrigerator at 4°C for subsequent analysis of parameters including ammonium nitrogen, nitrate nitrogen, water content, soluble organic carbon, and rhizosphere secretion. The remaining portion underwent quick-freezing with liquid nitrogen and was stored at −80°C for molecular analysis.

2.3 Determination of rhizosphere exudates

Root exudates were collected via *ex-situ* incubation in 5 mM calcium chloride for 6 h, and then the total amount of amino acids was determined by an automatic amino acid analyzer (Hitachi L8900). The total amount of organic acids in the rhizosphere soil was detected with high-performance liquid chromatography (HPLC).

2.4 DNA extraction and library construction for 16S rRNA amplicon sequencing

DNA was extracted by the CTAB method and DNA quality was determined using a NanoDrop 1,000 spectrophotometer (Thermo Fisher Scientific, Wilmington, United States). Bacterial abundance was then determined by qPCR using a Roche LightCycler480II fluorescence quantitative PCR instrument. The bacterial 16S rRNA gene was amplified by polymerase chain reaction (PCR) using primer pair 338F (5′-ACTCCTACGGGGAGGCAGCA3′) and 806R (5′-GGACTACHVGGGTWTCTAAT-3′) (Langille et al., 2013). The amplicon samples were sequenced at MajorbioBio-Pharm Technology Co. Ltd. (Shanghai, China) using the Illumina MiSeq platform. After removing low quality reads, remaining sequences were divided into OTUs at 97% similarity using Uparse (version 7.0.1090) and were analyzed for other bioinformatic statistics.

2.5 Data analysis

Soil physicochemical properties have been determined in a previous study and the results of this data were used (Wang et al., 2021). One-way analysis of variance (ANOVA) was performed using SPSS 26.0 to determine differences in microbial composition and microbial α-diversity between treatments. Correlations between environmental factors, bacterial abundance, and species α-diversity were then plotted using origin2022b, and correlation heatmaps were utilized to assess the correlation between environmental factors, bacterial abundance, and species α-diversity, and differences in means were considered statistically significant if $p < 0.05$. Non-metric multidimensional scaling (NMDS) was used to investigate the effect of treatments on microbial community composition at the microbial OTU level. To compare α-diversity among treatments, OTU data were analyzed using the phylogenetic diversity (PD) metric and Shannon index. Redundancy analysis (RDA) was performed by Canoco5 where the statistical methods used to assess the significance of environmental factors were Monte Carlo tests, and ANOSIM (analysis of similarity) based on the OTU's Bray-Curtis distances was used to measure the effects of fertilizer application and rhizosphere effects on the composition of the bacterial community.

Full length 16S rRNA sequences of common pathogens were retrieved from NCBI, and were used as query to blast against our sequences using TBtools. Hit sequences with >=94% identity were considered as the same genus of respective pathogen. To reveal the potential effects of fertilization practices on microbial interactions, OTUs with abundance greater than 0.5% were used to construct microbial networks with Spearman using the "psych" package in R (version 3.6.3), and were visualized with Gephi 0.9.2. and set the set the *p*-value threshold to 0.01 and the correlation coefficient threshold to 0.7 to filter out the relationships with less than a certain correlation or frequency of co-occurrence. Complexity of the network and highlight important relationships. and various topological features of the bacterial networks were computed to infer the network characteristics.

3 Results

3.1 Soil bacterial abundance

The abundance of rhizosphere bacteria significantly responded to fertilizer treatments (Table 1), demonstrating an escalating trend with higher proportions of organic fertilizers (Supplementary Figure S1). Notably, F3 exhibited the highest bacterial abundance at 1.43×10^{11} copies g^{-1} dry soil, while F1 had the lowest at 2.96×10^{10} copies g^{-1}. In non-rhizosphere soils, the impact of fertilizer treatments on bacterial abundance was less pronounced, showing no significant differences among treatments. Interestingly, bacterial abundance in the F4 treatment receiving only chemical fertilizer was much higher in the rhizosphere soil than in the non-rhizosphere. Rhizosphere bacterial 16S rRNA gene abundance showed a positive correlation with total amino acids, while non-rhizosphere abundance correlated positively with soil water content (Supplementary Figure S2).

3.2 Soil microbial diversity

A total of 2,240,027 high-quality sequences with an average length of 432 bp were obtained in this study, and a total of 3,092

operational taxonomic units (OTUs) were classified at 97% sequence similarity cutoff. Differences in microbial diversity existed between the rhizosphere and non-rhizosphere (Table 1). In the F2 treatment receiving equal proportion of organic and chemical fertilizers, the Shannon index of the rhizosphere microbes was lower than that of the non-rhizosphere soil (Figure 1A). Organic fertilizer enhanced microbial PD in both rhizosphere and bulk soils, even if it was applied at the minimum level (25%). An increasing proportion of organic fertilizer further increased the PD index, which remained relatively stable at all other treatments (Figure 1B). However, the impact of organic fertilizer application on the Shannon index was ambiguous (Figure 1A). These findings suggest that organic fertilizer sustains a higher microbial functional diversity. Further analysis indicated that the PD index positively correlated with amino acids content and DOC in rhizosphere soil and with nitrate-N in non-rhizosphere soil (Supplementary Figure S2).

3.3 Soil microbial community composition

Actinobacteria, *Proteobacteria*, and *Chloroflexi* dominated both rhizosphere and non-rhizosphere soils, with the relative abundance of *Actinobacteria* at 37 and 29%, and *Chloroflexi* at 22 and 29%, respectively. Compared to the F0 treatment receiving only chemical fertilizer, the application of organic fertilizer enhanced the relative abundance of *Actinobacteria* while decreasing that of *Chloroflexi*, in both rhizosphere and non-rhizosphere soils. The abundance of *Proteobacteria* remained relatively stable in all treatments (Figure 2A). At the genus level, the dominant genera observed in the oilseed rape soil were mostly uncultured (norank_c_JG37-AG-4, 2.30–14.39%; norank_p_*Saccharibacteria*, 2.19–12.43%, and norank_f_ODP1230B8.23, 2.25–7.94%). These bacterial genera responded significantly to fertilizer treatments. Apart from the F3 treatment that receiving 75% of organic fertilizer, the relative abundance of Norank_c_JG37-AG-4 group demonstrated a decreasing trend along increasing proportion of applied organic fertilizers. Meanwhile, the relative abundance of norank_p_*Saccharibacteria* and norank_f_ODP1230B8.23 differed in soil compartments, showing dominance in rhizosphere and non-rhizosphere soils, respectively (Figure 2B).

NMDS, ANOSIM and PERMANOVA analysis all indicated that the microbial communities differed between rhizosphere and non-rhizosphere soils, as well as among treatments receiving different fertilizer applications (Figure 3, Table 2; Supplementary Table S1).

Redundancy analysis (RDA) highlighted the importance of DOC in influencing rhizosphere bacterial community structure, while nitrate nitrogen in shaping non-rhizosphere microbial community structure (Figure 4A). In addition, factors such as organic acids and DOC were also significantly associated with bacterial community structure in the rhizosphere and non-rhizosphere soil fertilization treatments, respectively (Figures 4B,C).

TABLE 1 Rhizosphere effects and fertilizer treatments on soil bacterial abundance and α-diversity.

Group	Abundance (16S rRNA)		Shannon index		Phylogenetic diversity	
	F	*p*-value	*F*	*p*-value	*F*	*p*-value
REs	8.728	0.006**	9.999	0.004**	5.563	0.025*
Fs	2.105	0.105	2.381	0.074	26.442	0.000**
REs*Fs	2.287	0.083	1.534	0.218	0.470	0.757

REs, Rhizosphere effects; Fs, Fertilization treatments; REs*Fs, Interaction of rhizosphere effect and fertilization treatments.

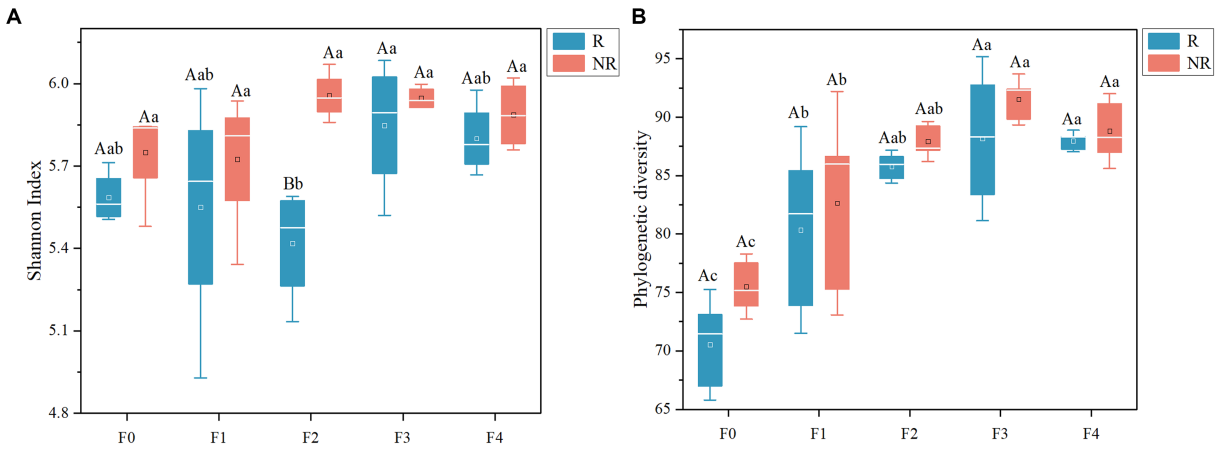

FIGURE 1
Phylogenetic diversity **(A)** and Shannon index **(B)** of bacterial communities in soil. Uppercase letters indicate differences between rhizosphere and non-rhizosphere between each group of fertilizer treatments; lowercase letters indicate differences between fertilizer treatments ($p < 0.05$).

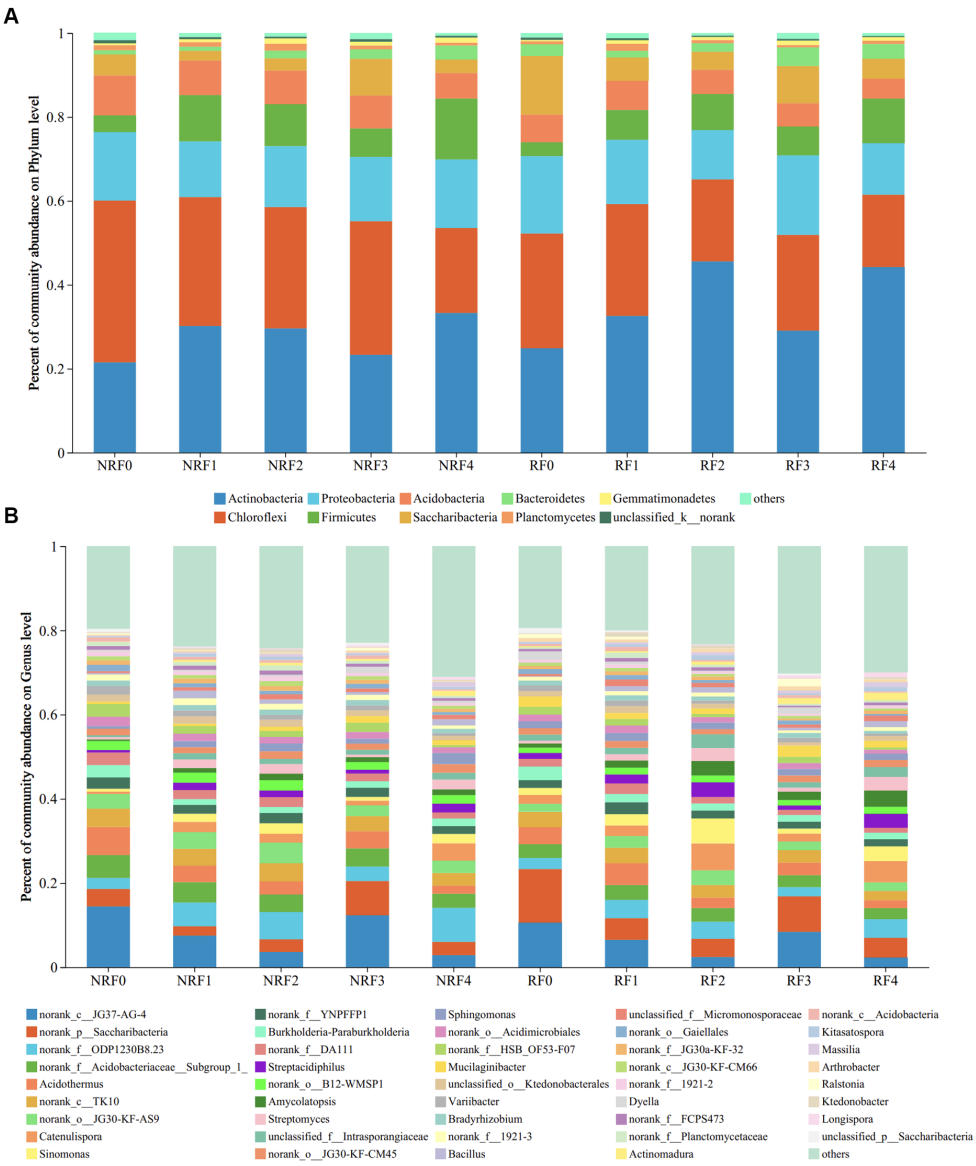

FIGURE 2
Community composition at the phylum level **(A)** and Genus level **(B)**.

3.4 Pathogenic bacteria abundance in organic fertilization treatments

Soil pathogenic bacteria analysis revealed that *Ralstonia solanacearum* (*R. solanacearum*) and *Clavibacter michiganensis subsp. Michiganensis* (Cmm) accounted for a comparatively high relative abundance at the OTU level of 0.95–3.8 and 1.00–5.75%, respectively. And their relative abundance was generally higher in the rhizosphere than in non-rhizosphere soils (Table 3). Other pathogenic bacteria *Xanthomonas arboricola pv. Juglandis* (*X. juglandis*) and *Pseudomonas syringae* (Pst) had a lower relative abundance of less than 1% (Table 3). The highest abundance of *R. solanacearum* was found in both rhizosphere and non-rhizosphere soils of F0 treatment receiving chemical fertilizer alone, and organic fertilizer application reduced its abundance. In contrast, the relative abundance of Cmm was enhanced in treatments with organic fertilizers, and this phenomenon was more evident in non-rhizosphere soils. The rest pathogens with lower relative abundance were also slightly enriched in treatments receiving combined organic-chemical fertilizers than chemical fertilizer alone.

3.5 Co-occurrence network analysis of soil bacterial communities

Fertilization and rhizosphere effects influenced microbial networks (Supplementary Table S2). *Actinobacteria* and *Chloroflexi* were the keystone taxa comprising most of the highly connected nodes in both rhizosphere and non-rhizosphere microbial networks, neither of which, however, formed clear modules. There were more positive edges in the rhizosphere network. In the rhizosphere microbial networks of different fertilization treatments, keystone taxa shifted from *Chloroflexi* in the F0 treatment to *Actinobacteria* in

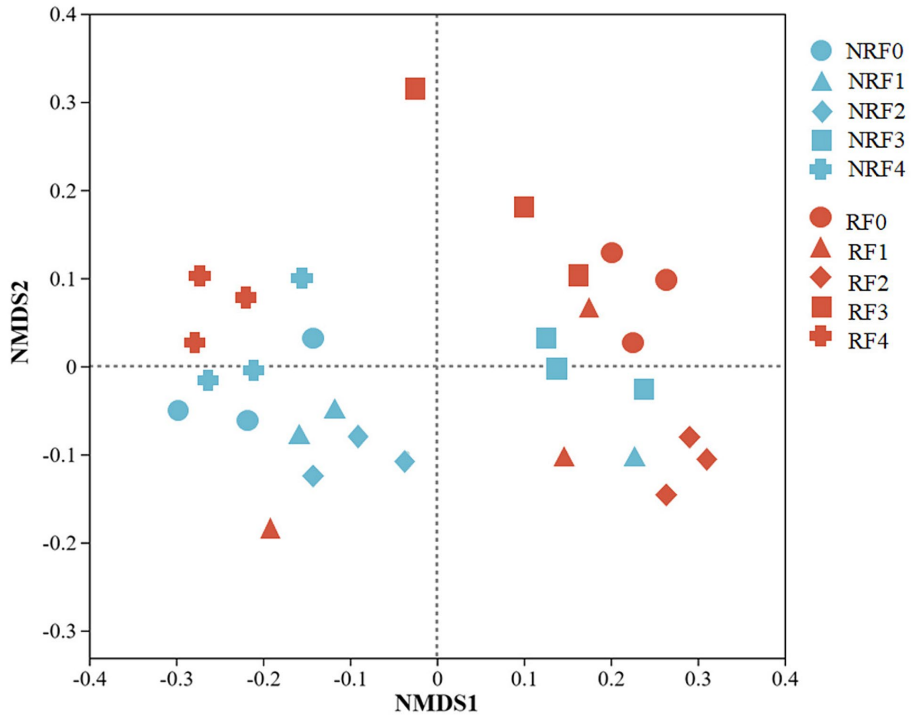

FIGURE 3
Non-metric Multidimensional Scale ordination of bacterial communities.

TABLE 2 Intergroup similarity analysis of rhizosphere effects and fertilization treatments (Adonis).

Adonis	MeanSqs	R^2	P
REs	0.206	0.087	0.030*
F	0.263	0.545	0.001**

treatments with organic fertilizers (Figure 5). The F3 treatment, which received 75% of organic fertilizer, had highly connected nodes from more taxa, including *Chloroflexi*, *Actinobacteria*, and *Proteobacteria*, and exhibited a trend of modularity (Figure 5, RF3). Positive interactions were predominant, especially in the treatments with higher proportions of organic fertilizers. In non-rhizosphere microbial networks, there were generally more diverse keystone taxa in all treatments, but no clear modules were formed (Figure 5, NRF0-NRF4).

4 Discussion

Organic fertilizer applications provide sustained nutrient supply, enrich soil structure, and promote long-term soil health (Liu et al., 2021). But nutrient contents of organic fertilizers vary widely and their release is often slow. Additionally, animal manure or compost-derived organic fertilizers may carry pathogens and contaminants like antibiotic resistance genes, bringing concerns for their application (Xu et al., 2020; Wei et al., 2022). So, as an integrated nutrient management practice, the combined application of chemical and organic fertilizers offers several benefits, such as providing a balanced nutrient supply and mitigating the environmental risks associated with the excessive use of synthetic fertilizers (Liu et al., 2022; Wu et al., 2022). However, balancing the application rates of chemical and organic fertilizers and determining the optimal ratio and timing of application can be challenging. Soil microbial diversity and functionality can be a potential indictor.

Some short-term field studies have reported reduced soil bacterial diversity with organic fertilizer application (Tian et al., 2015), others emphasize the enriching potential of organic fertilizers, attributing to their nutrient-rich content, thus promoting bacterial growth and increasing bacterial population and diversity (Ji et al., 2018; Feng et al., 2021). However, the optimal fertilizer rate is still controversial and may be potentially influenced by varying soil types and crops. Application of 10–30% organic fertilizer significantly increased bacterial diversity in a maize pot experiment by Han et al. (2021). In the current study, the most pronounced effect was observed with the application of 75% organic fertilizer, consistent with some previous studies (Ren et al., 2021; Yang et al., 2023). Additionally, the dry weight of the aboveground oilseed rape biomass was the highest in the F3 treatment, indicating a better growth of oilseed rape under 75% of organic fertilization (Yang, 2019). Normally, the application of different rates of organic and chemical fertilizers coordinates the availability of different nutrients (Bao et al., 2020), and can lead to distinct responses of microbial populations (Lin et al., 2019), consequently, the effect of fertilizer application on microbial community assemblage and plant growth differs.

Fertilizer application changes environmental factors including contents of ammonium nitrogen, nitrate nitrogen, and DOC, therefore significantly affecting bacterial abundance and diversity. *Actinobacteria* abundance increased after the application of organic fertilizer. In

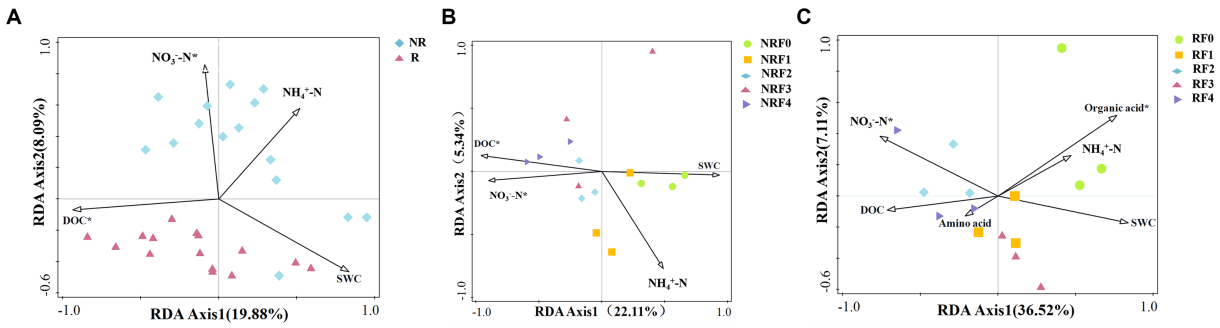

FIGURE 4
Redundancy analysis of soil bacterial community structure and soil physicochemical properties in oilseed rape with different fertilizer treatments. **(A)** Rhizosphere and non-rhizosphere soil bacterial community structure; **(B)** Rhizosphere fertilization treatment soil bacterial community structure; **(C)** Non-rhizosphere fertilization treatment soil bacterial community structure.

TABLE 3 The relative abundance of pathogenic bacteria in soil samples.

		R. solanacearum	Cmm	*A. tumefaciens*	*X. juglandis*	Pst
NR	F0	3.26 ± 1.14a	1.00 ± 0.11c	0.08 ± 0.02c	0.00 ± 0.00c	0.00 ± 0.00c
	F1	1.01 ± 0.20b	4.03 ± 1.04a	0.08 ± 0.03c	0.023 ± 0.01bc	0.01 ± 0.01bc
	F2	0.95 ± 0.12b	2.21 ± 0.20b	0.14 ± 0.05ab	0.04 ± 0.03b	0.02 ± 0.01ab
	F3	1.88 ± 0.35b	2.94 ± 0.71b	0.17 ± 0.06ab	0.05 ± 0.04b	0.01 ± 0.00b
	F4	1.16 ± 0.56b	2.78 ± 0.27b	0.18 ± 0.06a	0.17 ± 0.01a	0.02 ± 0.00a
R	F0	3.80 ± 1.33a	3.75 ± 0.36b	0.23 ± 0.08b	0.00 ± 0.00c	0.01 ± 0.00bc
	F1	2.20 ± 1.17ab	3.59 ± 0.30b	0.1 ± 0.05c	0.01 ± 0.01c	0.00 ± 0.00c
	F2	1.01 ± 0.09b	5.75 ± 0.89a	0.14 ± 0.01bc	0.04 ± 0.01bc	0.02 ± 0.00ab
	F3	2.90 ± 1.09ab	3.27 ± 0.51b	0.56 ± 0.08a	0.12 ± 0.12ab	0.02 ± 0.01a
	F4	1.00 ± 0.41b	4.86 ± 0.77a	0.19 ± 0.03bc	0.16 ± 0.03a	0.01 ± 0.01ab

contrast, the relative abundance of *Chloroflexi* was higher at F0. Studies have reported that *Chloroflexi* is oligotrophic, adapted to nutrient-limited environments, and sensitive to changes in nitrogen and carbon levels (Trivedi et al., 2016; Dai et al., 2019; Romero-Salas et al., 2021). In contrast, *Actinobacteria* can rapidly decompose organic matter, which increases levels of carbon and other nutrients to improve the soil environment. Thus its relative abundance increases with the application of organic fertilizers (Yan et al., 2021). This selective effect helps to maintain the balance of soil ecosystems, but may also trigger certain microbial diseases.

Ralstonia solanacearum can cause plant greening and is one of the most common soil-borne diseases. The application of organic manure from swine manure alters the composition of the soil microbial community and reduces the community of *Ralstonia solanacearum* (Gorissen et al., 2004). However, it is widely known that organic fertilizer application may introduce exogenous pathogens. Potential pathogenic bacteria such as *Pseudomonas*, *Flavobacterium*, and *Bacillus* were detected in more than 13% of organic fertilizer products (Xu et al., 2022). Our results showed that the combined application of organic manure with chemical fertilizers significantly suppressed *R. solanacearum* compared to chemical fertilizers alone. In addition, Cmm was similarly abundant in F0 treatment and other treatment receiving organic fertilizers, and other pathogens did not show increasing abundance with increasing proportion of organic fertilizer applied (Table 3), suggesting that these pathogens were not introduced solely, if not at all, by organic fertilizer application in this study.

Although many studies have shown that organic fertilizers inhibit a wide range of plant soil-borne diseases, soil diseases are usually caused by multiple soil pathogens, and it is difficult to effectively inhibit multiple pathogens by applying a single organic fertilizer alone; therefore, there is a need for more in-depth research on the application of fertilizer mixtures, such as the mixing of multiple organic fertilizers, organic fertilizers, and biocontrol formulations, as well as mixing of organic fertilizers with induced activators (Liu et al., 2017; Yang et al., 2022). In addition to this, the application of organic fertilizers after soil fumigation can activate beneficial soil microorganisms, promote soil health, and increase crop yield (Li Q. et al., 2022).

The microbial networks of F2 and F3 treatments receiving 50 and 75% of organic fertilizers application had the highest number of nods and edges in the rhizosphere and non-rhizosphere soils, respectively, suggesting high complexity and stability of these microbial communities (Okuyama and Holland, 2007). Complex networks often support more diverse functions, resulting in increased efficiency of resource cycling and information transfer (Morriën et al., 2017; Wagg et al., 2019), which also improve the stability of microbial communities (Wang et al., 2017; Ji et al., 2020). Positive and negative associations, which indicate cooperation and competition among species, respectively, are key network attributes (Deng et al., 2015). It has been

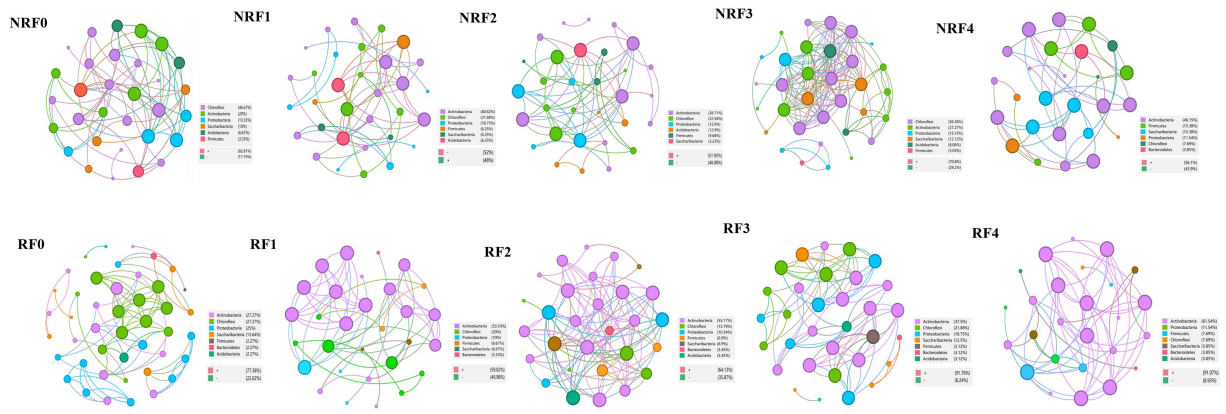

FIGURE 5
Co-occurrence network analysis based on Spearman's correlation analysis for connectivity and module partitioning based on selected OTUs. (R,NR) Rhizosphere and non-rhizosphere; (NRF) Non-rhizosphere soil fertilization treatment; (RF) Rhizosphere soil fertilization treatment.

suggested that a high positive correlation may lead to dependence and mutual collapse (Coyte et al., 2015), and conversely, the negative correlation may stabilize co-oscillations in microbial communities and enhance network stability (Zhou et al., 2020). Yang et al. found a higher negative correlation in microbial networks under the combination of organic and inorganic fertilizers, which suggests that the combined application of fertilizers resulted in microbial communities with higher network stability (Yang et al., 2023). However, it should be noted that co-occurrence networks infer biological interactions based on co-occurrences or absence of sequences, it is important to exercise caution when drawing conclusions from microbial networks (Faust, 2021).

Studies have reported that plant roots impact the soil microbial community by releasing a substantial amount of exudates, including primary metabolites such as amino acids, organic acids, sugars, and carboxylic acids (Li et al., 2018). This release enhances the carbon and nitrogen substrate nutrients for microbial growth, turning the rhizosphere into a favorable microhabitat for the rapid colonization of specific microorganisms (Ulbrich et al., 2022; Steinauer et al., 2023). Simultaneously, these secretions exhibit selectivity in promoting the growth and colonization of particular soil microbes with certain potential metabolic profiles (Bulgarelli et al., 2013; Li et al., 2020; He et al., 2022). Plants recruit beneficial microbial groups through rhizospheric exudates, increasing rhizobacterial abundance and a decrease in diversity (Ling et al., 2022), aligning with our research findings that rhizosphere effects significantly influenced the rhizosphere microbial diversity and abundance.

Research indicates that specific plant metabolites, such as organic acids, amino acids, and hormones, can serve as signaling molecules, activators, and attractants, influencing the composition of microbial communities (Baetz and Martinoia, 2014). Many studies have shown that different rhizosphere secretions attract different microbial communities. For instance, organic acid secretion was found to attract *Comamonadacea* against pathogenic bacteria; Arabidopsis thaliana attracts and stimulates specific *Pseudomonas* colonies by releasing long-chain amino acids, etc. (Yuan et al., 2018; Wen et al., 2020). Our study also observed significant differences between rhizosphere and non-rhizosphere soil microbial communities, and organic acids was recognized as a pivotal driver in the formation of these differences. Together, these studies highlight the intricate interactions among fertilization, crop root exudates and soil microbial communities.

The complexity and negative correlations of rhizosphere microbial networks are lower than those in non-rhizosphere environments, which could be attributed to the loss of diversity and enriching effects of rhizosphere secretions (Chen Y. et al., 2023), driven by changes in rhizosphere resource availability and niche differentiation (Zhao et al., 2020). Currently, many studies are exploring applications of rhizosphere effect in plant restoration. For instance, the halophyte L. sinense under salt stress can attract and recruit beneficial rhizosphere bacteria through root exudates, and the recruited B. flexus KLBMP 4941 enhances seedling salt tolerance through intricate plant physiological regulatory mechanisms (Xiong et al., 2020). Similarly, Luo et al. investigated the succession trajectories and oscillations of rhizosphere microbial symbiotic networks in S. alfredii, aiming to deepen understanding and design stable bioremediation microbial communities (Luo et al., 2021). Understanding the interactions and feedback loop involving fertilization, crop root exudates, the soil microbial community and soil properties, offers a new avenue for sustainable agricultural production.

5 Conclusion

The study demonstrates that the application of combined organic fertilizer and chemical fertilizer, together with rhizosphere effects, fosters a more stable and conducive soil bacterial community, and enhances oilseed rape growth. Nonetheless, the research primarily focused on the seedling stage, prolonged investigations will be necessary to understand the comprehensive impacts of fertilization on bacterial community structure and function, and reveal the best ratio of organic to chemical fertilizers in oilseed rape cultivation.

Data availability statement

The datasets presented in this study can be found in online repositories. The names of the repository/repositories and accession number(s) can be found in the article/Supplementary material.

Author contributions

JW: Conceptualization, Data curation, Investigation, Validation, Visualization, Writing – original draft, Writing – review & editing. HQ: Funding acquisition, Resources, Supervision, Writing – review & editing. LZ: Investigation, Supervision, Validation, Writing – review & editing. YT: Investigation, Supervision, Writing – review & editing. JL: Conceptualization, Investigation, Visualization, Writing – review & editing. HX: Investigation, Methodology, Supervision, Validation, Writing – review & editing. BZ: Conceptualization, Data curation, Funding acquisition, Resources, Supervision, Validation, Visualization, Writing – review & editing.

Funding

The author(s) declare that financial support was received for the research, authorship, and/or publication of this article. The study was supported by the Science Research Project Fund of Hubei Provincial Department of Education, China (B2020147); the National Key Research and Development Program of China (2021YFD1901203 and 2023YFD1900900); and the Hunan Science Fund for Distinguished Young Scholars (2022JJ10057).

Conflict of interest

The authors declare that the research was conducted in the absence of any commercial or financial relationships that could be construed as a potential conflict of interest.

Publisher's note

All claims expressed in this article are solely those of the authors and do not necessarily represent those of their affiliated organizations, or those of the publisher, the editors and the reviewers. Any product that may be evaluated in this article, or claim that may be made by its manufacturer, is not guaranteed or endorsed by the publisher.

Supplementary material

The Supplementary material for this article can be found online at: https://www.frontiersin.org/articles/10.3389/fmicb.2024.1374199/full#supplementary-material

References

Ali, S., and Khan, N. (2021). Delineation of mechanistic approaches employed by plant growth promoting microorganisms for improving drought stress tolerance in plants. *Microbiol. Res.* 249:126771. doi: 10.1016/j.micres.2021.126771

Baetz, U., and Martinoia, E. (2014). Root exudates: the hidden part of plant defense. *Trends Plant Sci.* 19, 90–98. doi: 10.1016/j.tplants.2013.11.006

Bao, Y., Feng, Y., Stegen, J. C., Wu, M., Chen, R., Liu, W., et al. (2020). Straw chemistry links the assembly of bacterial communities to decomposition in paddy soils. *Soil Biol. Biochem.* 148:107866. doi: 10.1016/j.soilbio.2020.107866

Brtnicky, M., Mustafa, A., Hammerschmiedt, T., Kintl, A., Trakal, L., Beesley, L., et al. (2023). Pre-activated biochar by fertilizers mitigates nutrient leaching and stimulates soil microbial activity. *Chem. Biol. Technol. Agric.* 10:430. doi: 10.1186/s40538-023-00430-7

Bulgarelli, D., Schlaeppi, K., Spaepen, S., van Themaat, E. V. L., and Schulze-Lefert, P. (2013). Structure and functions of the bacterial microbiota of plants. *Annu. Rev. Plant Biol.* 64, 807–838. doi: 10.1146/annurev-arplant-050312-120106

Chen, W., Zhang, X., Hu, Y., and Zhao, Y. (2023). Effects of different proportions of organic fertilizer in place of chemical fertilizer on microbial diversity and community structure of pineapple rhizosphere soil. *Agronomy* 14:59. doi: 10.3390/agronomy14010059

Chen, Y., Li, Y., Qiu, T., He, H., Liu, J., Duan, C., et al. (2023). High nitrogen fertilizer input enhanced the microbial network complexity in the paddy soil. *Soil Ecology Letters* 6:205. doi: 10.1007/s42832-023-0205-3

Chen, Y., Zhang, X., Yang, X., Lv, Y., Wu, J., Lin, L., et al. (2020). Emergy evaluation and economic analysis of compound fertilizer production: a case study from China. *J. Clean. Prod.* 260:121095. doi: 10.1016/j.jclepro.2020.121095

Coyte, K. Z., Schluter, J., and Foster, K. R. (2015). The ecology of the microbiome: networks, competition, and stability. *Science* 350, 663–666. doi: 10.1126/science.aad2602

Cui, X., Zhang, Y., Gao, J., Peng, F., and Gao, P. (2018). Long-term combined application of manure and chemical fertilizer sustained higher nutrient status and rhizospheric bacterial diversity in reddish paddy soil of central South China. *Sci. Rep.* 8:8. doi: 10.1038/s41598-018-34685-0

Dai, H., Zang, H., Zhao, Y., Qian, X., Liu, K., Wang, D., et al. (2019). Linking bacterial community to aggregate fractions with organic amendments in a sandy soil. *Land Degrad. Dev.* 30, 1828–1839. doi: 10.1002/ldr.3383

Deng, S., Caddell, D. F., Xu, G., Dahlen, L., Washington, L., Yang, J., et al. (2021). Genome wide association study reveals plant loci controlling heritability of the rhizosphere microbiome. *ISME J.* 15, 3181–3194. doi: 10.1038/s41396-021-00993-z

Deng, Y., Zhang, P., Qin, Y., Tu, Q., Yang, Y., He, Z., et al. (2015). Network succession reveals the importance of competition in response to emulsified vegetable oil amendment for uranium bioremediation. *Environ. Microbiol.* 18, 205–218. doi: 10.1111/1462-2920.12981

Fahey, C., Koyama, A., Antunes, P. M., Dunfield, K., and Flory, S. L. (2020). Plant communities mediate the interactive effects of invasion and drought on soil microbial communities. *ISME J.* 14, 1396–1409. doi: 10.1038/s41396-020-0614-6

Faust, K. (2021). Open challenges for microbial network construction and analysis. *ISME J.* 15, 3111–3118. doi: 10.1038/s41396-021-01027-4

Feng, H., Fu, R., Hou, X., Lv, Y., Zhang, N., Liu, Y., et al. (2021). Chemotaxis of beneficial Rhizobacteria to root exudates: the first step towards root–microbe rhizosphere interactions. *Int. J. Mol. Sci.* 22:655. doi: 10.3390/ijms22136655

Francioli, D., Schulz, E., Lentendu, G., Wubet, T., Buscot, F., and Reitz, T. (2016). Mineral vs. organic amendments: microbial community structure, activity and abundance of agriculturally relevant microbes are driven by Long-term fertilization strategies. *Front. Microbiol.* 7:1446. doi: 10.3389/fmicb.2016.01446

Garzón, E., González-Andrés, F., García-Martínez, V. M., and De Paz, J. M. (2011). Mineralization and nutrient release of an organic fertilizer made by flour, meat, and crop residues in two vineyard soils with different pH levels. *Commun. Soil Sci. Plant Anal.* 42, 1485–1496. doi: 10.1080/00103624.2011.581719

Gorissen, A., van Overbeek, L. S., and van Elsas, J. D. (2004). Pig slurry reduces the survival of *Ralstonia solanacearum* biovar 2 in soil. *Can. J. Microbiol.* 50, 587–593. doi: 10.1139/w04-042

Han, J., Dong, Y., and Zhang, M. (2021). Chemical fertilizer reduction with organic fertilizer effectively improve soil fertility and microbial community from newly cultivated land in the loess plateau of China. *Appl. Soil Ecol.* 165:103966. doi: 10.1016/j.apsoil.2021.103966

He, H., Peng, M., Ru, S., Hou, Z., and Li, J. (2022). A suitable organic fertilizer substitution ratio could improve maize yield and soil fertility with low pollution risk. *Front. Plant Sci.* 13:663. doi: 10.3389/fpls.2022.988663

He, T., Xu, Z.-J., Wang, J.-F., Wang, F.-P., Zhou, X.-F., Wang, L.-L., et al. (2022). Improving cadmium accumulation by *Solanum nigrum* L. via regulating rhizobacterial community and metabolic function with phosphate-solubilizing bacteria colonization. *Chemosphere* 287:132209. doi: 10.1016/j.chemosphere.2021.132209

Ji, L., Ni, K., Wu, Z., Zhang, J., Yi, X., Yang, X., et al. (2020). Effect of organic substitution rates on soil quality and fungal community composition in a tea plantation with long-term fertilization. *Biol. Fertil. Soils* 56, 633–646. doi: 10.1007/s00374-020-01439-y

Ji, L., Wu, Z., You, Z., Yi, X., Ni, K., Guo, S., et al. (2018). Effects of organic substitution for synthetic N fertilizer on soil bacterial diversity and community composition: a 10-year field trial in a tea plantation. *Agric. Ecosyst. Environ.* 268, 124–132. doi: 10.1016/j.agee.2018.09.008

Kanthilanka, H., Ramilan, T., Farquharson, R. J., and Weerahewa, J. (2023). Optimal nitrogen fertilizer decisions for rice farming in a cascaded tank system in Sri Lanka: an analysis using an integrated crop, hydro-nutrient and economic model. *Agric. Syst.* 207:103628. doi: 10.1016/j.agsy.2023.103628

Kumari, M., Sheoran, S., Prakash, D., Yadav, D. B., Yadav, P. K., Jat, M. K., et al. (2024). Long-term application of organic manures and chemical fertilizers improve the organic carbon and microbiological properties of soil under pearl millet-wheat cropping system in North-Western India. *Heliyon* 10:e25333. doi: 10.1016/j.heliyon.2024.e25333

Langille, M. G. I., Zaneveld, J., Caporaso, J. G., McDonald, D., Knights, D., Reyes, J. A., et al. (2013). Predictive functional profiling of microbial communities using 16S rRNA marker gene sequences. *Nat. Biotechnol.* 31, 814–821. doi: 10.1038/nbt.2676

Li, D., Qu, C., Cheng, X., Chen, Y., Yan, H., and Wu, Q. (2023). Effect of different fertilization strategies on the yield, quality of Euryales semen and soil microbial community. *Front. Microbiol.* 14:366. doi: 10.3389/fmicb.2023.1310366

Li, H., Xue, J.-f., Gao, Z.-q., N-w, X., and Yang, Z.-p. (2018). Response of yield increase for dryland winter wheat to tillage practice during summer fallow and sowing method in the loess plateau of China. *J. Integr. Agric.* 17, 817–825. doi: 10.1016/S2095-3119(17)61806-9

Ling, N., Wang, T., and Kuzyakov, Y. (2022). Rhizosphere bacteriome structure and functions. *Nat. Commun.* 13:448. doi: 10.1038/s41467-022-28448-9

Lin, Y., Ye, G., Kuzyakov, Y., Liu, D., Fan, J., and Ding, W. (2019). Long-term manure application increases soil organic matter and aggregation, and alters microbial community structure and keystone taxa. *Soil Biol. Biochem.* 134, 187–196. doi: 10.1016/j.soilbio.2019.03.030

Li, Q., Zhang, D., Song, Z., Ren, L., Jin, X., Fang, W., et al. (2022). Organic fertilizer activates soil beneficial microorganisms to promote strawberry growth and soil health after fumigation. *Environ. Pollut.* 295:118653. doi: 10.1016/j.envpol.2021.118653

Li, R., Liu, J., Li, J., and Sun, C. (2020). Straw input can parallelly influence the bacterial and chemical characteristics of maize rhizosphere. *Environ. Pollut. Bioavailability* 32, 1–11. doi: 10.1080/26395940.2019.1710260

Liu, H., Xiong, W., Zhang, R., Hang, X., Wang, D., Li, R., et al. (2017). Continuous application of different organic additives can suppress tomato disease by inducing the healthy rhizospheric microbiota through alterations to the bulk soil microflora. *Plant Soil* 423, 229–240. doi: 10.1007/s11104-017-3504-6

Liu, J., Shu, A., Song, W., Shi, W., Li, M., Zhang, W., et al. (2021). Long-term organic fertilizer substitution increases rice yield by improving soil properties and regulating soil bacteria. *Geoderma* 404:115287. doi: 10.1016/j.geoderma.2021.115287

Liu, T., Wang, S., Chen, Y., Luo, J., Hao, B., Zhang, Z., et al. (2023). Bio-organic fertilizer promoted phytoremediation using native plant leymus chinensis in heavy metal(loid)s contaminated saline soil. *Environ. Pollut.* 327:121599. doi: 10.1016/j.envpol.2023.121599

Liu, W., Cheng, Y., Guo, J., Duan, Y., Wang, S., Xu, Q., et al. (2022). Long-term manure inputs induce a deep selection on agroecosystem soil antibiotic resistome. *J. Hazard. Mater.* 436:129163. doi: 10.1016/j.jhazmat.2022.129163

Li, Y., Wei, J., Ma, L., Wu, X., Zheng, F., Cui, R., et al. (2024). Enhancing wheat yield through microbial organic fertilizer substitution for partial chemical fertilization: regulation of nitrogen conversion and utilization. *J. Soil Sci. Plant Nutr.* 2024, 1–9. doi: 10.1007/s42729-023-01597-6

Luo, J., Guo, X., Tao, Q., Li, J., Liu, Y., Du, Y., et al. (2021). Succession of the composition and co-occurrence networks of rhizosphere microbiota is linked to cd/Zn hyperaccumulation. *Soil Biol. Biochem.* 153:108120. doi: 10.1016/j.soilbio.2020.108120

Lu, W., Hao, Z., Ma, X., Gao, J., Fan, X., Guo, J., et al. (2024). Effects of different proportions of organic fertilizer replacing chemical fertilizer on soil nutrients and fertilizer utilization in Gray Desert soil. *Agronomy* 14:228. doi: 10.3390/agronomy14010228

Maltas, A., Kebli, H., Oberholzer, H. R., Weisskopf, P., and Sinaj, S. (2018). The effects of organic and mineral fertilizers on carbon sequestration, soil properties, and crop yields from a long-term field experiment under a Swiss conventional farming system. *Land Degrad. Dev.* 29, 926–938. doi: 10.1002/ldr.2913

Manoharan, L., Kushwaha, S. K., Ahrén, D., and Hedlund, K. (2017). Agricultural land use determines functional genetic diversity of soil microbial communities. *Soil Biol. Biochem.* 115, 423–432. doi: 10.1016/j.soilbio.2017.09.011

Morriën, E., Hannula, S. E., Snoek, L. B., Helmsing, N. R., Zweers, H., De Hollander, M., et al. (2017). Soil networks become more connected and take up more carbon as nature restoration progresses. *Nat. Commun.* 8:349. doi: 10.1038/ncomms14349

Okuyama, T., and Holland, J. N. (2007). Network structural properties mediate the stability of mutualistic communities. *Ecol. Lett.* 11, 208–216. doi: 10.1111/j.1461-0248.2007.01137.x

Pang, Z., Chen, J., Wang, T., Gao, C., Li, Z., Guo, L., et al. (2021). Linking plant secondary metabolites and plant microbiomes: a review. *Front. Plant Sci.* 12:276. doi: 10.3389/fpls.2021.621276

Peng, C, Lai, S, Luo, X, Lu, J, Huang, Q, and Chen, W (2016). Effects of long term rice straw application on the microbial communities of rapeseed rhizosphere in a paddy-upland rotation system. *Sci. Total Environ.* 557-558: 231–239. doi: 10.1016/j.scitotenv.2016.02.184

Qaswar, M., Yiren, L., Jing, H., Kaillou, L., Mudasir, M., Zhenzhen, L., et al. (2020). Soil nutrients and heavy metal availability under long-term combined application of swine manure and synthetic fertilizers in acidic paddy soil. *J. Soils Sediments* 20, 2093–2106. doi: 10.1007/s11368-020-02576-5

Ren, J., Liu, X., Yang, W., Yang, X., Li, W., Xia, Q., et al. (2021). Rhizosphere soil properties, microbial community, and enzyme activities: short-term responses to partial substitution of chemical fertilizer with organic manure. *J. Environ. Manag.* 299:113650. doi: 10.1016/j.jenvman.2021.113650

Romero-Salas, E. A., Navarro-Noya, Y. E., Luna-Guido, M., Verhulst, N., Crossa, J., Govaerts, B., et al. (2021). Changes in the bacterial community structure in soil under conventional and conservation practices throughout a complete maize (*Zea mays* L.) crop cycle. *Appl. Soil Ecol.* 157:103733. doi: 10.1016/j.apsoil.2020.103733

Searchinger, T. D., Wirsenius, S., Beringer, T., and Dumas, P. (2018). Assessing the efficiency of changes in land use for mitigating climate change. *Nature* 564, 249–253. doi: 10.1038/s41586-018-0757-z

Steinauer, K., Thakur, M. P., Emilia Hannula, S., Weinhold, A., Uthe, H., van Dam, N. M., et al. (2023). Root exudates and rhizosphere microbiomes jointly determine temporal shifts in plant-soil feedbacks. *Plant Cell Environ.* 46, 1885–1899. doi: 10.1111/pce.14570

Tian, W., Wang, L., Li, Y., Zhuang, K., Li, G., Zhang, J., et al. (2015). Responses of microbial activity, abundance, and community in wheat soil after three years of heavy fertilization with manure-based compost and inorganic nitrogen. *Agric. Ecosyst. Environ.* 213, 219–227. doi: 10.1016/j.agee.2015.08.009

Trivedi, P., Delgado-Baquerizo, M., Anderson, I. C., and Singh, B. K. (2016). Response of soil properties and microbial communities to agriculture: implications for primary productivity and soil health indicators. *Front. Plant Sci.* 7:990. doi: 10.3389/fpls.2016.00990

Ulbrich, T. C., Rivas-Ubach, A., Tiemann, L. K., Friesen, M. L., and Evans, S. E. (2022). Plant root exudates and rhizosphere bacterial communities shift with neighbor context. *Soil Biol. Biochem.* 172:108753. doi: 10.1016/j.soilbio.2022.108753

Vezzani, F. M., Anderson, C., Meenken, E., Gillespie, R., Peterson, M., and Beare, M. H. (2018). The importance of plants to development and maintenance of soil structure, microbial communities and ecosystem functions. *Soil Tillage Res.* 175, 139–149. doi: 10.1016/j.still.2017.09.002

Wagg, C., Schlaeppi, K., Banerjee, S., Kuramae, E. E., and van der Heijden, M. G. A. (2019). Fungal-bacterial diversity and microbiome complexity predict ecosystem functioning. *Nat. Commun.* 10:798. doi: 10.1038/s41467-019-12798-y

Wang, D., Yang, J., Liao, R., Yuan, H., Zhou, H., Lv, D., et al. (2021). Effects of chemical and organic fertilizers on root secretion of oilseed rape during nutritive growth period. *Soil Fertil. China* 2021, 95–102.

Wang, J., Song, Y., Ma, T., Raza, W., Li, J., Howland, J. G., et al. (2017). Impacts of inorganic and organic fertilization treatments on bacterial and fungal communities in a paddy soil. *Appl. Soil Ecol.* 112, 42–50. doi: 10.1016/j.apsoil.2017.01.005

Wang, J., Wang, F., Sha, Z., and Cao, L. (2023). Enhancing soil nitrogen supply and maintaining rice yield through partial replacement of chemical nitrogen with food waste-derived organic fertilizer. *Plant Soil* 492, 625–639. doi: 10.1007/s11104-023-06207-z

Wei, Z., Shen, W., Feng, K., Feng, Y., He, Z., Li, Y., et al. (2022). Organic fertilizer potentiates the transfer of typical antibiotic resistance gene among special bacterial species. *J. Hazard. Mater.* 435:128985. doi: 10.1016/j.jhazmat.2022.128985

Wen, T., Yuan, J., He, X., Lin, Y., Huang, Q., and Shen, Q. (2020). Enrichment of beneficial cucumber rhizosphere microbes mediated by organic acid secretion. *Hortic. Res.* 7:154. doi: 10.1038/s41438-020-00380-3

Wu, S., Zhuang, G., Bai, Z., Cen, Y., Xu, S., Sun, H., et al. (2018). Mitigation of nitrous oxide emissions from acidic soils by *Bacillus amyloliquefaciens*, a plant growth-promoting bacterium. *Glob. Chang. Biol.* 24, 2352–2365. doi: 10.1111/gcb.14025

Wu, X., Hu, H., Li, S., Zhao, J., Li, J., Zhang, G., et al. (2022). Chemical fertilizer reduction with organic material amendments alters co-occurrence network patterns of bacterium-fungus-nematode communities under the wheat–maize rotation regime. *Plant Soil* 473, 605–623. doi: 10.1007/s11104-022-05314-7

Xiong, Y.-W., Li, X.-W., Wang, T.-T., Gong, Y., Zhang, C.-M., Xing, K., et al. (2020). Root exudates-driven rhizosphere recruitment of the plant growth-promoting rhizobacterium *Bacillus flexus* KLBMP 4941 and its growth-promoting effect on the coastal halophyte *Limonium sinense* under salt stress. *Ecotoxicol. Environ. Saf.* 194:110374. doi: 10.1016/j.ecoenv.2020.110374

Xu, Y., Gao, Y., Tan, L., Wang, Q., Li, Q., Wei, X., et al. (2022). Exploration of bacterial communities in products after composting rural wastes with different components: Core microbiome and potential pathogenicity. *Environ. Technol. Innov.* 25:102222. doi: 10.1016/j.eti.2021.102222

Xu, Y., Li, H., Shi, R., Lv, J., Li, B., Yang, F., et al. (2020). Antibiotic resistance genes in different animal manures and their derived organic fertilizer. *Environ. Sci. Eur.* 32:381. doi: 10.1186/s12302-020-00381-y

Yan, B., Liu, N., Liu, M., Du, X., Shang, F., and Huang, Y. (2021). Soil actinobacteria tend to have neutral interactions with other co-occurring microorganisms, especially under oligotrophic conditions. *Environ. Microbiol.* 23, 4126–4140. doi: 10.1111/1462-2920.15483

Yang, J. (2019). Effects of Different Fertilization Treatments on Microbial Nitrification and Denitrification in Rhizosphere Soils in Subtropical Red Soils. thesis. Hunan Normal University; 22.

Yang, S., Shu, R., Yin, X., Long, Y., and Yuan, J. (2022). Response of soil microbial community structure mediated by sulfur-induced resistance against kiwifruit bacterial canker. *Front. Microbiol.* 13:463. doi: 10.3389/fmicb.2022.883463

Yang, X., Cheng, J., Franks, A. E., Huang, X., Yang, Q., Cheng, Z., et al. (2023). Loss of microbial diversity weakens specific soil functions, but increases soil ecosystem stability. *Soil Biol. Biochem.* 177:108916. doi: 10.1016/j.soilbio.2022.108916

Yuan, J., Zhao, J., Wen, T., Zhao, M., Li, R., Goossens, P., et al. (2018). Root exudates drive the soil-borne legacy of aboveground pathogen infection. *Microbiome* 6:156. doi: 10.1186/s40168-018-0537-x

Yu, G.-H., Chen, C.-M., He, X.-H., Zhang, X.-Z., and Li, L.-N. (2020). Unexpected bulk density and microstructures response to long-term pig manure application in a Ferralic Cambisol soil: implications for rebuilding a healthy soil. *Soil Tillage Res.* 203:104668. doi: 10.1016/j.still.2020.104668

Zhang, K., Khan, Z., Khan, M. N., Luo, T., Luo, L., Bi, J., et al. (2024). The application of biochar improves the nutrient supply efficiency of organic fertilizer, sustains soil quality and promotes sustainable crop production. *Food Energy Secur.* 13:520. doi: 10.1002/fes3.520

Zhang, L, Niu, J, Lu, X, Zhao, Z, Li, K, Wang, F, et al (2023). Dosage effects of organic manure on bacterial community assemblage and phosphorus transformation profiles in greenhouse soil. *Front. Microbiol.* 14. doi: 10.3389/fmicb.2023.1188167

Zhao, S., Liu, J., Banerjee, S., Zhou, N., Zhao, Z., Zhang, K., et al. (2020). Biogeographical distribution of bacterial communities in saline agricultural soil. *Geoderma* 361:114095. doi: 10.1016/j.geoderma.2019.114095

Zhao, Z., Ma, Y., Zhang, A., Chen, Y., Zheng, Z., Zheng, W., et al. (2023). Response of apple orchard bacteria co-occurrence network pattern to long-term organic fertilizer input. *Appl. Soil Ecol.* 191:105035. doi: 10.1016/j.apsoil.2023.105035

Zheng, H., Wang, X., Chen, L., Wang, Z., Xia, Y., Zhang, Y., et al. (2017). Enhanced growth of halophyte plants in biochar-amended coastal soil: roles of nutrient availability and rhizosphere microbial modulation. *Plant Cell Environ.* 41, 517–532. doi: 10.1111/pce.12944

Zheng, W., Zeng, S., Bais, H., LaManna, J. M., Hussey, D. S., Jacobson, D. L., et al. (2018). Plant growth-promoting Rhizobacteria (PGPR) reduce evaporation and increase soil water retention. *Water Resour. Res.* 54, 3673–3687. doi: 10.1029/2018WR022656

Zhou, H., Gao, Y., Jia, X., Wang, M., Ding, J., Cheng, L., et al. (2020). Network analysis reveals the strengthening of microbial interaction in biological soil crust development in the mu us Sandy land, northwestern China. *Soil Biol. Biochem.* 144:107782. doi: 10.1016/j.soilbio.2020.107782

frontiers | Frontiers in Microbiology

TYPE Mini Review
PUBLISHED 18 March 2024
DOI 10.3389/fmicb.2024.1342331

OPEN ACCESS

EDITED BY
Yichao Shi,
Agriculture and Agri-Food Canada (AAFC), Canada

REVIEWED BY
Federica Caradonia,
University of Modena and Reggio Emilia, Italy
Fasih Ullah Haider,
Chinese Academy of Sciences (CAS), China
Bhaskar Gupta,
Government General Degree College, Singur, India

*CORRESPONDENCE
Iryna Kulkova
✉ i.kulkova@itp.edu.pl

RECEIVED 21 November 2023
ACCEPTED 04 March 2024
PUBLISHED 18 March 2024

CITATION
Kulkova I, Wróbel B and Dobrzyński J (2024) *Serratia* spp. as plant growth-promoting bacteria alleviating salinity, drought, and nutrient imbalance stresses. *Front. Microbiol.* 15:1342331. doi: 10.3389/fmicb.2024.1342331

Serratia spp. as plant growth-promoting bacteria alleviating salinity, drought, and nutrient imbalance stresses

Iryna Kulkova*, Barbara Wróbel and Jakub Dobrzyński

Institute of Technology and Life Science – National Research Institute, Raszyn, Poland

In agricultural environments, plants are often exposed to abiotic stresses including temperature extremes, salt stress, drought, and heavy metal soil contamination, which leads to significant economic losses worldwide. Especially salt stress and drought pose serious challenges since they induce ionic toxicity, osmotic stress, and oxidative stress in plants. A potential solution can be the application of bacteria of the *Serratia* spp. known to promote plant growth under normal conditions Thus the mini-review aims to summarize the current knowledge on plant growth promotion by *Serratia* spp. (under the conditions of salinity stress, drought, and nutrient deficit) and highlight areas for development in the field. So far, it has been proven that *Serratia* spp. strains exhibit a variety of traits contributing to enhanced plant growth and stress tolerance, such as phytohormone production, ACC deaminase activity, nitrogen fixation, P and Zn solubilization, antioxidant properties improvement, and modulation of gene expression. Nevertheless, further research on *Serratia* spp. is needed, especially on two subjects: elucidating its mechanisms of action on plants at the molecular level and the effects of *Serratia* spp. on the indigenous soil and plant microbiota and, particularly, the rhizosphere. In both cases, it is advisable to use omics techniques to gain in-depth insights into the issues. Additionally, some strains of *Serratia* spp. may be phytopathogens, therefore studies to rule out this possibility are recommended prior to field trials. It is believed that by improving said knowledge the potential of *Serratia* spp. to stimulate plant growth will increase and strains from the genus will serve as an eco-friendly biofertilizer in sustainable agriculture more often.

KEYWORDS

***Serratia* spp., plant growth-promotion bacteria, salinity stress, drought stress, nutritional imbalance stress**

1 Introduction

In the agricultural environment, plants are often exposed to abiotic stresses such as temperature extremes, salt stress, drought, nutrient deficiencies, and heavy metals contamination of soils. These stressors have a significant impact on global agriculture, causing significant economic losses (Faisol et al., 2022; Hewedy et al., 2022; Suleimenova et al., 2023; Wróbel et al., 2023). Salt stress and drought are among the most damaging environmental stresses, which causes plants to simultaneously develop ionic toxicity, osmotic stress, and oxidative stress (Ma et al., 2020; Kulkova et al., 2023). Therefore, eco-friendly solutions such as plant growth-promoting bacteria are needed (Dobrzyński et al., 2022a, 2023a,b).

Serratia spp. is a genus of gram-negative, facultatively anaerobic bacteria belonging to the Enterobacteriaceae family (Grimont and Grimont, 2015). This highly diverse genus grows in a variety of habitats including water, soil, plants, and humans. While some *Serratia* species, in particular *Serratia marcescens* are known to cause opportunistic infections in humans and plant diseases, other strains have gained attention due to their potential as plant growth-promoting bacteria (PGPB) (Hasan et al., 2020; Soenens and Imperial, 2020). *Serratia* spp. strains, as endophytic and rhizospheric microorganisms, when interacting with plants not only contribute positively to stimulating plant growth, increase yields, and improve soil quality under normal conditions, but also can be used in environments exposed to various abiotic and biotic stresses (Verma et al., 2019). Furthermore, plant growth promotion through *Serratia* spp. can reduce dependence on synthetic fertilizers, contributing to sustainable and environmentally friendly agricultural practices (Sood et al., 2019).

Salt- and drought-tolerant bacteria have different mechanisms of tolerance to the abiotic stresses (Gamalero and Glick, 2022). Some of the main mechanisms of *Serratia* spp. promoting plant growth under normal, saline, and drought conditions include: (i) production of phytohormones; (ii) ACC deaminase production; (iii) facilitation of nutrient availability (P or Zn solubilization); (iv) uptake of reactive oxygen species (ROS); (v) osmolytes production; exopolysaccharides (EPS) production; (vi) ion homeostasis in plants; (vii) expression of genes encoding salt and drought stress tolerance (Saikia et al., 2018; Mahdi et al., 2021; Nordstedt and Jones, 2021; Ahmad et al., 2022). In addition to *Serratia* spp., PGPB include, for instance, bacteria of the following genera: *Azotobacter*, *Azospirillum*, *Bacillus*, *Paenibacillus*, *Pseudomonas*, and *Rhizobium* (Gopalakrishnan et al., 2015; Aasfar et al., 2021; Dobrzyński et al., 2021, 2022a,b; Cruz-Hernández et al., 2022; Górska et al., 2024). However, *Serratia* spp., compared to most known bacterial plant growth promoters, is not studied as extensively, particularly with regard to its potential to promote plant growth by modulating the native soil or plant microbiota and, importantly, in the mitigation of plant abiotic stresses including salinity stress, drought stress, and nutritional imbalance stress. Nevertheless, despite the insufficient understanding of the mechanisms governing the modes of action of *Serratia* spp. under stress conditions, some *Serratia* spp. strains have been shown to improve plant growth under salt and drought stress conditions (Table 1).

To our knowledge, this mini-review is the first review of plant growth promotion by bacteria of the genus *Serratia* spp. The mini-review aims to provide an overview of the protective role of *Serratia* spp. against various abiotic stresses such as salinity, drought, and nutrient deficiency. Based on recent studies, important features of *Serratia* spp. that stimulate plant growth under normal conditions are also discussed. Additionally, the aim of the mini-review is to delineate areas that require further research, particularly more detailed studies elucidating the molecular mechanisms of action of various *Serratia* spp. traits that mitigate abiotic stresses in plants.

2 Mini-review methodology

The mini-review analysis was conducted using a variety of keywords such as: abiotic stress, oxidative stress, osmotic stress, ionic stress, salinity stress, drought stress, PGPB, *Serratia*, plant growth-promoting traits, plant physiology, ROS, lipid peroxidation, antioxidant activity, expression of genes, and nutrient imbalance stress. The data were extracted from six databases, namely Google Scholar, Web of Science, Scopus, freefullpdf, Researchgate, and Sciencedirect. Thereby, 98 articles published between 2005 and 2024 were selected. Thence, information was obtained on salinity stress (33 articles), drought stress (24 articles), nutrient uptake (28 articles), and plant growth stimulation under normal conditions (20 articles) by bacteria of genus *Serratia*.

3 *Serratia* spp. strains as plant growth-promoting bacteria in normal and nutrient deficiency conditions

To date, a large number of studies has been published on the effects of different *Serratia* sp. strains on plant growth promotion. As previously evidenced, phytohormone production, AHL, ACC deaminase, nitrogen fixation, P and Zn solubilization, and biofilm formation play crucial roles in stimulating plant growth under normal conditions through the activity of *Serratia* spp. strains (Martínez et al., 2018; Hakim et al., 2021; Debnath et al., 2023).

Importantly, studies using bacteria of *Serratia* spp. have been carried out on plants cultivated under different cultivation conditions. For instance, after inoculation of rice plants with *S. glossinae* GS2 and *S. fonticola* GS2, studies conducted in a climate chamber showed a significant increase in plant growth parameters and chlorophyll content (Jung et al., 2017b, 2020). Interestingly, Jung et al. (2017a,b), by liquid chromatography, also showed that the rhizospheric strains *S. glossinae* GS2 and *S. fonticola* GS2 are capable of producing quorum-sensing (QS) signaling molecules (N-hexanoyl-L-homoserine lactone and N-octanoyl-L-homoserine lactone) that play an important role in biofilm formation and plant-microbe interactions. Besides, Zhang et al. (2022), in growth chamber experiment, revealed that *S. marcescens* PLR inoculation increases the expression of auxin biosynthesis genes in *Arabidopsis* roots and the expression of nutrient transporter genes (N, P, K, and S), which in turn promotes lateral root formation and benefits plant growth. In another pot experiment (on wheat), a genomic analysis of *S. marcescens* OK482790 revealed the presence of key nitrogen cycle genes (Hamada and Soliman, 2023). The strain produces lytic enzymes and antimicrobial compounds and reduces ammonia, which suggests its potential role in wheat plant growth. On the other hand, in a greenhouse experiment, Zheng et al. (2022) reported that *S. marcescens* X-45 may promote plant growth by modifying the taxonomic composition of inoculated plants, which probably contributed to the symbiotic nitrogen-fixing effect and consequently to the growth of inoculated plants.

It has also been reported that after the application of *Serratia* spp. strains, not only did the growth parameters of plants such as *Origanum* L., chamomile, and turmeric improve, but also the essential oil content of the plants increased significantly (Alraey et al., 2019; Mostafa et al., 2019; Jagtap et al., 2023). *S. marcescens* AL2-16 also enhanced the growth and biomass of the medical plant *Achyranthes aspera* L. growth (Devi et al., 2016).

Also, there is research where strains of *Serratia* spp. were used to stimulate plant growth under field conditions. For instance, two strains of *S. liquefaciens* (B.AT and B.A10) showed the ability to, e.g., fix nitrogen, produce IAA, siderophores, and EPS, and enhance plant growth and chlorophyll and carotenoid content (Samet et al., 2022).

TABLE 1 Overview of salt and plant drought tolerance mechanisms mediated by *Serratia* spp. strains.

Strains of *Serratia* spp.	Plant species	Experiments	Salinity/ drought stress	PGPB traits	Results	References
S. fonticola S1T1	Cucumber (*Cucumis sativus* L.)	Greenhouse; pot experiment; isolation and molecular characterization using 16S rRNA; evaluation of plant growth dynamics; determination of leaf relative water content (LRWC), electrolytic leakage from leaves, antioxidant enzymes activity; analyses endogenous abscisic acid (ABA), gene expression using qRT-PCR	200 mM NaCl	Production of phytohormones, solubilization of phosphate, production of siderophores and ACC deaminase	Increase of biomass, root length, shoot length, chlorophyll content and LRWC; decrease of levels of MDA, electrolytic leakage, H_20_2, superoxide anion (SOA) and ABA content; increase of CAT, SOD, gene expression *HKT1, NHX, SOS1*	Moon et al. (2023)
S. marcescens	Eggplant (*Solanum melongena*)	Greenhouse; evaluation of plant growth dynamics; SPAD values and lipid peroxidation; mineral element analysis; antioxidant enzymes activity	200 mM NaCl	Production of ACC deaminase	Increase of shoot fresh weight, shoot dry weight, stem length, leaf area and chlorophyll; decrease of the levels of MDA and Na^+ and Cl^-; increase of SOD, APX, GR	Turhan et al. (2020)
S. proteamaculans ATCC35475	Lettuce (*Lactuca sativa L*)	Greenhouse; evaluation of plant growth dynamics; analysis of inorganic elements and chlorophyll II content; antioxidant enzymes activity	Soil salinity (EC = 1.5 and 7.0 dS m^{-1})	Production of EPS	Increase of fresh weight, dry weight, leaf length, leaf area, chlorophyll content, GR and APX	Han and Lee (2005)
S. marcescens	Pepper (*Capsicum annuum*)	*In vitro*; pot experiment; isolation and molecular characterization using 16S rRNA; screening of bacteria for plant growth promoting traits; evaluation of plant growth dynamics; determination of chlorophyll content and proline	60, 120, and 240 mM NaCl; drought stress	Phosphate solubilization, production of siderophore, ammonia, ACC deaminase, EPS	Increase of fresh plant weight, shoot length, primary root length, no. of secondary roots, no. of leaves, dry plant weight; increase of chlorophyll a, chlorophyll b, proline	Maxton et al. (2018)
S. plymuthica RR-2-5-10; *S. rhizophila* e-p10	Cucumber (*Cucumis sativum* L.)	*In vitro*; greenhouse; plant growth-promoting traits	Soil salinity (EC =659 mS m^{-1})	HCN, production of IAA, ACC deaminase, protease	Increase of dry weight, plant height and fruit yield.	Egamberdieva et al. (2011)

(Continued)

10.3389/fmicb.2024.1342331

TABLE 1 (Continued)

Strains of *Serratia* spp.	Plant species	Experiments	Salinity/ drought stress	PGPB traits	Results	References
S. plymuthica DT8	Jujube (Ziziphus jujuba)	Pot experiment; isolation and molecular characterization using 16S rRNA; evaluation of drought tolerance and plant growth-promoting traits; evaluation of plant growth dynamics; antioxidant enzyme activity and MDA contents	Drought stress	Phosphate solubilization, nitrogen fixation, production of IAA, ACC deaminase, EPS	Increase of plant height, shoot dry matter weight, root dry matter weight; Decrease of the levels of MDA and ethylene content; Increase of SOD, POD, IAA, ABA, RWC, RAS/RS ratio and soil aggregate stability;	Zhang et al. (2020)
Serratia sp. 1–9	Wheat (*Triticum aestivum*)	Greenhouse; isolation and molecular characterization using 16S rRNA; evaluation of drought tolerance and plant growth-promoting traits; evaluation of plant growth dynamics	Drought stress	Auxin; growth in N-free media	Increase of shoot and root dry weight, plant biomass and root	Wang et al. (2014)
S. plymuthica MBSA-MJ1	Petunia (*Petunia* × *hybrida*) (), impatiens (*Impatiens walleriana*), and pansy (*Viola* × *wittrockiana*)	*In vitro*; greenhouse; whole-genome sequencing of strain; taxonomy and phylogenetic comparison; evaluation of drought tolerance and plant growth-promoting traits; evaluation of plant growth dynamics	Drought stress	Production of ACC deaminase	Increase of flower number, shoot and root biomass, shoot dry biomass.	Nordstedt and Jones, 2021

10.3389/fmicb.2024.1342331

Interestingly, Nascente et al. (2019) conducted a field experiment noting that the efficacy of *Serratia* spp. strains may be dependent on the nitrogen dose. The application of *Serratia* sp. BRM 32114 resulted in a significant increase in rice yield, stomatal conductance in plants, and nitrogen, calcium, and magnesium content in the soil at relatively low nitrogen fertilization rates (0, 20, 40, and 80 kg N ha-1) compared to the control. In contrast, higher amounts of nitrogen (120 kg ha $^{-1}$) reduced the beneficial effects of BRM 32114 on rice plants compared to the control (Nascente et al., 2019).

In addition, an important PGPB trait is the ability to solubilize insoluble phosphorus compounds in the soil and thus make their bioavailable forms available to plants. Among the mechanisms enabling phosphorus solubilization are the organic acids production (e.g., malic acid, lactic acid, and acetic acid) and the production of phosphatases including acid (ACP, EC 3.1.3.2) and alkaline (ALK, EC 3.1.3.1) (Behera et al., 2017; Barra et al., 2018). To date, many works have described the significant role of PGPB, including strains from the genus *Serratia,* in solubilizing insoluble phosphorus. For example, a statistically significant increase in N, P, and K content in plants was observed after maize inoculation with *Serratia* sp. QW45 (Zhang et al., 2018). Similar results were obtained in a study conducted by Zafar-ul-Hye et al. (2017) where inoculation of wheat seeds with *S. ficaria* W10 (alone or in combination with *Enterobacter cloacae* W6) significantly increased the concentration of N, P, and K in shoots and grains of plants. In addition, the aforementioned phosphate-solubilizing (also EPS- and auxin-producing) bacteria significantly improved growth parameters, spike number, and wheat yield; this fact indicates their potential as a biofertilizer for plants, especially those in nutrient-poor soils (Zafar-ul-Hye et al., 2017). Besides, plant growth stimulation through phosphate solubilization was also observed in strains such as *Serratia* sp. S2, *S. marcescens* CDP-13 (Dogra et al., 2019), *Serratia* sp. KPS-14 (Hanif et al., 2020), *Serratia* sp. LX2 (Guo et al., 2021), and *S. plymuthica* BMA1 (Borgi et al., 2020).

Also, several reports show that *Serratia* sp. S119 can stimulate the growth of peanut and corn due to its ability to solubilize inorganic phosphate, thereby supporting plants in environments low in available P (Anzuay et al., 2017; Ludueña et al., 2018). Ludueña et al. (2023) revealed that the root exudates obtained from plants grown under P-deficient conditions promote colonization and biofilm formation of the strain *Serratia* sp. S119 and stimulate its ability to solubilize phosphate and ACC deaminase activity.

Importantly, bacteria of *Serratia* spp. can also promote growth in nitrogen-poor soils (Zaheer et al., 2016). For instance, inoculation with *Serratia* sp. 5D resulted in a 30.85% increase in a chickpea grain yield in nutrient-poor areas (N, P, K), compared to the uninoculated control (Zaheer et al., 2016). Moreover, in nitrogen-poor cultivation, the strain *Serratia* sp. ZM synthesizes more IAA, thereby supporting root and plant growth (Ouyang et al., 2017).

It has also been documented that *Serratia* spp. strains can be potential candidates for combating Zn deficiency by increasing the bioavailability of the element to plants through various mechanisms (Table 2).

In conclusion, *Serratia* spp. demonstrates potential as a plant growth-promoting bacteria (PGPB) with diverse mechanisms. Understanding these mechanisms is crucial for harnessing their full potential in sustainable agriculture. Therefore, further research is needed to determine the mechanisms of, for instance, solubilization of phosphorus, the vast majority of which is unavailable to plants in the soil. Knowledge of whether a *Serratia* spp. strains solubilize phosphorus via the production of organic acids or phosphatases could contribute to more extensive exploitation of the potential of such a strain. Additionally, research on *Serratia* spp. should be conducted under field conditions, as this brings PGPB closer to commercialization.

4 Alleviation of salinity stress in plants by *Serratia* spp.

Long-term salinity causes ion toxicity due to increased concentrations of Na^+ and Cl^- ions, which leads to nutrient imbalance and decreased osmotic potential of the soil; such conditions induce oxidative stress (Egamberdieva et al., 2018). More specifically, oxidative stress is induced by the production of toxic ROS mainly including hydrogen peroxide (H_2O_2), singlet oxygen ($^1O_2$), superoxide ions superoxide anion ($O_2^{\bullet-}$), hydroxyl radical ($HO^\bullet$), peroxy radical ($ROO^\bullet$), alkoxyl radicals ($RO^\bullet$), and reactive nitrogen species (RNS) (Gupta et al., 2022; Szechyńska-Hebda et al., 2022). The ROS cause lipid peroxidation, inactivation of antioxidant enzymes (CAT, POD, SOD, APX, GR), reduced photosynthetic rates, membrane permeability and denaturation of DNA, RNA, and proteins, which activates programmed cell death (Nawaz et al., 2020; Mousavi et al., 2022).

Some recent studies have revealed the beneficial effects of *Serratia* spp. strains under saline conditions on various crops such as maize (*Zea mays* L.) (Becze et al., 2021), wheat (*Triticum aestivum* L.) (Desoky et al., 2020), and quinoa (*Chenopodium quinoa* Willd.) (Mahdi et al., 2021). For example, studies under controlled conditions by Becze et al. (2021) showed that after inoculation with *S. fonticola* BB17 at NaCl concentrations of 1–3 g L^{-1}, the biomass and chlorophyll a + b content of maize plants increased significantly. Similarly, inoculation of maize with *S. liquefaciens* KM4 with 80 and 160 mM NaCl increased photosynthetic efficiency (chlorophyll a, b, a + b and carotenoids). Interestingly, the authors attributed these results to enhancing the expression of genes mediating the photosynthesis (RuBisCO coding genes: *rbcL* and *rbcS*). Another study also evaluated the effect of strain from *Serratia* spp. on genes expression. El-Esawi et al. (2018) documented that maize inoculated with *S. liquefaciens* KM4 showed significantly less oxidative damage compared to the control group; the strain up-regulated the expression of the most important stress-related genes (CAT, SOD, APX, H^+-PPase, HKT1, and NHX1), which in turn alleviated the toxicity of Na^+ and Cl^- ions, thus enhancing plant tolerance to salinity. Similar beneficial effects were observed in a study on wheat inoculation with *S. marcescens* M8 at different salinity levels (150 mM and 300 mM NaCl) (Desoky et al., 2020). In this study, increases in enzymatic and non-enzymatic antioxidant activities (CAT, POD, SOD, AsA, GsH, α-TOC) and significant reductions in Na^+ levels and oxidative stress biomarkers (H_2O_2 and $O_2^{\bullet-}$) alleviated the deleterious effects of salinity stress and enhanced wheat growth.

ACC deaminase is crucial for mitigating salt stress in wheat by *Serratia* spp. strains (Barra et al., 2016; Acuña et al., 2019). Zahir et al. (2009) reported that *S. proteamaculans* M35, exhibiting ACC deaminase activity at different salinity conditions (ES = 1.63–15.0 ds m^{-1}), significantly increased biometric parameters of wheat plants and improved K^+/Na^+ ratio. The positive effect of ACC deaminase under salinity stress was also showed in a study by Nadeem et al. (2013)

TABLE 2 Effective *Serratia* spp. with Zn solubilizing mechanism.

Strains of *Serratia* spp.	Plants	Insoluble Zn form	Plant growth promoting traits	References
S. nematodiphilia TM 56	Rice (*Oryza sativa* L.)	ZnO, $ZnCO_3$, and $Zn_3(PO4)_2$	Zn, P solubilization, IAA production, nitrogen fixation, siderophore production, cellulose degradation, organic acid production	Othman et al. (2022)
Serratia sp.	Rice (*Oryza sativa* L.)	$ZnSO_4$ and ZnO	Zn solubilization	Idayu (2017)
Serratia sp. TM9	Rice (*Oryza sativa* L. cultivar MR219)	$ZnSO_4$ and ZnO	Zn solubilization	Idayu et al. (2017)
S. marcescens	Rice (*Oryza sativa* L.)	ZnO, $ZnCO_3$, and $ZnPO_4$	Zn, P solubilization, siderophore production. IAA production; ammonia production, EPS production	Upadhayay et al. (2022)
S. marcescens FA-4	Wheat (*Triticum aestivum* L.), Rice (*Triticum aestivum* L.)	ZnO, $ZnCO_3$, ZnS	Zn solubilization, ACC-deaminase activity. N2 fixation, EPS activity, siderophore activity, antifungal activity	Abaid-Ullah et al. (2015) and Shakeel et al. (2023)
S. liquefaciens FA-2	Wheat (*Triticum aestivum* L.)	ZnO, $ZnCO_3$	Zn solubilization, ACC-deaminase activity. N2 fixation, EPS activity, siderophore activity, antifungal activity	Abaid-Ullah et al. (2015)
Serratia sp.	Maize (*Zea mays* L.)	ZnO	Zn solubilization, ACC deaminase activity, ammonia production, GA_3 production	Kour et al. (2019)
S. marcescens AF8I1	Carrot (*Daucus carota* L.)	ZnO, $[ZnCO_3]_2$ $[Zn(OH)_2]_3$, ZnCO	Zn, P, K solubilization, IAA, ammonia production, chitinolytic activity, siderophore activity	Fiodor et al. (2023)

where wheat seeds after inoculation with *S. ficaria* W10 were sown in naturally saline fields (EC = 1.0–15.0 dS m^{-1}), which significantly increased germination percentage, germination rate, wheat seed rate, and plant yield, compared to the uninoculated control. Additionally, the ACC deaminase producing strain *S. marcescens* CDP-13 minimized oxidative damage, thereby increasing wheat plant tolerance under various levels of salt stress (150 mM, 175 mM and 200 mM NaCl) (Singh and Jha, 2016a). Similar results were obtained using the ACC deaminase-producing strain of *Serratia* sp. SL-12 in wheat grown on saline soil. The authors observed that *Serratia* sp. SL-12 increased plant growth parameters, facilitating nutrient uptake (Singh and Jha, 2016b). Furthermore, the ACC deaminase producing consortium consisting of *S. ficaria* W10, *Pseudomonas putida*, and *P. fluorescens* improved the physiology, growth, and yield characteristics of wheat (Sohaib et al., 2020). Despite the fact that ACC deaminase is known to reduce ethylene levels by degrading ACC and thus reducing the effects of stress on plants, the molecular mechanism of action of *Serratia* spp. strains in alleviating the effects of drought stress in plants is still relatively poorly understood. On the other hand, explanatory studies have emerged showing how halotolerant strain responds to salinity at the level of the proteome. ACC deaminase-producing *S. plymuthica* Sp2 was molecularly studied using a proteomic approach (Novello et al., 2022). Overall, the study revealed that the levels of proteins involved in salt stress responses (4.4% NaCl) were increased, while the levels of proteins involved in metabolism and strand structure were decreased. The main proteins with increased expression in the Sp2 proteome were DsbA, ATP, Porin OmpA, Porin OmpC, and LpoB (Novello et al., 2022).

In addition, it was recently reported that *S. rubidaea* strain ED1, which produces siderophores, cellulase, ammonia, and indole-3-acetic acid (IAA) through its ability to solubilize phosphate and insoluble zinc compounds, increased seed germination and seedling growth of quinoa under salt stress conditions (Mahdi et al., 2021).

Numerous studies have confirmed the potential of *Serratia* spp. strains as biofertilizers promoting plant growth while improving physiological, biochemical, and molecular parameters under salt stress conditions. Nevertheless, we believe that there is a need for further studies of halotolerant *Serratia* spp. strains which have shown tolerance to salinity from 5.8 to 10% NaCl and significant potential in promoting plant growth under normal conditions (George et al., 2013; Hamane et al., 2023; Jagtap et al., 2023). Screening strains of *Serratia* spp. (exhibiting stimulation under normal conditions) for plant growth promotion under saline conditions could increase the list of strains that mitigate the effects of said stress and contribute to the selection of the best ones. Importantly, research is also needed to explain how specific PGP traits affect the expression of genes

responsible for mitigating the effects of salinity stress. Such studies should be carried out using omics approach, which will allow a deeper insight into, for example, the plant proteome after the introduction of *Serratia* spp.

5 Mitigation of drought stress by *Serratia* spp.

In almost all regions of the world, drought stress is one of the most serious problems recognized as one of the factors limiting crop productivity (Kour and Yadav, 2022). In response to drought stress, plants have lower stomatal conductance, leading to reduced CO_2 uptake and consequently a decrease in the photosynthesis rate (Saberi Riseh et al., 2021). Plants exposed to drought stress reduce leaf water potential, transpiration rate, and turgor factor, leading to reduced relative water content (RWC) and plant cell damage or death (Kasim et al., 2021).

There are various microorganisms that can effectively help plants under water deficit conditions (Abdelaal et al., 2021). Experiments conducted under drought conditions have shown that *Serratia* spp. strains are capable of effectively stimulating plant growth (Khan and Singh, 2021). In terms of alleviating drought stress, the best studied species of *Serratia* spp. is *S. odorifera.* ACC deaminase-producing strain *S. odorifera* (accession number KC425221) provided tolerance to drought stress by regulating ethylene levels in plants (Ullah et al., 2020; Gul et al., 2023). For instance, a positive effect of *S. odorifera* application was found on wheat in a study by Bangash et al. (2013). Besides, under water deficit conditions, *S. odorifera* (alone or in combination with biocarbon) was able to significantly improve soil nutrition (N, P, and K) and plant growth parameters of barley and maize, compared to the control (Ullah et al., 2020; Gul et al., 2023). The studied strain also significantly increased photosynthetic parameters (chlorophyll a, b, and a + b), NPK content, and SOD, POD, and CAT activities in fresh leaves.

The capacity to mitigate the effects of drought was also observed in other bacteria from *Serratia* spp. The ACC deaminase- and EPS-producing strain *S. marcescens* RRNII not only improved the physiological status and productivity of wheat crops, but also increased micronutrient contents (Zn and Fe) in grains (Khan and Singh, 2021). Interestingly, the EPS produced by the bacteria, under drought stress conditions, provide a microenvironment that retains water, thereby protecting the bacteria from drying out by increasing water availability in the plants (Zhang et al., 2020). The role of EPS-producing bacteria from *Serratia* spp. in promoting growth of maize and rice under drought conditions has also been demonstrated in the studies of Yaseen et al. (2020) and Pang et al. (2020). Furthermore, according to Wang et al. (2012) and Shinde and Borkar (2018), osmolytic proline may also play an important role in the plant response to drought stress by protecting plants from excessive dehydration. Wang et al. (2012) reported that after inoculation of cucumber (*Cucumis sativa* L.) seedlings with a BBS consortium (*Bacillus cereus* AR156, *Bacillus subtilis* SM21, and *Serratia* sp. XY21), leaf proline content increased 4-fold compared to the control. However, in a study by Shinde and Borkar (2018), inoculation of sorghum (*Sorghum bicolor*) seeds with *S. marcescens* L1SC8 and *S. marcescens* L2FmA4 resulted in a significant increase in proline content, which also proved to be beneficial in mitigating the effects of drought stress.

In summary, strains of *Serratia* spp. may help plants tolerate drought through mechanisms such as the production of ACC deaminase, EPS, various phytohormones, increased nutrient uptake, induction of osmolyte, and antioxidant accumulation. However, it is worth adding that the biochemical and molecular mechanisms governing the resistance and tolerance to drought stress induced by *Serratia* spp. strains are still unclear, thus further research is needed. As in the case of mechanisms related to salinity stress, studies using omics methods at the level of the transcriptome or proteome are needed to elucidate the detailed effects of PGP traits on plants under drought conditions.

6 Conclusions and future prospective

In sustainable agriculture, *Serratia* spp. holds promise as a valuable tool enhancing both crop yields and quality while aiding plants in managing abiotic stresses. Nevertheless, further research into the mechanisms of action of these bacteria is crucial to fully realize their potential in agricultural practice. As previously mentioned, there is insufficient knowledge regarding the impact of PGP Serratia spp. on the expression of genes associated with growth and protection against abiotic stresses in various plants. We believe that these issues should continue to be investigated, particularly using omics methods. Expanding our knowledge of these mechanisms may also lead to improvements in the effectiveness of *Serratia* spp. strains in important plants, for instance wheat, maize, soya or rice.

Furthermore, studies on the impact of *Serratia* spp. strains on the native microbiota are particularly relevant, especially on the rhizosphere microbiota which belongs to the plant-microbiome axis and seems to be the most significant. To the best of our knowledge, there has been only one publication to date describing this issue, which is insufficient to assess the impact of *Serratia* spp. on the native rhizosphere microbiota. Further studies on a wide range of plants, soils, and different climate types are therefore needed to determine repeatable patterns. Obtaining information on the increase or decrease in abundance of the crucial taxa (e.g., Proteobactera, Actinobacteriota, Acidobacteriota) involved in main soil biochemical processes, may contribute to the development of different optimized formulations with increased efficiency in promoting plant growth. In addition, insights into the native microbiota after application of *Serratia* spp. are also needed to assess bacterial and fungal diversity, the disruption of which may contribute to a decline in soil quality and yield. Research on *Serratia* spp. strains that promote plant growth should also be expanded to determine the potential for biofilm formation, which could optimize rhizosphere colonization.

At the end, it should also be noted that some strains of *Serratia* can be plant and human pathogens, which has been overlooked in the context of research on PGPB. Therefore, prior to field studies, it is vital to examine whether the genomes of PGPB strains contain genes associated with virulence.

Author contributions

IK: Writing – original draft, Conceptualization. BW: Writing – original draft. JD: Writing – review & editing, Supervision.

Funding

The author(s) declare that no financial support was received for the research, authorship, and/or publication of this article.

Acknowledgments

English language revision and translation assistance provided by Katarzyna Rafalska.

Conflict of interest

The authors declare that the research was conducted in the absence of any commercial or financial relationships that could be construed as a potential conflict of interest.

Publisher's note

All claims expressed in this article are solely those of the authors and do not necessarily represent those of their affiliated organizations, or those of the publisher, the editors and the reviewers. Any product that may be evaluated in this article, or claim that may be made by its manufacturer, is not guaranteed or endorsed by the publisher.

References

Aasfar, A., Bargaz, A., Yaakoubi, K., Hilali, A., Bennis, I., Zeroual, Y., et al. (2021). Nitrogen fixing Azotobacter species as potential soil biological enhancers for crop nutrition and yield stability. *Front. Microbiol.* 12:628379. doi: 10.3389/fmicb.2021.628379

Abaid-Ullah, M., Hassan, M. N., Jamil, M., Brader, G., Shah, M. K. N., Sessitsch, A., et al. (2015). Plant growth promoting rhizobacteria: an alternate way to improve yield and quality of wheat (*Triticum aestivum*). *Int. J. Agric. Biol.* 17, 51–60.

Abdelaal, K., AlKahtani, M., Attia, K., Hafez, Y., Király, L., and Künstler, A. (2021). The role of plant growth-promoting Bacteria in alleviating the adverse effects of drought on plants. *Biology* 10:520. doi: 10.3390/biology10060520

Acuña, J. J., Campos, M., Mora, M. D. L. L., Jaisi, D. P., and And Jorquera, M. A. (2019). ACCD-producing rhizobacteria from an Andean Altiplano native plant (Parastrephia quadrangularis) and their potential to alleviate salt stress in wheat seedlings. *Appl. Soil Ecol.* 136, 184–190. doi: 10.1016/j.apsoil.2019.01.005

Ahmad, H. M., Fiaz, S., Hafeez, S., Zahra, S., Shah, A. N., Gul, B., et al. (2022). Plant growth-promoting Rhizobacteria eliminate the effect of drought stress in plants: a review. *Front. Plant Sci.* 13:875774. doi: 10.3389/fpls.2022.875774

Alraey, D. A., Haroun, S. A., Omar, M. N., Abd-ElGawad, A. M., El-Shobaky, A. M., and Mowafy, A. M. (2019). Fluctuation of essential oil constituents in *Origanum syriacum* subsp. *sinaicum* in response to plant growth promoting Bacteria. *J. Essent. Oil-Bear. Plants* 22, 1022–1033. doi: 10.1080/0972060X.2019.1661794

Anzuay, M. S., Ciancio, M. G. R., Ludueña, L. M., Angelini, J. G., Barros, G., Pastor, N., et al. (2017). Growth promotion of peanut (*Arachis hypogaea* L.) and maize (*Zea mays* L.) plants by single and mixed cultures of efficient phosphate solubilizing bacteria that are tolerant to abiotic stress and pesticides. *Microbiol. Res.* 199, 98–109. doi: 10.1016/j.micres.2017.03.006

Bangash, N., Khalid, A., Mahmood, T., and Siddique, M. T. (2013). Screening rhizobacteria containing ACC-deaminase for growth promotion of wheat under water stress. *Pak. J. Bot.* 45, 91–96.

Barra, P. J., Inostroza, N. G., Acuña, J. J., Mora, M. L., Crowley, D. E., and Jorquera, M. A. (2016). Formulation of bacterial consortia from avocado (*Persea americana* mill.) and their effect on growth, biomass and superoxide dismutase activity of wheat seedlings under salt stress. *Appl. Soil Ecol.* 102, 80–91. doi: 10.1016/j.apsoil.2016.02.014

Barra, P. J., Viscardi, S., Jorquera, M. A., Duran, P. A., Valentine, A. J., and De La Luz Mora, M. (2018). Understanding the strategies to overcome phosphorus–deficiency and aluminum–toxicity by ryegrass endophytic and rhizosphere Phosphobacteria. *Front. Microbiol.* 9:1155. doi: 10.3389/fmicb.2018.01155

Becze, A., Vincze, E. B., Varga, H. M., and Gyongyver, M. (2021). Effect of plant growth promoting rhizobacteria on *Zea mays* development and growth under heavy metal and salt stress condition. *Environ. Eng. Manag. J.* 20, 547–557. doi: 10.30638/eemj.2021.053

Behera, B. C., Yadav, H., Singh, S. K., Mishra, R. R., Sethi, B. K., Dutta, S. K., et al. (2017). Phosphate solubilization and acid phosphatase activity of *Serratia* sp. isolated from mangrove soil of Mahanadi river delta, Odisha, India. *J. Genet. Eng. Biotechnol.* 15, 169–178. doi: 10.1016/j.jgeb.2017.01.003

Borgi, M. A., Saidi, I., Moula, A., Rhimi, S., and Rhimi, M. (2020). The attractive *Serratia plymuthica* BMA1 strain with high rock phosphate-solubilizing activity and its effect on the growth and phosphorus uptake by *Vicia faba* L. *Plants. Geomicrobiol. J.* 37, 437–445. doi: 10.1080/01490451.2020.1716892

Cruz-Hernández, M. A., Mendoza-Herrera, A., Bocanegra-García, V., and Rivera, G. (2022). *Azospirillum* spp. from plant growth-promoting bacteria to their use in bioremediation. *Microorganisms* 10:1057. doi: 10.3390/microorganisms10051057

Debnath, S., Chakraborty, S., Langthasa, M., Choure, K., Agnihotri, V., Srivastava, A., et al. (2023). Non-rhizobial nodule endophytes improve nodulation, change root exudation pattern and promote the growth of lentil, for prospective application in fallow soil. *Front. Plant Sci.* 14:1152875. doi: 10.3389/fpls.2023.1152875

Desoky, E.-S. M., Saad, A. M., El-Saadony, M. T., Merwad, A.-R. M., and Rady, M. M. (2020). Plant growth-promoting rhizobacteria: potential improvement in antioxidant defense system and suppression of oxidative stress for alleviating salinity stress in *Triticum aestivum* (L.) plants. *Biocatal. Agric. Biotechnol.* 30:101878. doi: 10.1016/j.bcab.2020.101878

Devi, K. A., Pandey, P., and Sharma, G. D. (2016). Plant growth-promoting endophyte *Serratia marcescens* AL2-16 enhances the growth of *Achyranthes aspera* L., a medicinal plant. *HAYATI J. Biosci.* 23, 173–180. doi: 10.1016/j.hjb.2016.12.006

Dobrzyński, J., Jakubowska, Z., and Dybek, B. (2022a). Potential of *Bacillus pumilus* to directly promote plant growth. *Front. Microbiol.* 13:1069053. doi: 10.3389/fmicb.2022.1069053

Dobrzyński, J., Jakubowska, Z., Kulkova, I., Kowalczyk, P., and Kramkowski, K. (2023a). Biocontrol of fungal phytopathogens by *Bacillus pumilus*. *Front. Microbiol.* 14:1194606. doi: 10.3389/fmicb.2023.1194606

Dobrzyński, J., Wierzchowski, P. S., Stępień, W., and Górska, E. B. (2021). The reaction of cellulolytic and potentially cellulolytic spore-forming bacteria to various types of crop management and farmyard manure fertilization in bulk soil. *Agronomy* 11:772. doi: 10.3390/agronomy11040772

Dobrzyński, J., Wróbel, B., and Górska, E. B. (2022b). Cellulolytic properties of a potentially lignocellulose-degrading Bacillus sp. 8E1A strain isolated from bulk soil. *Agronomy* 12:665. doi: 10.3390/agronomy12030665

Dobrzyński, J., Wróbel, B., and Górska, E. B. (2023b). Taxonomy, ecology, and cellulolytic properties of the genus *Bacillus* and related genera. *Agriculture* 13:1979. doi: 10.3390/agriculture13101979

Dogra, N., Yadav, R., Kaur, M., Adhikary, A., Kumar, S., and Ramakrishna, W. (2019). Nutrient enhancement of chickpea grown with plant growth promoting bacteria in local soil of Bathinda, northwestern India. *Physiol. Mol. Biol. Plants* 25, 1251–1259. doi: 10.1007/s12298-019-00661-9

Egamberdieva, D., Kucharova, Z., Davranov, K., Berg, G., Makarova, N., Azarova, T., et al. (2011). Bacteria able to control foot and root rot and to promote growth of cucumber in salinated soils. *Biol. Fertil. Soils* 47, 197–205. doi: 10.1007/s00374-010-0523-3

Egamberdieva, D., Wirth, S., and Abd_Allah, E. F. (2018). "Plant hormones as key regulators in plant-microbe interactions under salt stress" in *Plant microbiome: Stress response microorganisms for sustainability*. eds. D. Egamberdieva and P. Ahmad (Singapore: Springer Singapore), 165–182.

El-Esawi, M., Alaraidh, I., Alsahli, A., Alzahrani, S., Ali, H., Alayafi, A., et al. (2018). *Serratia liquefaciens* KM4 improves salt stress tolerance in maize by regulating redox potential, ion homeostasis, Leaf gas exchange and stress-related gene expression. *IJMS* 19:3310. doi: 10.3390/ijms19113310

Faisol, A., Indarto, I., Novita, E., and Budiyono, B. (2022). Assessment of agricultural drought based on CHIRPS data and SPI method over West Papua–Indonesia. *J. Water Land Dev.* 52, 44–52. doi: 10.24425/jwld.2021.139942

Fiodor, A., Ajijah, N., Dziewit, L., and Pranaw, K. (2023). Biopriming of seed with plant growth-promoting bacteria for improved germination and seedling growth. *Front. Microbiol.* 14:1142966. doi: 10.3389/fmicb.2023.1142966

Gamalero, E., and Glick, B. R. (2022). Recent advances in bacterial amelioration of plant drought and salt stress. *Biology* 11:437. doi: 10.3390/biology11030437

George, P., Gupta, A., Gopal, M., Thomas, L., and Thomas, G. V. (2013). Multifarious beneficial traits and plant growth promoting potential of *Serratia marcescens* KiSII and Enterobacter sp. RNF 267 isolated from the rhizosphere of coconut palms (*Cocos nucifera* L.). *World J. Microbiol. Biotechnol.* 29, 109–117. doi: 10.1007/s11274-012-1163-6

Gopalakrishnan, S., Sathya, A., Vijayabharathi, R., Varshney, R. K., Gowda, C. L., and Krishnamurthy, L. (2015). Plant growth promoting rhizobia: challenges and opportunities. *3 Biotech.* 5, 355–377. doi: 10.1007/s13205-014-0241-x

Górska, E. B., Stępień, W., Hewelke, E., Lata, J. C., Gworek, B., Gozdowski, D., et al. (2024). Response of soil microbiota to various soil management practices in 100-year-old agriculture field and identification of potential bacterial ecological indicator. *Ecol. Indic.* 158:111545. doi: 10.1016/j.ecolind.2024.111545

Grimont, F., and Grimont, P. A. (2015). "*Serratia*" in *Bergey's manual of systematics of archaea and bacteria* (New Jersey, US: Wiley), 1–22.

Gul, F., Khan, I. U., Rutherford, S., Dai, Z.-C., Li, G., and Du, D.-L. (2023). Plant growth promoting rhizobacteria and biochar production from *Parthenium hysterophorus* enhance seed germination and productivity in barley under drought stress. *Front. Plant Sci.* 14:1175097. doi: 10.3389/fpls.2023.1175097

Guo, S., Feng, B., Xiao, C., Wang, Q., Zhou, Y., and Chi, R. (2021). Effective Solubilization of rock phosphate by a phosphate-tolerant bacterium *Serratia* sp. *Geomicrobiology* 38, 561–569. doi: 10.1080/01490451.2021.1903623

Gupta, A., Mishra, R., Rai, S., Bano, A., Pathak, N., Fujita, M., et al. (2022). Mechanistic insights of plant growth promoting Bacteria mediated drought and salt stress tolerance in plants for sustainable agriculture. *IJMS* 23:3741. doi: 10.3390/ijms23073741

Hakim, S., Naqqash, T., Nawaz, M. S., Laraib, I., Siddique, M. J., Zia, R., et al. (2021). Rhizosphere engineering with plant growth-promoting microorganisms for agriculture and ecological sustainability. *Front. Sustain. Food Syst.* 5:617157. doi: 10.3389/fsufs.2021.617157

Hamada, M. A., and Soliman, E. R. S. (2023). Characterization and genomics identification of key genes involved in denitrification-DNRA-nitrification pathway of plant growth-promoting rhizobacteria (*Serratia marcescens* OK482790). *BMC Microbiol.* 23:210. doi: 10.1186/s12866-023-02941-7

Hamane, S., El Yemlahi, A., Hassani Zerrouk, M., El Galiou, O., Laglaoui, A., Bakkali, M., et al. (2023). Plant growth promotion and biocontrol potentiality of endophytes isolated from root nodules of *Sulla flexuosa* L. *Int. J. Agron.* 2023, 1–9. doi: 10.1155/2023/2451806

Han, H. S., and Lee, K. D. (2005). Physiological responses of soybean-inoculation of *Bradyrhizobium japonicum* with PGPR in saline soil conditions. *Res. J. Agric. Biol. Sci.* 1, 216–221.

Hanif, M. K., Malik, K. A., Hameed, S., Saddique, M. J., Ayesha, F. K., Naqqash, T., et al. (2020). Growth stimulatory effect of AHL producing *Serratia* spp. from potato on homologous and non-homologous host plants. *Microbiol. Res.* 238:126506. doi: 10.1016/j.micres.2020.126506

Hasan, M. F., Islam, M. A., and Sikdar, B. (2020). First report of *Serratia marcescens* associated with black rot of *Citrus sinensis* fruit, and evaluation of its biological control measures in Bangladesh. *F1000Research*. 9:9. doi: 10.12688/f1000research.27657.2

Hewedy, O. A., Mahmoud, G. A. E., Elshafey, N. F., Khamis, G., Karkour, A. M., Abdel Lateif, K. S., et al. (2022). Plants take action to mitigate salt stress: ask microbe for help, phytohormones, and genetic approaches. *J. Water Land Dev.* 55, 1–16. doi: 10.24425/jwld.2022.142299

Idayu, O. N. M. (2017). Inoculation of zinc-solubilizing Bacteria with different zinc sources and rates for improved growth and zinc uptake in Rice. *IJAB* 19, 1137–1140. doi: 10.17957/IJAB/15.0396

Idayu, O. N. M., Othman, R., Saud, H. M., and Megat Wahab, P. E. (2017). Effects of root colonization by zinc-solubilizing bacteria on rice plant (*Oryza sativa* MR219) growth. *Agric. Nat. Resour.* 51, 532–537. doi: 10.1016/j.anres.2018.05.004

Jagtap, R. R., Mali, G. V., Waghmare, S. R., Nadaf, N. H., Nimbalkar, M. S., and Sonawane, K. D. (2023). Impact of plant growth promoting rhizobacteria *Serratia nematodiphila* RGK and *Pseudomonas plecoglossicida* RGK on secondary metabolites of turmeric rhizome. *Biocatal. Agric. Biotechnol.* 47:102622. doi: 10.1016/j.bcab.2023.102622

Jung, B. K., Ibal, J. C., Pham, H. Q., Kim, M.-C., Park, G.-S., Hong, S.-J., et al. (2020). Quorum sensing system affects the plant growth promotion traits of *Serratia fonticola* GS2. *Front. Microbiol.* 11:536865. doi: 10.3389/fmicb.2020.536865

Jung, B. K., Khan, A. R., Hong, S.-J., Park, G.-S., Park, Y.-J., Kim, H.-J., et al. (2017a). Quorum sensing activity of the plant growth-promoting rhizobacterium *Serratia glossinae* GS2 isolated from the sesame (*Sesamum indicum* L.) rhizosphere. *Ann. Microbiol.* 67, 623–632. doi: 10.1007/s13213-017-1291-1

Jung, B. K., Khan, A. R., Hong, S.-J., Park, G.-S., Park, Y.-J., Park, C. E., et al. (2017b). Genomic and phenotypic analyses of *Serratia fonticola* strain GS2: a rhizobacterium isolated from sesame rhizosphere that promotes plant growth and produces N-acyl homoserine lactone. *J. Biotechnol.* 241, 158–162. doi: 10.1016/j.jbiotec.2016.12.002

Kasim, W. A., Osman, M. E. H., Omar, M. N., and Salama, S. (2021). Enhancement of drought tolerance in *Triticum aestivum* L. seedlings using *Azospirillum brasilense* NO40 and *Stenotrophomonas maltophilia* B11. *Bull. Natl. Res. Cent.* 45:95. doi: 10.1186/s42269-021-00546-6

Khan, A., and Singh, A. V. (2021). Multifarious effect of ACC deaminase and EPS producing Pseudomonas sp. and *Serratia marcescens* to augment drought stress tolerance and nutrient status of wheat. *World J. Microbiol. Biotechnol.* 37:198. doi: 10.1007/s11274-021-03166-4

Kour, R., Jain, D., Bhojiya, A. A., Sukhwal, A., Sanadhya, S., Saheewala, H., et al. (2019). Zinc biosorption, biochemical and molecular characterization of plant growth-promoting zinc-tolerant bacteria. *3 Biotech.* 9:421. doi: 10.1007/s13205-019-1959-2

Kour, D., and Yadav, A. N. (2022). Bacterial mitigation of drought stress in plants: current perspectives and future challenges. *Curr. Microbiol.* 79:248. doi: 10.1007/s00284-022-02939-w

Kulkova, I., Dobrzyński, J., Kowalczyk, P., Bełżecki, G., and Kramkowski, K. (2023). Plant growth promotion using *Bacillus cereus*. *IJMS* 24:9759. doi: 10.3390/ijms24119759

Ludueña, L. M., Anzuay, M. S., Angelini, J. G., McIntosh, M., Becker, A., Rupp, O., et al. (2018). Strain *Serratia* sp. S119: a potential biofertilizer for peanut and maize and a model bacterium to study phosphate solubilization mechanisms. *Appl. Soil Ecol.* 126, 107–112. doi: 10.1016/j.apsoil.2017.12.024

Ludueña, L. M., Valdés, P. F., Anzuay, M. S., Dalmasso, R., Angelini, J. G., Tejerizo, G. T., et al. (2023). Impact of phosphorus deficiency on the interaction between the biofertilizer strain *Serratia* sp. S119 with peanut (*Arachis hypogaeae* L.) and maize (*Zea mays* L.) plants. *Plant Soil* 487, 639–653. doi: 10.1007/s11104-023-05963-2

Ma, Y., Dias, M. C., and Freitas, H. (2020). Drought and salinity stress responses and microbe-induced tolerance in plants. *Front. Plant Sci.* 11:591911. doi: 10.3389/fpls.2020.591911

Mahdi, I., Hafidi, M., Allaoui, A., and Biskri, L. (2021). Halotolerant endophytic bacterium *Serratia rubidaea* ED1 enhances phosphate Solubilization and promotes seed germination. *Agriculture* 11:224. doi: 10.3390/agriculture11030224

Martínez, O. A., Encina, C., Tomckowiack, C., Droppelmann, F., Jara, R., Maldonado, C., et al. (2018). *Serratia* strains isolated from the rhizosphere of rauli (*Nothofagus alpina*) in volcanic soils harbour PGPR mechanisms and promote raulí plantlet growth. *J. Soil Sci. Plant Nutr.* 18, 804–819. doi: 10.4067/S0718-95162018005002302

Maxton, A., Singh, P., and Masih, S. A. (2018). ACC deaminase-producing bacteria mediated drought and salt tolerance in *Capsicum annuum*. *J. Plant Nutr.* 41, 574–583. doi: 10.1080/01904167.2017.1392574

Moon, Y.-S., Khan, M., Khan, M. A., and Ali, S. (2023). Ameliorative symbiosis of *Serratia fonticola* (S1T1) under salt stress condition enhance growth-promoting attributes of *Cucumis sativus* L. *Symbiosis* 89, 283–297. doi: 10.1007/s13199-023-00897-w

Mostafa, A., Khalafallah, M., AboSedera, S., Fathy, H., and Higazy, A. (2019). Different methods of bacterial inoculation on the yield of chamomile blossoms and essential oil. *Global J. Environ. Sci. Manag.* 5, 237–248.

Mousavi, S. S., Karami, A., Saharkhiz, M. J., Etemadi, M., and Ravanbakhsh, M. (2022). Microbial amelioration of salinity stress in endangered accessions of Iranian licorice (*Glycyrrhiza glabra* L.). *BMC Plant Biol.* 22:322. doi: 10.1186/s12870-022-03703-9

Nadeem, S. M., Zahir, Z. A., Naveed, M., and Nawaz, S. (2013). Mitigation of salinity-induced negative impact on the growth and yield of wheat by plant growth-promoting rhizobacteria in naturally saline conditions. *Ann. Microbiol.* 63, 225–232. doi: 10.1007/s13213-012-0465-0

Nascente, A. S., Lanna, A. C., De Sousa, T. P., Chaibub, A. A., De Souza, A. C. A., and De Filippi, M. C. C. (2019). N fertilizer dose-dependent efficiency of *Serratia* spp. for improving growth and yield of upland Rice (*Oryza sativa* L.). *Int. J. Plant Prod.* 13, 217–226. doi: 10.1007/s42106-019-00049-5

Nawaz, A., Shahbaz, M., Asadullah, Imran, A., Marghoob, M. U., Imtiaz, M., et al. (2020). Potential of salt tolerant PGPR in growth and yield augmentation of wheat (*Triticum aestivum* L.) under saline conditions. *Front. Microbiol.* 11:2019. doi: 10.3389/fmicb.2020.02019

Nordstedt, N. P., and Jones, M. L. (2021). Genomic analysis of *Serratia plymuthica* MBSA-MJ1: a plant growth promoting Rhizobacteria that improves water stress tolerance in greenhouse ornamentals. *Front. Microbiol.* 12:653556. doi: 10.3389/fmicb.2021.653556

Novello, G., Gamalero, E., Massa, N., Cesaro, P., Lingua, G., Todeschini, V., et al. (2022). Proteome and physiological characterization of halotolerant nodule endophytes: the case of *Rahnella aquatilis* and *Serratia plymuthica*. *Microorganisms* 10:890. doi: 10.3390/microorganisms10050890

Othman, N. M. I., Othman, R., Zuan, A. T. K., Shamsuddin, A. S., Zaman, N. B. K., Sari, N. A., et al. (2022). Isolation, characterization, and identification of zinc-solubilizing Bacteria (ZSB) from wetland Rice fields in peninsular Malaysia. *Agriculture* 12:1823. doi: 10.3390/agriculture12111823

Ouyang, L., Pei, H., and Xu, Z. (2017). Low nitrogen stress stimulating the indole-3-acetic acid biosynthesis of *Serratia* sp. ZM is vital for the survival of the bacterium and its plant growth-promoting characteristic. *Arch. Microbiol.* 199, 425–432. doi: 10.1007/s00203-016-1312-7

Pang, Z., Zhao, Y., Xu, P., and Yu, D. (2020). Microbial diversity of upland Rice roots and their influence on Rice growth and drought tolerance. *Microorganisms* 8:1329. doi: 10.3390/microorganisms8091329

Saberi Riseh, R., Ebrahimi-Zarandi, M., Gholizadeh Vazvani, M., and Skorik, Y. A. (2021). Reducing drought stress in plants by encapsulating plant growth-promoting Bacteria with polysaccharides. *IJMS* 22:12979. doi: 10.3390/ijms222312979

Saikia, J., Sarma, R. K., Dhandia, R., Yadav, A., Bharali, R., Gupta, V. K., et al. (2018). Alleviation of drought stress in pulse crops with ACC deaminase producing rhizobacteria isolated from acidic soil of Northeast India. *Sci. Rep.* 8:3560. doi: 10.1038/s41598-018-21921-w

Samet, M., Ghazala, I., Karray, F., Abid, C., Chiab, N., Nouri-Ellouz, O., et al. (2022). Isolation of bacterial strains from compost teas and screening of their PGPR properties on potato plants. *Environ. Sci. Pollut. Res.* 29, 75365–75379. doi: 10.1007/s11356-022-21046-8

Shakeel, M., Hafeez, F. Y., Malik, I. R., Farid, A., Ullah, H., Ahmed, I., et al. (2023). *Serratia marcescens* strain FA-4 enhances zinc content in rice grains by activating the zinc translocating enzymes. *SABRAO J. Breed. Genet.* 52, 495–507. doi: 10.54910/sabrao2023.55.2.21

Shinde, K. S., and Borkar, S. (2018). Seed bacterialization induced proline content in *Sorghum bicolor* crop under severe drought condition. *Int. J. Chem. Stud* 6, 1191–1194.

Singh, R. P., and Jha, P. N. (2016a). Alleviation of salinity-induced damage on wheat plant by an ACC deaminase-producing halophilic bacterium *Serratia* sp. SL- 12 isolated from a salt lake. *Symbiosis* 69, 101–111. doi: 10.1007/s13199-016-0387-x

Singh, R. P., and Jha, P. N. (2016b). The multifarious PGPR *Serratia marcescens* CDP-13 augments induced systemic resistance and enhanced salinity tolerance of wheat (*Triticum aestivum* L.). *PLoS One* 11:e0155026. doi: 10.1371/journal.pone.0155026

Soenens, A., and Imperial, J. (2020). Biocontrol capabilities of the genus Serratia. *Phytochem. Rev.* 19, 577–587. doi: 10.1007/s11101-019-09657-5

Sohaib, M., Zahir, Z. A., Khan, M. Y., Ans, M., Asghar, H. N., Yasin, S., et al. (2020). Comparative evaluation of different carrier-based multi-strain bacterial formulations to mitigate the salt stress in wheat. *Saudi J. Biol. Sci.* 27, 777–787. doi: 10.1016/j.sjbs.2019.12.034

Sood, G., Kaushal, R., Panwar, G., and Dhiman, M. (2019). Effect of indigenous plant growth-promoting Rhizobacteria on wheat (*Triticum Aestivum* L.) productivity and soil nutrients. *Commun. Soil Sci. Plant Anal.* 50, 141–152. doi: 10.1080/00103624.2018.1556282

Suleimenova, N., Togisbayeva, A., Orynbasarova, G., Kuandykova, E., and Yerekeyeva, S. (2023). Ecological assessment of soil contamination with heavy metals due to the application of mineral fertilisers. *J. Water Land Dev.* 56, 74–80. doi: 10.24425/jwld.2023.143747

Szechyńska-Hebda, M., Ghalami, R. Z., Kamran, M., Van Breusegem, F., and Karpiński, S. (2022). To be or not to be? Are reactive oxygen species, antioxidants, and stress signalling universal determinants of life or death? *Cells* 11:4105. doi: 10.3390/cells11244105

Turhan, E., Kiran, S., Ates, Ç., Ates, O., Kusvuran, S., and Ellialtioglu, S. S. (2020). Ameliorative effects of inoculation with *Serratia marcescens* and grafting on growth of eggplant seedlings under salt stress. *J. Plant Nutr.* 43, 594–603. doi: 10.1080/01904167.2019.1690662

Ullah, N., Ditta, A., Khalid, A., Mehmood, S., Rizwan, M. S., Ashraf, M., et al. (2020). Integrated effect of algal biochar and plant growth promoting Rhizobacteria on physiology and growth of maize under deficit irrigations. *J. Soil Sci. Plant Nutr.* 20, 346–356. doi: 10.1007/s42729-019-00112-0

Upadhayay, V. K., Khan, A., Singh, J., and Singh, A. V. (2022). Bacterial assisted improved zn consignment in root and shoot of rice plant by zinc solubilizing *Serratia marcescence* bearing plant probiotic traits. *Adv. Biores.* 13, 1–08. doi: 10.15515/abr.0976-4585.13.1.108

Verma, M., Mishra, J., and Arora, N. K. (2019). "Plant growth-promoting rhizobacteria: diversity and applications" in *Environmental biotechnology: for sustainable future*. eds. R. C. Sobti, N. K. Arora and R. Kothari (Berlin: Springer), 129–173.

Wang, S., Ouyang, L., Ju, X., Zhang, L., Zhang, Q., and Li, Y. (2014). Survey of plant drought-resistance promoting Bacteria from *Populus euphratica* tree living in arid area. *Indian J. Microbiol.* 54, 419–426. doi: 10.1007/s12088-014-0479-3

Wang, C.-J., Yang, W., Wang, C., Gu, C., Niu, D.-D., Liu, H.-X., et al. (2012). Induction of drought tolerance in cucumber plants by a consortium of three plant growth-promoting Rhizobacterium strains. *PLoS One* 7:e52565. doi: 10.1371/journal.pone.0052565

Wróbel, M., Śliwakowski, W., Kowalczyk, P., Kramkowski, K., and Dobrzyński, J. (2023). Bioremediation of heavy metals by the genus *Bacillus*. *IJERPH* 20:4964. doi: 10.3390/ijerph20064964

Yaseen, R., Hegab, R., Kenawey, M., and Eissa, D. (2020). Effect of super absorbent polymer and bio fertilization on maize productivity and soil fertility under drought stress conditions. *Egypt.J. Soil Sci.* 60, 377–395. doi: 10.21608/ejss.2020.35386.1372

Zafar-Ul-Hye, M., Aslam, U., Muqaddas, B., and Hussain, M. B. (2017). Connotation of *Enterobacter cloacae*-W6 and *Serratia ficaria*-W10 with or without carriers for improving growth, yield and nutrition of wheat. *Soil Environ.* 36, 182–189. doi: 10.25252/SE/17/41169

Zaheer, A., Mirza, B. S., Mclean, J. E., Yasmin, S., Shah, T. M., Malik, K. A., et al. (2016). Association of plant growth-promoting *Serratia* spp. with the root nodules of chickpea. *Res. Microbiol.* 167, 510–520. doi: 10.1016/j.resmic.2016.04.001

Zahir, Z. A., Ghani, U., Naveed, M., Nadeem, S. M., and Asghar, H. N. (2009). Comparative effectiveness of Pseudomonas and *Serratia* sp. containing ACC-deaminase for improving growth and yield of wheat (*Triticum aestivum* L.) under salt-stressed conditions. *Arch. Microbiol.* 191, 415–424. doi: 10.1007/s00203-009-0466-y

Zhang, Y., Kang, X., Liu, H., Liu, Y., Li, Y., Yu, X., et al. (2018). Endophytes isolated from ginger rhizome exhibit growth promoting potential for *Zea mays*. *Arch. Agron. Soil Sci.* 64, 1302–1314. doi: 10.1080/03650340.2018.1430892

Zhang, M., Yang, L., Hao, R., Bai, X., Wang, Y., and Yu, X. (2020). Drought-tolerant plant growth-promoting rhizobacteria isolated from jujube (*Ziziphus jujuba*) and their potential to enhance drought tolerance. *Plant Soil* 452, 423–440. doi: 10.1007/s11104-020-04582-5

Zhang, C., Yu, Z., Zhang, M., Li, X., Wang, M., Li, L., et al. (2022). *Serratia marcescens* PLR enhances lateral root formation through supplying PLR-derived auxin and enhancing auxin biosynthesis in Arabidopsis. *J. Exp. Bot.* 73, 3711–3725. doi: 10.1093/jxb/erac074

Zheng, J., Liu, C., Liu, J., and Zhuang, J. Y. (2022). Study of the effect of bacterial-mediated legume plant growth using bacterial strain *Serratia marcescens* N1.14 X-45. *Front. Microbiol.* 13:988692. doi: 10.3389/fmicb.2022

frontiers | Frontiers in Microbiology

TYPE Original Research
PUBLISHED 17 May 2024
DOI 10.3389/fmicb.2024.1367184

OPEN ACCESS

EDITED BY
Jianling Fan,
Nanjing University of Information Science and Technology, China

REVIEWED BY
Qiuxia Wang,
Chinese Academy of Agricultural Sciences, China
Asit Mandal,
Indian Institute of Soil Science (ICAR), India

*CORRESPONDENCE
Pu Shen
✉ shenpupeanut@126.com

RECEIVED 08 January 2024
ACCEPTED 06 May 2024
PUBLISHED 17 May 2024

CITATION
Yang L, Wang C, He X, Liang H, Wu Q, Sun X, Liu M and Shen P (2024) Multi-year crop rotation and quicklime application promote stable peanut yield and high nutrient-use efficiency by regulating soil nutrient availability and bacterial/fungal community. *Front. Microbiol.* 15:1367184. doi: 10.3389/fmicb.2024.1367184

Multi-year crop rotation and quicklime application promote stable peanut yield and high nutrient-use efficiency by regulating soil nutrient availability and bacterial/fungal community

Liyu Yang[1], Caibin Wang[1], Xinhua He[2], Haiyan Liang[1], Qi Wu[1], Xuewu Sun[1], Miao Liu[1] and Pu Shen[1]*

[1]Shandong Peanut Research Institute/Key Laboratory of Peanut Biology, Genetic & Breeding, Ministry of Agriculture and Rural Affairs, Shandong Academy of Agricultural Sciences, Qingdao, Shandong, China, [2]College of Resources and Environment, Southwest University, Chongqing, China

Diversifying cultivation management, including different crop rotation patterns and soil amendment, are effective strategies for alleviating the obstacles of continuous cropping in peanut (*Arachis hypogaea* L.). However, the peanut yield enhancement effect and temporal changes in soil chemical properties and microbial activities in response to differential multi-year crop rotation patterns and soil amendment remain unclear. In the present study, a multi-year localization experiment with the consecutive application of five different cultivation managements (including rotation with different crops under the presence or absence of external quicklime as soil amendment) was conducted to investigate the dynamic changes in peanut nutrient uptake and yield status, soil chemical property, microbial community composition and function. Peanut continuous cropping led to a reduction in peanut yield, while green manure-peanut rotation and wheat-maize-peanut rotation increased peanut yield by 40.59 and 81.95%, respectively. A combination of quicklime application increased yield by a further 28.76 and 24.34%. Alterations in cultivation management also strongly affected the soil pH, nutrient content, and composition and function of the microbial community. The fungal community was more sensitive than the bacterial community to cultivation pattern shift. Variation in bacterial community was mainly attributed to soil organic carbon, pH and calcium content, while variation in fungal community was more closely related to soil phosphorus content. Wheat-maize-peanut rotation combined with quicklime application effectively modifies the soil acidification environment, improves the soil fertility, reshapes the composition of beneficial and harmful microbial communities, thereby improving soil health, promoting peanut development, and alleviating peanut continuous cropping obstacles. We concluded that wheat-maize-peanut rotation in combination with quicklime application was the effective practice to improve the soil fertility and change the composition of potentially beneficial and pathogenic microbial communities in the soil, which is strongly beneficial for building a healthy soil micro-ecology, promoting the growth and development of peanut, and reducing the harm caused by continuous cropping obstacles to peanut.

KEYWORDS

peanut, crop rotation pattern, continuous cropping obstacle, bacterial/fungal community, quicklime

Introduction

Peanut is one of the most widely cultivated economic crops and an important source of edible oil in the world (Bertioli et al., 2016). The global demand for peanut has continued to grow over the past decade. Recently, peanut continuous cropping has become common due to the growing land crisis for peanut production. However, continuous cropping leads to peanut growth and development abnormalities, severe diseases, significant yield reductions, posing a risk to the supply of edible oils (Chen et al., 2014; Li et al., 2018, 2022; Yu et al., 2024). As a result, selecting suitable cropping method to eliminate the adverse effects of continuous cropping obstacles is a challenge for the peanut plantation and industry.

Recent evidence have indicated that the overall alteration of the soil microcosm system was the leading cause of continuous cropping obstacles (Liu et al., 2020, 2021; Xiao et al., 2024). This is represented by the imbalance of soil nutrients and soil microbiota, self-toxic effect of chemo-sensitive substances, and alteration of soil pH (Shen et al., 2019). After growing the same crop continuously for a long time, specific nutrient is selectively absorbed by and removed from crops, resulting in nutrient imbalance in soil (Pervaiz et al., 2020). Besides nutrient imbalance, continuous cropping is often accompanied by soil acidification. Numerous studies have shown that plant roots secreted organic acids during growth, and long-term cultivation of the same crop could lead to the accumulation of specific organic acids in soil (Tan et al., 2017; Bai et al., 2019). Nitrogen (N) is an important nutrient for the development of most crops, and the selective uptake of NH_4^+ by some crops including rice, maize, and sorghum results in a persistent deficit of NH_4^+ in soil, which produce saline acidity and further aggravate the acidification in continuous cropping soil (Fageria and Baligar, 2005). In addition, some secondary metabolites, such as phenols and terpenoids, are secreted by root systems during crop development and have very strong chemosensory activity. With the increase of cropping years, these chemo-sensitive substances will accumulate in soil and become self-toxic to crop (including peanut), making the crop less resistant, decreasing the yield and further aggravating the continuous cropping obstacles (Li et al., 2014a).

Soil microorganisms are directly involved in decomposing of soil organic matter, nutrient transformation and soil-borne diseases (Fierer et al., 2020). In recent years, increased studies showed that soil microflora dysbiosis was a fundamental cause of continuous cropping obstacles. For instance, the diversity, function and co-occurrence networks of soil fungi and bacteria were significantly affected by continuous cropping with interannual variations (Liu et al., 2020, 2021). The dominant fungi from the continuous cropping soil showed significantly inhibitory effects on the growth and development of crops, further suggesting that the altered microorganisms caused by continuous cropping was the fundamental cause of constant cropping obstacles (Liu et al., 2021). Studies also showed that a strong correlation exists between continuous cropping obstacles in peanut plantation with changes in soil microbial communities and compositions (Li et al., 2018, 2022). With continuously increasing cropping years, the number of pathogenic fungi in soil and inter-rhizosphere also increased, while the number of bacteria and actinomycetes decreased significantly. The abundance and/or diversity of plant beneficial bacteria including *Alteromonadales*, *Burkholderiales*, *Flavobacteriales*, *Pseudomonadales*, *Rhizobiales*, and *Rhodospirillales*, have a decreased propensity with continuous cropping (Chen et al., 2014). At the same time, fungi in soil trended to increase pathogenic fungi and simplify of beneficial fungal communities (Chen et al., 2012; Li et al., 2014b). Li et al. (2018) treated peanut seedling with bacterial suspensions extracted from continuous-cropping soil and found that such bacterial suspensions markedly suppressed peanut growth. Therefore, an imbalance in the soil microbial community structure can be a leading cause of continuous cropping obstacles for peanut.

The formation of continuous cropping obstacles is related to the deterioration of soil chemical properties and microbial community structure disorders. Therefore, applying rational cultivation patterns to improve soil chemical properties and change microbial community structure becomes an effective approach to eliminate continuous cropping obstacles in agricultural production (Kagawa et al., 2022; Wang et al., 2022). It has shown in studies that changes in cultivation managements (including the reasonable application of crop rotation and soil amendments) can effectively reduce the harmful effects of continuous cropping obstacles (Aparicio and Costa, 2007; Huang et al., 2015; Zhang et al., 2022a). Reasonable crop rotation is an effective agronomic management strategy to reduce continuous cropping obstacles. The multiple crops introduced by crop rotation can balance soil nutrients and improve soil fertility due to different nutrient ecological niches (Passaris et al., 2021). Moreover, by continuously changing hosts, it can break the specialized parasitic pathogens and oligophagous pests, and reduce the pest and disease hazards caused by continuous cropping (Carrière et al., 2020). The different inter-root environments brought by different crops are conducive to the construction of a healthy soil microbial community, further reducing the damage caused by continuous cropping (He et al., 2019). Differences in the crop species used for crop rotation make different crop rotation patterns have different mitigating effects on the cropping obstacles (Venter et al., 2016; Sumner, 2018; Massigoge et al., 2024). Green manure rotation and wheat-maize rotation are the two main crop rotation patterns in peanut cultivation process, however, the literature on effect of different crop rotation patterns on the alleviation of continuous cropping obstacles in peanut and the underlying mechanism of its regulation are lacking is scarce. Quicklime is an important soil amendment. Applying quicklime by increasing external calcium to soil is a common method of soil disinfection and plays an essential role in increasing soil pH of acid soil caused by continuous cropping, and reconstructing the composition structure of microorganisms, mitigating the continuous cropping obstacles to crop production (You et al., 2015; Lu et al., 2021). Exploring effective agricultural management measures is a meaningful way to alleviate and eliminate continuous cropping obstacles. Recently, although studies have recently focused on the effects of various cultivation managements on peanut continuous cropping obstacles, there is still a paucity of evidence regarding how the multi-year cultivation management affects peanut growth, soil chemical properties, and microbial community structure in peanut continuous cropping system.

To explore the characteristics of peanut continuous cropping obstacles and the intrinsic mechanisms in the application of different cultivation managements (including rotation with different crops under the presence or absence of external quicklime) for consecutive years to alleviate peanut continuous cropping obstacles, we investigate the effects of different cultivation managements on peanut yield, soil chemical properties and microbial community composition and

function in peanut cropping soil at different cropping year. The effects of different long-term cultivation management on peanut growth performance and soil nutrient availability were assessed by measuring the yield and nutrient of peanut and determining properties of soil organic matter, available nitrogen, phosphorus, potassium and calcium nutrients. Bacterial and fungal communities in the soil were determined using Illumina MiSeq platform. We hypothesize that different cultivation management and cropping year could alter soil chemistry and shape microbial community structure, thereby offering a beneficial environment for peanut growth, alleviating peanut continuous cropping obstacles, and thus increasing the yield and nutrient content of peanut. This study increases our understanding of the mechanism of different cultivation management that change soil chemical properties and drive alternations in the composition and function of the microbial community to mitigate continuous cropping obstacles for peanut. The results of this study will provide a theoretical and practical basis for high-quality cultivation and sustainable peanut production.

Materials and methods

Study site description and experimental design

This multi-year localization experiment was conducted at a typically acidic brown soil (*Haplic Luvisols*, the FAO soil classification system) in a major peanut production area, Laixi County, Shandong (E120°29′, N36° 48′, 227 m above the sea level), China. At the experimental sites peanut has never been planted in this brown soil that is developed from weathered acid parent rocks. The average annual temperature was 11.5°C, and the average annual rainfall was 635.8 mm.

In a randomly complete block design with three replicates for each treatment, five continuously experimental treatments were examined: (1) T1, annual summer peanut and winter fallow; (2) T2, annual summer peanut and winter ryegrass without quicklime application; (3) T3, annual summer peanut and winter ryegrass plus quicklime application; (4) T4, summer peanut rotated with maize and winter wheat; (5) T5, summer peanut rotated with maize and winter wheat plus quicklime application. Nitrogen, phosphorus (P), and potassium (K) fertilizers were based on the local fertilization practice. With 600 kg CaO (quicklime)/hm^2, a total of 750 kg/hm^2 ternary compound fertilizer (15%N: 15% P_2O_5: 15% K_2O) were applied containing 112.5 kg N/hm^2, 112.5 kg P_2O_5/hm^2, 112.5 kg K_2O/hm^2.

Soil and plant sampling and analyses

A common local peanut variety of Huayu 33 was seeded in early May and harvested in mid-September for selected experimental years. There was one peanut seed in each plant hole with a planting distance of 15 cm. Sowing rate 180,000 plants/m^2. Soil at year1 (Base), year 3 (T1-3Y, T2-3Y, T3-3Y, T4-3Y, T5-3Y) and 5 (T1-5Y, T2-5Y, T3-5Y, T4-5Y, T5-5Y) were collected. The basic soil chemical properties mainly included soil pH, soil organic matter (SOC), soil available nitrogen (AN), available phosphorus (AP), available potassium (AK) and calcium (Ca) nutrients. After peanut harvest, soils at 0–20 cm depth were collected with a 10 cm auger. Soil samples were air-dried and passed through a 2 mm sieve and further ground to pass a 0.25 mm sieve to determine soil properties. Soil pH was measured using a pH meter (Orion 2 Star, Thermo Fisher Scientific, United States). Organic C was determined using a potassium dichromate volumetric method (Walkley, 1935). Alkali hydrolyzed or available N was determined using 1 mol/L NaOH alkali hydrolysis, 2% boric acid absorption, and 0.01 mol/L HCl titration (Mulvaney and Khan, 2001). Available P was extracted with 0.5 mol/L $NaHCO_3$ and determined by UV–vis spectrophotometry (Olsen and Sommers, 1982). Available K was extracted with 1 mol/L ammonium acetate and determined by flame photometry (Lu et al., 2024). Soil Ca^{2+} concentration was determined by inductively coupled plasma atomic emission spectrometry (Agilent ICP 720-OES, Varian Inc., Darmstadt, Germany) (Dahlquist and Knoll, 1978). The initial properties of soil were as follows: pH 5.68, SOC 1.1 g/kg, AN 61.05 mg/kg, AP37.10 mg/kg, AK 114.4 mg/kg, Ca 4.42 g/kg. Concentrations of kernel N, P, K, and Ca were determined by an inductively coupled plasma atomic emission spectrometry (Agilent ICP 720-OES, Varian Inc., Darmstadt, Germany).

DNA extraction, amplification and sequencing

Total genomic DNA of 33 soil samples was extracted separately using the Fast DNA® Spin Kit for Soil (MP Biomedicals, United States) according to the manufacturer's instructions. The concentration and purity of DNA were then examined with 1% agarose gels. The V3-V4 region of the bacterial 16S rRNA gene was amplified using primers 515F (5′-GTGCCAGCMGCCGCGG-3′) and 806R (5′-GGACTACH VGGGTWTCTAAT-3′). The ITS1 region of the fungal gene was amplified using the primers ITS1F (5′-CTTGGTCATTTAGAGG AAGTAA-3′) and ITS2R (5′-GCTGCGTTCTTCATCGATGC-3′). All PCR reactions were conducted using a TransGen Kit (TransGen AP221-02: TransStart Fastpfu DNA Polymerase, TransGen Biotech, Beijing, China) with 20 μL reaction system, including 4 μL FastPluBuffer, 0.4 μL FastPfu Polymerase, 2 μL dNTPs, 0.8 μL of each forward and reverse primers, 0.2 μL Bovine Serum Albumin and 10 ng template DNA. DNA was amplified using ABI GeneAmp® 9,700 (Life Technologies, Foster City, CA) under the following conditions: 95°C for 5 min, followed by 95°C for 3 min, 30 cycle of 95°C for 30 s, 55°C for 30 s, 72°C for 45 s and elongation at 72°C for 10 min. After purifying, all PCR products were used to construct sequencing libraries by using the TruSeq™ DNA Sample Prep Kit (Illumina). Ultimately, the constructed libraries were sequenced on an Illumina HiSeq2500 platform at Majorbio Bio-Pharm Technology (Shanghai, China).

Calculation and statistical analyses

After sequencing, the generated raw data were first spliced based on overlap relationships using the fast-length adjustment of short reads (FLASH) software (version 1.2.11). Using a Uparse (version 7.0.1090) software, non-repetitive sequences with >97% similarity (excluding single sequences) were categorized into operational taxonomic units (OTUs). The Ribosomal Database Project (RDP)

classifier was used to analyze the taxonomy of OTU representative sequences to obtain the taxonomic information of species corresponding to each OTU. The bacteria were identified using the SILVA database,[1] and fungi were identified using the Unite database.[2] Alpha diversity (Shannon diversity index) (Shannon, 1948) was used to reflect the abundance and diversity of the microbial community using mothur software (version v.1.30.2). Principal coordinates analysis (PCoA) plots were used to evaluate the effects of different treatments on soil microbial composition based on the Bray-Curtis distances via "vegan" (version 2.6–4) from R package (version 3.3.1). The Mantel test analysis, redundancy analysis (RDA) and Pearson correlation heatmap were adopted to reveal the relationship between soil environmental variables and bacterial and fungal community composition. The Pearson' s correlation coefficients were also used to investigate the correlation between environment variables environmental factors. These analyses were performed by "vegan" package and visualized by "ggcor" package (version v.0.9.8) under R environment. OTUs of bacteria were mapped to the FAPROTAX (Functional Annotation of Prokaryotic Taxa) database[3] to predict potential metabolic functions of the detected soil bacteria. The *p*-values generated from the Welch's t-test were used to measure the functional difference between the two different groups. Functions of identified fungi were classified via FUNGuild database[4] (Nguyen et al., 2016). Co-occurrence network analysis was performed to detect the connections within bacterial-bacterial, bacterial-fungal and fungal-fungal taxa. The top 100 bacteria and fungi in relative abundance in each of the different libraries were selected for Person's correlation analysis. A correction represents a strong ($r > 0.8$) and significant correlation ($p < 0.01$). The generated networks were visualized with the Gephi software (version v.0.9.6) (Bastian et al., 2009). Differences in soil properties, plant nutrients, and yield among the five treatments were subjected to analyses of variance (ANOVA) using SAS 9.4 (SAS, Inc., Cary, NC). The least significant difference (*t*-test) test was used to separate the significant differences between treatments at a 0.05 probability level.

Results

Effects of different cultivation managements on the pod yield of peanut

The formation of peanut yield was impacted by cultivation management measures (Figure 1). In the first year of cultivation, there was no significant difference in peanut yield between treatments. In the third year of cultivation, peanut yields under the T2 (green manure rotation) and T4 treatment (wheat-maize rotation) were 1.31 and 2.55 times higher than that in T1 treatment (continuous cropping). In the fifth year of cultivation, T2 and T4 increase peanut yield by 40.59 and 81.95% compared to T1. These results indicated that crop rotation measure could significantly increase peanut yield compared to continuous cropping measures and wheat-maize rotation measure have more pronounced enhancement effect on peanut yield than green manure rotation measures. In addition, compared to treatment without quicklime (T2 and T4), peanut yield was significantly ($p < 0.05$) increased in the treatment with quicklime application (T3 and T5). At the fifth cropping year, compared to T2 and T4, T3 and T5 increase peanut yield by 28.76 and 24.34%. These results indicated that quicklime application could improve the effect of crop rotation measures on peanut yield enhancement.

Effects of different cultivation managements on nutrient elements in peanut kernels

The absorption of nutrient elements in peanut kernels was affected by continuous cropping. Different cultivation managements exhibited various effects on different nutrient elements in peanut kernels (Figure 2). Nitrogen uptake by kernel decreases with increasing years of continuous crop. Application of green manure (T2) and crop rotation (T4) could effectively improve the uptake of N by the kernels. Compared with T1-3Y, N absorption in peanut kernels increased by 8.0 and 1.7% in T3-3Y and T5-3Y. Compared with T1-5Y, N absorption increased by 25.0 and 22.9% in T3-5Y and T5-5Y, respectively. The Ca content of peanut kernels was basically unaffected by the continuous cropping years or crop rotation patterns, but was significantly increased by quicklime application.

Effects of different cultivation managements on the soil properties

As seen in Figure 3, soil pH exhibited a decreasing trend with increasing years of continuous cropping, by 0.31 and 0.45 units in T1-3Y and T1-5Y, compared to Base. Concentrations of SOC increased with the introduction of other crops. The highest value of AN was observed in T2-3Y. Compared with T1, soil AP and AK was elevated under T4, but decreased under a further quicklime application (T5). Soil Ca did not show significantly interannual differences. At the same cropping year, soil Ca was significantly increased by T2 (green manure rotation) and T4 (wheat-maize rotation) treatments compared to T1, and was obviously further increased with the application of quicklime.

Differences in microbial composition under different continuous cropping years and cultivation managements

After sequencing the 16 S rRNA gene and fungal rRNA internal transcribed spacer (ITS) region, a total of 1,282,970 and 2,199,255 sequences were obtained from 11 soil samples, respectively. Soil bacterial abundance increased with the peanut cropping years, and was significantly higher at the year 5, compared to year 1 and 3 (Supplementary Table S1), as well as higher under T2-T5 than under T1. Soil fungal abundance was less affected by the peanut cultivation years. Consistent with the trend in bacterial abundance, soil fungal

1 http://www.arb-silva.de
2 http://unite.ut.ee/index.php
3 http://www.loucalab.com/archive/FAPROTAX/lib/php/index.php?section=Home
4 http://www.stbates.org/guilds/app.php

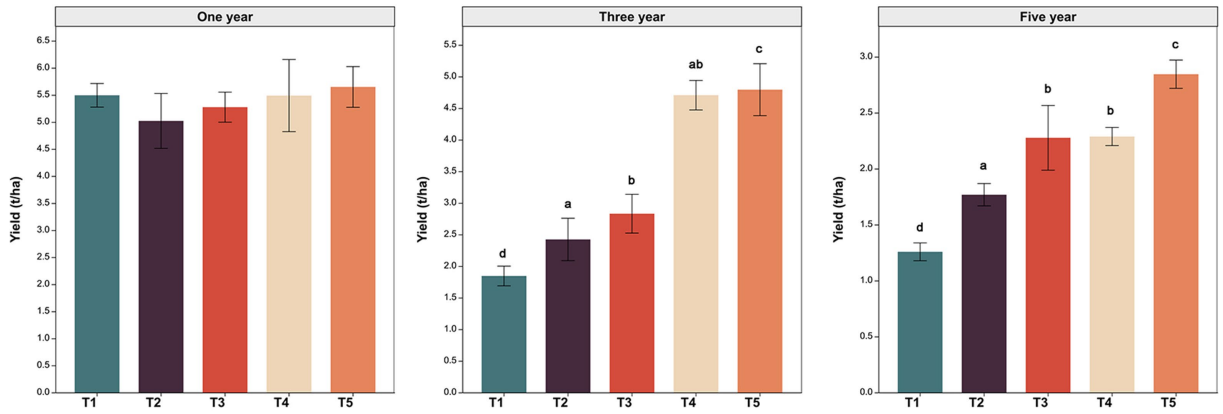

FIGURE 1
Peanut yield in year 1, 3 and 5 under five different cultivation managements. T1: No treatment; T2: Green manure rotation; T3: Green manure rotation+Quicklime; T4: Wheat-maize rotation; T5: Wheat-maize rotation +Quicklime. Different superscript letters indicate significant differences among treatments (t-test, $p < 0.05$).

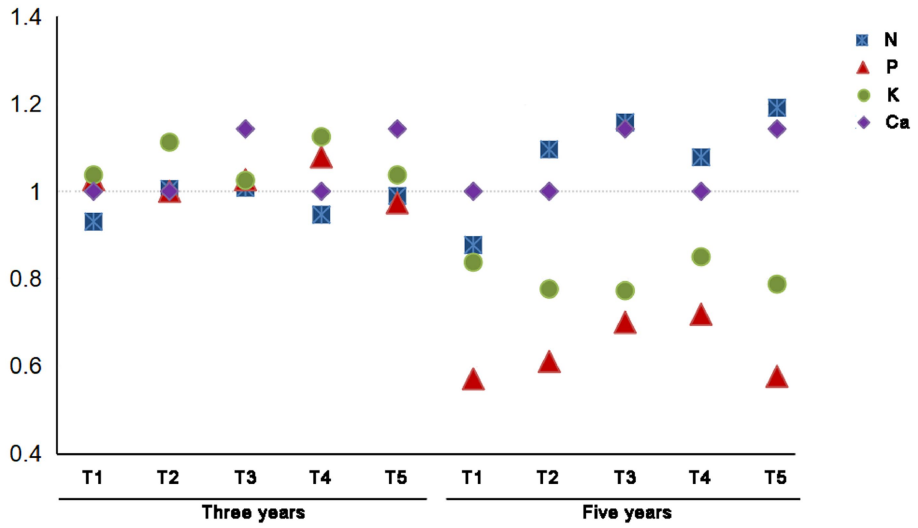

FIGURE 2
Difference of nutrient elements in peanut kernels under different cultivation managements at different cropping years. The change of ratio was relative to Base treatments.

abundance was also higher under T2-T5 than under T1. Additionally, bacterial and fungal abundances were lower in treatments with quicklime (T3 and T5) than in those without quicklime application (T2 and T4) at the same cropping year. This result may be related to the germicidal effect of quicklime.

There existed differences in the α-diversity of soil bacteria and fungi under different cropping years and cultivation practice treatment conditions (Figure 4). For bacteria, by comparing the Shannon index, the diversity index of soil bacteria increased with planting years. The bacterial diversity index was significantly higher in soil samples with quicklime application than in other soil samples under the same planting year conditions, indicating that quicklime is an essential driver for increasing bacterial diversity. For fungi, the Shannon index did not differ significantly between planting years and cultivation practices. However, the Shannon index of fungi in soil with applied cultivation practices (T2-T5) was greater than that of fungi in continuous crop soils (T1) in the same cultivation years. This result indicates that continuous crop cultivation measures can decrease fungal diversity.

Changes in microbial community composition under different continuous cropping years and cultivation managements

Soil bacterial and fungal communities were altered by different cultivation years and practices. In the present study, a principal coordinate analysis (PCoA) analysis was performed to measure the effects of different years and cultivation practices on the bacterial fungi in the soil. As shown in Figure 5A, the year of cultivation was the most influential factor in the structure of the soil bacterial

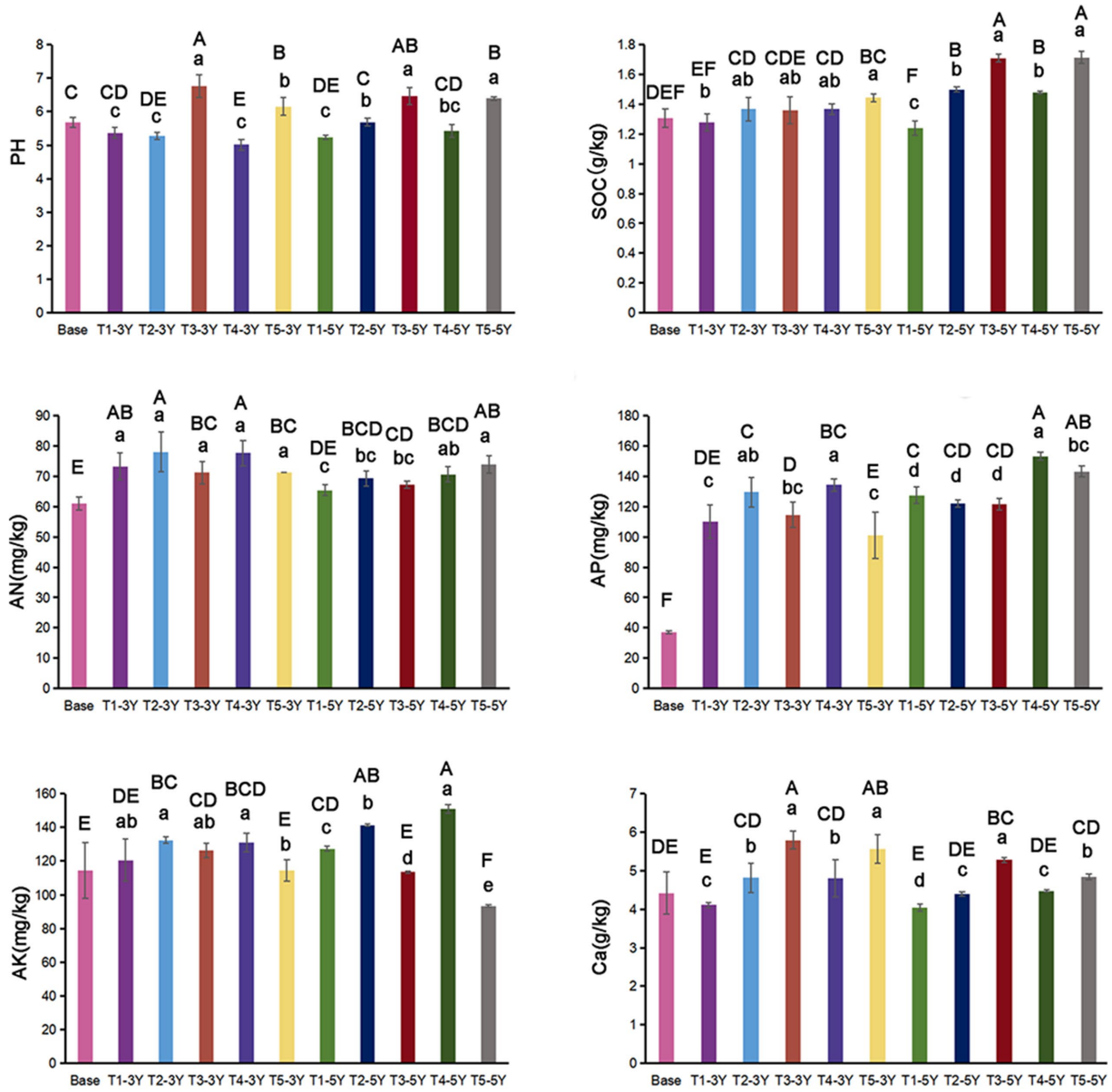

FIGURE 3
Soil properties under different cultivation managements at different cropping years. Lowercase letters indicate differences between cultivation managements in the same year, and capital letters indicate differences between all treatments.

community. Regardless of cultivation practices, soil libraries with the same cultivation years were grouped into the same cluster. In the same cultivation year, the bacterial community in the soil treated with and without quicklime was clustered into two different clusters. This indicated that the overall similarity of the bacterial community structure was high between the wheat-maize rotation with quicklime and the green manure with quicklime. This suggests that quicklime also had a more significant influence on the bacterial community structure of continuous peanut fields during the cultivation year.

The fungal communities showed different patterns from bacteria. The separated PCoA plot (Figure 5B) showed that, regardless of cropping year, the fungal communities of each treatment were divided into two groups: soil under the green manure rotation and soil under the wheat-maize rotation. Moreover, under the same rotation pattern, the fungal communities were divided into two distinct groups by the presence or absence of quicklime application. These results indicate that the difference in rotation pattern was the primary driver of fungal community change for fungal communities. Quicklime application is an essential inducer of fungal community change under certain cultivation practices.

Based on the OTU classification results, the species and relative abundance of bacteria and fungi in all samples were analyzed at the phylum level (Figure 5C). Soil bacterial species under all treatments covered twenty-three bacterial phyla and six fungal phyla. Among all treatments, *Actinobacteria*, *Proteobacteria*, and *Chloroflexi* were the dominant soil bacterial taxa. However, bacterial phyla composition and relative abundance differed significantly under

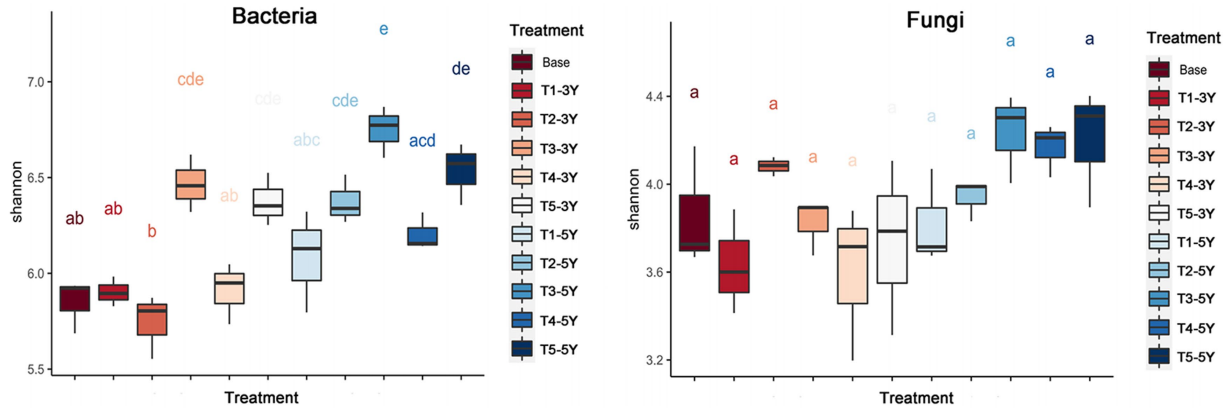

FIGURE 4
Alpha diversity of soil bacteria and fungi in each sample.

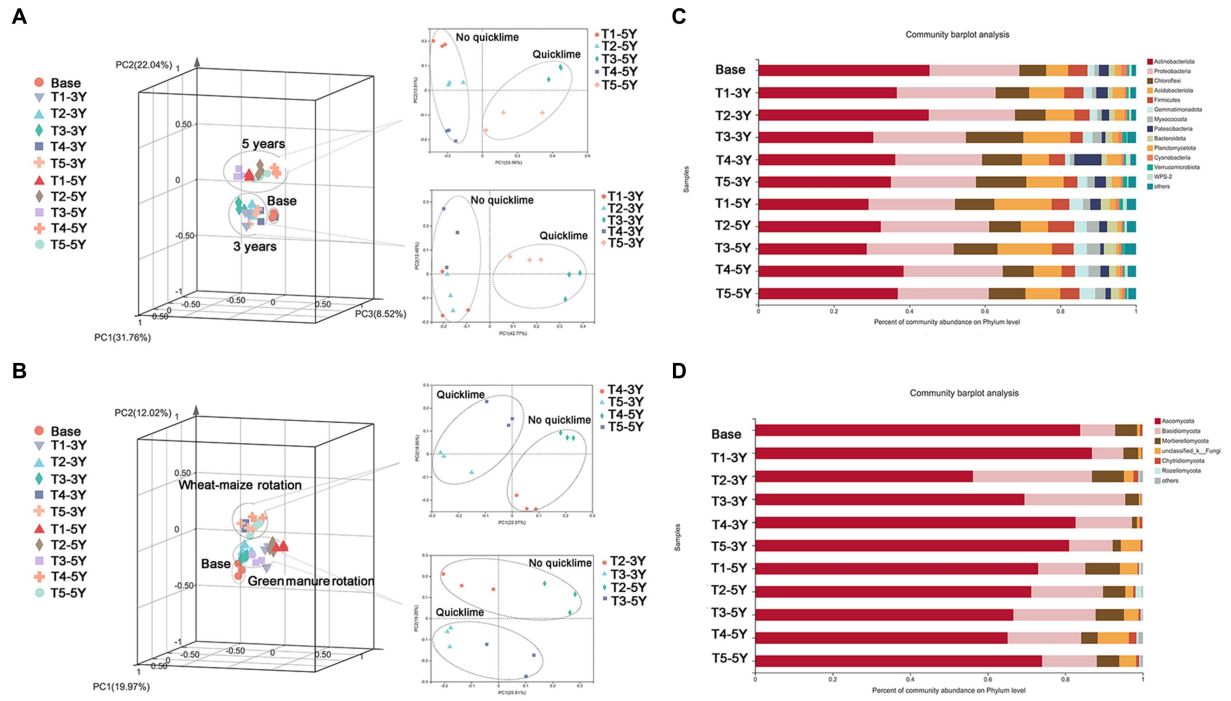

FIGURE 5
The effects of different cultivation practices on soil microbial composition. Principal coordinates analysis (PCoA) plots showing the effects of different cultivation measures on soil bacterial **(A)** and fungal **(B)** composition under different years of continuous peanut cropping based on Bray-Curtis distances. Relative abundance of bacterial **(C)** and fungal **(D)** phyla communities in each sample.

different cropping years and cultivation managements. The abundance of *Actinobacteria* varied from 28.70 to 45.34%, while the proportion of *Proteobacteria* in each sample ranged from 22.51 to 28.69%. Different cultivation practices contributed differently to the alteration of the bacterial community structure in terms of the proportion of major bacterial phyla under different treatments. For example, the percentage of *Actinobacteria* in the soil library was lower in the quicklime application than in the non-quicklime treatment. Therefore, the percentage of *Actinobacteria* was significantly reduced by quicklime application treatment. For the fungal community taxonomic composition (Figure 5D), *Ascomycota*, *Basidiomycota*, and *Mortierellomycota* were the three most dominant soil fungal taxa in all treatments. Although the species composition of soil fungal communities was similar at the phylum level under different continuous cultivation patterns, there were significant differences in the relative abundance of major soil fungal genera under different cultivation practices at the genus level. For instance, as a critical class of fungal genera in *Ascomycota*, the relative abundance of *Leptosphaerulina* increased significantly as crop years increased. However, there was a decreasing trend under green manure rotation and wheat-maize rotation. Additionally, the relative abundance of *Leptosphaerulina* showed a

further decrease in the quicklime-applied soil under the same planting year conditions.

Correlation analysis between different microbial abundances and soil factors under different cultivation managements

To measure the relationship between the different microbial communities in the samples and soil environmental variables and to assess the correlation between microbial taxa and soil environmental variables, mantel test analysis was used to clarify which soil chemical factor was the main ecological driver influencing the microbial community composition (Figure 6A). Soil pH ($p < 0.01$), Ca ($p < 0.01$) and SOC ($p < 0.05$) exhibited significant correlations with bacterial community. For fungi, AP in soil ($p < 0.05$) was the main driver of fungal community composition.

We further correlated soil chemical properties with bacterial and fungal communities at the genus level using an RDA test (Figure 6B). Soil chemical properties had a significant effect on the abundance of fungi and bacteria at the genus level. Soil pH and Ca had a significant effect on the distribution of bacterial communities. These results were consistent with the results of the Mantel test, showing that these two soil variables were positively correlated. Soil pH positively correlated with the abundance of *Arthrobacter*, *Bacillus*, and *Nocardioiders*. In contrast, soil pH negatively correlated with the abundance of *Sphingomonas* and *Gaiellales*. Soil Ca content positively correlated with the abundance of *Arthrobacter*, while negatively correlated with the abundance of *Nocardioiders*, *Bacillus*, *Sphingomonas*, and *Gaiellales*. Despite the positive correlation between soil pH and Ca content, the dominant influential factors in the bacterial community, they had different regulatory effects on specific bacterial genera, such as *Bacillus* and *Nocardioiders*. Among the top 50 abundant bacteria, *Arthrobacter*, *Acidobacteriales* and *Elsterales*, showed significant correlations ($p < 0.05$) with both soil Ca and pH, indicating that changes in the abundance of these bacteria were closely related to the application of quicklime (Supplementary Figure S1).

Additionally, the mental test revealed that soil AP was critical variable driving changes in fungal community (Figure 6C). A positive correlation between AP and AN was shown by the RDA results. Both soil AP and AN positively correlated with the abundance of *Penicillium*, *Fasuriam*, *Tausonia*, and *Chaetomiacrae*, but negatively correlated with the abundance of *Mortierella*. Among the top 50 abundant fungi, *Papiliotrema*, *Tremellomycetes*, *Phaeosphaeriopsis*, *Oidiodendron*, and *Chaetomidium* displayed strong correlations ($p < 0.05$) with soil Ca and pH, demonstrating that quicklime treatment had a direct impact on changes in these fungi' abundance (Supplementary Figure S1).

Microbial collinearity network structure analysis

The interactions between bacterial and fungal communities in soils under different cropping years and cultivation practices were analyzed through co-occurrence networks. The complex relationship between bacteria and fungi was exhibited by calculating the network topology. As shown in Figure 7, the soil bacterial-fungal interactions network in different cultivation practices at the same cropping years were significantly different. The soil bacterial-fungal interactions network depended on different cropping years under the same cultivation managements (Supplementary Table S2). The number of edges had the highest value in the T2-3Y soils compared to other treatments. Microbial networks in soils under different tillage practices were affected by the application of quicklime. Compared to non-quicklime treatments, the proportion of fungal-fungal interactions among all interactions was increased by the application of quicklime. Additionally, the proportion of overall bacterial interactions accounted by bacteria positively associated with bacterial interactions.

The betweenness centrality score could reflect the core microorganisms that play a crucial role in the bacterial-fungal interaction network (Supplementary Table S2). By analyzing the betweenness centrality scores of co-occurrence networks under different treatments, soil bacteria and fungi with the highest abundance differed from these bacteria and fungi with the highest betweenness centrality scores. These results suggested that bacteria and fungi with high abundance did not necessarily play the most critical role in the co-occurrence network. Additionally, the abatement effect of different cultivation managements on the continuous cropping obstacles may depend more on the result of the joint action of multiple microorganisms.

Effects of different cultivation managements on microbial functional diversity

To measure the effect of different cultivation practices used to alleviate continuous cropping obstacles in peanut on the functional diversity of microorganisms, we predicted bacterial and fungal microbial functions in soil by using FAPROTAX database and FUNGuild database, respectively. The FAPROTAX database analysis results indicated significant differences in the metabolic functional groups of soil bacteria under different cultivation practices (Figure 8; Supplementary Table S3). The functions of the bacteria detected in this study were classified into 53 functional descriptions. Among these, green manure rotation and wheat-maize rotation practices increased the functional groups of bacteria with soil chemoheterotrophy (chemoheterotrophy and aerobic_chemoheterotrophy) and nitrogen fixation compared to continuous cropping soils. The addition of quicklime further altered soil functional groups of bacteria under the influence of these two rotation patterns. Adding quicklime significantly changed the functional groups of bacteria related to nitrogen cycling, such as nitrite denitrification, nitrous oxide denitrification, nitrogen fixation, and nitrate respiration, compared to the green manure rotation and wheat-maize rotation practice under non-quicklime application ($p < 0.05$).

In the present study, FUNGuild was used to investigate the functions of the fungi in all soil samples (Figure 8). Results showed that fungal trophic types could be divided into three types: saprotroph, pathotroph, and symbiotroph. The remaining types were complex trophic types. The ecological functional groups of fungal communities differed significantly among different crop years and cultivation practices. As active decomposers in the ecosystem, saprophytic fungi could decompose organic compounds such as plant and animal

10.3389/fmicb.2024.1367184

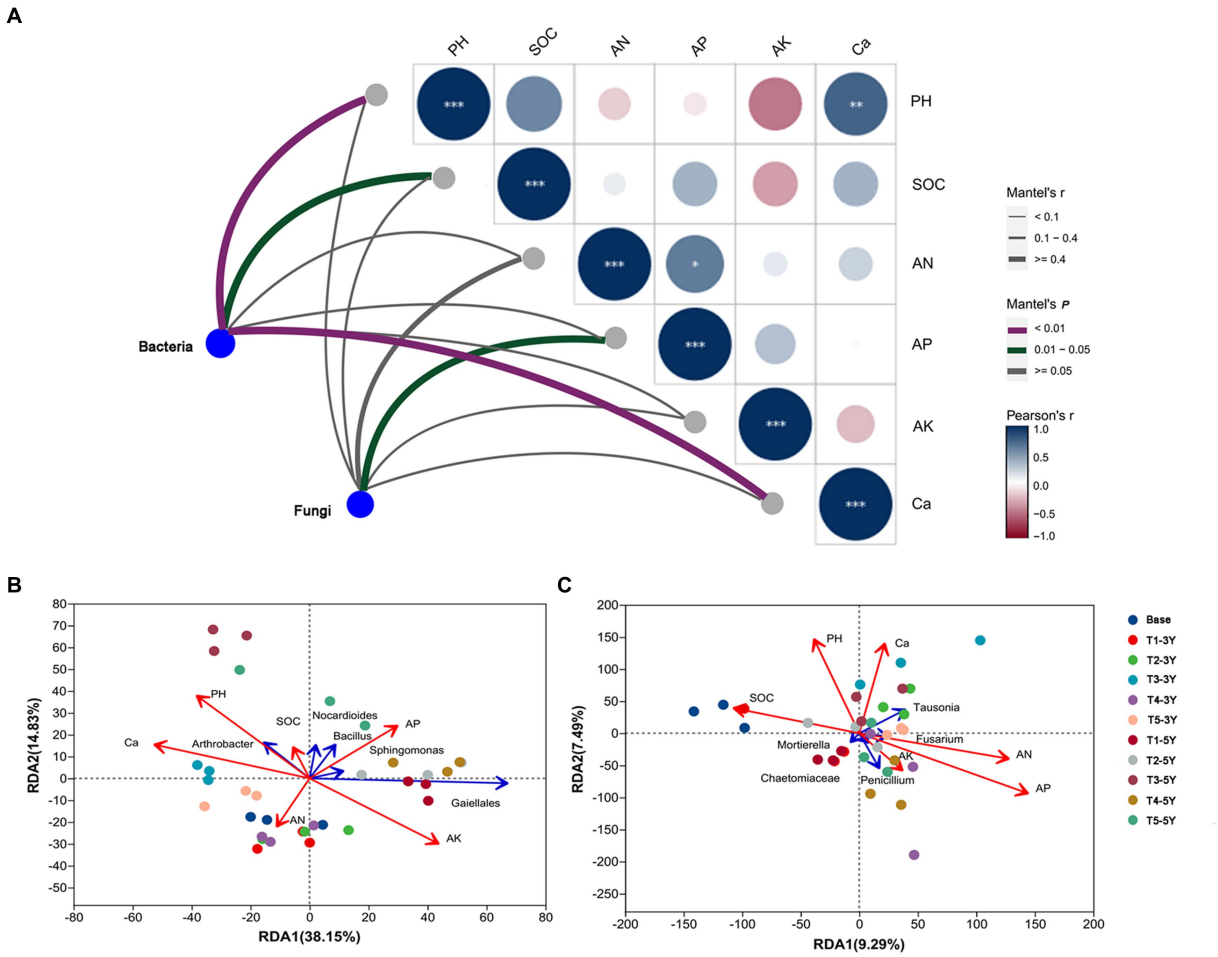

FIGURE 6
Correlation analysis of bacterial and fungal composition with soil variable factors. **(A)** Mantel tests depicting the association of bacterial composition (16 S OTUs) and fungal composition (ITS OTUs) with soil variable factors. The width of the Mantel edge represents the Mantel *r*-value. The color of the edge represents statistical significance. The color gradient of the Pearson correlation indicates the pairwise correlation of the soil variable factors. The number of asterisks represents the significance level. *$0.01 < p < 0.05$, **$0.001 < p < 0.01$, ***$p < 0.001$. The redundancy analysis (RDA) of bacterial **(B)** and fungal **(C)** communities and soil variable factors. The five most abundant bacterial and fungal genera of bacteria and fungi are shown in this figure.

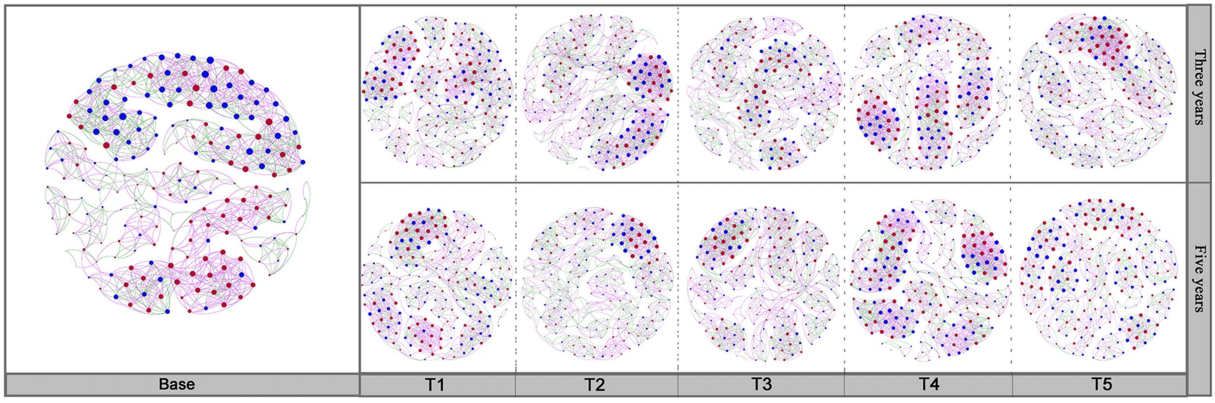

FIGURE 7
The co-occurrence network of soil bacteria and fungi in each sample. The network was constructed based on a correlation analysis. The nodes represent unique OTUs. The blue node represents bacteria. The red node represents fungi. The size of each node is proportional to its degree. Purple links represent positive correlations. Green links represent negative correlations between nodes.

10.3389/fmicb.2024.1367184

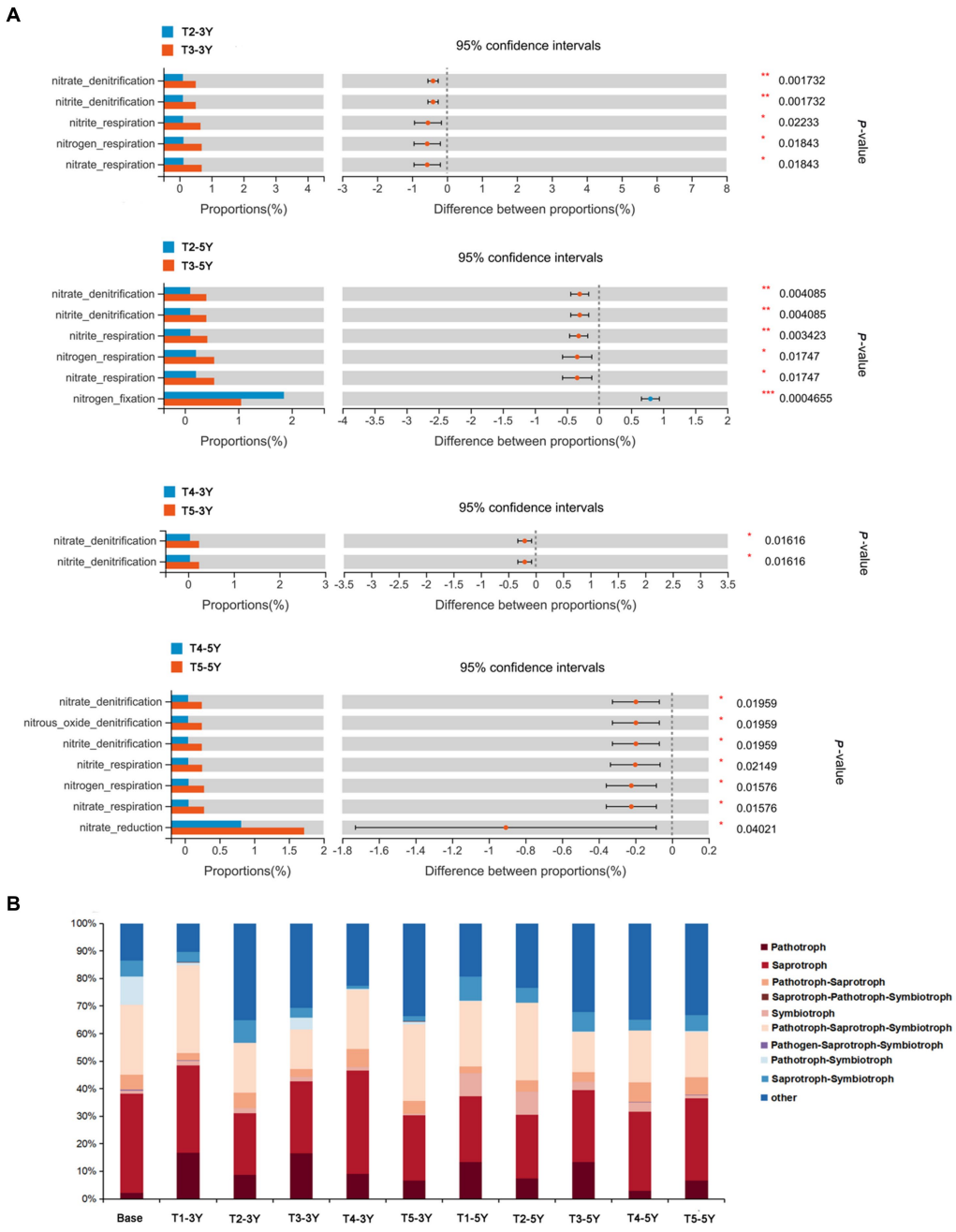

FIGURE 8
Functions of bacteria and fungi in soils under different cultivation managements at different cropping years. **(A)** Comparison of bacteria associated with nitrogen metabolism in soils in T2-*vs*-T3 and T4-*vs*-T5. Differences between the treatments was measured by Welch' s *t*-test. The number of asterisks represents the significance level. *$0.01 < p < 0.05$, **$0.001 < p < 0.01$, ***$p < 0.001$. **(B)** Trophic mode of fungi in soil under different treatments. The proportion of different trophic fungi was represented by different colors.

residues, and play an essential role in soil nutrient cycling. In most samples, saprophytic fungi were the dominant group and showed a decreasing trend with the increase in continuous cropping years. The proportion of saprophytic fungi did not change significantly after green manure measures under 3 years of continuous crop growth. The proportion of saprophytic fungi increased with rotation patterns (green manure rotation and wheat-maize rotation) at the same cropping year. Moreover, the application of quicklime was an essential driver of fungal community change. It was shown by FUNGuild functional predictions that the proportion of the pathotroph-symbiotroph type in fungi was increased by superimposed quicklime compared to a single application of green manure rotation and wheat-maize rotation measures. On the other hand, the proportion of the pathotrophic-saprotrophic fungi decreased compared to a single application of green manure and wheat-maize rotation. These results suggested that quicklime application caused the fungi to adopt a more complex survival strategy and to increase metabolic functional diversity to adapt to changes in the survival environment.

Discussion

Peanut is one of China's major oil crops (Yang L. et al., 2022). Due to the extremely limited *per capita* arable land in China, coupled with a single farming system, the proportion of intensive peanut production is increasing (Li et al., 2022). Peanut continuous cropping has led to soil environmental degradation and significant yield reduction. Changes in cultivation managements (including different crop rotation patterns and the addition of soil amendments) have been shown to be effective measures for eliminating continuous cropping obstacles of many crops (Aparicio and Costa, 2007; Zhang et al., 2022a), but the underlying mechanisms remain to be revealed. In the current study, we analyzed the effects of different cultivation managements on peanut yield, soil chemical properties and microbial community dynamics. The results of this study will expand our understanding of the mitigating effects of different cultivation managements on continuous cropping obstacles in peanut, and provide important clues for future research (Wang et al., 2023).

Wheat-maize-peanut rotation is more beneficial to eliminate continuous cropping obstacles in peanut than green manure-peanut rotation

Crop rotation is an effective agronomic method for improving soil chemical properties and enzyme activity, balancing the ratio of soil nutrients, and increasing crop yield (Venter et al., 2016; Sumner, 2018). Systemic changes in soil ecology brought about by crop rotation, especially its effect on microorganisms, can significantly alleviate continuous cropping obstacles (Shen et al., 2021; Singh and Kumar, 2021; Wang et al., 2022). It has been proven in previous studies that multiple crop rotation can introduce different types of organic residues into the soil, thus increasing the accumulation of organic matter in the soil (Berzsenyi et al., 2000; Govaerts et al., 2008). The process of soil N and P cycling through metabolic compensations is promoted by increasing organic matter, primarily organic C (Vogel et al., 2014). A balanced availability of nutrients is promoted by the coupled cycle of C-N-P (Schmidt et al., 2011), which in turn eliminates continuous cropping obstacles and promotes crop growth. Green manure-peanut rotation and wheat-maize-peanut rotation are two important ways of peanut rotation cropping patterns. As a source of bio-organic fertilizer, green manure has a balanced nutrient content and high fertilizer efficiency, playing an active role in promoting the cultivation of fertility and microbial diversity (Elfstrand et al., 2007; Ye et al., 2014; Du et al., 2020). Ryegrass has well-developed fibrous roots. When used as a green manure measure, its well-developed root system being decomposed in soil can enrich a large amount of nutrients in the tillage layer. This can increase soil organic matter content, enhance soil fertility without applying organic matter, and change the soil microbial community structure (He et al., 2020; Yang et al., 2023). In the current study, available N, P, and K in soil were obviously influenced by green manure-peanut rotation based on RDA results. Compared with continuous cropping, green manure-peanut increased SOC, AN, and AK in soil, and N concentrations in peanut kernels were increased (Figures 2, 3). Additionally, it has been proven in a recent study that the application of ryegrass as green manure could facilitate crop growth by changing bacterial communities. The soil nutrient cycle process was accelerated due to the increased relative abundance of soil microbes associated with nutrition nutrient cycling (e.g., *Proteobacteria*, *Bacteroidetes*, *Acidobacteria*, and *Gemmatimonadetes*) under the application of ryegrass (He et al., 2020). Similarly, it was demonstrated in the FAPROTAX functional analysis used in the current study that bacteria with chemoheterotrophy and nitrogen fixation functions were more pronounced in soil with green manure application (Figure 8; Supplementary Table S3). Moreover, the relative abundance of microorganisms related to nitrogen metabolism (*Actinobacteriota*) and carbon metabolism (*Bacteroidota* and *Myxococcota*) increased with the application of green manure (Figure 5). It was indicated that green manure-peanut rotation increase the available soil nutrients by increasing the relative abundance of soil microorganisms associated with nutrient cycling. Consequently, peanut growth is promoted, alleviating the damage caused by peanut continuous cropping.

It has been established that multi-crop rotations are a more effective cultivation practice to improve the sustainability and stability of agricultural systems than single crop rotation (Liu et al., 2022; Wang et al., 2023). Crop yield benefits could increase with crop species diversity in the crop rotation within a certain range (Smith et al., 2023). In the current study, the average peanut yield increased sequentially under T1 (continuous cropping), T2 (green manure rotation) and T4 (wheat-maize rotation) treatments. SOC, soil AP and AK in wheat-maize rotation soil (T3) were higher than those in continuous cropping soil (T1) and exhibited an increasing trend with increasing cropping years. This result indicated that as continuous cropping obstacle mitigation practice for peanut, the yield enhancement effect of wheat-maize-peanut rotation is stronger than that of green manure-peanut rotation. In the third year of cropping, AP was higher in the T4 treatment than in T2, and in the fifth year of cropping, AN, AP, and AK in the soil were higher in the T4 treatment than in T2. These results indicated that the wheat-maize-peanut rotation is more effective in maintaining and even increasing soil fertility than the green manure-peanut rotation, and that the fertility promotion effect increases with the number of cropping year. This result is most likely due to the introduction of more crops with different nutrient requirements in the T4 crop rotation system, resulting in a more balanced soil nutrient environment and thus easier soil fertility maintenance (Breza et al., 2022; Liang et al., 2023). It has already been shown in previous studies that multi-crop rotation could enhance soil microbial community diversity, optimize soil microbial community structure and function, and promote soil health (Liu et al., 2022). Li et al. (2022) showed that changes in soil microbial community composition (with an increase in beneficial microorganisms and a decrease in pathogenic microorganisms) and soil properties caused by multi-crop rotation could alleviate continuous cropping obstacles of peanut. In our results, the alpha diversity of the bacterial and fungal communities in the T4 soil was higher than that in T1 soil. This is consistent with the finding of a previous study reported by Li et al. (2018), who found that crop rotation could increase the diversity of microorganisms in peanut continuous cropping soil. For bacteria, among the top 10 most abundant phyla, the relative abundance of half of these phyla increased due to T4 treatment. *Actinobacteriota*, *Proteobacteria*, and *Bacteroidota* (Wegner and Liesack, 2016) were reported to have the capability to decompose organic matter and promote humus formation, while *Chloroflexi* and *Myxococcota* are able to promote nitrogen and carbon cycling (Kragelund et al., 2007; Ohore et al., 2022). The increased

relative abundance of these microorganisms may become a powerful driving force for soil organic matter and nutrient cycling and transformation, and to accelerate the transformation and supply of soil nutrients, promote the peanut development. The increase in pathogenic fungi was considered one of the critical causes of continuous cropping obstacles. Multi-crop rotation has become an important method for managing soil-borne fungal diseases, in part because of its ability to increase the diversity of soil fungal community. Diverse fungal community could contribute to reducing pathogenic fungi through mechanisms such as competition, antagonism, and induce systemic resistance, thereby reducing crop disease incidence (Govaerts et al., 2008; Bainard et al., 2017; Frąc et al., 2018; Liu et al., 2020). In this study, we found that the diversity of fungi was increased under T4 treatment. This increase in diversity may have improved functional adaptability or resistance to disturbance of the peanut cropping system. Additionally, according to the results of the co-occurrence network analysis, the implementation of T4 increased the number of interactions between fungi, which in turn increased the competition between fungi. Therefore, we believe that wheat-maize rotation can suppress the accumulation of pathogenic fungi by enhancing mutual competition among fungi, thus building a soil environment conducive to peanut growth and development.

The application of quicklime is an efficient measure to further alleviate continuous cropping obstacles in peanut

Peanut is a crop sensitive to continuous cropping (Chen et al., 2012; Li et al., 2014a). One of the fundamental reasons for the continuous cropping obstacles is the self-toxic effect caused by secretion from the peanut root system. Organic acids, such as phenolic, cetyl, and oleic acids, have been shown in previous studies to be the primary peanut chemosensitive substances in continuous cropping soils (Liu et al., 2010; Li et al., 2014a). Organic acid accumulation occurs with continuous cropping, creating an acidic soil environment. Soil acidification makes peanut more susceptible to pathogenic bacterial and fungal infestations (Zhou et al., 2014). Applying quicklime is effective to increase soil pH (Mayfield et al., 2004; Liang et al., 2021; Zhao et al., 2022). In the present study, we found that quicklime superimposed with T2 and T4 treatments increased peanut yield compared with these two treatments alone. Presumably, this occurs because residues from green manure and wheat-maize rotation have smaller-molecule organic acids during decomposition. The organic acids produced by the decomposition of root residues generated during green manure and crop rotation application could be neutralized by quicklime application. Consequently, the self-toxic effects of organic acids in the soil on peanut could be alleviated, facilitating the development of green manure and wheat-maize rotation potential.

Calcium is one of the essential nutrients in plant growth and development and has the functions of stabilizing cell membranes and cell walls and enhancing plant tolerance against environmental stresses (Lee and Seo, 2021). In addition, Ca^{2+}, as an essential second messenger of signal transduction, could participate in several physiological and biochemical processes of plant growth, development, and stress resistance (Yang S. et al., 2022). Peanut is a calcium-sensitive crop. It has been shown in previous studies that when peanut is deficient in calcium, photosynthetic products do not function well, and the photosynthetic material conversion rate is lowered. Peanut pod development was hindered, and the kernel became smaller when there is a lack of Ca^{2+} (Yang et al., 2017). Applying exogenous calcium to peanut can promote the transfer of nutrients from plant roots and stems to pods, regulate peanut growth, and improve peanut yield and quality (Basu et al., 2008). In this study, we found that a large amount of Ca^{2+} was introduced by applying quicklime, resulting in a significant increase in soil calcium content and peanut plant calcium uptake, improved peanut growth, and increased yield.

The plant growth environment is closely related to the microflora in the soil, and its microbial community dynamics are likely to directly affect plant health and efficient nutrient utilization. It has been proven in a recent study that the application of quicklime has a significant effect on changing the relative abundance of beneficial and pathogenic microorganisms in the soil (Zhang et al., 2022b). This can stimulate the potential of soil microorganisms to promote plant growth. Using high-throughput sequencing, Shen et al. (2018) found that quicklime effectively increased the abundance and diversity of inter-root soil bacterial community, and alleviated the continuous cropping obstacles by suppressing pathogenic microbes such as *Aeromonas*, *Pseudoxanthomonas* and *Saccharomyces* under tobacco plantation. Previous studies showed that soil microbial types and community composition could be significantly altered by the exogenous application of calcium, which in turn affects the resistance, growth, and development of peanut (Ci et al., 2020). Haggag and Timmusk (2008) showed that *Paenibacillus polymyxa* was effective in the biocontrol of peanut crown rot disease. *Lysinibacillus* and *Pseudomonas* were proven had the ability to inhibit aflatoxin activity, degrade aflatoxin or produce aflatoxin inhibitors (Wang et al., 2013; Gong et al., 2019). In this study, the Mantel test revealed that variation in bacterial community abundance was significantly correlated with soil Ca^{2+} concentration. Compared with the group without quicklime application, the relative abundance of peanut growth beneficial bacteria in the soil, such as *Paenibacillus*, *Lysinibacillus*, and *Pseudomonas*, increased with quicklime application. The increased relative abundance of these bacterial genera may promote peanut growth by reducing the occurrence of peanut crown rot disease and aflatoxin infection. Fungal diseases are the largest category of plant diseases caused by pathogenic microorganisms. Li et al. (2014b) proved that years of continuous peanut crops could significantly result in the accumulation of pathogenic microorganisms and decrease the abundance of plant-beneficial fungi in the soil, leading to reduced peanut yields. *Penicillium* and *Fusarium*, critical pathogenic fungi, have been reported to cause peanut fruit rot and root rot diseases (Rajeendran et al., 2017). The results of the present study showed that *Penicillium* and *Fusarium* were the dominant genera of the soil fungal community (Figure 5). The relative abundance of *Penicillium* and *Fusarium* was lower in the quicklime application than in the non-quicklime application. The decline of pathogenic fungi in continuous cropping soil reduced soil-borne diseases and might be one of the fundamental reasons for the improved peanut yield under quicklime application. In the present study, the combined application of quicklime with cultivation practice increased peanut yield more than the cultivation practice alone. *Arthrobacter*, *Bryobacter*, *Candidatus_Solibacter*, and *Acidothermus* are the key genera for decomposing organic matter and utilizing carbon sources in soil (Rime et al., 2015; Yu et al., 2016). In our results, by analyzing the correlation between microbial community change and cultivation measure, we found that the community changes in

Arthrobacter, Bryobacter, Candidatus_Solibacter, and *Acidothermus* exhibited a significant correlation ($p \leq 0.05$) with the calcium content of soil. We speculated that quicklime application might enhance the decomposition of organic matter in soil and the utilization of carbon sources by altering soil bacterial community, thus improving the growth of peanut and alleviating continuous cropping obstacles.

In addition, it is worth noting that while crop rotation (T2, T4) and crop rotation in combined with quicklime application (T3, T5) are superior to continuous cropping (T1) in guaranteeing peanut yields, there is a tendency for the yield advantages of these four cultivation managements tend to decline year after year. It has been shown that different crop rotation patterns have different soil mineral nutrient content and soil water retention capacity due to different cultivated crops (Zhang et al., 2019; Cui and Yan, 2022). Although crop rotation plays an important role in improving the multifunctionality of soil ecosystems and maintaining the yield stability of the main crop, for main crop with sensitive mineral fertilizer and water requirements, multi-year crop rotation cannot make up for the differences in mineral fertilizer requirements and water-fertilizer coupling effects of the main crop, and the differences in different crop rotation patterns will decrease with the increase in the number of cropping years (Liu et al., 2023). In addition, the effects of different soil types on the stable yield effect of crop rotation are different (Van Doren Jr et al., 1976; Fiorini et al., 2020). In the future, it is still necessary to further explore the optimization of fertilization and water supply measures under different soil types, combined with different crop rotation systems on the sustainability of stable crop yield. Nevertheless, without considering other factors, the results of the present study suggested that wheat-maize-peanut rotation with quicklime application is an effective peanut yield stabilization measure than the other four cultivation measures.

Conclusion

This study provides evidence that cultivation management plays a significant role in changing soil chemistry and shaping the composition and functions of bacterial and fungal communities on a time scale. Peanut continuous cropping leads to increased soil acidification, reduced soil fertility and induced an increase in pathogenic bacteria and fungi. Compared with peanut continuous cropping, the application of crop rotation increased microbial diversity and effectively enhanced the microbial functions associated with carbon and nitrogen cycling. Importantly, crop rotation with quicklime application effectively modifies the soil acidification environment, increases contents of Ca and SOC in soil and changes the relative abundance of potentially beneficial and pathogenic bacteria and fungi, thereby promoting plant development and yield of peanut. Moreover, variation in bacterial community is mainly attribute to soil pH, Ca and SOC content, while variation in fungal community was more closely related to soil P content. In addition, compared to peanut continuous cropping, the application of green manure-peanut rotation and wheat-maize-peanut rotation increase peanut yield by 40.59 and 81.95%, respectively. Whereas the combination of these two rotation patterns with quicklime application further increase peanut yield by 28.76 and 24.34%. Peanut yield was highest in wheat-maize-peanut rotation combined with quicklime application treatment. Therefore, during actual production, the combination of wheat-maize-peanut rotation with quicklime application was an effective measure to improve soil fertility and microecology, alleviate peanut cropping obstacles and promote the sustainable development of peanut production. Since this study was conducted only in peanut fields with brown soil, additional investigations in various agricultural regions are still required to verify the effectiveness of this measure.

Data availability statement

The datasets presented in this study can be found in online repositories. The names of the repository/repositories and accession number(s) can be found below: https://www.ncbi.nlm.nih.gov/, PRJNA901660.

Author contributions

LY: Writing – original draft, Writing – review & editing. CW: Conceptualization, Investigation, Supervision, Writing – review & editing. XH: Project administration, Validation, Writing – review & editing. HL: Data curation, Formal analysis, Methodology, Software, Writing – review & editing. QW: Data curation, Formal analysis, Methodology, Writing – review & editing. XS: Investigation, Methodology, Writing – review & editing. ML: Validation, Writing – review & editing. PS: Writing – review & editing, Writing – original draft.

Funding

The author(s) declare that financial support was received for the research, authorship, and/or publication of this article. This work was supported by the Shandong Provincial Natural Science Foundation (ZR2021QC096, ZR2022MC074), Talent Project for Agricultural Science and Technology Innovation Engineering of Shandong Academy of Agricultural Sciences (CXGC2021B33), National Natural Science Foundation of China (41501330, 33201918), Major Scientific and Technological Innovation Projects in Shandong Province, China (2019JZZY010702).

Conflict of interest

The authors declare that the research was conducted in the absence of any commercial or financial relationships that could be construed as a potential conflict of interest.

Publisher's note

Supplementary material

The Supplementary material for this article can be found online at: https://www.frontiersin.org/articles/10.3389/fmicb.2024.1367184/full#supplementary-material

References

Aparicio, V., and Costa, J. L. (2007). Soil quality indicators under continuous cropping systems in the Argentinean Pampas. *Soil Till. Res.* 96:155–165. doi: 10.1016/j.still.2007.05.006

Bainard, L. D., Navarro-Borrell, A., Hamel, C., Braun, K., Hanson, K., and Gan, Y. (2017). Increasing the frequency of pulses in crop rotations reduces soil fungal diversity and increases the proportion of fungal pathotrophs in a semiarid agroecosystem. *Agric. Ecosyst. Environ.* 240, 206–214. doi: 10.1016/j.agee.2017.02.020

Bai, Y. X., Wang, G., Chen, Y. D., Shi, P. Y., Yang, C. C., Yang, H. W., et al. (2019). Soil acidification in continuously cropped tobacco alters bacterial community structure and diversity via the accumulation of phenolic acids. *Sci. Rep.* 9:12499. doi: 10.1038/s41598-019-48611-5

Bastian, M., Heymann, S., and Jacomy, M. (2009). Gephi: an open source software for exploring and manipulating networks. *Proc. Int. AAAI Conf. Web Soc. Media* 3, 361–362. doi: 10.1609/icwsm.v3i1.13937

Basu, M., Bhadoria, P. B., and Mahapatra, S. C. (2008). Growth, nitrogen fixation, yield and kernel quality of peanut in response to lime, organic and inorganic fertilizer levels. *Bioresour. Technol.* 99, 4675–4683. doi: 10.1016/j.biortech.2007.09.078

Bertioli, D. J., Cannon, S. B., Froenicke, L., Huang, G., Farmer, A. D., Cannon, E. K., et al. (2016). The genome sequences of Arachis duranensis and Arachis ipaensis, the diploid ancestors of cultivated peanut. *Nat. Genet.* 48, 438–446. doi: 10.1038/ng.3517

Berzsenyi, Z., Győrffy, B., and Lap, D. Q. (2000). Effect of crop rotation and fertilisation on maize and wheat yields and yield stability in a long-term experiment. *Eur. J. Agron.* 13, 225–244. doi: 10.1016/S1161-0301(00)00076-9

Breza, L. C., Mooshammer, M., Bowles, T. M., Jin, V. L., Schmer, M. R., Thompson, B., et al. (2022). Complex crop rotations improve organic nitrogen cycling. *Soil Biol. Biochem.* 177:108911. doi: 10.1016/j.soilbio.2022.108911

Carrière, Y., Brown, Z. S., Aglasan, S., Dutilleul, P., Carroll, M. W., Head, G. P., et al. (2020). Crop rotation mitigates impacts of corn rootworm resistance to transgenic Bt corn. *Proc. Natl. Acad. Sci. U. S. A.* 117, 18385–18392. doi: 10.1073/pnas.2003604117

Chen, M., Li, X., Yang, Q., Chi, X., Pan, L., Chen, N., et al. (2014). Dynamic Succession of Soil Bacterial Community during Continuous Cropping of Peanut (Arachis hypogaea L.). *PloS One*, 9:e101355. doi: 10.1371/journal.pone.0101355

Chen, M., Li, X., Yang, Q., Chi, X., Pan, L., Chen, N., et al. (2012). Soil eukaryotic microorganism succession as affected by continuous cropping of peanut-pathogenic and beneficial fungi were selected. *PLoS One* 7:e40659. doi: 10.1371/journal.pone.0040659

Ci, D., Tang, Z., Ding, H., Cui, L., Zhang, G., Li, S., et al. (2020). The synergy effect of arbuscular mycorrhizal fungi symbiosis and exogenous calcium on bacterial community composition and growth performance of peanut (*Arachis hypogaea* L.) in saline alkali soil. *J. Microbiol.* 59, 51–63. doi: 10.1007/s12275-021-0317-3

Cui, Z., and Yan, B. (2022). Crop yield and water use efficiency in response to long-term diversified crop rotations. *Front. Plant Sci.* 13:1024898. doi: 10.3389/fpls.2022.1024898

Dahlquist, R. L., and Knoll, J. W. (1978). Inductively coupled plasma-atomic emission spectrometry: analysis of biological materials and soils for major, trace, and ultra-trace elements. *Appl. Spectrosc.* 32, 1–30. doi: 10.1366/000370278774331828

Du, Y., Cui, B., Wang, Z., Sun, J., and Niu, W. (2020). Effects of manure fertilizer on crop yield and soil properties in China: a meta-analysis. *Catena* 193:104617. doi: 10.1016/j.catena.2020.104617

Elfstrand, S., Båth, B., and Mårtensson, A. (2007). Influence of various forms of green manure amendment on soil microbial community composition, enzyme activity and nutrient levels in leek. *Appl. Soil Ecol.* 36, 70–82. doi: 10.1016/j.apsoil.2006.11.001

Fageria, N., and Baligar, V. (2005). Enhancing nitrogen use efficiency in crop plants. *Adv. Agron.* 88, 97–185. doi: 10.1016/S0065-2113(05)88004-6

Fierer, N., Wood, S. A., and de Mesquita, C. P. (2020). How microbes can, and cannot, be used to assess soil health. *Soil Biol. Biochem.* 153:108111. doi: 10.1016/j.soilbio.2020.108111

Fiorini, A., Boselli, R., Maris, S. C., Santelli, S., Perego, A., Acutis, M., et al. (2020). Soil type and cropping system as drivers of soil quality indicators response to no-till: a 7-year field study. *Appl. Soil Ecol.* 155:103646. doi: 10.1016/j.apsoil.2020.103646

Frąc, M., Hannula, S. E., Bełka, M., and Jędryczka, M. (2018). Fungal biodiversity and their role in soil health. *Front. Microbiol.* 9:707. doi: 10.3389/fmicb.2018.00707

Gong, A., Dong, F., Hu, M., Kong, X., Wei, F., Gong, S., et al. (2019). Antifungal activity of volatile emitted from *Enterobacter asburiae* Vt-7 against aspergillus flavus and aflatoxins in peanuts during storage. *Food Control* 106:106718. doi: 10.1016/j.foodcont.2019.106718

Govaerts, B., Mezzalama, M., Sayre, K. D., Crossa, J., Lichter, K., Troch, V., et al. (2008). Long-term consequences of tillage, residue management, and crop rotation on selected soil micro-flora groups in the subtropical highlands. *Appl. Soil Ecol.* 38, 197–210. doi: 10.1016/j.apsoil.2007.10.009

Haggag, W. M., and Timmusk, S. (2008). Colonization of peanut roots by biofilm-forming *Paenibacillus polymyxa* initiates biocontrol against crown rot disease. *J. Appl. Microbiol.* 104, 961–969. doi: 10.1111/j.1365-2672.2007.03611.x

He, H., Li, W., Zhang, Y., Cheng, J., Jia, X., Li, S., et al. (2020). Effects of Italian ryegrass residues as green manure on soil properties and bacterial communities under an Italian ryegrass (*Lolium multiflorum* L.)-rice (*Oryza sativa* L.) rotation. *Soil Till. Res.* 196:104487. doi: 10.1016/j.still.2019.104487

He, Z., Mao, R., Dong, J., Liang, Z., Zhang, H., and Liu, L. (2019). Remediation of deterioration in microbial structure in continuous *Pinellia ternata* cropping soil by crop rotation. *Can. J. Microbiol.* 654, 282–295. doi: 10.1139/cjm-2018-0409

Huang, M., Liang, T., Wang, L., and Zhou, C. (2015). Effects of no-tillage systems on soil physical properties and carbon sequestration under long-term wheat-maize double cropping system. *Catena* 128, 195–202. doi: 10.1016/j.catena.2015.02.010

Kagawa, K., Gonai, T., Ichige, H., Fujita, Y., Terakado, I., Shimizu, A., et al. (2022). Effect of hot water drip irrigation treatment of continuous cropping soil before replanting on growth and yields of young Japanese pear trees. *Horticult. J.* 91, 501–507. doi: 10.2503/hortj.UTD-362

Kragelund, C., Levantesi, C., Borger, A., Thelen, K., Eikelboom, D., Tandoi, V., et al. (2007). Identity, abundance and ecophysiology of filamentous Chloroflexi species present in activated sludge treatment plants. *FEMS Microbiol. Ecol.* 59, 671–682. doi: 10.1111/j.1574-6941.2006.00251.x

Lee, H., and Seo, P. J. (2021). Ca^{2+}talyzing initial responses to environmental stresses. *Trends Plant Sci.* 26, 849–870. doi: 10.1016/j.tplants.2021.02.007

Liang, J., Yu, X., Cao, Y., Zhang, J., Yan, N., et al. (2021). Effect of Quicklime on microbial community in strong acidic soil. *J. Plant Nutr. Soil Sci.* 21:1771–1781. doi: 10.1007/s42729-021-00478-0

Liang, Z., Zhan, X., Cheng, J., Ma, B., Cong, W., Zhang, C., et al. (2023). Designing diversified crop rotations to advance sustainability: a method and an application. *Sustain. Prod. Consump.* 40, 532–544. doi: 10.1016/j.spc.2023.07.018

Li, H., Li, C., Song, X., Liu, Y., Gao, Q., Zheng, R., et al. (2022). Impacts of continuous and rotational cropping practices on soil chemical properties and microbial communities during peanut cultivation. *Sci. Rep.* 12, 1–12. doi: 10.1038/s41598-022-06789-1

Liu, C., Feng, X., Xu, Y., Kumar, A., Yan, Z., Zhou, J., et al. (2023). Legume-based rotation enhances subsequent wheat yield and maintains soil carbon storage. *Agron. Sustain. Dev.* 43:64. doi: 10.1007/s13593-023-00918-4

Liu, C., Plaza-Bonilla, D., Coulter, J. A., Kutcher, H. R., Beckie, H. J., Wang, L., et al. (2022). Diversifying crop rotations enhances agroecosystem services and resilience. *Adv. Agron.* 173, 299–335. doi: 10.1016/bs.agron.2022.02.007

Liu, P., Wan, S. B., Jiang, L. H., Wang, C. B., Liu, Z. H., Zhao, H. J., et al. (2010). Autotoxic potential of root exudates of peanut (*Arachis hypogaea* L.). *Allelopath. J.* 26, 197–205,

Liu, Q., Wang, S., Li, K., Qiao, J., Guo, Y., Liu, Z., et al. (2021). Responses of soil bacterial and fungal communities to the long-term monoculture of grapevine. *Appl. Microbiol. Biot.* 105, 7035–7050. doi: 10.1007/s00253-021-11542-1

Liu, Z., Liu, J., Yu, Z., Yao, Q., Li, Y., Liang, A., et al. (2020). Long-term continuous cropping of soybean is comparable to crop rotation in mediating microbial abundance, diversity and community composition. *Soil Till. Res.* 197:104503. doi: 10.1016/j.still.2019.104503

Li, X., Ding, C., Hua, K., Zhang, T., Zhang, Y., Zhao, L., et al. (2014a). Soil sickness of peanuts is attributable to modifications in soil microbes induced by peanut root exudates rather than to direct allelopathy. *Soil Biol. Biochem.* 78, 149–159. doi: 10.1016/j.soilbio.2014.07.019

Li, X., Ding, C., Zhang, T., and Wang, X. (2014b). Fungal pathogen accumulation at the expense of plant-beneficial fungi as a consequence of consecutive peanut monoculturing. *Soil Biol. Biochem.* 72, 11–18. doi: 10.1016/j.soilbio.2014.01.019

Li, X., Jousset, A., de Boer, W., Carrión, V. J., Zhang, T., Wang, X., et al. (2018). Legacy of land use history determines reprogramming of plant physiology by soil microbiome. *ISME J.* 13, 738–751. doi: 10.1038/s41396-018-0300-0

Lu, W., Hao, Z., Ma, X., Gao, J., Fan, X., Guo, J., et al. (2024). Effects of different proportions of organic fertilizer replacing chemical fertilizer on soil nutrients and fertilizer utilization in gray desert soil. *Agronomy* 14:228. doi: 10.3390/agronomy14010228

Lu, Y., Gao, P., Wang, Y., Li, W., Cui, X., Zhou, J., et al. (2021). Earthworm activity optimized the rhizosphere bacterial community structure and further alleviated the yield loss in continuous cropping lily (*Lilium lancifolium* Thunb.). *Sci. Rep.* 11:20840. doi: 10.1038/s41598-021-99597-y

Massigoge, I., Baral, R., Sofía, C., Denson, E., Paula, G. H., Guareschi, C., et al. (2024). Exploring alternative crop rotations to continuous winter wheat for agricultural intensification in the US central great plains. *Agric. Syst.* 216:103879. doi: 10.1016/j.agsy.2024.103879

Mayfield, J. L., Ozanne, L. K., Mitchell, C. C., Simonne, E. H., and Sibley, J. L. (2004). Laboratory and greenhouse evaluation of quicklime sources for suitability as agricultural liming materials. *Commun. Soil Sci. Plant* 35, 1167–1183. doi: 10.1081/CSS-120030596

Mulvaney, R. L., and Khan, S. A. (2001). Diffusion methods to determine different forms of nitrogen in soil hydrolysates. *Soil Sci. Soc. Am. J.* 65, 1284–1292. doi: 10.2136/sssaj2001.6541284x

Nguyen, N. H., Song, Z., Bates, S. T., Branco, S., Tedersoo, L., Menke, J. R., et al. (2016). FUNGuild: an open annotation tool for parsing fungal community datasets by ecological guild. *Fungal Ecol.* 20, 241–248. doi: 10.1016/j.funeco.2015.06.006

Ohore, O. E., Wei, Y., Wang, J., Wang, Y., Ifon, B., Liu, W., et al. (2022). Vertical characterisation of phylogenetic divergence of microbial community structures, interaction, and sustainability in estuary and marine ecosystems. *Sci. Total Environ.* 851:158369. doi: 10.1016/j.scitotenv.2022.158369

Olsen, S. L., and Sommers, L. E. (1982). "Phosphorus" in *Methods of soil analysis. Part 2: Chemical and microbiological properties*. eds. A. L. Page, R. H. Miller and D. R. Keeney. *2nd* ed (Madison: American Society of Agronomy), 403–427.

Passaris, N., Flower, K. C., Ward, P. R., and Cordingley, N. (2021). Effect of crop rotation diversity and windrow burning of residue on soil chemical composition under long-term no-tillage. *Soil Till. Res.* 213:105153. doi: 10.1016/j.still.2021.105153

Pervaiz, Z. H., Iqbal, J., Zhang, Q., Chen, D., Wei, H., and Saleem, M. (2020). Continuous cropping alters multiple biotic and abiotic indicators of soil health. *Soil Syst.* 4:59. doi: 10.3390/soilsystems4040059

Rajeendran, A., Nulit, R., Yien, C. Y., Ibrahim, M. H., and Kalhori, N. (2017). Isolation and molecular identification of colletotrichum gloeosporioides from infected peanut seeds. *Int. J. Plant Sci.* 19, 1–8. doi: 10.9734/ijpss/2017/35838

Rime, T., Hartmann, M., Brunner, I., Widmer, F., Zeyer, J., and Frey, B. (2015). Vertical distribution of the soil microbiota along a successional gradient in a glacier forefield. *Mol. Ecol.* 24, 1091–1108. doi: 10.1111/mec.13051

Schmidt, M. W., Torn, M. S., Abiven, S., Dittmar, T., Guggenberger, G., Janssens, I. A., et al. (2011). Persistence of soil organic matter as an ecosystem property. *Nature* 478, 49–56. doi: 10.1038/nature10386

Shannon, C. E. (1948). A mathematical theory of communication. *Bell Syst. Tech. J.* 27, 379–423. doi: 10.1002/j.1538-7305.1948.tb01338.x

Shen, G., Zhang, S., Liu, X., Jiang, Q., and Ding, W. (2018). Soil acidification amendments change the rhizosphere bacterial community of tobacco in a bacterial wilt affected field. *Appl. Microbiol. Biotechnol.* 102, 9781–9791. doi: 10.1007/s00253-018-9347-0

Shen, J., Tao, Q., Dong, Q., Luo, Y., Luo, J., He, Y., et al. (2021). Long-term conversion from rice-wheat to rice-vegetable rotations drives variation in soil microbial communities and shifts in nitrogen-cycling through soil profiles. *Geoderma* 404:115299. doi: 10.1016/j.geoderma.2021.115299

Shen, P., Wang, C., Wu, Z., Wang, C., Zhao, H., Shan, S., et al. (2019). Peanut macronutrient absorptions characteristics in response to soil compaction stress in typical brown soils under various tillage systems. *Soil Sci. Plant Nutr.* 65, 148–158. doi: 10.1080/00380768.2019.1579043

Singh, J., and Kumar, S. (2021). Responses of soil microbial community structure and greenhouse gas fluxes to crop rotations that include winter cover crops. *Geoderma* 385:114843. doi: 10.1016/j.geoderma.2020.114843

Smith, M. E., Vico, G., Costa, A., Bowles, T., Gaudin, A. C. M., Hallin, S., et al. (2023). Increasing crop rotational diversity can enhance cereal yields. *Commun. Earth Environ.* 4:89. doi: 10.1038/s43247-023-00746-0

Sumner, D. R. (2018). "Crop rotation and plant productivity" in *Handbook of Agricultural Productivity*. 1st edn. Ed. M. Rechcigl (Boca Raton: CRC Press), 273–314.

Tan, Y., Cui, Y., Li, H., Kuang, A., Li, X., Wei, Y., et al. (2017). Rhizospheric soil and root endogenous fungal diversity and composition in response to continuous Panax notoginseng cropping practices. *Microbiol. Res.* 194, 10–19. doi: 10.1016/j.micres.2016.09.009

Van Doren Jr, D. M., Triplett, G. B. Jr., and Henry, J. E. (1976). Influence of long term tillage, crop rotation, and soil type combinations on corn yield. *Soil Sci. Soc. Am. J.* 40, 100–105. doi: 10.2136/sssaj1976.03615995004000010027x

Venter, Z. S., Jacobs, K., and Hawkins, H. J. (2016). The impact of crop rotation on soil microbial diversity: a meta-analysis. *Pedobiologia* 59, 215–223. doi: 10.1016/j.pedobi.2016.04.001

Vogel, C., Mueller, C. W., Höschen, C., Buegger, F., Heister, K., Schulz, S., et al. (2014). Submicron structures provide preferential spots for carbon and nitrogen sequestration in soils. *Nat. Commun.* 5:2947. doi: 10.1038/ncomms3947

Walkley, A. (1935). An examination of methods for determining organic carbon and nitrogen in soils. *J. Agric. Sci.* 25, 598–609. doi: 10.1017/S0021859600019687

Wang, F., Zhang, X., Wei, M., Wang, Y., Liang, Z., and Xia, P. (2022). Appropriate crop rotation alleviates continuous cropping barriers by changing rhizosphere microorganisms in Panax notoginseng. *Rhizosphere* 23:100568. doi: 10.1016/j.rhisph.2022.100568

Wang, K., Yan, P. S., Ding, Q., Wu, Q., Wang, Z., and Peng, J. (2013). Diversity of culturable root-associated/endophytic bacteria and their chitinolytic and aflatoxin inhibition activity of peanut plant in China. *World J. Microb. Biotechnol.* 29, 1–10. doi: 10.1007/s11274-012-1135-x

Wang, S., Xiong, J., Yang, B., Yang, X., Du, T., Steenhuis, T. S., et al. (2023). Diversified crop rotations reduce groundwater use and enhance system resilience. *Agric. Water Manage.* 276:108067. doi: 10.1016/j.agwat.2022.108067

Wegner, C. E., and Liesack, W. (2016). Microbial community dynamics during the early stages of plant polymer breakdown in paddy soil. *Environ. Microbiol.* 18, 2825–2842. doi: 10.1111/1462-2920.12815

Xiao, Z., Lu, C., Wu, Z., Li, X., Ding, K., Zhu, Z., et al. (2024). Continuous cropping disorders of eggplants (*Solanum melongena* L.) and tomatoes (*Solanum lycopersicum* L.) in suburban agriculture: microbial structure and assembly processes. *Sci. Total Environ.* 909:168558. doi: 10.1016/j.scitotenv.2023.168558

Yang, L., Wu, Q., Liang, H., Yin, L., and Shen, P. (2022). Integrated analyses of transcriptome and metabolome provides new insights into the primary and secondary metabolism in response to nitrogen deficiency and soil compaction stress in peanut roots. *Front. Plant Sci.* 13:948742. doi: 10.3389/fpls.2022.948742

Yang, R., Song, S., Chen, S., Du, Z., and Kong, J. (2023). Adaptive evaluation of green manure rotation for a low fertility farmland system: impacts on crop yield, soil nutrients, and soil microbial community. *Catena* 222:106873. doi: 10.1016/j.catena.2022.106873

Yang, S., Li, L., Zhang, J., Geng, Y., Guo, F., Wang, J., et al. (2017). Transcriptome and differential expression profiling analysis of the mechanism of Ca^{2+} regulation in peanut (*Arachis hypogaea*) pod development. *Front. Plant Sci.* 8:1609. doi: 10.3389/fpls.2017.01609

Yang, S., Wang, J., Tang, Z., Li, Y., Zhang, J., Guo, F., et al. (2022). Calcium/calmodulin modulates salt responses by binding a novel interacting protein SAMS1 in peanut (*Arachis hypogaea* L.). *Crop J.* 11, 21–32. doi: 10.1016/j.cj.2022.06.007

Ye, X., Liu, H., Li, Z., Wang, Y., Wang, Y., Wang, H., et al. (2014). Effects of green manure continuous application on soil microbial biomass and enzyme activity. *J. Plant Nutr.* 37, 498–508. doi: 10.1080/01904167.2013.867978

You, C., Jiang, L., Xi, F., Wang, W., Li, M., Xu, Z., et al. (2015). Comparative evaluation of different types of soil conditioners with respect to their ability to remediate consecutive tobacco monoculture soil. *Int. J. Agric. Biol.* 17, 969–975. doi: 10.17957/IJAB/15.0017

Yu, T., Hou, X., Fang, X., Razavi, B., Zang, H., Zeng, Z., et al. (2024). Short-term continuous monocropping reduces peanut yield mainly via altering soil enzyme activity and fungal community. *Environ. Res.* 245:117977. doi: 10.1016/j.envres.2023.117977

Yu, Z., Li, Y., Wang, G., Liu, J., Liu, J., Liu, X., et al. (2016). Effectiveness of elevated CO2 mediating bacterial communities in the soybean rhizosphere depends on genotypes. *Agric. Ecosyst. Environ.* 231, 229–232. doi: 10.1016/j.agee.2016.06.043

Zhang, Y., Gao, Y., Zhang, Y., Huang, D., Li, X., Gregorich, E., et al. (2022a). Effect of long-term tillage and cropping system on portion of fungal and bacterial necromass carbon in soil organic carbon. *Soil Till. Res.* 218:105307. doi: 10.1016/j.still.2021.105307

Zhang, Y., Wang, R., Wang, H., Wang, S., Wang, X., and Li, J. (2019). Soil water use and crop yield increase under different long-term fertilization practices incorporated with two-year tillage rotations. *Agric. Water Manage.* 221, 362–370. doi: 10.1016/j.agwat.2019.04.018

Zhang, Y., Ye, C., Su, Y. S., Peng, W., Lu, R., Liu, Y., et al. (2022b). Soil acidification caused by excessive application of nitrogen fertilizer aggravates soil-borne diseases: evidence from literature review and field trials. *Agric. Ecosyst. Environ.* 340:108176. doi: 10.1016/j.agee.2022.108176

Zhao, L., Jiang, W., Chen, R., Wang, H., Duan, Y., Chen, X., et al. (2022). Quicklime and superphosphate alleviating apple replant disease by improving acidified soil. *ACS Omega* 7, 7920–7930. doi: 10.1021/acsomega.1c06876

Zhou, J., Kang, L., Wang, H., Yang, T., and Dai, C. C. (2014). Liquid laccase production by Phomopsis liquidambari B3 accelerated phenolic acids degradation in long-term cropping soil of peanut. *Acta. Agr. Scand.* 64, 683–693. doi: 10.1080/09064710.2014.953987

frontiers | Frontiers in Microbiology

TYPE Original Research
PUBLISHED 31 May 2024
DOI 10.3389/fmicb.2024.1408622

OPEN ACCESS

EDITED BY
Yichao Shi,
Agriculture and Agri-Food Canada (AAFC), Canada

REVIEWED BY
Rafael Jorge Leon-Morcillo,
Spanish National Research Council (CSIC), Spain
Lin Chen,
Chinese Academy of Forestry, China

*CORRESPONDENCE
Peifang Chong
✉ zhongpf@gsau.edu.cn

RECEIVED 28 March 2024
ACCEPTED 21 May 2024
PUBLISHED 31 May 2024

CITATION
Bao X, Chong P, He C, Wang X and Zhang F (2024) Mechanism on the promotion of host growth and enhancement of salt tolerance by *Bacillaceae* isolated from the rhizosphere of *Reaumuria soongorica*. *Front. Microbiol.* 15:1408622. doi: 10.3389/fmicb.2024.1408622

Mechanism on the promotion of host growth and enhancement of salt tolerance by *Bacillaceae* isolated from the rhizosphere of *Reaumuria soongorica*

Xinguang Bao[1], Peifang Chong[1]*, Cai He[2], Xueying Wang[1] and Feng Zhang[1]

[1]College of Forest of Gansu Agriculture University, Lanzhou, China, [2]Wuwei Academy of Forestry, Wuwei, China

Salt stress is a major abiotic stress that affects the growth of *Reaumuria soongorica* and many psammophytes in the desert areas of Northwest China. However, various Plant Growth-Promoting Rhizobacteria (PGPR) have been known to play an important role in promoting plant growth and alleviating the damaging effects of salt stress. In this study, three PGPR strains belonging to *Bacillaceae* were isolated from the rhizosphere of *Reaumuria soongorica* by morphological and molecular identification. All isolated strains exhibited capabilities of producing IAA, solubilizing phosphate, and fixing nitrogen, and were able to tolerate high levels of NaCl stress, up to 8–12%. The results of the pot-based experiment showed that salt (400 mM NaCl) stress inhibited *Reaumuria soongorica* seedlings' growth performance as well as biomass production, but after inoculation with strains P2, S37, and S40, the plant's height significantly increased by 26.87, 17.59, and 13.36%, respectively ($p < 0.05$), and both aboveground and root fresh weight significantly increased by more than 2 times compared to NaCl treatment. Additionally, inoculation with P2, S37, and S40 strains increased the content of photosynthetic pigments, proline, and soluble protein in *Reaumuria soongorica* seedlings under NaCl stress, while reducing the content of malondialdehyde and soluble sugars. Metabolomic analysis showed that strain S40 induces *Reaumuria soongorica* seedling leaves metabolome reprogramming to regulate cell metabolism, including plant hormone signal transduction and phenylalanine, tyrosine, and tryptophan biosynthesis pathways. Under NaCl stress, inoculation with strain S40 upregulated differential metabolites in plant hormone signal transduction pathways including plant hormones such as auxins (IAA), cytokinins, and jasmonic acid. The results indicate that inoculation with *Bacillaceae* can promote the growth of *Reaumuria soongorica* seedlings under NaCl stress and enhance salt tolerance by increasing the content of photosynthetic pigments, accumulating osmoregulatory substances, regulating plant hormone levels This study contributes to the enrichment of PGPR strains capable of promoting the growth of desert plants and has significant implications for the psammophytes growth and development in desert regions, as well as the effective utilization and transformation of saline-alkali lands.

KEYWORDS

***Reaumuria soongorica*, plant growthpromoting rhizobacteria (PGPR), salt stress, plant hormones, metabolites**

1 Introduction

Data indicate that the area of saline soils worldwide exceeds 833 million hectares, accounting for 8.7% of the Earth's surface area from the Global Saline Soils Map published by the Food and Agriculture Organization of the United Nations in 2021. China's saline soil totals 36.9 million hectares, comprising 4.4% of the global saline soil (Yang et al., 2022). Saline soils are mainly distributed in arid and semi-arid regions and have become a global issue affecting vegetation restoration and agricultural productivity. Under salt stress, the massive accumulation of Na^+ and Cl^- within plant cells leads to ionic imbalance, the production of reactive oxygen species, oxidative damage, and disruption of plant metabolic functions, inhibiting plant growth (Kibria et al., 2017; Sunita et al., 2020). Various physical, chemical, hydraulic engineering, and biological methods are employed in agriculture to ameliorate saline soils. At present, microbial improvement of saline-alkali soils is recognized as one of the most environmentally friendly and sustainable measures and has become a hot research topic. Practical evidence has demonstrated that some beneficial microbes can promote plant growth and help plants resist biotic and abiotic stresses. Based on their effects on plant growth, nutrient cycling, and soil structure, beneficial microbes can be categorized into plant growth-promoting rhizobacteria (PGPR), nitrogen-fixing bacteria, arbuscular mycorrhizal fungi, and ectomycorrhizal fungi (Coban et al., 2022).

PGPR are soil bacteria that reside in the plant root vicinity and promote plant growth, either directly or indirectly, through their vital activities, helping plants cope with various biotic and abiotic stresses (Aguirre-Monroy et al., 2019; Gupta et al., 2019). Studies have found that PGPRs mediate the increase in soil nutrient availability and produce plant growth hormones to directly promote plant growth; for instance, nitrogen-fixing bacteria convert atmospheric nitrogen into plant-usable forms of $NO3^-$ or $NH4^+$ (Mukherjee and Sen, 2015), phosphate-solubilizing bacteria enhance soil phosphorus availability (Amri et al., 2023), siderophore-producing strains increase soil bioavailability of iron (Saha et al., 2016), and PGPR can promote plant growth by producing plant growth hormones, such as exogenous IAA, to stimulate root development and the formation of lateral and adventitious roots (Li et al., 2022). On the other hand, PGPR can indirectly support plant growth by suppressing the deleterious effects of biotic and abiotic stresses. For example, inoculation with *Azospirillum* and *Azotobacter* species significantly promoted growth and enhanced salt tolerance of cherry tomato under different salinity levels (El-Beltagi et al., 2022), and the addition of *Enterobacter cancerogenus* JY65 promoted the growth of rice under NaCl stress with significantly increased plant biomass, plant height, and root length (Peng et al., 2023). There is also evidence that plant secondary metabolites are involved (Sunita et al., 2020; Pang et al., 2021; Koza et al., 2022; Kumar et al., 2023). The *Bacillus subtilis* strain WM13-24 isolated from the rhizosphere of *Haloxylon ammodendron* promotes plant growth by producing volatile organic compounds that stimulate lateral root and root hair development (He et al., 2023). Flavonoids, as active molecules mediating communication between PGPR and plants, involve in PGPR-mediated plant tolerance to abiotic stresses, especially salinity stress (Wang et al., 2022). Thus, PGPR plays a key role in plant growth and development as well as in addressing various environmental stresses. Therefore, rhizosphere microbes certainly deserve as "second genome" of plants (Maeda and Dudareva, 2012).

However, competition exists between introduced microbes and indigenous microbial communities, and PGPR can only function effectively if they adapt to local soil environments (Al-Turki and Abdullah, 2021). Thus, many researchers have begun to isolate and screen new PGPR from special environments such as saline-alkali lands and arid deserts. Halotolerant PGPR strains isolated from salt mine soils induce salinity tolerance in wheat by enhancing the expression of SOS genes (Haroon et al., 2022). Similarly, halotolerant PGPR strains isolated from coastal saline soil improve nitrogen fixation and alleviate salt stress in rice plants (Khumairah et al., 2022). The *Enterobacter cancerogenus* JY65 isolated from extremely desert saline-lkali soil promotes the growth of rice under salt stress by producing IAA (Peng et al., 2023). Synthetic bacterial community derived from the root of the desert plant *Indigofera argenteaa* confer salt stress resilience to tomato (Schmitz et al., 2022). It is evident that PGPRs play a crucial role in the growth and stress resistance of crops, but research is primarily focused on crops, with few developments and research of PGPR for plants native to the northwest deserts. Through long-term monitoring, it has been found that *Reaumuria soongorica*, a small shrub of the *Tamaricaceae* family and a halophyte widely distributed in desert areas, is one of the typical dominant shrub species in the arid and semi-arid deserts of Northwest China (Ma et al., 2005; Bai et al., 2009). Therefore, this study isolated and screened PGPR strains with growth-promoting traits from the rhizosphere of the desert plant *Reaumuria soongorica,* and evaluated their growth-promoting effects and stress resistance on the host through pot experiments from physiological and metabolic perspectives. Elucidation of the mechanisms through which PGPRs promote plant growth and enhance salt tolerance holds immense importance for desert plant growth, as well as for bioremediation, advancement, and utilization of saline-alkali soil.

2 Materials and methods

2.1 Isolation and screening of PGPR strains

The rhizosphere soil of *Reaumuria soongorica* used in this experiment was collected in April 2023 from the Liangucheng National Nature Reserve in Minqin, Gansu. High-throughput cultivation and identification methods were employed to isolate and screen IAA-producing PGPR (Zhang et al., 2021). A sample of 10 g of soil was dissolved in 90 mL of sterile physiological saline and incubated on a shaker at 30°C, 180 r/min for 30 min. Gradient dilutions were prepared sequentially to produce 10^{-3}, 10^{-4}, and 10^{-5} dilutions. Various dilutions were inoculated into 96-well Lauria Bertani (LB) liquid culture plates, and after incubation, 30–40% of the wells exhibited visible bacterial growth, which indicated that each bacterial culture originated from a single cell, thus ensuring a high proportion of pure cultures. The pure cultures were then transferred to two 96-well LB liquid culture plates containing 0.1% L-tryptophan and incubated at 30°Cfor 2 days. Subsequently, an equal volume of Salkowski reagent (prepared from 50 mL of 35% perchloric acid and 1 mL of 0.5 M $FeCl_3$ solution) was added to one of the plates, and after 30 min of color development in the dark, the appearance of a pink coloration indicated the ability to produce IAA. Cultures from corresponding wells with deeper coloration on the other plate were selected for streak purification and then incubated at 30°C for 3 days.

Single colonies were picked and isolated by streaking, and stored at −80°C for preservation.

2.2 Salt tolerance and plant growth-promoting function test of primary screened strains

Primary Screened strains were inoculated on LB solid medium containing 4, 6, 8, 10, and 12% NaCl to test the NaCl tolerance of strains. The ability of the strains to produce IAA was evaluated using a colorimetric assay (Kumar and Audipudi, 2015). Briefly, the strains were inoculated into LB liquid mediums containing 0.1% L-tryptophan and then incubated at 30°C for 2 days. After centrifugation at 6000 rpm for 10 min, 2 mL of the supernatant was mixed with 2 mL of Salkowski reagent, and color development was observed for 30 min. Absorbance was measured at 530 nm and IAA content was determined based on a standard curve. The ability of the bacterial isolates to solubilize phosphate was tested using the plate assay method (Nautiyal, 1999; Amri et al., 2023). After inoculating fresh bacterial suspension on PVK and NBRIP agar media and incubating at 30°C for 3 days, the appearance of a solubilization halo around the colonies indicated phosphate solubilization capability; the diameters of the strains and solubilization halos were recorded. Isolates were inoculated onto Ashby medium and considered to have nitrogen-fixing ability if they could still grow on Ashby medium after three successive transfers. All the above tests were repeated three times.

2.3 Morphological observation and molecular identification of dominant strains

The dominant bacterial strains isolated above were activated on LB solid mediums and incubated at 30°C for 48 h, with continuous observations and recordings of colony color, shape, margin, elevation, and surface characteristics. Gram staining was performed according to the instructions of the Biosharp Gram Staining Kit. Bacterial DNA was extracted using a bacterial DNA extraction kit. The 16S rDNA sequence fragments of the strains were amplified using the universal primers 27F (5'-AGAGTTTGATCMTGGCTCAG-3′) and 1492R (5'-TACGGYTACCTTGTTACGACTT-3′). The total PCR reaction system was 50 μL, including 2× PCR Taq Mix 25 μL, template DNA 1.0 μL, primer 27F (10μmmol/L) 1 μL, primer 1492R (10 μmmol/L) 1 μL, BSA 1 μL, and ddH_2O 21 μL. The PCR thermal cycling conditions were 95°C for 2 min for initial denaturation, followed by 31 cycles of 95°C for 15 s (denaturation), 53°C for 15 s (annealing), 72°C for 15 s (extension), and a final extension at 72°C for 5 min. Products were checked by 1.5% agarose electrophoresis. Samples were then sent to Guangdong Meige Gene Technology Co., Ltd. for Sanger sequencing. The obtained 16S rRNA gene sequences were analyzed using the EzTaxon[1] online database. A phylogenetic tree was constructed using the Maximum Likelihood Estimate method in MEGA 11.0 software, calculating evolutionary distances with the General Time Reversible (GTR) model, with bootstrap testing repeated 500 times to determine the taxonomic status of the isolated strains.

2.4 Preparation of the bacterial inoculum

According to the growth-promoting function and identification results, 3 strains of *Bacillaceae* were selected for the pot experiment, which was P2, S37, and S40, respectively. After the above spare strains were prepared by growing every strain in LB at 28°C for 48 h, the cultures were harvested and diluted with sterile normal saline (0.9% NaCl) to a final OD of 1.0 at 600 nm (~ 10^9 CFU mL^{-1}), and bacterial inoculums were prepared.

2.5 Design and treatments of experiment, and plant growth conditions

Uniformly sized *Reaumuria soongorica* seeds, harvested in 2021 from Qingtuhu in Minqin County, were selected and disinfected with a 1% sodium hypochlorite solution for 30 min, then rinsed five times with sterile water. In April 2023, the seeds were sown in trays. The seedlings were transplanted into plastic flower pots with a diameter of 24.8 cm and a height of 28 cm, with one plant per pot, when they reached a height of 5 cm. The plastic flower pots contained 5 kg of a substrate mixture of soil, sandy soil, and humus (1,2,1), totaling 100 pots. After acclimatization of the seedlings, those with uniform growth were selected for treatment. The experiment included a control (CK, no NaCl or growth-promoting bacteria added), NaCl treatments (S, only 400 mM NaCl added), and treatments with the three strains P2, S37, and S40 alone, as well as combined treatments of NaCl and strains (P2 + S, S37 + S, S40 + S). Each treatment had six replicates; three replicates were used for biomass measurement, and three for physiological and metabolite measurements. Previous research by our team indicated that *Reaumuria soongorica* seedlings could survive under 400 and 500 mM NaCl stress, but growth was severely inhibited (Yan et al., 2022). NaCl is one of the main salts in saline-alkali soils (Chen et al., 2021). Therefore, this study selected 400 mM NaCl for salt stress treatment. To avoid osmotic shock, each pot was watered with 500 mL of NaCl solution per day for 3 consecutive days, reaching a total volume of 1,500 mL; controls and single-strain treatments were watered with an equal volume of water. Two days after the NaCl stress treatment, 100 mL of the bacterial inoculum was applied to the root area of the plants, while controls were inoculated with an equal volume of sterile physiological saline. Inoculation was repeated every 15 days using the same methodology for a total of three times. *Reaumuria soongorica* seedlings grew under natural conditions at the experimental site of Gansu Agricultural University, located in Anning District, Lanzhou City, Gansu Province (36°5′N, 103°42′E), which is in a mid-temperate climate zone with distinct inland climate characteristics, clear seasonal changes, ample sunlight, and dry weather.

2.6 Growth index measurement of *Reaumuria soongorica* seedlings

Sampling was conducted 56 days after treatment of the *Reaumuria soongorica* seedlings. Photographs were taken with a digital camera

1 https://www.ezbiocloud.net/apps

before sampling, and a ruler was used to measure the height of the seedlings; then, destructive sampling was carried out, collecting the aboveground and underground parts of the plants and bringing them back to the laboratory in a low-temperature sampling box, washed with pure water, and surface moisture was blotted with filter paper before weighing the fresh weight. The total root length was determined using the LA-S root analysis system (WSEEN, China).

2.7 Physiological index measurement of *Reaumuria soongorica* seedlings

A sample of 0.3 g fresh leaf tissue was placed in a 2 mL centrifuge tube, along with a small amount of quartz sand, and 600 mL of pre-cooled extract solution was added along with 20 zirconium oxide beads. The sample was ground for 5 min at 30 Hz using a Tissue Grinde (DROIDE, China), the homogenate was then transferred to a 10 mL centrifuge tube, and the 2 mL centrifuge tube was rinsed three times with 4 mL of extract solution to 10 mL centrifuge tube. The content of chlorophyll a, chlorophyll b, total chlorophyll, and carotenoids were measured using spectrophotometry (Li, 2000). Malondialdehyde (MDA) content was determined using the thiobarbituric acid colorimetric method (Li, 2000); proline content was measured using the acid ninhydrin method; soluble sugar content was assessed using the anthrone colorimetric method (Li, 2000); and soluble protein content was determined using the Coomassie Brilliant Blue G-250 method (Li, 2000). Na^+ and K^+ content was measured using the flame photometric method (Fang et al., 2018).

2.8 Widely targeted metabolome analysis using LC–MS/MS

The leaves of *Reaumuria soongorica*, treated for a duration of 56 days, were collected as samples for widely targeted metabolomics analysis. Three biological replicates were taken, and all samples were immediately frozen in liquid nitrogen and stored at −80°C. The S40 strain with the most effective growth promotion was chosen for metabonomics analysis. The freeze-dried samples were crushed and extracted using the procedure reported by Meng et al. (2022). The quality control (QC) sample was prepared by mixing an equal aliquot of the supernatants from all of the samples to evaluate the reproducibility and stability of the whole LC–MS/MS analysis. The sample analysis was performed using a UHPLC system (Sciex, United States) with an ACQUITY UPLC HSS T3 column (1.8 μm 2.1 × 100 mm, Waters, United States), coupled to a QTrap 6,500+ Mass Spectrometer (Sciex, United States). Metabolome raw data collected by LC–MS/MS were processed using SIMCA software (Version 16.0.2), including peak extraction, retention time, peak area, logarithmic transform, etc. Differential metabolites (DEMs) were screened based on p-value <0.05 among the metabolites with variable importance in projection (VIP) >1.0. In addition, the metabolic pathway enrichment of differential metabolites was analyzed by using KEGG[2] databases. Metabolome analysis was conducted by Shanghai Biotree Biomedical Technology Company (Shanghai, China).

2 http://www.genome.jp/kegg/

2.9 Statistical analysis

All experiments were designed with three replicates and analyzed using SPSS 26.0 software for one-way analysis of variance (ANOVA). Duncan's multiple range test was used for significant difference comparisons between groups ($\alpha = 0.05$), and graphs were created using Origin 2021 and Adobe Illustrator 2022 software.

3 Results

3.1 Screening and identification results of PGPR strains

3.1.1 Tolerance to NaCl stress and growth-promoting activity of dominant strains

A total of 142 bacterial strains were isolated from the rhizosphere of *Reaumuria soongorica* in the desert regions of the Northwest. These strains exhibited various growth-promoting functions, including the capability of producing IAA, fixing nitrogen, and solubilizing organic and inorganic phosphorus. For further study, this research selected strains P2, S37, and S40, which not only have multiple growth-promoting functions but also can tolerate high levels of NaCl stress, up to 8%. Specific NaCl tolerance concentrations and growth-promoting functions are shown in Table 1.

3.1.2 Morphological observation and gram staining results of dominant strains

Gram staining of strains P2, S37, and S40 showed positive results, with short rod-shaped cells with blunt ends, occurring in pairs or chains. On LB agar plates, the colonies were yellow, with smooth, moist surfaces and irregular edges. The colonies were opaque with uneven margins (see Figure 1), pre and preliminarily identified as *Bacillus*.

3.1.3 Molecular identification results of dominant strains

The 16S rDNA sequencing results of strains P2, S37, and S40 were compared and analyzed. The phylogenetic tree based on the 16S rRNA gene sequences, as shown in Figure 2, indicated that the dominant strains P2 and S40 belong to the *Bacillus*, and S37 belongs to the *Peribacillus*. which was consistent with morphological identification results. In addition, the gene fragment of strain P2 was 1,385 bp in length, which was the same branch as *Bacillus pumilus* KCTC 13622^T and had a similarity of 99.93%. The gene sequence length of strain S37 was 1,388 bp, belonging to the same branch as *Peribacillus frigoritolerans* DSM 8801^T, with a similarity of 100%. The gene fragment of strain S40 was 1,384 bp, belonging to the same branch as *Bacillus tequilensis* KCTC 13622^T, with a similarity of 100%. So, combining morphological and molecular biological characteristics, P2, S37, and S40 could be preliminarily determined as *Bacillus pumilus, Peribacillus frigoritolerans, Bacillus tequilensis*, respectively. The 16S rDNA sequences of P2, S40, and S37 strains have been deposited in the NCBI database with GenBank accession numbers PP515614, PP515615, and PP515616, respectively.

10.3389/fmicb.2024.1408622

TABLE 1 NaCl tolerance concentrations and the growth promoting function of the dominant strains.

Name	E.coli	P2	S37	S40
Maximal tolerable dose of NaCl (%)	8%	12%	8%	12%
IAA (μg mL-1)	20.66 ± 0.88^{d}	50.91 ± 1.36^{c}	80.39 ± 1.54^{a}	61.99 ± 1.19^{b}
Nitrogen fixation	–	***	***	***
Inorganic phosphorus solubilization (D/d)	–	1.35 ± 0.07^{a}	1.30 ± 0.04^{a}	1.39 ± 0.13^{a}
Organic phosphorus solubilization (D/d)	–	2.72 ± 0.10^{a}	1.78 ± 0.08^{b}	1.63 ± 0.15^{b}

D/d, diameter halo/diameter colony; IAA, indole acetic acid; +, presence of activity; −, absence of activity; Mean values labeled with the same superscript letter within the same line were not significantly different at $p < 0.05$ following Duncan's test; *E.coli*, Control strain *Escherichia coli*.

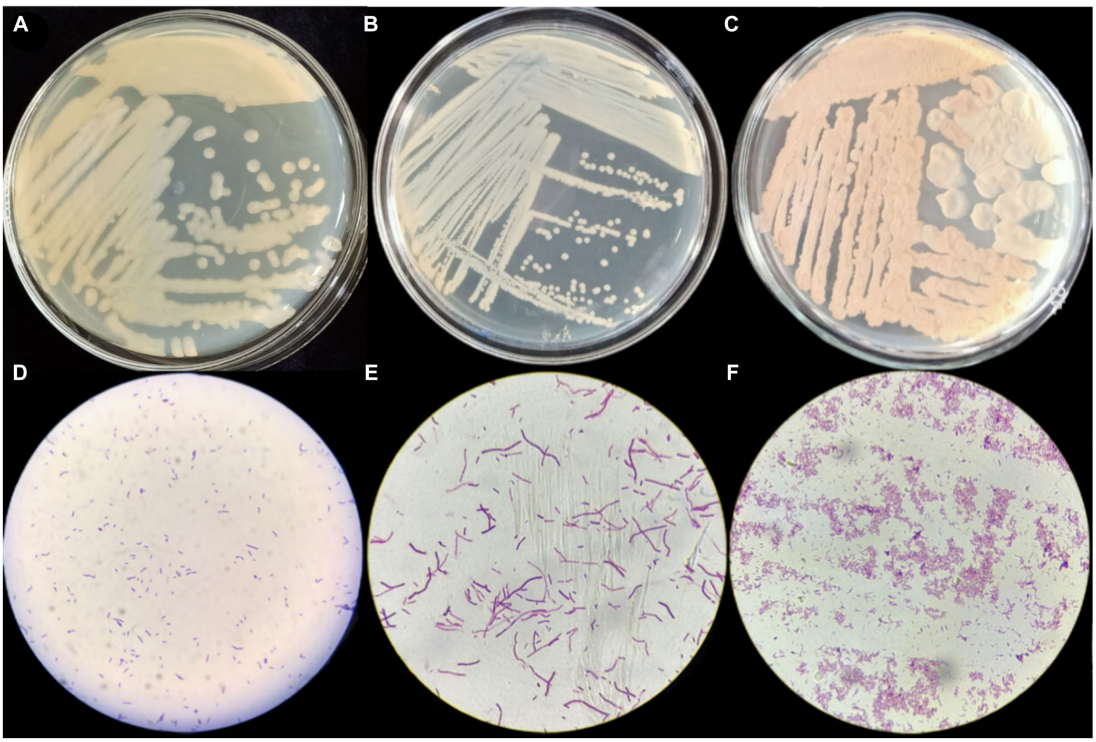

FIGURE 1
Morphological characteristics and Gram staining results of strains P2, S37, and S40. **(A–C)** The morphological structure diagrams of strains P2, S37, and S40; **(D–F)** the 100x microscope images of Gram's stain of strains P2, S37, and S40.

3.2 *Bacillaceae* improved growth and enhanced salt tolerance of *Reaumuria soongorica* seedlings under NaCl stress

3.2.1 *Bacillaceae* promoted the growth of *Reaumuria soongorica* seedlings

Inoculation with the three *Bacillaceae* strains had a significant impact on the growth and salt tolerance of *Reaumuria soongorica* seedlings (Figures 3, 4). Inoculation with strains P2, S37, and S40 showed no significant difference in seedling height compared to the control, but the aboveground fresh weight increased significantly by 83.17, 72.54, and 94.54% ($p < 0.05$), respectively. Inoculation also increased the total root length and fresh weight of *Reaumuria soongorica* seedlings, with P2 and S40 single-strain treatment groups showing a significant increase in total root length by 48.00 and 29.62% over the control, respectively; and P2, S37, and S40 single-strain treatment groups showing a significant increase in root fresh weight by 94.75, 68.86, and 94.98% ($p < 0.05$) over the control, respectively. NaCl stress significantly reduced the height, aboveground, and root fresh weight, and of *Reaumuria soongorica* seedlings, but inoculation with P2, S37, and S40 strains resulted in a significant increase in seedling height by 26.87, 17.59, and 13.36% ($p < 0.05$) compared to NaCl treatment, and more than doubled the aboveground and root fresh weight. Thus, inoculation with strains P2, S37, and S40 had positive effects on *Reaumuria soongorica* growth and Salt tolerance.

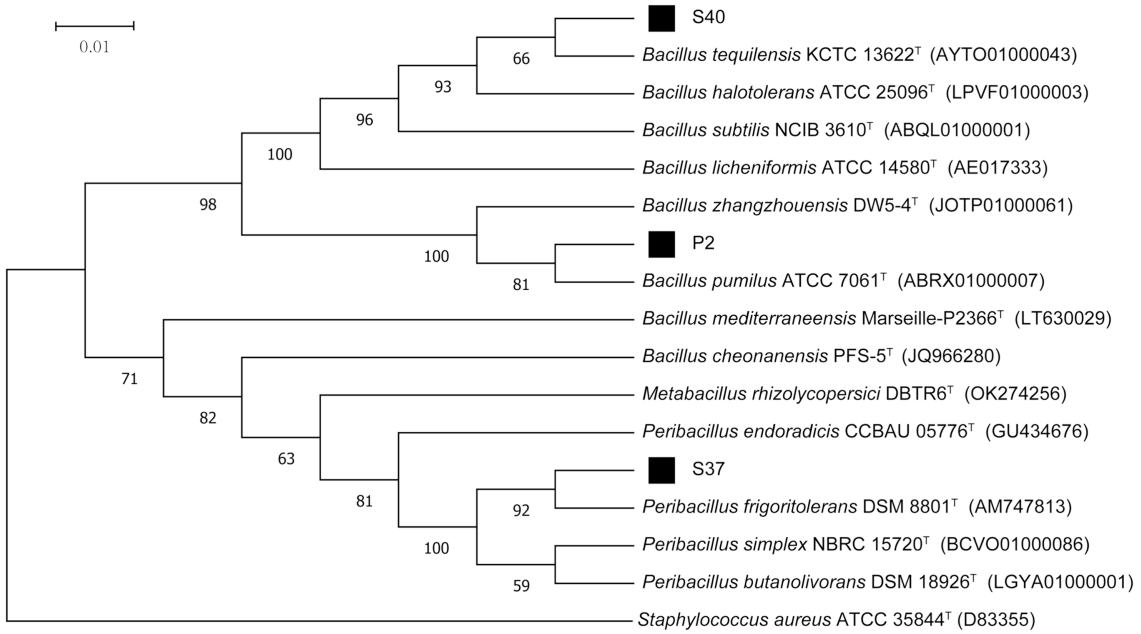

FIGURE 2
The phylogenetic tree of strains P2, S37, and S40 based on 16S rDNA sequencing results. *Staphylococcus aureus* ATCC 35844^T is an outgroup; Superscript T are type strains; the scale length is 1% base difference.

3.2.2 Effect of *Bacillaceae* on photosynthetic pigment content in *Reaumuria soongorica* seedling leaves

Shown in Table 2, inoculation with P2, S37, and S40 strains upregulated the photosynthetic pigment content in the leaves of *Reaumuria soongorica* seedlings. Specifically, inoculation with strain S40 resulted in a significant increase in the content of chlorophyll a, b, and carotenoids by 22.95, 20.14, and 24.33% ($p < 0.05$) over the control. Under NaCl stress, the contents of chlorophyll a, b, and total chlorophyll in the leaves of *Reaumuria soongorica* seedlings were significantly reduced by 23.08, 21.48, and 22.81% compared to the control. However, after inoculation with P2, S37, and S40 strains, the four photosynthetic pigments in the leaves of *Reaumuria soongorica* seedlings were significantly higher than those in the NaCl treatment and significantly exceeded control levels. Compared to the NaCl treatment, inoculation with strain S40 significantly increased the content of chlorophyll a, b, total chlorophyll, and carotenoids in *Reaumuria soongorica* seedling leaves by 87.00, 85.47, 86.74, and 20.81%, respectively ($p < 0.05$). Thus, inoculation with strains P2, S37, and S40 increased the content of photosynthetic pigments in leaves of *Reaumuria soongorica* seedlings, and the effect was more obvious under NaCl stress.

3.2.3 Effect of *Bacillaceae* on osmotic adjustment substances content in *Reaumuria soongorica* seedling leaves

Inoculation with P2, S37, and S40 strains significantly affected the contents of osmotic substances in *Reaumuria soongorica* seedlings (Table 3). The proline and soluble protein content in the leaves of *Reaumuria soongorica* seedlings inoculated with strains P2, S37, and S40 were significantly higher than the control, with strain S40 showing a significant increase of 38.60 and 26.12%, respectively; but, soluble sugar content in the leaves of *Reaumuria soongorica* seedlings significantly decreased after inoculated with P2, S37, and S40 strains, by 13.66, 13.77, and 13.83%, respectively ($p < 0.05$). Under NaCl stress, the proline content in the leaves of *Reaumuria soongorica* seedlings inoculated with P2, S37, and S40 strains showed no significant change, while the soluble protein content was significantly increased by 19.98, 23.57, and 24.25% ($p < 0.05$) compared to the NaCl treatment. However, compared to the NaCl treatment, the soluble sugar content in the leaves of *Reaumuria soongorica* seedlings stress significantly decreased by 10.44, 10.51, and 10.48%, respectively ($p < 0.05$). Overall, inoculation with strains P2, S37, and S40 regulated the contents of osmoprotectants in leaves of *Reaumuria soongorica* seedlings, maintaining ion homeostasis, and preventing oxidative damage.

3.2.4 Effect of *Bacillaceae* on malondialdehyde content in *Reaumuria soongorica* seedling

Malondialdehyde (MDA) is one of the most common indicators used to detect lipid peroxidation in cells and tissues. Inoculation with P2, S37, and S40 strains, the MDA content in the leaves of *Reaumuria soongorica* seedlings were significantly reduced by 28.54, 15.14, and 24.31% ($p < 0.05$) compared to the control; and under NaCl stress, the MDA contents were significantly reduced by 25.41, 30.62, and 34.85% ($p < 0.05$) compared to the NaCl treatment (Table 3). Thus, inoculation with strains P2, S37, and S40 had positive effects on preventing oxidative damage of *Reaumuria soongorica* seedlings and preserving the cell membrane structure.

3.2.5 Effect of *Bacillaceae* on Na^+, K^+ content in *Reaumuria soongorica* seedling

Under NaCl stress, inoculation with P2, S37, and S40 strains, Na^+, K^+ contents, and the Na^+- K^+ ratio were significantly downregulated (Table 4). Inoculation with strains P2, S37, and S40 showed no significant difference in Na^+, K^+ contents, and the Na^+- K^+ ratio compared to the control. Under NaCl stress, Na^+, K^+ contents, and the

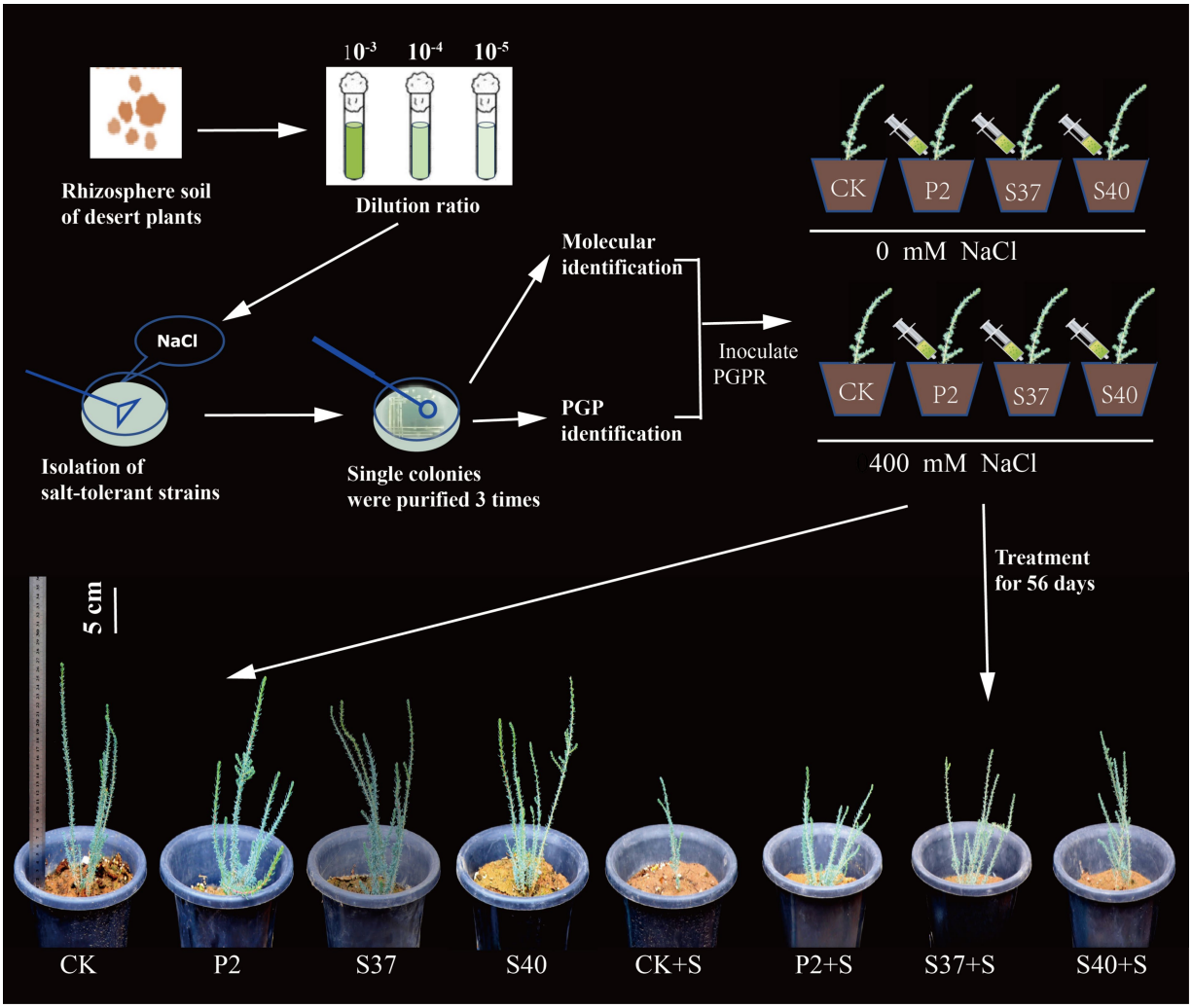

FIGURE 3
Experimental processing flowchart and the growth states of *Reaumuria soongorica* seedlings after inoculation with strains P2, S37, and S40.

Na^+- K^+ ratio in the leaves of *Reaumuria soongorica* seedlings were significantly increased by 173.90, 23.45, and 121.81%, respectively ($p < 0.05$) compared to the control. However, after inoculation with P2, S37, and S40 strains, Na^+ contents in the leaves of *Reaumuria soongorica* seedlings were significantly decreased by 35.80, 30.59, and 35.92%, respectively ($p < 0.05$) compared to the NaCl treatment; K^+ contents were significantly decreased by 21.13, 17.07, and 25.57%, respectively ($p < 0.05$); the Na^+- K^+ ratio was significantly decreased by 18.47, 16.13, and 13.91%, respectively ($p < 0.05$). The results showed that inoculation with strains P2, S37, and S40 decreased Na^+ content and Na^+- K^+ ratio in leaves of *Reaumuria soongorica* seedlings under NaCl stress to re-establish ion balance, and alleviated the toxicity of salt stress.

3.3 Effect of *Bacillus* S40 on metabolites in *Reaumuria soongorica* seedling leaves under NaCl stress

3.3.1 Classification of metabolites

Based on the above results, inoculated with P2 and S37 strains, the growth indexes such as plant height, total root length, biomass, and physiological indexes such as photosynthetic pigment and osmotic adjustment substance MDA of Reaumuria soongorica seedlings under salt stress showed the same trend as the S40 strain. S40 strain had the best effect of promoting growth. Therefore, only the S40 strain was selected for metabolism analysis in this study. After filtering and normalizing the raw data of the targeted metabolome, a total of 400 metabolites were obtained, including 59 flavonoids, 54 alkaloids, 49 phenolic compounds, 46 terpenoids, 26 lipids, 24 lignans and coumarins, 23 organic acids and derivatives, 22 amino acids and derivatives, 19 phenylpropanoids, 16 carbohydrates and alcohols, 14 plant hormones, 10 nucleosides and derivatives, 8 quinones, 7 aromatic compounds, 4 organic acids and derivatives, 2 vitamins, and 26 other metabolites (Supplementary Table S1).

3.3.2 Differential analysis of metabolites

Based on the *p*-value <0.05 among the metabolites with variable importance in projection (VIP) >1.0, 37 differential metabolites (DEMs) were screened (Supplementary Table S2). In the 3D PCA plot, biological replicates for each of the four different treatments clustered together in different areas, suggesting that there were significant differences in metabolites (Figure 5A). Volcano plots (Figures 5B–D)

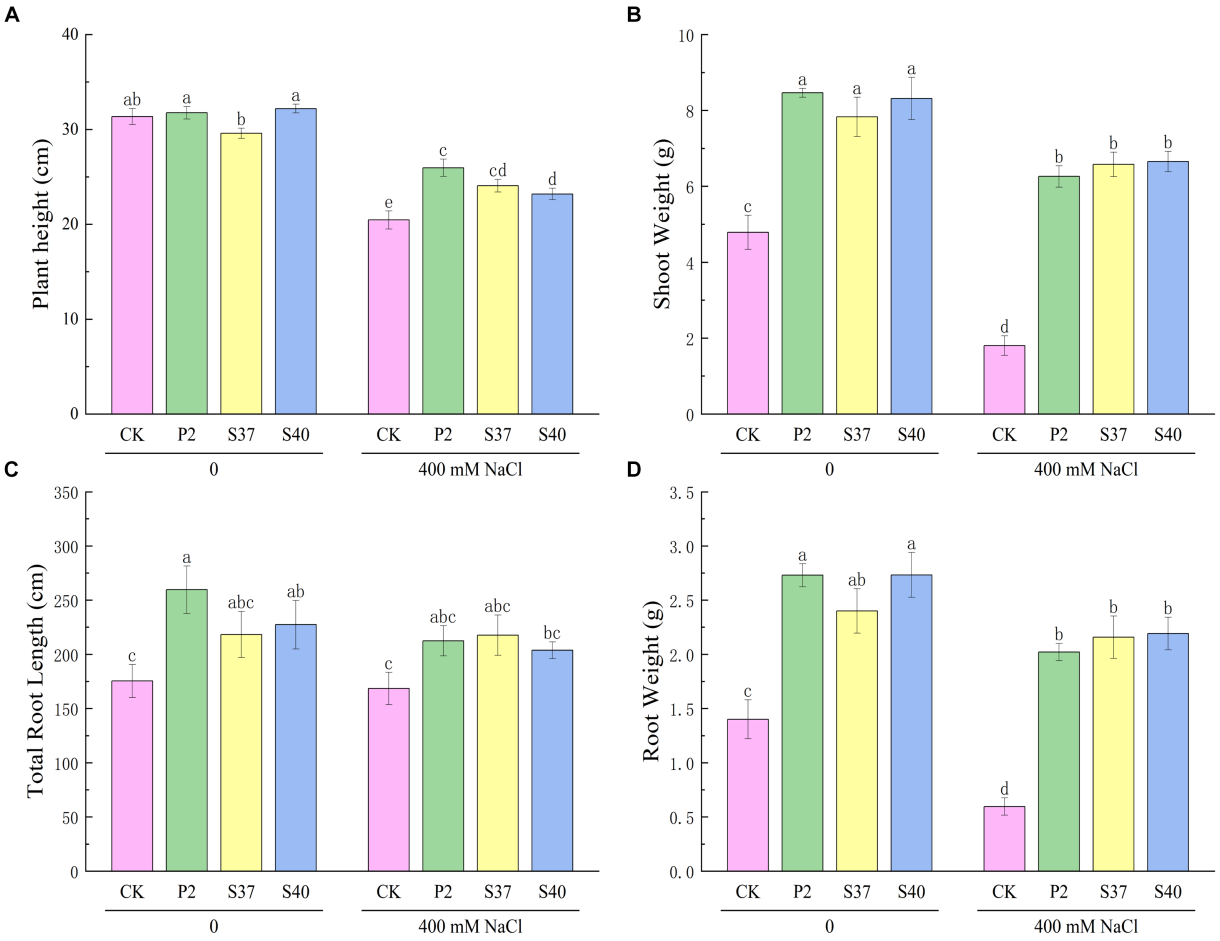

FIGURE 4
The effect of strains P2, S37, and S40 on the growth of *Reaumuria soongorica* seedlings under NaCl stress. **(A)** Plant height, **(B)** Shoot Weight, **(C)** Total Root Length, and **(D)** Root Weight. Mean values labeled with the same superscript letter within the same line were not significantly different at $p < 0.05$ following Duncan's test.

TABLE 2 The content of photosynthetic pigments in the leaves of *Reaumuria soongorica* seedlings after inoculation with strains P2, S37, and S40.

NaCl level	Strain NO.	Chlorophyll a (mg L^{-1} FW)	Chlorophyll b (mg L^{-1} FW)	Total Chlorophyll (mg L^{-1} FW)	Carotenoids (mg·g^{-1}FW)
0 mM NaCl	CK	0.52 ± 0.02^{d}	0.10 ± 0.01^{cd}	0.63 ± 0.04^{d}	0.13 ± 0.01^{b}
	P2	0.60 ± 0.04^{cd}	0.13 ± 0.01^{abc}	0.73 ± 0.05^{c}	0.16 ± 0.01^{a}
	S37	0.61 ± 0.03^{c}	0.12 ± 0.00^{bc}	0.73 ± 0.03^{c}	0.16 ± 0.02^{ab}
	S40	0.65 ± 0.04^{bc}	0.12 ± 0.01^{abc}	0.77 ± 0.04^{bc}	0.16 ± 0.01^{a}
400 mM NaCl	CK	0.40 ± 0.01^{e}	0.08 ± 0.01^{d}	0.49 ± 0.01^{e}	0.15 ± 0.01^{ab}
	P2	0.69 ± 0.02^{ab}	0.14 ± 0.01^{ab}	0.83 ± 0.02^{ab}	0.18 ± 0.01^{a}
	S37	0.72 ± 0.03^{ab}	0.13 ± 0.01^{ab}	0.85 ± 0.03^{ab}	0.16 ± 0.01^{a}
	S40	0.75 ± 0.01^{a}	0.15 ± 0.01^{a}	0.89 ± 0.02^{a}	0.18 ± 0.00^{a}

Mean values labeled with the same superscript letter within the same line were not significantly different at $p < 0.05$ following Duncan's test.

exhibited trends in differential metabolite changes between different treatment groups ($p < 0.05$). There were 19 differential metabolites (12 upregulated, 7 downregulated) between the control (CK) and S treatment, with significant upregulation of 5'-S-Methyl-5′-thioadenosine, N-((−)-jasmonoyl)-S-isoleucine, L-Ornithine, eriodictyol, and 2′-hydroxygenistein ($\log_2$(Fold Change) > 1), and significant downregulation of amygdalin, and physcion ($\log_2$(Fold Change) < 0.5); 16 differential metabolites (10 upregulated, 6 downregulated) between the control (CK) and S40 treatment, with significant upregulation of 5'-S-Methyl-5′-thioadenosine, pyrrolidone carboxylic acid, and p-hydroxyphenylacetylglycine ($\log_2$(Fold Change) > 1), and significant downregulation of chrysin, cauloside A,

TABLE 3 The content of osmotic adjustment substances and MDA contents in the leaves of *Reaumuria soongorica* seedlings after inoculation with strains P2, S37, and S40.

NaCl level	Strain NO.	Proline content (μg·g^{-1}FW)	Soluble protein content (μg·g^{-1}FW)	Soluble sugar content (mg·g^{-1}FW)	MDA content (μmol·g-1FW)
0 mM NaCl	CK	100.35 ± 5.83^{b}	6.20 ± 0.34^{c}	14.35 ± 0.32^{a}	3.65 ± 0.27^{d}
	P2	153.07 ± 10.57^{a}	7.98 ± 0.44^{b}	9.96 ± 0.26^{b}	2.61 ± 0.19^{e}
	S37	136.11 ± 7.04^{a}	7.68 ± 0.09^{b}	8.22 ± 0.59^{c}	3.10 ± 0.16^{e}
	S40	139.08 ± 8.53^{a}	7.81 ± 0.49^{b}	7.42 ± 0.11^{c}	2.76 ± 0.16^{e}
400 mM NaCl	CK	150.49 ± 6.72^{a}	7.68 ± 0.33^{b}	11.16 ± 0.20^{b}	6.44 ± 0.08^{a}
	P2	140.55 ± 11.05^{a}	9.21 ± 0.18^{a}	8.03 ± 0.73^{c}	4.80 ± 0.24^{b}
	S37	132.90 ± 4.22^{a}	9.49 ± 0.16^{a}	7.26 ± 0.47^{c}	4.47 ± 0.13^{bc}
	S40	135.44 ± 6.84^{a}	9.54 ± 0.20^{a}	7.54 ± 0.39^{c}	4.19 ± 0.14^{c}

Mean values labeled with the same superscript letter within the same line were not significantly different at $p < 0.05$ following Duncan's test.

TABLE 4 The content of Na^+, K^+ contents, and the Na^+- K^+ ratio in the leaves of *Reaumuria soongorica* seedlings after inoculation with strains P2, S37, and S40.

NaCl level	Strain NO.	Na^+ content (mg·g^{-1} DW)	K^+ content (mg·g^{-1} DW)	Na^+/K^+ ratio
0 mM NaCl	CK	32.91 ± 1.04^{c}	15.03 ± 0.21^{bc}	2.19 ± 0.07^{c}
	P2	39.33 ± 0.84^{c}	16.47 ± 0.62^{b}	2.39 ± 0.14^{c}
	S37	37.61 ± 1.18^{c}	15.37 ± 0.57^{bc}	2.45 ± 0.01^{c}
	S40	34.53 ± 0.90^{c}	15.1 ± 0.52^{bc}	2.29 ± 0.14^{c}
400 mM NaCl	CK	90.14 ± 3.47^{a}	18.56 ± 0.26^{a}	4.86 ± 0.12^{a}
	P2	57.87 ± 2.78^{b}	14.64 ± 0.87^{c}	3.96 ± 0.21^{b}
	S37	62.56 ± 2.18^{b}	15.39 ± 0.82^{bc}	4.07 ± 0.26^{b}
	S40	57.76 ± 4.58^{b}	13.81 ± 0.58^{c}	4.18 ± 0.25^{b}

Mean values labeled with the same superscript letter within the same line were not significantly different at $p < 0.05$ following Duncan's test.

and N-D-Glucosylarylamine (log_2(Fold Change) < 0.5); 32 differential metabolites (20 upregulated, 12 downregulated) between S40 + S and S treatment, with significant upregulation of eicosenoic acid, talatisamine, 7-ethoxycoumarin, dihydrokavain, epicatechin, quillaic acid, 3-hydroxy-4-methoxycinnamic acid, and epicatechin gallate (log_2(Fold Change) > 1), and significant downregulation of 4-hydroxycoumarin, sclareol, and alpha-hexylcinnamaldehyde (log_2(Fold Change) < 0.5). The heatmap of 37 differential metabolites analysis for different treatment samples was shown in Figure 5E, and hierarchical clustering analysis was performed on the differential metabolites. There was an obvious separation in metabolites between the control (CK) and the NaCl treatments (S), the control (CK) and S40, and S40 and S40 + S treatments. Overall, there were significant differences in metabolites of leaves *Reaumuria soongorica* seedlings in different treatments.

3.3.3 KEGG enrichment analysis of differential metabolites

Using Arabidopsis as a model organism, differential metabolites were mapped to KEGG metabolic pathways for pathway and enrichment analyses. KEGG heatmap based on the relative abundance of differential metabolites and the classification of pathways was shown in Figure 6A, which displays the total amount of annotated differential metabolites in a certain KEGG metabolic pathway in different samples. Under NaCl stress, the total amount of N-((−)-jasmonoyl)-S-isoleucine, (J)-Jasmonic acid, and 5'-S-Methyl-5′-thioadenosine were significantly up-regulated compared with the control (CK) ($p < 0.05$), and they were annotated to plant hormone signal transduction and zeatin biosynthesis pathway, while the amount of D-fructose 6-phosphate was significantly down-regulated compared with the control (CK) ($p < 0.05$), and it was annotated to carbon fixation in photosynthetic organisms, starch and sucrose metabolism and galactose metabolism pathway. However, inoculation with the S40 strain, the amount of D-fructose 6-phosphate was significantly up-regulated compared with the NaCl treatments (S) ($p < 0.05$), while the amount of epicatechin, chrysin, eriodictyol, and sclareol were significantly down-regulated compared with NaCl treatments (S) ($p < 0.05$), and they were annotated to flavonoid biosynthesis and diterpenoid biosynthesis pathway. The Sankey bubble diagram (Figure 6B) shows the enrichment analysis of the top fifteen KEGG metabolic pathways of differential metabolites in leaves of *Reaumuria soongorica* seedlings. Five pathways were significantly enriched, including plant hormone signal transduction, flavonoid biosynthesis, biosynthesis of various plant secondary metabolites, D-amino acid metabolism, and tropane, piperidine, and pyridine alkaloids biosynthesis ($p < 0.05$). L-phenylalanine is involved in the biosynthesis of various plant secondary metabolites, D-amino acid metabolism, tropane, piperidine, and pyridine alkaloids biosynthesis, the biosynthesis of phenylalanine, tyrosine, and tryptophan, cyanogenic amino acids, phenylalanine metabolism, and phenylpropanoid biosynthesis. These results indicate that inoculation with strain S40 induces plant metabolome reprogramming to regulate cell metabolism, including plant hormone signal transduction and phenylalanine, tyrosine, and tryptophan biosynthesis pathways.

4 Discussion

Desert plants live in environments with various abiotic stresses such as nutrient deficiency, drought, and salinization. PGPR can help plants cope with adversity in various ways; however, whether it is a single isolate or SynCum, it must be adapted to the target environment to exert its growth-promoting function (Saad et al., 2020; Schmitz et al., 2022). Therefore, this study isolated and screened PGPR with various growth-promoting functions and salt resistance from the

10.3389/fmicb.2024.1408622

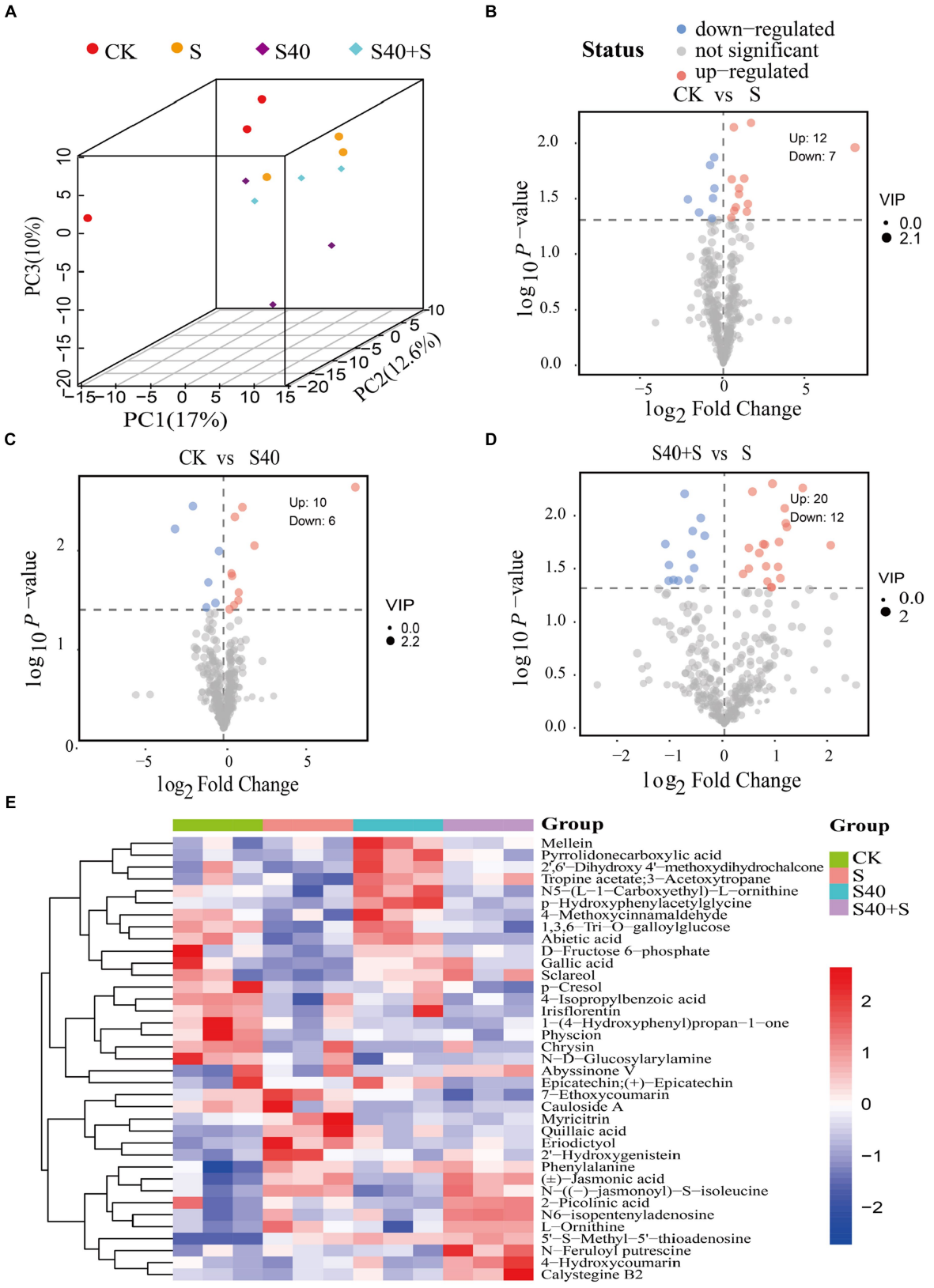

FIGURE 5
Differential metabolites in leaves of *Reaumuria soongorica* seedlings. **(A)** Score scatter plot 3D of PCA model. **(B–D)** The volcano maps between different groups, each dot represented a metabolite, the x-axis represents the fold change of the comparison of various substances (taking the logarithm of base 2), the y-axis represents the negative logarithm of *p*-value (taking the negative logarithm of base 10). **(E)** Hierarchical clustering heatmap of differential metabolites, red indicates that the substance is highly expressed in the group where it is located, and blue indicates that the substance is low in the group where it is located.

10.3389/fmicb.2024.1408622

FIGURE 6
Enrichment analysis of top fifteen KEGG metabolic pathways of differential metabolites in leaves of *Reaumuria soongorica* seedlings. **(A)** KEGG heatmap for different groups, with color blocks representing the relative content of all differential metabolites annotated in the corresponding positional pathway. **(B)** Sankey bubble combination diagram, with the horizontal axis representing the ratio of the number of differential metabolites in this pathway to the number of metabolites annotated in this pathway. The redder the bubbles, the more significant the enrichment of differential metabolites in this pathway; the larger the bubble, the more differential metabolites there are.

rhizosphere of the desert plant *Reaumuria soongorica* using high-throughput bacterial culture and identification methods. Through molecular identification, the dominant strains were identified as belonging to the *Bacillaceae*. This study found that inoculation with strains P2, S37, and S40 significantly improved growth indicators such as plant height, total root length, and biomass, and notably increased salt stress tolerance in *Reaumuria soongorica* seedlings. This increase is attributed to PGPR's ability to regulate plant photosynthetic pigment synthesis and improve photosynthesis efficiency, as well as to promote plant nutrient absorption through phosphate solubilization and nitrogen fixation. Inoculation with strain S40 can relieve salt stress in plants by regulating the synthesis of primary metabolites such as phenylalanine, tyrosine, proline, and secondary metabolites such as IAA, cytokinins, and jasmonic acid (Sunita et al., 2020; Koza et al., 2022; Liu et al., 2023). The *Bacillus* and *Peribacillus* strains screened in this study promote the growth of *Reaumuria soongorica* and enhance its salt stress tolerance by inducing systemic tolerance in the plant. A schematic diagram summarizing the mechanisms by which *Bacillaceae* promotes the growth of *Reaumuria soongorica* seedlings and enhances resistance to salt stress is presented in Figure 7.

4.1 *Bacillaceae* plays a significant role in promoting healthy plant growth

Bacillus, widely studied as a Plant Growth-Promoting Rhizobacteria (PGPR), was known for its biological control and growth promoting effects. Studies have found that *Bacillus licheniformis* and *Bacillus velezensis* promote the growth of rice (Devi et al., 2023); *Bacillus megaterium* induces systemic resistance-related metabolites to promote the growth of Arabidopsis (Liu et al., 2023); *Bacillus paralicheniformis* enhances cotton growth by significantly increasing root length and the content of brassinosteroids (Xu et al., 2023). In this study, three PGPR strains were isolated and identified as *Bacillus pumilus*, *Peribacillus frigoritolerans*, and *Bacillus tequilensis*. These PGPR strains not only produce IAA and have the ability to solubilize phosphate and fix nitrogen—characteristics of ideal PGPR—but also play a crucial role in promoting the growth of desert plants and enhancing their stress resistance, especially in barren desert environments. Pot experiments showed that under NaCl stress, the height, total root length, and fresh weight of *Reaumuria soongorica* seedlings were significantly reduced compared to the control, but inoculation with strains P2, S37, and S40 significantly increased the shoot and root fresh weight of *Reaumuria soongorica* seedlings compared to the NaCl treatment. This indicates that inoculation with *Bacillaceae* has positive effects on *Reaumuria soongorica* growth and salt tolerance.

4.2 *Bacillaceae* promotes plant growth and alleviates salt stress by regulating photosynthesis

In higher plants, chlorophyll a, chlorophyll b, and carotenoids are the most critical photosynthetic pigments and are essential for plant photosynthesis. Under salt stress, plants may experience disturbances in leaf area and stomatal conductance, leading to insufficient water and mineral nutrient absorption, resulting in malnutrition; excess salt can lead to chloroplast degradation, block the biosynthesis of chlorophyll and carotenoids, reduce photosynthetic efficiency, and affect plant growth (Kibria et al., 2017; Sunita et al., 2020; Kumar et al., 2021). However, PGPR can produce IAA, siderophores, and hydrolytic enzymes, and can solubilize phosphates, thereby improving chlorophyll content and membrane integrity (Jalmi and Sinha, 2022). Cherry tomato plants inoculated with PGPR have higher chlorophyll content in their leaves than uninoculated plants (El-Beltagi et al., 2022). In this study, chlorophyll a, b, and total chlorophyll in *Reaumuria soongorica* seedling leaves under NaCl stress were significantly reduced compared to the control, consistent with the previous research results (Yan et al., 2022). After inoculation with strains P2, S37, and S40, chlorophyll a, b, and carotenoids in *Reaumuria soongorica* seedling leaves under NaCl stress were significantly higher than those treated with NaCl and significantly higher than control levels. Metabolomic results showed that after inoculation with strain S40, the content of glutamate, which is involved in chlorophyll synthesis, was significantly increased in *Reaumuria soongorica* seedlings, providing a material basis for the increase in chlorophyll. Strains P2, S37, and S40 enhanced the synthesis of photosynthetic pigments by promoting phytohormone production, thus improving *Reaumuria soongorica* photosynthesis and leading to a significant accumulation of *Reaumuria soongorica* biomass, consistent with previous research findings (El-Beltagi et al., 2022; Slimani et al., 2023). It indicates that inoculation with *Bacillaceae* can promote photosynthesis by increasing the content of photosynthetic pigments, thereby promoting the growth of the plant and enhancing its salt tolerance.

4.3 *Bacillaceae* induces the osmoprotectants to alleviate salt ion toxicities

One of the plant's stress response mechanisms to adverse conditions is the synthesis of osmoprotectants, which increase the solute concentration inside cells, lower the water potential, and enable plants to absorb water from the environment to sustain growth. Proline is a vital substance required for plant survival under abiotic stress. As a compatible osmolyte, it can chelate salt ions to maintain internal osmotic balance and interact with proteins to increase their solubility (Selim et al., 2021). Studies have shown that *Bacillus flexus* KLBMP 4941 promotes the growth of the halophyte Suaeda salsa under salt stress by regulating the Na^+/K^+ homeostasis (Xiong et al., 2020). Salt-tolerant *Bacillus* KKD1 alleviates salt stress in wheat by regulating osmotic balance and ion homeostasis to protect plant growth (Wu et al., 2022). In this study, the inoculation of strains P2, S37, S40 increased the proline and soluble protein content in *Reaumuria soongorica* seedling leaves compared to the NaCl treatment, indicating that these strains can induce *Reaumuria soongorica* seedling to synthesize proline and soluble proteins, maintaining osmotic balance in plant cells under salt stress and preventing water loss, consistent with previous research findings (Slimani et al., 2023). However, the soluble sugar content in leaves of *Reaumuria soongorica* seedlings inoculated with strains P2, S37, and S40 was significantly reduced, a result inconsistent with previous studies (El-Beltagi et al., 2022), which may be due to the involvement of soluble sugars in plant metabolism under 400 mM NaCl stress, providing energy or being converted into secondary metabolites. MDA is the end product of lipid peroxidation and an important

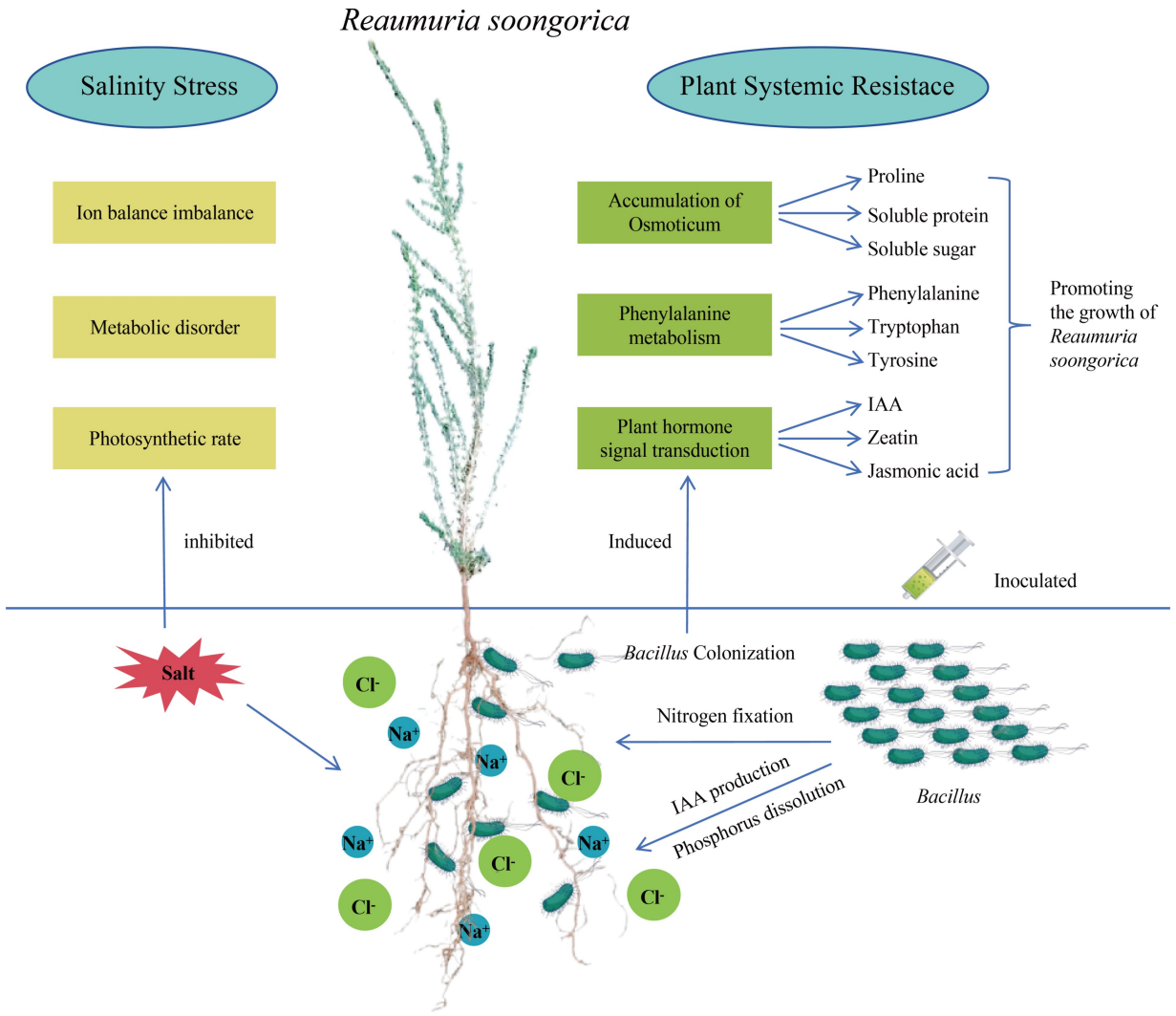

FIGURE 7
Pattern diagram of *Bacillus subtilis* promoting the growth of *Reaumuria soongorica* seedlings and enhancing salt tolerance mechanism.

indicator of lipid peroxidation and plasma membrane damage. Inoculation with strains P2, S37, and S40 significantly reduced MDA content in *Reaumuria soongorica* seedling leaves under both NaCl stress and non-stress conditions. It indicated that inoculation with *Bacillaceae* can promote the growth of the plant and enhance its salt tolerance by regulating the accumulation of osmoprotectants, preventing oxidative damage, and preserving the integrity of the cell membrane structure.

4.4 *Bacillus* S40 modulates the synthesis pathways of phenylalanine, tyrosine, and tryptophan to promote plant growth and increase salt tolerance

Phenylalanine, tyrosine, and tryptophan are precursors of natural products such as alkaloids, flavonoid compounds, plant auxins, and cell wall components. Phenylalanine is catalyzed by phenylalanine ammonia-lyase to form cinnamic acid and coumaric acid, which are further hydroxylated and methoxylated to form phenylpropanoid compounds such as caffeic acid and ferulic acid, eventually leading to the synthesis of complex secondary metabolites like coumarins, lignins, and flavonoids, which are used in plant defense against various biotic and abiotic stresses (Maeda and Dudareva, 2012; Ham et al., 2022; Liu et al., 2023). In this study, inoculation with strain S40 significantly increased the content of phenylalanine in the leaves of *Reaumuria soongorica* seedlings compared to the control ($p < 0.05$) (Supplementary Table S1). Under NaCl stress, inoculation with strain S40 significantly increased the content of metabolites such as 4-hydroxycoumarin, sclareol, and alpha-hexylcinnamaldehyde in *Reaumuria soongorica* seedling compared to the NaCl treatment (Figure 5E). L-phenylalanine is involved in D-amino acid metabolism, the biosynthesis of phenylalanine, tyrosine, and tryptophan, cyanogenic amino acids, phenylalanine metabolism, phenylpropanoid biosynthesis, and other pathway (Figure 6B). Strain S40 induced the accumulation of phenylalanine in the leaves of *Reaumuria soongorica* seedlings, which are involved in the synthesis of secondary metabolites such as coumarins, and flavonoids. Studies have shown that inoculation with *Bacillus megaterium* BT22 promotes Arabidopsis growth by accumulating flavonoids and phenylpropanoid metabolites

(Liu et al., 2023). *Paenibacillus polymyxa* YC0136 induces tobacco systemic resistance by stimulating phenylpropanoid metabolism under pathogen-free conditions (Liu et al., 2020). Our study also proved this point, inoculation with strain S40 increases the content of phenylalanine in *Reaumuria soongorica* seedlings, thereby regulating the biosynthesis of plant coumarins, and flavonoid compounds.

4.5 *Bacillus* S40 modulates plant hormones to promote plant growth and increase salt tolerance

Plant hormones are significant signaling molecules between plants and microbes, involved in the regulation of plant growth and development, and they can also be treated as an important factor in mediating plant stress response (Liu et al., 2023). Abscisic acid, indole-3-acetic acid (IAA), cytokinins, jasmonic acid, salicylic acid, and gibberellins were well-known plant growth regulators (Waadt et al., 2022). Research indicates that PGPR can promote plant growth and enhance tolerance to biotic stress by producing phytohormones; they also regulate the homeostasis and signaling of endogenous hormones to support healthy growth under various stress conditions (Ha-Tran et al., 2021). In this study, the three selected strains all produced IAA. Inoculation with strains P2, S37, and S40, the total root length and root fresh weight of *Reaumuria soongorica* seedlings significantly increased compared to the NaCl treatment. Besides, our result showned that inoculation with strain S40 significantly increased the content of metabolites such as 5'-S-Methyl-5′-thioadenosine, jasmonic acid, and jasmonoyl aicd-isoleucine in the leaves of *Reaumuria soongorica* seedlings under NaCl stress (Figure 5E). These metabolites were involved in the plant hormone signal transduction and zeatin biosynthesis pathway. IAA, the first discovered plant hormone, primarily synthesizes via the tryptophan-dependent pathway in plants. PGPRs promote the growth of lateral and adventitious roots through the production of IAA, enhancing nutrient absorption efficiency (He et al., 2023). Strain S40 promoted the growth by the production of IAA and also induced the production of endogenous IAA in *Reaumuria soongorica* seedlings by regulating the biosynthesis of tryptophan. In higher plants, zeatin is the major naturally active cytokinin component that promotes cell division, cell expansion, chloroplast development, and other processes. Inoculation with *Bacillus megaterium* BT22 has been shown to promote Arabidopsis growth by modulating plant hormone signal transduction pathways, including auxins and cytokinins related to cell enlargement and division (Liu et al., 2023). After inoculation with strain S40, the 5'-S-Methyl-5′-thioadenosine content increased in the leaves of *Reaumuria soongorica* seedling compared to the control. This compound was known as one of the main metabolites in zeatin biosynthesis. The findings suggested that strain S40 could protect cells from salt stress damage by modulating cytokinins. Furthermore, Jasmonic acid, ubiquitous in higher plants, is synthesized from the unsaturated fatty acid α-linolenic acid through an enzymatic reaction pathway (Papadopoulou et al., 2023). *Pseudomonas* induced the expression of genes related to jasmonic acid synthesis and α-linolenic acid metabolism in tomato, providing resistance to abiotic stress (Papadopoulou et al., 2023). After inoculation with strain S40, the jasmonic acid and jasmonic acid-isoleucine content increased in the leaves of *Reaumuria soongorica* seedlings. It indicated that Jasmonic acid was an important regulator for the plant's response to abiotic stress. The results indicate that auxins, zeatin, and jasmonic acid are involved in the stress response of *Reaumuria soongorica* seedlings to stressors, and inoculation with *Bacillus* can alleviate salt stress in plants by modulating plant hormone signal transduction (Lephatsi et al., 2021; Liu et al., 2023).

5 Conclusion

The current study identified three strains of PGPR, isolated from the rhizosphere of the desert plant *Reaumuria soongorica*, as salt-tolerant *Bacillaceae* species, which are part of a crucial beneficial microbial population that can be utilized for the reclamation and improvement of saline soils and also for enhancing crop yields in desert regions. Pot experiments demonstrated that under NaCl stress, inoculation with strains P2, S37, and S40 increased the height, total root length, and biomass of *Reaumuria soongorica* seedlings. Strains P2, S37, and S40 promoted the healthy growth of *Reaumuria soongorica* seedlings under salt stress by modulating photosynthetic efficiency and the content of osmoregulatory substances. Comprehensive targeted metabolomic analysis of total metabolites in the leaves of *Reaumuria soongorica* seedlings revealed that inoculation with strain S40 modulated the metabolite content in the leaves, significantly upregulating metabolites involved in plant hormone signal transduction and the phenylalanine biosynthesis pathway. The results suggest that *Bacillaceae* primarily promotes plant growth and salt tolerance by increasing photosynthetic pigments to enhance photosynthetic efficiency, accumulating osmoregulatory substances, regulating hormone signal transduction. The study indicates that PGPR has a positive impact on soil physicochemical properties, nutrient content, and soil enzyme activities. This research focused solely on the effects of salt-tolerant *Bacillus* on plants, with further studies planned to investigate their impact on soil.

Data availability statement

The datasets presented in this study can be found in online repositories. The names of the repository/repositories and accession number(s) can be found in the article/Supplementary material.

Author contributions

XB: Conceptualization, Data curation, Investigation, Methodology, Validation, Visualization, Writing – original draft, Writing – review & editing. PC: Conceptualization, Funding acquisition, Project administration, Resources, Supervision, Writing – review & editing. CH: Investigation, Writing – review & editing. XW: Data curation, Investigation, Methodology, Writing – original draft. FZ: Data curation, Investigation, Methodology, Writing – original draft.

Funding

The author(s) declare financial support was received for the research, authorship, and/or publication of this article. The authors are

thankful to the Key Laboratory of Grassland Ecosystem (Gansu Agricultural University), Ministry of Education Open Project (KLGE-2022-15) for providing financial support. The authors are also thankful to the National Natural Foundation of China (32160407), and the Gansu Provincial Key Research and Development Program (23YFFA0065), for providing financial support.

Conflict of interest

The authors declare that the research was conducted in the absence of any commercial or financial relationships that could be construed as a potential conflict of interest.

Publisher's note

Supplementary material

The Supplementary material for this article can be found online at: https://www.frontiersin.org/articles/10.3389/fmicb.2024.1408622/full#supplementary-material

References

Aguirre-Monroy, A. M., Santana-Martínez, J. C., and Dussán, J. (2019). *Lysinibacillus sphaericus* as a nutrient enhancer during fire-impacted soil replantation. *Appl. Environ. Soil Sci.* 2019, 1–8. doi: 10.1155/2019/3075153

Al-Turki, A., and Abdullah, R. R. H. (2021). Native plant growth-promoting rhizobacteria for growth promotion of lettuce from Qassim, Saudi Arabia. *Pak. J. Biol. Sci.* 24, 773–779. doi: 10.3923/pjbs.2021.773.779

Amri, M., Rjeibi, M. R., Gatrouni, M., Mateus, D. M. R., Asses, N., Pinho, H. J. O., et al. (2023). Isolation, identification, and characterization of phosphate-solubilizing bacteria from Tunisian soils. *Microorganisms* 11:783. doi: 10.3390/microorganisms11030783

Bai, J., Gong, C. M., Chen, K., Kang, H. M., and Wang, G. (2009). Examination of antioxidative system's responses in the different phases of drought stress and during recovery in desert plant *Reaumuria soongorica* (pall.) maxim. *J. Plant Biol.* 52, 417–425. doi: 10.1007/s12374-009-9053-7

Chen, J. T., Aroca, R., and Romano, D. (2021). Molecular aspects of plant salinity stress and tolerance. *Int. J. Mol. Sci.* 22:4918. doi: 10.3390/ijms22094918

Coban, O., De Deyn, G. B., and van der Ploeg, M. (2022). Soil microbiota as game-changers in restoration of degraded lands. *Science* 375:abe0725. doi: 10.1126/science.abe0725

Devi, S., Sharma, S., Tiwari, A., Bhatt, A. K., Singh, N. K., Singh, M., et al. (2023). Screening for multifarious plant growth promoting and biocontrol attributes in *bacillus* strains isolated from indo gangetic soil for enhancing growth of rice crops. *Microorganisms* 11:1085. doi: 10.3390/microorganisms11041085

El-Beltagi, H. S., Ahmad, I., Basit, A., Abd El-Lateef, H. M., Yasir, M., Shah, S. T., et al. (2022). Effect of *Azospirillum* and *Azotobacter* species on the performance of cherry tomato under different salinity levels. *Gesunde Pflanzen* 74, 487–499. doi: 10.1007/s10343-022-00625-2

Fang, Y. J., Qin, Y. H., and Xiong, L. Z. (2018). Determination of Na^+, K^+ content in rice leaf (flame photometric method). *Bio-101*:e1010149. doi: 10.21769/BioProtoc.1010149

Gupta, P., Kumar, V., Usmani, Z., Rani, R., Chandra, A., and Gupta, V. K. (2019). A comparative evaluation towards the potential of *Klebsiella* sp. and *Enterobacter* sp. in plant growth promotion, oxidative stress tolerance and chromium uptake in *Helianthus annuus* (L.). *J. Hazard. Mater.* 377, 391–398. doi: 10.1016/j.jhazmat.2019.05.054

Ham, S. H., Yoon, A. R., Oh, H. E., and Park, Y. G. (2022). Plant growth-promoting microorganism *Pseudarthrobacter* sp. NIBRBAC000502770 enhances the growth and flavonoid content of *Geum aleppicum*. *Microorganisms* 10:1241. doi: 10.3390/microorganisms10061241

Haroon, U., Khizar, M., Liaquat, F., Ali, M., Akbar, M., Tahir, K., et al. (2022). Halotolerant plant growth-promoting rhizobacteria induce salinity tolerance in wheat by enhancing the expression of SOS genes. *J. Plant Growth Regul.* 41, 2435–2448. doi: 10.1007/s00344-021-10457-5

Ha-Tran, D. M., Nguyen, T. T. M., Hung, S. H., Huang, E. E., and Huang, C. C. (2021). Roles of plant growth-promoting Rhizobacteria (PGPR) in stimulating salinity stress defense in plants: a review. *Int. J. Mol. Sci.* 22:3154. doi: 10.3390/ijms22063154

He, A. L., Zhao, L. Y., Ren, W., Li, H. R., Pare, P. W., Zhao, Q., et al. (2023). A volatile producing *Bacillus subtilis* strain from the rhizosphere of Haloxylon ammodendron promotes plant root development. *Plant Soil* 486, 661–680. doi: 10.1007/s11104-023-05901-2

Jalmi, S. K., and Sinha, A. K. (2022). Ambiguities of PGPR-induced plant signaling and stress management. *Front. Microbiol.* 13:899563. doi: 10.3389/fmicb.2022.899563

Khumairah, F. H., Setiawati, M. R., Fitriatin, B. N., Simarmata, T., Alfaraj, S., Ansari, M. J., et al. (2022). Halotolerant plant growth-promoting rhizobacteria isolated from saline soil improve nitrogen fixation and alleviate salt stress in rice plants. *Front. Microbiol.* 13:905210. doi: 10.3389/fmicb.2022.905210

Kibria, M. G., Hossain, M., Murata, Y., and Hoque, M. A. (2017). Antioxidant defense mechanisms of salinity tolerance in rice genotypes. *Rice Sci.* 24, 155–162. doi: 10.1016/j.rsci.2017.05.001

Koza, N. A., Adedayo, A. A., Babalola, O. O., and Kappo, A. P. (2022). Microorganisms in plant growth and development: roles in abiotic stress tolerance and secondary metabolites secretion. *Microorganisms* 10:1528. doi: 10.3390/microorganisms10081528

Kumar, N. P., and Audipudi, A. V. (2015). Exploration of a novel plant growth promoting bacteria *Stenotrophomonas maltophilia* AVP 27 isolated from the chilli rhizosphere soil. *Int. J. Eng. Res. Gen. Sci.* 3, 265–273.

Kumar, V., Raghuvanshi, N., Pandey, A. K., Kumar, A., Thoday-Kennedy, E., and Kant, S. (2023). Role of halotolerant plant growth-promoting rhizobacteria in mitigating salinity stress: recent advances and possibilities. *Agriculture* 13:168. doi: 10.3390/agriculture13010168

Kumar, A., Singh, S., Mukherjee, A., Rastogi, R. P., and Verma, J. P. (2021). Salt-tolerant plant growth-promoting *Bacillus pumilus* strain JPVS11 to enhance plant growth attributes of rice and improve soil health under salinity stress. *Microbiol. Res.* 242:126616. doi: 10.1016/j.micres.2020.126616

Lephatsi, M. M., Meyer, V., Piater, L. A., Dubery, I. A., and Tugizimana, F. (2021). Plant responses to abiotic stresses and rhizobacterial biostimulants: metabolomics and epigenetics perspectives. *Meta* 11:457. doi: 10.3390/metabo11070457

Li, H. S. (2000). *Principles and techniques of plant physiology and biochemical experiment*. Beijing, China: Higer Education Press.

Li, Q., Li, H. C., Yang, Z., Cheng, X., Zhao, Y. C., Qin, L., et al. (2022). Plant growth-promoting rhizobacterium *Pseudomonas* sp. CM11 specifically induces lateral roots. *New Phytol.* 235, 1575–1588. doi: 10.1111/nph.18199

Liu, X., Du, Y., Na, X. F., Wang, M., Qu, Y., Ge, L. H., et al. (2023). Integrative transcriptome and metabolome revealed the molecular mechanism of *Bacillus megaterium* BT22-mediated growth promotion in *Arabidopsis thaliana*. *J. Plant Physiol.* 285:153995. doi: 10.1016/j.jplph.2023.153995

Liu, H., Wang, J., Sun, H. M., Han, X. B., Peng, Y. L., Liu, J., et al. (2020). Transcriptome profiles reveal the growth-promoting mechanisms of *Paenibacillus polymyxa* YC0136 on tobacco (*Nicotiana tabacum* L.). *Front. Microbiol.* 11:584174. doi: 10.3389/fmicb.2020.584174

Ma, J. Y., Chen, T., Qiang, W. Y., and Wang, G. (2005). Correlations between foliar stable carbon isotope composition and environmental factors in desert plant *Reaumuria soongorica* (pall.) maxim. *J. Integr. Plant Biol.* 47, 1065–1073. doi: 10.1111/j.1744-7909.2005.00129.x

Maeda, H., and Dudareva, N. (2012). The shikimate pathway and aromatic amino acid biosynthesis in plants. *Annu. Rev. Plant Biol.* 63, 73–105. doi: 10.1146/annurev-arplant-042811-105439

Meng, L., Zhou, R. Y., Lin, J. L., Wang, Q. J., Wang, P. M., Wang, W., et al. (2022). Integrated transcriptomics and nontargeted metabolomics analysis reveal key metabolic pathways in *ganoderma lucidum* in response to ethylene. *J. Fungi* 8:456. doi: 10.3390/jof8050456

Mukherjee, S., and Sen, S. K. (2015). Exploration of novel rhizospheric yeast isolate as fertilizing soil inoculant for improvement of maize cultivation. *J. Sci. Food Agric.* 95, 1491–1499. doi: 10.1002/jsfa.6848

Nautiyal, C. S. (1999). An efficient microbiological growth medium for screening phosphate solubilizing microorganisms. *FEMS Microbiol. Lett.* 170, 265–270. doi: 10.1111/j.1574-6968.1999.tb13383.x

Pang, Z. Q., Chen, J., Wang, T. H., Gao, C. S., Li, Z. M., Guo, L. T., et al. (2021). Linking plant secondary metabolites and plant microbiomes: a review. *Front. Plant Sci.* 12:621276. doi: 10.3389/fpls.2021.621276

Papadopoulou, A., Ainalidou, A., Mellidou, I., and Karamanoli, K. (2023). Metabolome and transcriptome reprogramming underlying tomato drought resistance triggered by a *Pseudomonas* strain. *Plant Physiol. Biochem.* 203:108080. doi: 10.1016/j.plaphy.2023.108080

Peng, M., Jiang, Z. H., Xiang, Z. W., Zhou, A. F., Wang, C., Wang, Z. Y., et al. (2023). Genomic features of a plant growth-promoting endophytic *Enterobacter cancerogenus* JY65 dominant in microbiota of halophyte *Suaeda salsa*. *Plant Soil* 496, 269–287. doi: 10.1007/s11104-023-06360-5

Saad, M. M., Eida, A. A., and Hirt, H. (2020). Tailoring plant-associated microbial inoculants in agriculture: a roadmap for successful application. *J. Exp. Bot.* 71, 3878–3901. doi: 10.1093/jxb/eraa111

Saha, M., Sarkar, S., Sarkar, B., Sharma, B. K., Bhattacharjee, S., and Tribedi, P. (2016). Microbial siderophores and their potential applications: a review. *Environ. Sci. Pollut. Res.* 23, 3984–3999. doi: 10.1007/s11356-015-4294-0

Schmitz, L., Yan, Z. C., Schneijderberg, M., de Roij, M., Pijnenburg, R., Zheng, Q., et al. (2022). Synthetic bacterial community derived from a desert rhizosphere confers salt stress resilience to tomato in the presence of a soil microbiome. *ISME J.* 16, 1907–1920. doi: 10.1038/s41396-022-01238-3

Selim, S., AbdElgawad, H., Alsharari, S. S., Atif, M., Warrad, M., Hagagy, N., et al. (2021). Soil enrichment with actinomycete mitigates the toxicity of arsenic oxide nanoparticles on wheat and maize growth and metabolism. *Physiol. Plant.* 173, 978–992. doi: 10.1111/ppl.13496

Slimani, A., Raklami, A., Benmrid, B., Oufdou, K., and Meddich, A. (2023). Salt-tolerant plant growth-promoting rhizobacteria mitigate salinity in barley by improving photosynthetic capacity, antioxidant activity, and soil fertility. *Biologia* 78, 3367–3379. doi: 10.1007/s11756-023-01541-0

Sunita, K., Mishra, I., Mishra, J., Prakash, J., and Arora, N. K. (2020). Secondary metabolites from halotolerant plant growth promoting rhizobacteria for ameliorating salinity stress in plants. *Front. Microbiol.* 11:567768. doi: 10.3389/fmicb.2020.567768

Waadt, R., Seller, C. A., Hsu, P. K., Takahashi, Y., Munemasa, S., and Schroeder, J. I. (2022). Plant hormone regulation of abiotic stress responses. *Nat. Rev. Mol. Cell Biol.* 23, 680–694. doi: 10.1038/s41580-022-00479-6

Wang, L. X., Chen, M. X., Lam, P. Y., Dini-Andreote, F., Dai, L., and Wei, Z. (2022). Multifaceted roles of flavonoids mediating plant-microbe interactions. *Microbiome* 10:233. doi: 10.1186/s40168-022-01420-x

Wu, X. H., Fan, Y., Wang, R., Zhao, Q., Ali, Q., Wu, H., et al. (2022). *Bacillus halotolerans* KKD1 induces physiological, metabolic and molecular reprogramming in wheat under saline condition. *Front. Plant Sci.* 13:978066. doi: 10.3389/fpls.2022.978066

Xiong, Y. W., Li, X. W., Wang, T. T., Gong, Y., Zhang, C. M., Xing, K., et al. (2020). Root exudates-driven rhizosphere recruitment of the plant growth-promoting rhizobacterium *Bacillus flexus* KLBMP 4941 and its growth-promoting effect on the coastal halophyte *Limonium sinense* under salt stress. *Ecotoxicol. Environ. Saf.* 194:110374. doi: 10.1016/j.ecoenv.2020.110374

Xu, J. Z., Qin, L. J., Xu, X. Y., Shen, H., and Yang, X. Y. (2023). *Bacillus paralicheniformis* RP01 enhances the expression of growth-related genes in cotton and promotes plant growth by altering microbiota inside and outside the root. *Int. J. Mol. Sci.* 24:7227. doi: 10.3390/ijms24087227

Yan, S. P., Chong, P. F., and Zhao, M. (2022). Effect of salt stress on the photosynthetic characteristics and endogenous hormones, and: a comprehensive evaluation of salt tolerance in *Reaumuria soongorica* seedlings. *Plant Signal. Behav.* 17:2031782. doi: 10.1080/15592324.2022.2031782

Yang, J. S., Yao, R. J., Wang, X. P., Xie, W. P., Zhang, X., Zhu, W., et al. (2022). Research on salt-affected soils in China: history, status quo and prospect. *Acta Pedol. Sin.* 59, 10–27. doi: 10.11766/trxb202110270578

Zhang, J. Y., Liu, Y. X., Guo, X. X., Qin, Y., Garrido-Oter, R., and Schulze-Lefert, P. (2021). High-throughput cultivation and identification of bacteria from the plant root microbiota. *Nat. Protoc.* 16, 988–1012. doi: 10.1038/s41596-020-00444-7

frontiers | Frontiers in Microbiology

TYPE Original Research
PUBLISHED 28 April 2025
DOI 10.3389/fmicb.2024.1384204

OPEN ACCESS

EDITED BY
Jianling Fan,
Nanjing University of Information Science and Technology, China

REVIEWED BY
Sami Abou Fayssal,
University of Forestry, Sofia, Bulgaria
Shouke Zhang,
Zhejiang Agriculture and Forestry University, China
Xingang Zhou,
Northeast Agricultural University, China

*CORRESPONDENCE
D. Wade Abbott
✉ wade.abbott@agr.gc.ca

RECEIVED 08 February 2024
ACCEPTED 06 May 2024
PUBLISHED 28 April 2025

CITATION
King ML, Bajwa B, Hanna N, Xing X, Low KE, Neuberger P, Hall E, Veltri M, Weighill B, Klassen L, Plain Eagle N, Big Bull W, Lynes LS, Montina T, Thomas PJ, Gorzelak MA and Abbott DW (2025) Comparative analysis of the soil microbiome and carbohydrate content of *Anthoxanthum nitens* (Sweetgrass) and other Poaceae grass tissues and associated soils. *Front. Microbiol.* 15:1384204. doi: 10.3389/fmicb.2024.1384204

Comparative analysis of the soil microbiome and carbohydrate content of *Anthoxanthum nitens* (Sweetgrass) and other Poaceae grass tissues and associated soils

Marissa L. King[1], Barinder Bajwa[1], Naomi Hanna[1], Xiaohui Xing[1], Kristin E. Low[1], Patrick Neuberger[1], Erin Hall[1], Michael Veltri[2], Brett Weighill[3,4], Leeann Klassen[1], Noreen Plain Eagle[5], William Big Bull[4], Laura S. Lynes[6], Tony Montina[2], Philippe J. Thomas[7], Monika A. Gorzelak[1] and D. Wade Abbott[1,2]*

[1]Lethbridge Research and Development Centre, Agriculture and Agri-Food Canada, Lethbridge, AB, Canada, [2]Department of Chemistry and Biochemistry, University of Lethbridge, Lethbridge, AB, Canada, [3]Department of Geography and Environment, University of Lethbridge, Lethbridge, AB, Canada, [4]Peigan Board of Education, Piikani Nation, Brocket, AB, Canada, [5]Piikani Nation Lands Department, Piikani Nation, Brocket, AB, Canada, [6]The Resilience Institute, Canmore, AB, Canada, [7]Environment and Climate Change Canada, National Wildlife Research Centre, Ottawa, ON, Canada

Sweetgrass (*Anthoxanthum nitens*) is a culturally and environmentally significant perennial grass to many Indigenous Peoples; however, little is known about the potential of Sweetgrass as a contributor to soil health, biodiversity, and climate adaptation. Here, a team of transdisciplinary experts from academia, a non-governmental organization, and a First Nation community collaborated to investigate the structural composition of the rhizomes, stems, and leaves of greenhouse-grown Sweetgrass in comparison to other Poaceae grass members found in a nearby field. The data shows that the monosaccharide composition of *A. nitens* was evenly distributed throughout the three tissues, and that cellulose was the predominant polysaccharide followed by glucuronoararbinoxylans. There were lesser amounts of xyloglucans, mixed-linkage glucans, homogalacturonans, and rhamnogalacturonans as the hemicellulosic and pectic polysaccharides, respectively. The carbohydrate composition seen in *A. nitens* was consistent with the other Poaceae grasses evaluated in this study, with the exception of *Setaria chondrachne*, which contained elevated pectin levels in its stems and leaves. Additionally, the analysis of the carbohydrate content within the soil samples revealed a higher abundance of carbohydrates within greenhouse soil when compared to field soil samples, with significantly more mannose, galactose, and galacturonic acid. Further, there were structural differences in the microbial communities across sampling sites, including a significant increase in the abundance of *Bacillus* spp. in the greenhouse soil. Overall, this study provides the glycome and associated soil microbial community baseline for greenhouse-grown Sweetgrass.

KEYWORDS

Sweetgrass, *Anthoxanthum nitens*, soil microbiome, glycomics, Indigenous knowledge, transdisciplinary

1 Introduction

Anthoxanthum nitens (Weber) Y. Schouten & Veldkamp (aka., *Hierochloe odorata* (L.) P. Beauv), commonly known as Sweetgrass, is a perennial Poaceae grass found throughout North America, Europe, and Asia. In Canada, Sweetgrass is considered a culturally and environmentally significant plant for First Nations, Inuit and Métis peoples and is commonly used for ceremonial protocol, medicine, as a material for weaving baskets or other crafts (Moerman, 1998; Kavasch and Baar, 1999; Shebitz and Kimmerer, 2005), or as a parable by Elders (Brant, 2022). Sweetgrass, especially the roots, are scented with a vanilla-like fragrance that is produced by coumarin (Ueyama et al., 1991). This volatile compound along with its coumadin and warfarin derivates have demonstrated anticoagulant activity (Sharifi-Rad et al., 2021). Additionally, coumarin and its 5,8-dihydroxycoumarin and 5-hydroxy-8-O-β-d-glucopyranosycoumarin derivatives have also been explored for their antioxidant properties. Sweetgrass extracts have previously shown a decrease in lipid oxidation in *in vitro* assays (Pukalskas et al., 2002) and rats administered ethanol (Dobrzyńska et al., 2013).

While the volatile and antioxidant properties of Sweetgrass have been well-documented, the carbohydrate profile, or glycome, of this plant remains relatively unknown. Sweetgrass has been previously analyzed for its fiber content in the search for sustainable materials to reinforce polymeric composites, revealing contents of 70.4% cellulose, 21.5% hemicellulose, and 8.1% lignin (Dalmis et al., 2020). However, this study did not investigate the polysaccharide profile within the plant and differences between its tissues. Using glycomics to profile the carbohydrate content of Sweetgrass, the potential Sweetgrass has for carbon sequestration can start to be revealed, as this rhizomatous grass stores carbon in its extensive rhizome network within soil (Winslow, 2000; Panchal et al., 2022). Sweetgrass has an expansive habitat much of which is vulnerable to the impacts of climate change, especially drought in prairie regions (Schneider, 2013). Thus, evaluating the carbon sequestration potential of Sweetgrass carbohydrates and the impact of a decline in abundance (Shebitz and Kimmerer, 2004) are important considerations.

The flow of carbohydrates within and between different ecosystems is deeply dependent on the composition of the soil microbial communities within each environment (Low et al., 2023). Plants interact with the soil microbial community through the production of root exudates, mucilage, and other secretions (Jones et al., 2009). Root exudates are primarily composed of carbohydrates, along with amino acids, organic acids, fatty acids, and secondary metabolites (Bais et al., 2006; Jones et al., 2009; Vranova et al., 2013). Exudate carbohydrates are quickly utilized by bacteria and fungi, which contributes to the assembly of the soil microbial community (Zhalnina et al., 2018). Depending on the exudate composition, plants can modify the soil through changing the soil pH, attracting beneficial microbes, and chelating or releasing toxic compounds (Vives-Peris et al., 2020). In addition to rhizodeposition, carbohydrates can also enter the soil through manure or compost, or as plant cell wall biomass in litter, where decomposition by soil microorganisms influences the turnover of soil organic matter (Schimel and Schaeffer, 2012). Unlike root exudates, recalcitrant cell wall polysaccharides require complex enzymatic pathways produced by capable microorganisms to be digested (Pérez et al., 2002). Overall, carbohydrates stemming from root exudates or cell wall litter not only mediate interaction between plants and soil microbiota, but also affect interactions between microbial members of the soil community (Sasse et al., 2018).

This study was conducted in partnership with the Piikani Nation, a proud First Nation community in southern Alberta, Canada and member of the Blackfoot Confederacy; the Resilience Institute, a climate-focused charity with a long-standing relationship with the Piikani Nation; two federal government departments: Environment and Climate Change Canada and Agriculture and Agri-Food Canada; and the University of Lethbridge. The Piikani Nation has ∼4,200 registered members, where an estimated 40% of the members live off reserve in urban centers that surround Nation lands. They occupy two reserves; the main reserve along Alberta Highway No. 3 covers an area of 42,6127 hectares (105,200 acres) and the timber reserve (No. 147B) located in the Porcupine Hills to the northwest corner covers an area of 2,979 hectares (7,360 acres). Similar to many Indigenous communities, the Piikani Nation commonly uses Sweetgrass for cultural purposes, but it is becoming harder to find on the land (Plain Eagle, 2023). Here, the monosaccharide composition of the rhizome, stem, and leaf fractions of greenhouse-grown Sweetgrass was determined and compared to other Poaceae grass members collected from a nearby field on Piikani Nation lands. The chemical structures of polysaccharides were investigated using glycosidic linkage analysis by gas chromatography-mass spectrometry (GC-MS) and gas chromatography-flame ionization detection (GC-FID) analyses. Additionally, greenhouse and field soils associated with each plant were assessed for their chemical and carbohydrate content. Lastly, greenhouse and field soil samples were assessed using 16S rRNA gene sequencing to determine the bacterial composition of the soil microbial communities as a function of their habitats and growing conditions.

2 Materials and methods

2.1 Collection of grass and soil samples

Prior to sample collection, the Piikani Nation and their community partners at the Resilience Institute, hosted a Sweetgrass Partnership Ceremony (September 9, 2022, Piikani Reserve 147 and 147B). Scientists from the University of Lethbridge and Agriculture and Agri-Food Canada, the president of the Resilience Institute, and invited guests joined Elders and other knowledge holders from the Piikani Nation for the ceremony. Elder Peter Strikes with a Gun gave a blessing for the collaborative work and expressed how Sweetgrass represented a symbol not just of their history, but of their future (Strikes with a Gun, 2022). Following the ceremony, a traditional Blackfoot meal was provided consisting of Saskatoon berry soup and fry bread. This Partnership Ceremony was an essential part of the research method for this study and paved the way for the collection of samples.

Guided by Piikani knowledge holders and students, six grass samples were collected from a 1 m^2 nursery bed located within a

greenhouse next to the Piikani Nation Secondary School (Brocket, AB, Canada; 49.54332°N, 113.75018°W) on October 4, 2022. Additionally, six grass samples were collected from a 5 m^2 section within a field on the main Piikani Reserve where Sweetgrass used to be commonly gathered (Brocket, AB, Canada; 49.54925°N, 113.73252°W; October 4, 2022). All plant samples were dug out and divided into leaf; stem; and rhizome tissues; each tissue sample was immediately frozen on dry ice and stored at −80°C. Soil and plant samples were freeze-dried and ball-milled to a fine powder using a Mixer Mill MM400 (Retsch, Germany), and stored at room temperature until processed further.

Soil samples associated with the plants collected from the greenhouse ($n = 6$) and field ($n = 6$) sampling sites, were also collected from the top layer (0–15 cm), and immediately frozen on dry ice and stored at −80°C until further processing. Soil samples were then sieved (2 mm) before being divided into two parts: one for 16S rRNA gene sequencing and microbial community analysis, and the second for glycomics. Additionally, six soil samples were collected from a "baseline" sampling site located adjacent to the greenhouse, which was the site originally used to collect soil for use in the greenhouse that was supplemented with bloodmeal as a fertilizer. Baseline soil samples were treated similarly to the greenhouse and field soils, except baseline soil samples were only studied using 16S rRNA gene sequencing.

2.2 Identification of grass species through ITS sequencing

To identify the grass species that were collected from the greenhouse and field sites, the internal transcribed spacer 1 (ITS1) region was used for DNA barcoding. DNA was extracted from all greenhouse leaf samples (50 mg) using the DNeasy Plant Pro kit (Qiagen, Canada) following the manufacturer's instructions. The ITS1 region was targeted for amplification by PCR using the primers: ITS-p5 (CCTTATCAYTTAGAGGAAGGAG) and ITS-p4 (CCGCTTAKTGATATGCTTAAA) (Cheng et al., 2016). Amplification was performed using iProof™ High-Fidelity DNA polymerase (Bio-Rad, Canada) with PCR cycles as follows: initial denaturation step of 98°C for 1 min before 16 cycles of: 98°C for 10 s, 58–0.5°C $cycle^{-1}$ for 20 s, and 72°C for 1 min, before 30 cycles of: 98°C for 10 s, 52°C for 20 s, and 72°C for 1 min, with a final extension at 72°C for 5 min. PCR products (~750 bp) were sent for Sanger sequencing (Eurofins Genomics, Canada), and sequencing results were paired using Sequencher (version 5.4.6) and run through NCBI's nucleotide BLAST suite (Altschul et al., 1990).

2.3 Preparation of alcohol insoluble residue

Alcohol insoluble residue (AIR) of rhizome, stem, and leaf sections of the greenhouse and field grass samples, along with the soil collected from each collection site, were prepared according to the literature (Pattathil et al., 2012) with modifications (Wood et al., 2018; Klassen et al., 2023). Briefly, 100 mg of each ball-milled plant sample and 10 g of each ball-milled soil sample was suspended in 40 mL of 80% (v/v) ethanol and placed on a rotator for 8 h, for a total of three washes, followed by a single wash of acetone and methanol, each for 20 min. Samples were centrifuged (3,000 × *g*, 30 min) between solvent washes and the supernatant was discarded. The residue after the final wash was vacuum-dried by SpeedVac (Thermo Scientific, USA).

2.4 Preparation of partially methylated alditol acetates from plant cell walls

Cell wall residue from AIR was de-starched by incubation with α-amylase (E-BLAAM, Megazyme) in 100 mM maleic acid buffer (pH 6.0) containing 100 mM NaCl and 3 mM $CaCl_2$ for 8 h at 70°C followed by incubation with amyloglucosidase (E-AMGDFPD, Megazyme) for 4 h at 50°C. The de-starched samples were extensively dialyzed (MWCO 3.5 kDa) against deionized water and then freeze-dried. For linkage analysis of neutral sugars, 5 mg of each AIR was permethylated by 0.6 mL of methyl iodide in 1 mL of dimethyl sulfoxide (DMSO) with the presence of excess amount of sodium hydroxide (NaOH) (Jones et al., 2020; Low et al., 2020; Badhan et al., 2022). The methylation product was cleaned up by partition between dichloromethane and 10% (v/v) acetic acid over ice one time and then with deionized water three times. The final lower phase was evaporated to dryness, and then the methylation process was repeated two more times. The per-*O*-methylated samples were subsequently hydrolyzed to monosaccharides with 2 mL of 4 M trifluoroacetic acid (TFA) for 4 h at 100°C, reduced with 10 mg of sodium borodeuteride ($NaBD_4$, 99 atom % D, Alfa Aesar) dissolved in 1 mL of deionized water for 16 h at room temperature (Low et al., 2020), and then per-acetylated with 2.5 mL of mixture of acetic anhydride and TFA (5:1, v/v) at 60°C for 1 h (Voiges et al., 2012; Robb et al., 2022; Chang et al., 2023). The resulting partially methylated alditol acetates (PMAAs) were redissolved in 3 mL of dichloromethane, and washed with saturated deionized water solution of sodium bicarbonate then deionized water three times. After that, the lower phase was passed through a glass wool-plugged Pasteur pipette loaded with anhydrous sodium sulfate powder (Yu et al., 2017), followed by evaporation to dryness and redissolved in ethyl acetate for GC-MS analysis. In a separate experiment, uronic acids in approximately 5 mg of dry AIR powder were carboxyl reduced to 6,6-dideuterated neutral sugars by $NaBD_4$ reduction of their methyl esters generated by weak methanolysis (0.5 M methanolic HCl, 80°C, 20 min) (Chong et al., 2019; Hosain et al., 2019; Muhidinov et al., 2020), followed by converting to PMAAs using the same procedure as described above. Two technical replicates were conducted for each sample.

2.5 GC-MS analysis of PMAAs

All PMAA samples were tested on an Agilent 7890A-5977B GC-MS system (Agilent Technologies, Santa Clara, CA) installed with a medium-polarity Supelco SP-2380 column (60 m × 0.25 mm × 0.2 μm; Sigma-Aldrich, USA) with a constant flow rate of helium (0.8 mL min^{-1}). Samples were injected at an inlet temperature

of 250°C with a 10:1 split ratio. The oven temperature was programmed to start at 120°C (hold 1 min) followed by increasing at 3°C min^{-1} to 200°C (hold 50 min) then 3°C min^{-1} to 250°C (hold 20 min). The EI-MS spectra of the PMAAs were interpreted by comparing them with those of reference derivatives and by referring to the literature (Carpita and Shea, 1989). The glycosidic linkage composition (mol%) was calculated following the published protocol (Pettolino et al., 2012). Visualization of the plant glycosidic linkage data was carried out using R (version 4.2.2) in R-studio (version 2022.02.3 Build 492) with the packages: ggplot2 (Wickham, 2016) and reshape2 (Wickham, 2007). Correlations amongst the glycosidic linkages present within the rhizome, stem, and leaf tissues of the greenhouse and field plants were analyzed with principal component analysis (PCA) plots using R in R-studio with the packages: dplyr (Wickham et al., 2023), forcats (Wickham, 2023), and ggplot2 (Wickham, 2016). Polysaccharide compositions were estimated from the linkage data (Supplementary Tables S3, S4) by adapting the published calculations from Pettolino et al. (2012).

2.6 Analysis of total carbohydrate content and monosaccharide composition of soil samples

In experimental duplicates, ball-milled air powder of soil (250 mg) was hydrolyzed by magnetic stirring in 1 mL of 12 M H_2SO_4 for 2 h, followed by adding 11 mL of deionized water to dilute the acid and then incubation at 100°C for 2 h with magnetic stirring. The hydrolysate was transferred to a 50 mL tube, along with 12 mL of deionized water used to wash the original tube for hydrolysis. Samples were centrifuged three times (3,000 × *g*, 10 min), where between spins the resulting supernatants were pooled with three deionized water washes of the pellet. 5 M NaOH solution (2 mL) was added to neutralize each supernatant. The resulting hydrolysates of soil samples were filtered (0.2 μm) for monosaccharide analysis using high-performance anion-exchange chromatography with pulsed amperometric detection (HPAEC-PAD), while hydrolysates were not filtered for the soil total carbohydrate assay.

The total carbohydrate contents of the soil AIRs were determined calorimetrically using the phenol-sulphuric acid assay (Dubois et al., 1956). Briefly, 2 mL of the above-mentioned hydrolysate was mixed with 50 μL of 80% phenol water solution, immediately followed by adding 3 mL of 18 M H_2SO_4. The solutions were vortexed and then cooled to room temperature followed by reading the absorbance at 490 nm with a Varian Cary 300 UV-Vis spectrophotometer (Agilent Technologies, Santa Clara, CA) against a reagent blank prepared from 2 mL of deionized water instead of the hydrolysate. The carbohydrate content of each soil sample was measured against a calibration curve prepared from 20 to 60 μg mL^{-1} of glucose solution. Total carbohydrate content was calculated based on the soil dry weight, where the mean ± standard deviation (n = 2) was used to plot the data in GraphPad Prism (version 8.0.2).

Absolute monosaccharide quantification was performed using HPAEC-PAD on all greenhouse and field soil samples. HPAEC-PAD was performed with a Dionex ICS-3000 chromatography system (Thermo Scientific) equipped with an autosampler and a pulsed amperometric (PAD) detector. 10 μL of each hydrolyzed sample was injected onto an analytical (3 × 150 mm) CarboPac PA20 column (Thermo Scientific) with a CarboPac PA20 guard column (Thermo Scientific). Neutral and uronic acid sugar samples were eluted at a flow rate of 0.3 mL min^{-1} with a background of NaOH (buffer A), and a gradient of sodium acetate (NaOAc; buffer B) (Supplementary Table S1) at 15°C, where amino sugars were eluted similarly but with a different gradient (Supplementary Table S2). The elution of each run was monitored with a PAD detector (standard quadratic waveform). For quantification of neutral and uronics, a mixture of monosaccharides was used in a known concentration series with the following concentrations for a 1X solution with 99 μM maltotriose used as an internal standard (ISTD): 119 μM fucose (Fuc), 132 μM arabinose (Ara), 132 μM ribose (Rib), 110 μM galactose (Gal), 110 μM glucose (Glc), 110 μM mannose (Man), 132 μM xylose (Xyl), 121 μM rhamnose (Rha), 110 μM glucosamine (GlcN), 101 μM guluronic acid (GulA), 98 μM galacturonic acid (GalA), 101 μM mannuronic acid (ManA), and 101 μM glucuronic acid (GlcA). For amino sugar quantification, a mixture of monosaccharides was used in a known concentration series with the following concentrations for a 1X solution with 99 μM maltotriose used as an ISTD: 112 μM GlcN, 112 μM galactosamine (GalN), and 112 μM mannosamine (ManN). Monosaccharide quantification was performed using Chromeleon software (Thermo Scientific) from triplicate HPAEC-PAD injections. The mean ± standard deviation (n = 3) was used to plot the data in GraphPad Prism (version 8.0.2). To compare differences in the amount of monosaccharides in the greenhouse and field soils, a two-way analysis of variance (ANOVA) test using a false discovery approach was conducted using GraphPad Prism (version 8.0.2).

2.7 16S rRNA gene sequencing of soil microbial communities

DNA was extracted from all baseline, field, and greenhouse rhizosphere soil samples (250 mg, 2 mm sieved) using the PowerSoil Pro kit (Qiagen, Canada) following the manufacturer's instructions. Purified DNA samples were sent to Génome Québec (Montréal, QC, Canada) for Illumina MiSeq PE250 16S rRNA gene sequencing using the primers 515F (GTGCCAGCMGCCGCGGTAA) and 806R (GGACTACHVGGGTWTCTAAT) targeting the V4 region. A total of 908,770 paired end reads were quality trimmed using Trimmomatic (Bolger et al., 2014) with a sliding window of 5:20. Trimmed fasta files were merged and classified using Kraken 2 (Wood et al., 2019) according to the Silva 138 SSU database. Bracken (Lu et al., 2017) was used to estimate bacterial and archaeal abundance at the genus level. Community analysis, statistics, and

plotting of the Bracken output files were performed using R (version 4.2.2) in R-studio (version 2022.02.3 Build 492) with the packages: phyloseq (McMurdie and Holmes, 2013), ggplot2 (Wickham, 2016), picante (Kembel et al., 2010), rioja (Juggins, 2022), and vegan (Oksanen et al., 2023).

Statistical analyses were carried out using normalized read abundances and classification at the genus level. Normalized read abundances were calculated with the "decostand()" function (method = total) from the vegan package (Oksanen et al., 2023). Non-metric multi-dimensional scaling (NMDS) analyses based on Bray-Curtis dissimilarity were performed using the vegdist() function of vegan (Oksanen et al., 2023), to visualize the separation between soil sampling sites. A permutational multivariant analysis of variance (PERMANOVA) was used to assess the effect of soil type on the compositions of rhizosphere-associated microbial communities, using the adonis2 function in vegan (Oksanen et al., 2023) with 999 permutations. Observed OTUs, Chao1, Shannon, and Simpson indices were calculated in R as a measure of community alpha diversity using the estimate richness function in the phyloseq package (McMurdie and Holmes, 2013). Changes in alpha diversity between the different sampling locations were assessed using the Kruskal-Wallis test with *post-hoc* Dunn's multiple comparison in GraphPad Prism (version 8.0.2).

2.8 Soil chemistry

Soils were very dry upon arrival in the lab and determined to contain 0% moisture using the thermogravimetric method and thus were only air-dried at room temperature for 24 h and ground to 2 mm. A subsample of each soil was fine ground to 60 μm. NO_3-N and NH_4-N were extracted from the 2 mm subsample using a 2.0 M KCl extraction at 25°C and measured with an Autoanalyzer 3 (EasyChem Pro, Systea Analytical Technology, Anagni, Italy). The 2 mm subsample was used to determine pH with a 2:1 soil slurry (water:soil) and an Orion Star 211 pH probe (ThermoFisher Scientific, USA). The 60 μm ground sample was analyzed for total carbon (TC) and total nitrogen (TN) using dry combustion with an Elemental analyzer (CE Instruments). Total organic carbon (TOC) was determined by acidification with 0.6 N HCl and inorganic carbon was calculated by determining the difference between TC and TOC. Changes in the soil physio-chemical data parameters were assessed in R-studio (version 2023.06.1 Build 524) using a Kruskal-Wallis test with a *post-hoc* two sided Dunn test, that included a Benjamani-Hochberg multiple comparisons correction factor from the FSA (version 0.9.5) package (Ogle et al., 2023).

3 Results

3.1 ITS sequencing

DNA barcoding using the ITS1 region was used to identify the grass species that were collected from the greenhouse and field sites. Based on the top BLAST hit, all six greenhouse samples were confirmed to be Sweetgrass (*A. nitens*, Table 1), whereas the field samples were identified as different grass species including blue wild rye (*Elymus glaucus*), Pumpelly's bromegrass (*Bromus pumpellianus*), couch grass (*Elymus repens*), and *Setaria chondrachne* (Table 1).

TABLE 1 Identification of grass species collected from the greenhouse and field sites within the Piikani Nation using ITS1 sequence similarity.

Sample	Top BLAST hit	Percent identity (%)
GH1	*Anthoxanthum nitens* voucher CMN:CAN	97.3
GH2	*Anthoxanthum nitens* voucher CMN:CAN	98.1
GH3	*Anthoxanthum nitens* voucher CMN:CAN	97.7
GH4	*Anthoxanthum nitens* voucher CMN:CAN	97.9
GH5	*Anthoxanthum nitens* voucher CMN:CAN	97.6
GH6	*Anthoxanthum nitens* voucher CMN:CAN	98.3
F1	*Elymus glaucus* strain QH-5	83.6
F2	*Bromus pumpellianus* voucher CAN:528978	96.3
F3	*Setaria chondrachne* voucher HCCN-PJ008548-PB-261	79.5
F4	*Elymus repens* isolate ER1	92.5
F5	*Elymus repens* isolate ER1	89.4
F6	*Elymus repens* isolate ER1	98.9

Top BLAST hit is displayed.

3.2 Glycosidic linkage composition of greenhouse-grown Sweetgrass rhizome, stem, and leaf sections

The rhizomes, stems, and leaves of greenhouse-grown Sweetgrass tissues were assessed for their polysaccharide content through monosaccharide composition and glycosidic linkage analysis. The comparison of the individual monosaccharides based on relative abundances within the three Sweetgrass tissue sections, revealed a consistent monosaccharide distribution throughout the plant (Figure 1A; Table 2). Glucose (Glc) was the predominant monosaccharide (58.1–59.3%), followed by xylose (Xyl; 22.3–26.8%), arabinose (Ara; 5.3–7.1%), uronic acids (Ur. acid; 4.8–5.5%), galactose (Gal; 2.7–3.9%), mannose (Man; 0.6–2.2%), and trace amounts of rhamnose (Rha; 0.7–0.9%) and fucose (Fuc; 0.1%). The primary glucose linkages were 4-Glc*p*, 4,6-Glc*p*, and t-Glc*p*, whereby all three linkages were abundant in the three Sweetgrass tissues (*A. nitens;* Figure 1B; Supplementary Table S3). As the samples were de-starched prior to undergoing glycosidic linkage analysis, a majority of the 4-Glc*p* was presumed to stem from cellulose, which is consistent with the previous study (Dalmis et al., 2020), while the 4,6-Glc*p* and t-Glc*p* linkages likely accounted for xyloglucans and mixed-linkage glucans. The second most abundant polysaccharide found throughout Sweetgrass was determined to be glucuronoararbinoxylans (GAX) based on the presence and relative abundances of the 4-Xyl*p*, 3,4-Xyl*p*, 2,4-Xyl*p*, t-Ara*f*, and t-GlcA*p* linkages (Figure 1B; Supplementary Table S3) (Izydorczyk and Biliaderis, 1995; Smith and Harris, 1999). Additionally, the presence of various rhamnose

10.3389/fmicb.2024.1384204

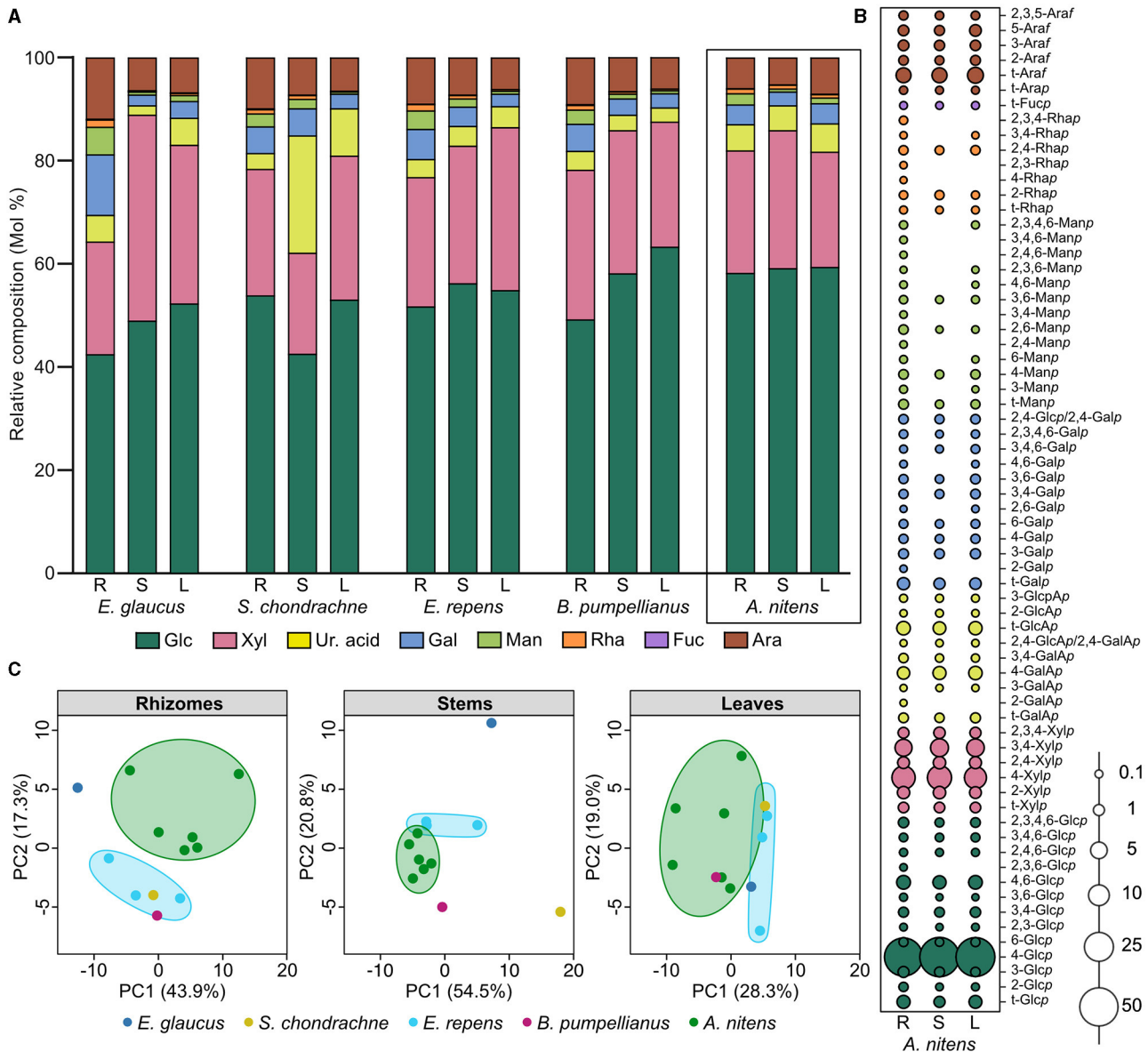

FIGURE 1
Carbohydrate content of greenhouse-grown Sweetgrass and other grass species. **(A)** Relative monosaccharide composition (mol%) of the cell walls present in the rhizome, stem, and leaf sections of greenhouse-grown Sweetgrass (*Anthoxanthum nitens*), and field grass species: *Elymus glaucus, Setaria chondrachne, Elymus repens,* and *Bromus pumpellianus*. **(B)** Relative composition (mol%) of glycosidic linkages present in the cell walls of greenhouse-grown Sweetgrass (*A. nitens*) rhizome, stem, and leaf sections. **(C)** Principal component analysis of glycosidic linkages obtained from the rhizome, stem, and leaf sections of each grass species; *E. glaucus* (dark blue), *S. chondrachne* (yellow), *E. repens* (light blue), and *B. pumpellianus* (fuchsia) collected from the field sampling site, and *A. nitens* (green) collected from the greenhouse.

linkages (i.e., t-Rha*p*, 2-Rha*p*, 4-Rha*p*, 2,3-Rha*p*, 2,4-Rha*p*, 3,4-Rha*p*, and 2,3,4-Rha*p*) is indicative of rhamnogalacturonans being present within Sweetgrass (Pettolino et al., 2012). However, these rhamnose linkages were sporadically present within the stem and leaf tissues of Sweetgrass, whereas all seven were present within the rhizomes (Figure 1B; Supplementary Table S3). In terms of uronic acid abundances within Sweetgrass, 4-GalA*p* and t-GalA*p* were present throughout the plant, therefore it was predicted that homogalacturonans (HGs) composed 1.4–4.1% of the total linkages in Sweetgrass.

3.3 Glycosidic linkage composition of the rhizome, stem, and leaf sections of other grass species collected from a nearby field

A higher degree of glycosidic diversity was seen between the three tissue sections of each field grass species. Interestingly, the stems of *S. chondrachne* contained the highest abundance of uronic acid (22.8%; Figure 1A; Table 2), mostly attributed to 4-GalA*p* and t-GlcA*p* whose abundances were increased within this section (Supplementary Figure S1). Additionally, *S. chondrachne*

10.3389/fmicb.2024.1384204

TABLE 2 Relative monosaccharide composition (Mol %) calculated from glycosidic linkage compositions for rhizome (R), stems (S), and leaves (L) harvested from *A. nitens*, *E. glaucus*, *B. pumpellianus*, *S. chondrachne*, and *E. repens*.

Monosaccharide	*A. nitens*			*E. glaucus*			*B. pumpellianus*			*S. chondrachne*			*E. repens*		
	R	S	L	R	S	L	R	S	L	R	S	L	R	S	L
Ara	6.0	5.3	7.1	11.9	6.4	6.8	9.1	6.6	6.1	10.0	7.3	6.5	9.0	7.3	6.2
Fuc	0.1	0.1	0.1	0.2	0.0	0.1	0.2	0.1	0.0	0.1	0.1	0.0	0.1	0.1	0.0
Gal	3.8	2.7	3.9	11.8	2.0	3.2	5.2	3.2	2.7	5.1	5.2	2.8	5.8	3.8	2.4
Glc	58.1	59.0	59.3	42.3	48.7	51.9	49.2	57.9	62.8	53.8	42.5	52.8	51.4	56.1	54.6
Man	2.2	0.6	1.1	5.3	0.6	1.2	2.8	0.9	0.6	2.5	1.9	0.4	3.6	1.6	0.6
Rha	0.9	0.7	0.7	1.4	0.3	0.4	0.9	0.4	0.3	0.9	0.7	0.2	1.2	0.6	0.3
Xyl	23.7	26.8	22.3	21.8	39.7	30.6	29.0	27.6	24.1	24.5	19.6	27.8	24.9	26.6	31.4
GalA	2.6	2.7	3.1	3.1	0.4	3.1	1.3	1.0	0.9	1.2	16.1	6.3	1.4	1.8	2.3
GlcA	2.5	2.1	2.4	2.0	1.5	2.1	2.4	2.0	1.9	1.9	6.6	2.8	2.2	2.0	1.8

Two separate experiments were conducted for each sample.

leaves also contained increased uronic acid levels (9.2%), with increased 4-GalA*p* and t-GlcA*p* but to a lesser extent than the stem section. Based on the abundances of these two uronic acid linkages, homogalacturonan is predicted to be more abundant within this field grass species. Specifically, based upon the proportion of 3,4-GalA*p* to 4-GalA*p* and the presence of rhamnose linkages (i.e., t-Rha*p*, 2,3- Rha*p*, 2,3,4- Rha*p*), where some of the GalA could be attributed to rhamnogalacturonan II (Pettolino et al., 2012). Further, the 4-ManA*p* linkage was only found in the stem and leaf tissues of *S. chondrachne* (Supplementary Figure S1). In contrast, the stem section of *E. glaucus* had the highest abundance of xylose (39.9%), whereas its rhizomes contained higher amounts of arabinose (11.9%), galactose (11.8%), mannose (5.3%), and rhamnose (1.4%) (Figure 1A; Table 2) in comparison to the other tissue sections of *E. glaucus*. Intriguingly, the leaves of *E. glaucus* had a similar neutral monosaccharide profile as the stems, and similar uronic acid content as the rhizomes. Increased levels of arabinose and galactose linkages such as t-Ara*p*, 6-Gal*p*, 3,6-Gal*p* are indicative of arabinogalactans, whereas the presence of mannose linkages (i.e., 4-Man*p*, 4,6-Man*p*) could be attributed to homomannan, glucomannan, or glucogalactomannan (Pettolino et al., 2012). With *E. repens* and *E. glaucus* being members of the same genus, the monosaccharide profiles of both showed comparable compositions. However, less dramatic proportions of xylose and galactose were seen in the *E. repens* stem and rhizome tissues, respectively (Figure 1A; Table 2). The stems and leaves of *B. pumpellianus* had similar profiles to each other, whereas the rhizomes of *B. pumpellianus* had increased levels of xylose (29.0%), arabinose (9.1%), galactose (5.2%), and mannose (2.8%) in comparison to its stem and leaf sections (Figure 1A; Table 2).

3.4 Comparison of glycosidic linkage compositions across plant sections and between different grass species

Amongst all grass species analyzed, the rhizome section of each plant contained an increased relative abundance of mannose and rhamnose (Figure 1A; Table 2), where a greater amount of diverse glycosidic linkages, such as 3,4-Rha*p*, 2-Rha*f*, 2,4,6-Man*p*, 4,6-Man*p*, 2,4-Man*p*, and 2-Gal*p*, were commonly found in the rhizomes but seldomly found in the other plant tissue sections of Sweetgrass and the field grasses (Supplementary Figure S1). The examination of the glycosidic linkage profiles of Sweetgrass and the field grasses revealed that the 2,4-GlcA*p*/2,4-GalA*p*, 3-GalA*p*, 2-Rha*p*, 2,3-Glc*p* linkages were consistently present in all three Sweetgrass tissues, but sporadically found in the field grass sections. Based on the linkage data for each plant tissue, PCA plotting revealed closely grouped data points belonging to the six greenhouse-grown Sweetgrass plants suggesting that these samples contained similar linkage compositions for their rhizome and stem sections (Figure 1C). The leaves of *B. pumpellianus* were aligned within the confidence interval of the leaves from Sweetgrass, indicating possible similarities between the two species. The most drastic difference in linkage compositions between greenhouse-grown Sweetgrass and the field grass species was seen in the rhizomes, where no overlap was observed (Figure 1C).

The major polysaccharides estimated to be present in the cell walls of all the grass species (Figure 2) were cellulose (24–52%) and glucuronoarabinoxylans (19–39%). Xyloglucan was calculated to be present in significant amounts (6–11%), while minor levels of arabinans, arabinogalactans, heteromannans, mixed linked glucans, rhamnogalacturonans, and homogalacturonans were detected in the majority of the samples. The stems of *S.*

10.3389/fmicb.2024.1384204

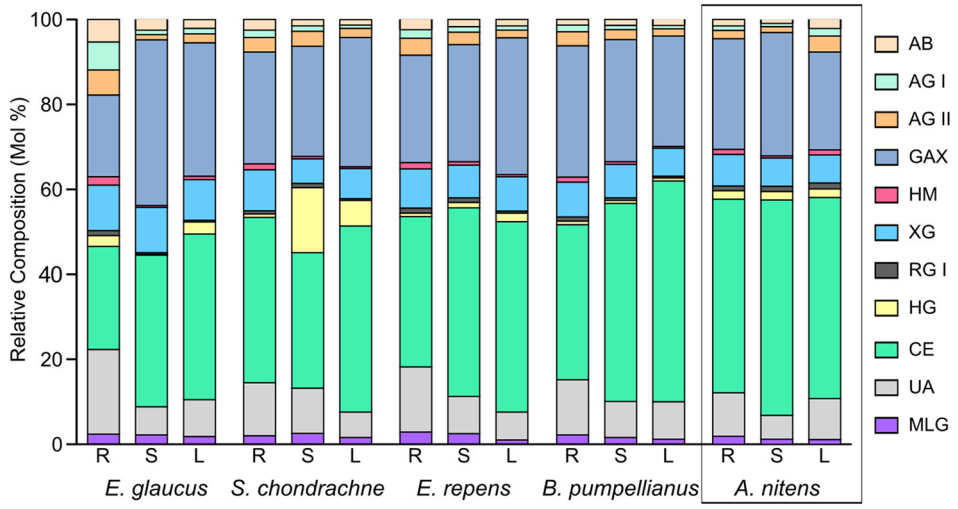

FIGURE 2
Averaged theorized polysaccharide composition for rhizome (R), stems (S), and leaves (L) from *A. nitens*, *E. glaucus*, *B. pumpellianus*, *S. chondrachne*, and *E. repens* ($n = 2$). Calculations were adapted from Pettolino et al. (2012). The following abbreviations were used for their respective polysaccharides: AB, arabinan; AG, arabinogalactan; GAX, glucuronoarabinoxylan; HM, heteromannan; XG, xyloglucan; RG, rhamnogalacturonan; HG, homogalacturonan; CE, cellulose; MLG, mixed linked glucan; UA, unassigned linkages.

chondrachne contained elevated levels of homogalacturonan (15%) whilst only comprising 1–3% of the cell walls in the tissues of other grass species. Homogeneity in the polysaccharide composition amongst the tissues in *A. nitens* and *E. repens* was observed, in which the relative composition of the polysaccharides were consistent between the tissues of the grass species.

3.5 Carbohydrate content of soils associated with greenhouse-grown Sweetgrass and other species collected from a nearby field

The total carbohydrate content was the highest amongst the greenhouse soil samples associated with the Sweetgrass plants at 10.1 ± 1.9% (Figure 3), whereby the field soil samples ranged from 4.6 ± 1.1 to 9.2 ± 1.8%. HPAEC-PAD analysis revealed that glucose was the most abundant monosaccharide within the soil samples, accounting for 30.2 μg mg^{-1} in the greenhouse samples and 9.7–20.9 μg mg^{-1} in the field samples (Figure 3). Further, significantly elevated amounts of glucose, galactose, mannose, xylose, and galacturonic acid were also seen in greenhouse soil samples ($P < 0.05$). In contrast, all field soil samples contained higher amounts of glucosamine in comparison to greenhouse soil, where this difference was significant ($P < 0.05$; Figure 3) in all except for the comparison between *B. pumpellianus* and greenhouse soils. Whereas, relatively consistent amounts of arabinose and xylose were seen amongst all soil samples, with lesser amounts of fucose, rhamnose, ribose, and other amino sugars and uronic acids.

3.6 16S microbial community analysis of greenhouse, field, and baseline soil samples

The greenhouse, field, and baseline soil samples significantly differed in their bacterial community composition (Figure 4A; PERMANOVA: $R^2 = 0.76$, $P = 0.001$). Richness indices (observed, Chao1) were significantly higher in greenhouse soil samples ($P < 0.05$; Figure 4B) in comparison to baseline soil samples. Furthermore, soil bacterial alpha-diversity (Shannon and Simpson indices) at the genus level was also significantly higher in greenhouse soil ($P < 0.05$; Figure 4B) in comparison to baseline but not field soil samples. Although field soil samples did not show significant differences in bacterial diversity, these samples were marginally higher in richness and alpha-diversity values compared to baseline samples. Further, the dendrogram shown in Figure 4C illustrates the clustering pattern of the samples according to the three sampling sites, where field and baseline samples are most related to each other.

Amongst all soil samples analyzed, the most abundant bacterial phyla were Actinobacteria and Proteobacteria, where on average, these phyla comprised 42% of the greenhouse, 51% of the baseline, and 47% of the field soil microbial communities (Figure 4C). Many of the genera belonging to these phyla were seen to have similar relative abundances across the three sampling sites (e.g., *Iamia, Mycobacterium, Pseudonocardia, Reyranella, Sphingomonas,* and uncultured *Xanthobacteraceae*; Figure 5). The six greenhouse soil samples contained a higher relative abundance of Firmicutes in comparison to baseline and field soil samples (Figure 4C), as an increased proportion of *Bacillus* members was seen in the greenhouse soil and members of the *Planifilum* genera were only detected in this sample (Figure 5). Additionally, members belonging to the JCM 18977 (Actinobacteria), and *Truepera* genera (Deinococcota) were also only detected in greenhouse soil samples.

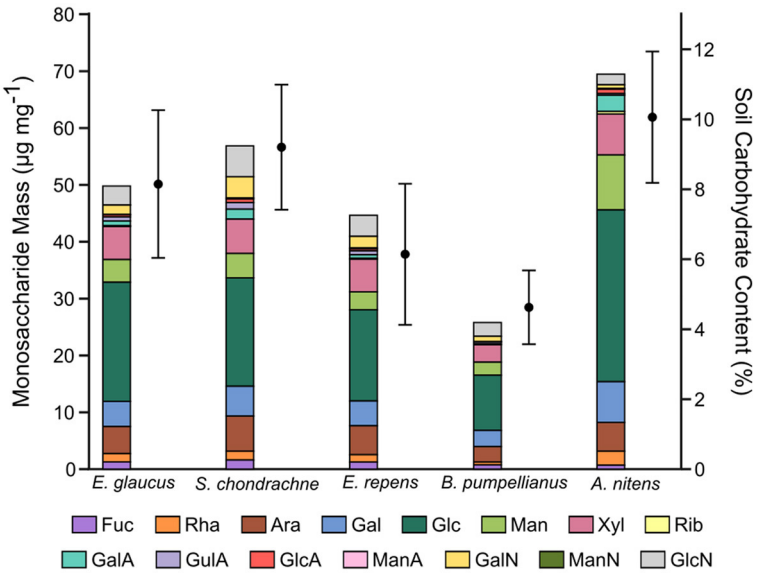

FIGURE 3
Carbohydrate content in greenhouse and field soil samples associated with Sweetgrass and other Poaceae grass species. Left *y*-axis: stacked bar chart of the masses for each monosaccharide present in the soil samples, determined by HPAEC-PAD analysis. Right *y*-axis: total carbohydrate content of each soil sample, determined by a colorimetric assay. Error bars represent the standard deviation of technical replicates ($n = 2$) from the colorimetric analysis of soil samples.

In contrast, there was a higher relative abundance of Chloroflexi seen in the field soil samples (Figure 4C), where uncultured *Anaerolineaceae* were drastically increased within these samples (Figure 5). The baseline field samples contained greater relative abundances of Verrucomicrobia and Actinobacteria, in comparison to the greenhouse and field soil samples (Figure 4C). Members belonging to the candidatus *Udaeobacter* and *Chtoniobacter* genera, and *Gaiella*, *Conexibacter*, *Solirubrobacter*, and *Nocardioides* genera were increased (Figure 5), an observation largely attributed to the increased relative abundances of Verrucomicrobia and Actinobacteria, respectively.

3.7 Soil chemistry

Soil chemical analysis revealed significantly higher total nitrogen, total carbon, total organic carbon, and NH_3-N in the greenhouse compared to baseline soils. Greenhouse soils had significantly higher NO_3-N than both baseline and field soils. Field soils had significantly higher pH values compared to the greenhouse soils (Table 3).

4 Discussion

Sweetgrass (*A. nitens*) and the four different field grass species analyzed within this study, are all Graminacous monocots belonging to the Poaceae family. Therefore, it is not surprising to see that these grass species have a similar polysaccharide profile to each other and to other Poaceae members (Smith and Harris, 1999; Gibeaut et al., 2005). In the glycomics analysis conducted here, cellulose and GAX were determined to be the predominant polysaccharides in Sweetgrass and the field grass species, where each species contained smaller proportions of other hemicelluloses (i.e., mixed-linkage glucans, xyloglucans, mannans) and pectic polysaccharides (i.e., homogalacturonan, rhamnogalacturonan) (Figure 2). In comparison, the cellulose content of Sweetgrass stems was previously reported to be 70.4% through gravimetric analysis (Dalmis et al., 2020). Xylan polysaccharides, such as heteroxylans, arabinoxylans, and GAX, typically represent 20–30% of the total cell wall content within Poaceae grass species (Hatfield et al., 2017), and were determined here to represent 19–32% of the tissue cell walls of various Poaceae species. Within the primary cell walls, Poaceae GAX typically contains more Ara*f* residues within the GAX backbone (Scheller and Ulvskov, 2010), where secondary cell walls also contain some GlcA*p* or MeGlcA*p* substituents as well (Peña et al., 2016). These Ara*f* residues are often esterified with coumaric or ferulic acids (Buanafina, 2009). In comparison, woody and herbaceous eudicots contain glucuronoxylans (Peña et al., 2016). It is hypothesized that commelinids, including Poaceae grasses, incorporate Ara*f* residues into glucuronoxylan polysaccharides to form GAX, whereby this addition may provide GAX with certain physical properties, allowing it to replace the function of xyloglucan and/or pectin as a cross linker (Carpita, 1996). The walls of the Poaceae are further distinguished by the presence of variable amounts of (1,3; 1,4)-linked β-glucans (Carpita and Gibeaut, 1993; Smith and Harris, 1999), where these are widely distributed as non-cellulosic matrix phase polysaccharides within the cell walls (Burton and Fincher, 2009). Here, the presence of the 3-Glc*p* and 4-Glc*p* linkages throughout all Sweetgrass and field grass tissue sections, indicates the presence of (1,3; 1,4)-glucans (Supplementary Figure S1; Supplementary Tables S3, S4).

The only striking difference in carbohydrate composition was seen in the stems of *S. chondrachne,* as these samples contained

10.3389/fmicb.2024.1384204

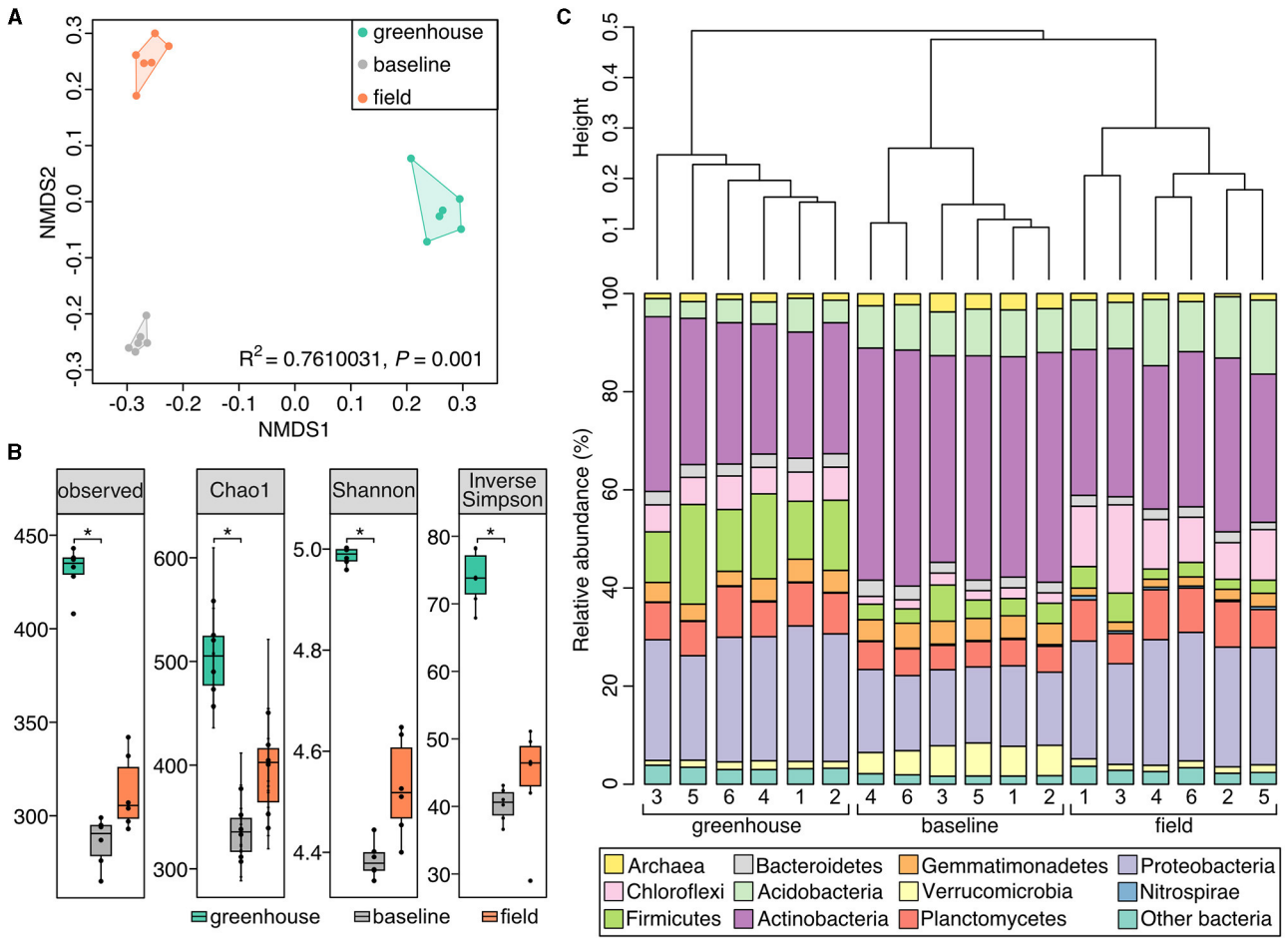

FIGURE 4
Soil microbial community composition differs between the three Piikani Nation sampling sites. **(A)** Non-metric multi-dimensional plot comparing the microbial communities of the soil samples collected from the greenhouse (teal), baseline (gray), and field (orange) sites. **(B)** Boxplots of the observed richness, Chao1, Shannon, and inversed Simpson diversity for each sample type. Boxplots and dots are colored to represent the different sample types: baseline (gray), greenhouse (teal), and field (orange). *Signifies a statistical difference ($P < 0.05$). **(C)** Dendrogram showing the similarity clustering of microbial community compositions between soil samples collected from greenhouse, baseline, and field plots in the Piikani Nation. Bar charts underneath, shows the relative community composition for each greenhouse, baseline, and field samples ($n = 6$) at the phylum level.

elevated levels of GalA and GlcA uronic acids (Figures 1A, 2; Table 2). This suggested an increased amount of HG within the stems of this plant. Pectins make up ~5% of growing cell walls in Poaceae species (Vogel, 2008), whereas it constitutes ~0.1% in mature cell walls (Ishii, 1997). Potentially, this increased abundance of pectin seen within *S. chondrachne* signifies that this plant was actively growing, as pectins allow for primary cell wall extension and plant growth to occur (Wolf and Greiner, 2012).

Carbohydrates commonly account for 5–20% of soil organic matter (Swincer et al., 1969). Here, the carbohydrate content of the soil AIR samples ranged from 4.6 to 10.1% (Figure 2), where the highest value was seen in the greenhouse soil. Greenhouse soil samples were enriched with statistically higher amounts of mannose, galactose, and galacturonic acid (Figure 3). The addition of bloodmeal has been previously shown to increase the total organic carbon within the soil (Ciavatta et al., 1997), positively impacting the relationship between soil microbial diversity and biomass (Bastida et al., 2021). Therefore, as bloodmeal was used to help initiate the greenhouse nursery bed soil, it is most likely that the fertilizer increased available nitrogen and organic carbon in the greenhouse soil (Table 3).

The available nutrients of each soil supported a particular microbial community that utilized enzymes to deconstruct available organic carbon (i.e., polysaccharides) into usable energy (i.e., monosaccharides). The high amount of glucose present with each sample is indicative of cellulose and hemicellulose deposition. Further, the presence of mannose, xylose, galactose, and arabinose within these soil samples suggests a role in hemicellulose turnover, as all four monosaccharides are present in hemicellulose polysaccharides. Proteobacteria, Firmicutes, Acidobacteria, Bacteroidetes, Actinobacteria, and Verrucomicrobia are all known phyla that contain cellulolytic members (López-Mondéjar et al., 2019) and were represented in each of the soils. The higher amount of monosaccharides related to hemicellulose turnover in the greenhouse soil again suggests a higher rate of turnover, which is supported by an increased abundance of members shown to

10.3389/fmicb.2024.1384204

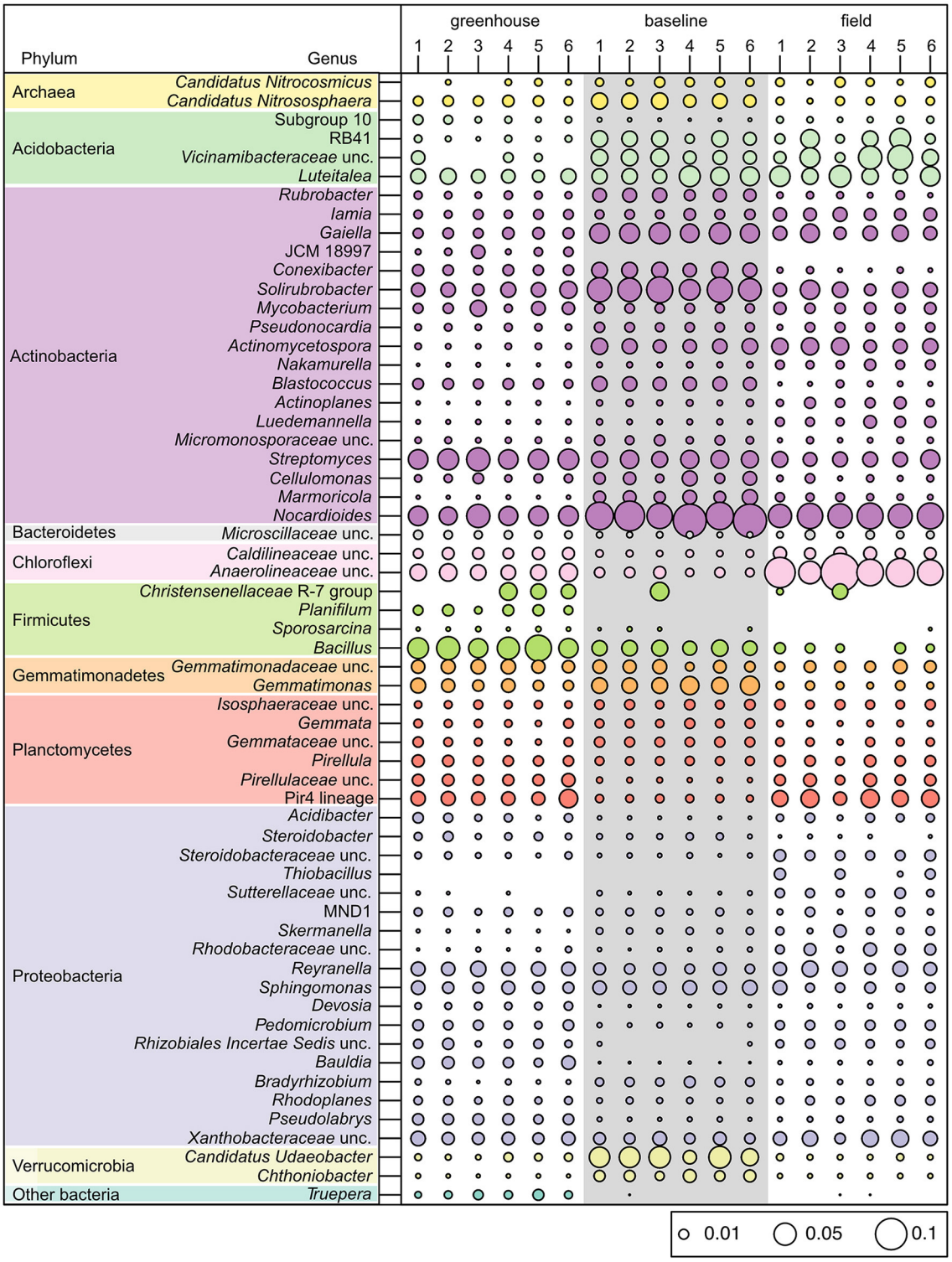

FIGURE 5
Bubble plot of different bacterial and archaeal genera that reached a minimum percentage of 1% relative read abundance in soil microbial communities collected from the greenhouse, baseline, and field sampling sites within the Piikani Nation ($n = 6$ for each sample type).

deconstruct hemicelluloses, such as *Bacillus* and *Streptomyces*. Assuming that the litter decomposition accounts for a fraction of soil monosaccharides, the abundances of GalA and GlcA observed can also be attributed to pectin degradation (Caffall and Mohnen, 2009) most likely by Proteobacteria, Firmicutes, and Bacteroidetes members. Whereas some of the GlcA may also come from bacterial cell wall polysaccharides (Vinnitskiy et al., 2015). As the amount of GlcA and GalA were higher in the greenhouse samples, and variable in the field samples, it suggests that there is higher cell and litter deposition and turnover in the greenhouse soil samples.

TABLE 3 Soil physiochemical parameters of baseline, field, and greenhouse soils affected by Sweetgrass (*A. nitens*).

Soil type	TN (g kg^{-1})	TC (g kg^{-1})	TOC (g kg^{-1})	pH	NO_3-N (μg g^{-1})	NH_3(μg g^{-1})
Greenhouse	0.071 ± 0.0025 (a)	1.67 ± 0.0879 (a)	1.57 ± 0.07 (a)	7.22 ± 0.07 (a)	482.12 ± 44.94 (a)	22.46 ± 4.13 (a)
Baseline	0.024 ± 0.0003 (b)	0.39 ± 0.0036 (b)	0.32 ± 0.01 (b)	8.15 ± 0.01 (ab)	3.34 ± 0.70 (b)	3.29 ± 0.11 (b)
Field	0.047 ± 0.0025 (ab)	0.63 ± 0.0274 (ab)	0.54 ± 0.03 (b)	8.47 ± 0.03 (b)	3.08 ± 0.25 (b)	7.68 ± 0.53 (ab)

Parameters include TN, total nitrogen; TC, total carbon; TOC, total organic carbon; pH, NO3-N, nitrate; NH3-N, ammonia ($n = 6$). Different letters (a, b) signifies a statistical difference ($P < 0.05$). $n = 6$.

In contrast, very little ManA and GulA were detected in the soil samples, where GulA was higher in the field samples. GulA and ManA are commonly used as indicators for the presence of alginate, a common polysaccharide in bacterial biofilms (Gheorghita et al., 2022). The production of extracellular polysaccharides by bacterial species, can facilitate prolonged cellular hydration and nutrient resupply in dry soil environments (Or et al., 2007). Additionally, this can affect the soil structure by promoting water retention and aggregate formation (Chenu and Roberson, 1996; Henao and Mazeau, 2009). Lastly, amino sugars are present in soil and account for a generous fraction of soil nitrogen content (Indorf et al., 2011). Amino sugars (i.e., MurN, GlcN, GalN, ManN) are also present in the cell wall components of both bacteria and fungi in the form of peptidoglycan and chitin, respectively (Joergensen, 2018). Here, GalN and GlcN were detected in each sample with higher amounts of both being seen in field soil samples (Figure 3), which can be presumably traced to bacterial and fungal cell wall metabolism (Amelung et al., 1999).

Correlating the soil microbiome with the plant and soil glycomes is challenging as the interactions are highly complex and variables in the current study were limited. The composition of soil microbiomes can vary to the extent where there is not a "typical" soil microbiome that can be found amongst different soil types (e.g., clay, loam). This statement is also true if multiple soil samples are collected from sites that are centimeters apart, due to the spatial variability of soil and specific characteristics of each sampling site (O'Brien et al., 2016). Thus, inconsistency seen between the total carbohydrate content of the field soil samples may be partially explained by differences in the soil sampling sites, where soil samples collected from the field site were inconsistent in the distances between sampling locations. In contrast, all six soil samples collected from the greenhouse were gathered from the same 1 m^2 nursery bed. Furthermore, the composition of above-ground plant species cannot be used to predict the soil microbiome composition, as many soil bacteria may be associated with a broad range of plant taxa. However, taxonomic analysis of soil samples can provide insight regarding ecological services that may be occurring in the soil (Banerjee and Van Der Heijden, 2023). These insights could potentially be used as biological indicators to assess soil conditions and health.

Several other factors such as; soil pH, nitrogen availability, soil organic matter, moisture, season, and temperature, can directly or indirectly influence the spatial structure of soil microbial communities, with pH having a profound impact on bacteria (Rousk et al., 2010; Murphy et al., 2016). A less alkaline pH in the greenhouse soil (Table 3) could contribute to the differences in community structure between the greenhouse, field and baseline soils (Figures 4, 5). While soil moisture was not measured in the field, the plants were collected during a drought (Supplementary Table S6) and soils were assessed to contain 0% moisture in the lab. In contrast, greenhouse soil samples were watered to field moist conditions. Previous studies have shown that drier soils result in more restrained microbial dispersion, as microbes are limited to soil pores (Jansson and Hofmockel, 2018). In terms of soil microbial members, the relative abundance of Actinobacteria has been shown to increase under dry conditions, where this phylum becomes established as a dominant group in the soil environment (Naylor et al., 2017; Preece et al., 2019). In contrast, the abundance of Proteobacteria is negatively correlated with drought conditions (Preece et al., 2019). Here, an elevated abundance of Actinobacteria and a decreased abundance of Proteobacteria were seen in baseline soil samples (Figure 4C). Further, the relative abundances of these two phyla were also slightly higher in field soil samples, in comparison to greenhouse samples.

Soil amendments, such as the use of organic fertilizers (i.e., bloodmeal) have been previously shown to increase the relative abundances of Firmicutes and Proteobacteria within a soil microbial community (Schlatter et al., 2019). Here, the abundance of Proteobacteria was similar between the greenhouse and field soils, and was significantly reduced in the baseline soils. However, the relative abundance of Firmicutes increased in greenhouse soil samples (Figure 4C), which is likely the result of the bloodmeal amendments (Francioli et al., 2016). Specifically, there was a drastic increase in the abundance of Firmicutes members belonging to the *Bacillus* genus (Figure 5). This result may reflect a "healthy soil microbiome" as *Bacillus* species are commonly associated with beneficial effects within a soil ecosystem, such as phosphate solubilization and siderophore production to aid in iron uptake (Fierer and Jackson, 2006). Additionally, *Bacillus* members are also associated with the promotion of plant growth (Lugtenberg and Kamilova, 2009) and disease suppression (Zhou et al., 2023), having a direct effect on plant health.

5 Conclusion

Through a collaboration with a climate-focused charity and a First Nations community, glycomics traits associated with greenhouse-grown Sweetgrass were determined to predominantly contain cellulose and GAX polysaccharides, with an even monosaccharide distribution between the rhizomes, stems, and leaves. Within the soil microbial communities associated with Sweetgrass, an increased relative abundance of Firmicutes members was seen in comparison to the baseline and field soils and bacterial members belonging to the *Planifilum, Truepera,* and

JCM 18977 were only detected in the greenhouse soil samples. These observations, along with the traditional knowledge of Piikani Nation provided by knowledge holders, will help inform future work regarding the re-introduction of greenhouse-grown Sweetgrass back into the environment. Further studies will be required to see if the traits associated with the greenhouse cultivated Sweetgrass persist in plants grown and harvested from the field.

Data availability statement

The data presented in the study are deposited in the NCBI repository, BioProject Accession No: PRJNA1110276.

Author contributions

MK: Writing – original draft, Visualization, Methodology, Data curation. BB: Writing – review & editing, Methodology. NH: Writing – review & editing, Methodology. XX: Writing – review & editing, Methodology. KL: Writing – review & editing, Methodology. PN: Writing – review & editing, Methodology. EH: Writing – review & editing, Methodology. MV: Writing – review & editing, Methodology. BW: Writing – review & editing, Resources, Methodology, Conceptualization. LK: Writing – review & editing, Visualization, Methodology. NP: Writing – review & editing, Resources, Funding acquisition. WB: Writing – review & editing, Resources, Funding acquisition. LL: Writing – review & editing, Funding acquisition. TM: Writing – review & editing, Supervision, Methodology, Funding acquisition. PT: Writing – review & editing, Funding acquisition. MG: Writing – review & editing, Supervision, Funding acquisition. DA: Writing – review & editing, Supervision, Funding acquisition, Conceptualization.

Funding

The author(s) declare financial support was received for the research, authorship, and/or publication of this article. Funding for this work was provided by AgriScience Projects Program Canadian Agricultural Projects and the Resilience Institute (Project No. ASP-265; J-003023), with contributions from the Environmental Cooperation's Environmental Justice and Climate Resilience fund. In-kind support was provided by the Piikani Nation.

Acknowledgments

We thank Jesse Plain Eagle and students from the Piikani Nation Secondary School for their assistance during the sample collections. We also thank the Resilience Institute for acting as a bridging organization between the science team and the Indigenous community.

Conflict of interest

The authors declare that the research was conducted in the absence of any commercial or financial relationships that could be construed as a potential conflict of interest.

Publisher's note

All claims expressed in this article are solely those of the authors and do not necessarily represent those of their affiliated organizations, or those of the publisher, the editors and the reviewers. Any product that may be evaluated in this article, or claim that may be made by its manufacturer, is not guaranteed or endorsed by the publisher.

Supplementary material

The Supplementary Material for this article can be found online at: https://www.frontiersin.org/articles/10.3389/fmicb.2024.1384204/full#supplementary-material

References

Altschul, S. F., Gish, W., Miller, W., Myers, E. W., and Lipman, D. J. (1990). Basic local alignment search tool. *J. Mol. Biol.* 215, 403–410. doi: 10.1016/S0022-2836(05)80360-2

Amelung, W., Zhang, X. D., Flach, K. W., and Zech, W. (1999). Amino sugars in native grassland soils along a climosequence in north america. *Soil Sci. Soc. Am. J.* 63, 86–92. doi: 10.2136/sssaj1999.03615995006300010014x

Badhan, A., Low, K. E., Jones, D. R., Xing, X., Milani, M. R. M., Polo, R. O., et al. (2022). Mechanistic insights into the digestion of complex dietary fibre by the rumen microbiota using combinatorial high-resolution glycomics and transcriptomic analyses. *Comput. Struct. Biotechnol. J.* 20, 148–164. doi: 10.1016/j.csbj.2021.12.009

Bais, H. P., Weir, T. L., Perry, L. G., Gilroy, S., and Vivanco, J. M. (2006). The role of root exudates in rhizosphere interactions with plants and other organisms. *Annu. Rev. Plant Biol.* 57, 233–266. doi: 10.1146/annurev.arplant.57.032905.105159

Banerjee, S., and Van Der Heijden, M. G. A. (2023). Soil microbiomes and one health. *Nat. Rev. Microbiol.* 21, 6–20. doi: 10.1038/s41579-022-00779-w

Bastida, F., Eldridge, D. J., García, C., Kenny Png, G., Bardgett, R. D., and Delgado-Baquerizo, M. (2021). Soil microbial diversity–biomass relationships are driven by soil carbon content across global biomes. *ISME J.* 15, 2081–2091. doi: 10.1038/s41396-021-00906-0

Bolger, A. M., Lohse, M., and Usadel, B. (2014). Trimmomatic: a flexible trimmer for Illumina sequence data. *Bioinformatics* 30, 2114–2120. doi: 10.1093/bioinformatics/btu170

Brant, J. (2022). Lessons from our Sweetgrass baskets: A wholistic vision of academic success for indigenous women in higher education. *Can. J. High. Educ.* 52, 27–40.

Buanafina, M. M. D. O. (2009). Feruloylation in grasses: current and future perspectives. *Mol. Plant* 2, 861–872. doi: 10.1093/mp/ssp067

Burton, R. A., and Fincher, G. B. (2009). (1,3;1,4)-β-D-glucans in cell walls of the poaceae, lower plants, and fungi: a tale of two linkages. *Mol. Plant* 2, 873–882. doi: 10.1093/mp/ssp063

Caffall, K. H., and Mohnen, D. (2009). The structure, function, and biosynthesis of plant cell wall pectic polysaccharides. *Carbohydr. Res.* 344, 1879–1900. doi: 10.1016/j.carres.2009.05.021

Carpita, N. C. (1996). Structure and biogenesis of the cell walls of grasses. *Annu. Rev. Plant Physiol. Plant Mol. Biol.* 47, 445–476. doi: 10.1146/annurev.arplant.47.1.445

Carpita, N. C., and Gibeaut, D. M. (1993). Structural models of primary cell walls in flowering plants: consistency of molecular structure with the physical properties of the walls during growth. *Plant J.* 3, 1–30. doi: 10.1111/j.1365-313x.1993.tb00007.x

Carpita, N. C., and Shea, E. M. (1989). *Linkage Structure of Carbohydrates by Gas Chromatography-Mass Spectrometry (GC-MS) of Partially Methylated Alditol Acetates*. Boca Raton, FL: CRC Press.

Chang, S.-C., Kao, M.-R., Saldivar, R. K., Díaz-Moreno, S. M., Xing, X., Furlanetto, V., et al. (2023). The Gram-positive bacterium *Romboutsia ilealis* harbors a polysaccharide synthase that can produce (1,3;1,4)-β-D-glucans. *Nat. Commun.* 14 :4526. doi: 10.1038/s41467-023-40214-z

Cheng, T., Xu, C., Lei, L., Li, C., Zhang, Y., and Zhou, S. (2016). Barcoding the kingdom Plantae: new PCR primers for ITS regions of plants with improved universality and specificity. *Mol. Ecol. Resour.* 16, 138–149. doi: 10.1111/1755-0998.12438

Chenu, C., and Roberson, E. B. (1996). Diffusion of glucose in microbial extracellular polysaccharide as affected by water potential. *Soil Biol. Biochem.* 28, 877–884. doi: 10.1016/0038-0717(96)00070-3

Chong, H. H., Cleary, M. T., Dokoozlian, N., Ford, C. M., and Fincher, G. B. (2019). Soluble cell wall carbohydrates and their relationship with sensory attributes in *Cabernet Sauvignon* wine. *Food Chem.* 298:124745. doi: 10.1016/j.foodchem.2019.05.020

Ciavatta, C., Govi, M., Sitti, L., and Gessa, C. (1997). Influence of blood meal organic fertilizer on soil organic matter: a laboratory study. *J. Plant Nutr.* 20, 1573–1591. doi: 10.1080/01904169709365358

Dalmis, R., Kökta,ş, S., Seki, Y., and Kilin,ç, A. Ç. (2020). Characterization of a new natural cellulose based fiber from *Hierochloe Odorata*. *Cellulose* 27, 127–139. doi: 10.1007/s10570-019-02779-1

Dobrzyńska, I., Szachowicz-Petelska, B., Skrzydlewska, E., and Figaszewski, Z. (2013). Effect of sweet grass (*Hierochloe odorata*) on the physico-chemical properties of liver cell membranes from rats intoxicated with ethanol. *Environ. Toxicol. Pharmacol.* 35, 247–253. doi: 10.1016/j.etap.2012.12.014

Dubois, M., Gilles, K. A., Hamilton, J. K., Rebers, P. A., and Smith, F. (1956). Colorimetric method for determination of sugars and related substances. *Anal. Chem.* 28, 350–356. doi: 10.1021/ac60111a017

Fierer, N., and Jackson, R. B. (2006). The diversity and biogeography of soil bacterial communities. *Proc. Natl. Acad. Sci. U. S. A.* 103, 626–631. doi: 10.1073/pnas.0507535103

Francioli, D., Schulz, E., Lentendu, G., Wubet, T., Buscot, F., and Reitz, T. (2016). Mineral vs. organic amendments: microbial community structure, activity and abundance of agriculturally relevant microbes are driven by long-term fertilization strategies. *Front. Microbiol.* 7:1446. doi: 10.3389/fmicb.2016.01446

Gheorghita, A. A., Li, Y. E., Kitova, E. N., Bui, D. T., Pfoh, R., Low, K. E., et al. (2022). Structure of the AlgKX modification and secretion complex required for alginate production and biofilm attachment in Pseudomonas aeruginosa. *Nat. Commun.* 13, 7631. doi: 10.1038/s41467-022-35131-6

Gibeaut, D. M., Pauly, M., Bacic, A., and Fincher, G. B. (2005). Changes in cell wall polysaccharides in developing barley (*Hordeum vulgare*) coleoptiles. *Planta* 221, 729–738. doi: 10.1007/s00425-005-1481-0

Hatfield, R. D., Rancour, D. M., and Marita, J. M. (2017). Grass cell walls: a story of cross-linking. *Front. Plant Sci.* 7:2056. doi: 10.3389/fpls.2016.02056

Henao, L. J., and Mazeau, K. (2009). Molecular modelling studies of clay–exopolysaccharide complexes: soil aggregation and water retention phenomena. *Mater. Sci. Eng. C* 29, 2326–2332. doi: 10.1016/j.msec.2009.06.001

Hosain, N. A., Ghosh, R., Bryant, D. L., Arivett, B. A., Farone, A. L., and Kline, P. C. (2019). Isolation, structure elucidation, and immunostimulatory activity of polysaccharide fractions from *Boswellia carterii* frankincense resin. *Int. J. Biol. Macromol.* 133, 76–85. doi: 10.1016/j.ijbiomac.2019.04.059

Indorf, C., Dyckmans, J., Khan, K. S., and Joergensen, R. G. (2011). Optimisation of amino sugar quantification by HPLC in soil and plant hydrolysates. *Biol. Fertil. Soils* 47, 387–396. doi: 10.1007/s00374-011-0545-5

Ishii, T. (1997). Structure and functions of feruloylated polysaccharides. *Plant Sci.* 127, 111–127. doi: 10.1016/S0168-9452(97)00130-1

Izydorczyk, M. S., and Biliaderis, C. G. (1995). Cereal arabinoxylans: advances in structure and physicochemical properties. *Carbohydr. Polym.* 28, 33–48. doi: 10.1016/0144-8617(95)00077-1

Jansson, J. K., and Hofmockel, K. S. (2018). The soil microbiome-from metagenomics to metaphenomics. *Curr. Opin. Microbiol.* 43, 162–168. doi: 10.1016/j.mib.2018.01.013

Joergensen, R. G. (2018). Amino sugars as specific indices for fungal and bacterial residues in soil. *Biol. Fertil. Soils* 54, 559–568. doi: 10.1007/s00374-018-1288-3

Jones, D. L., Nguyen, C., and Finlay, R. D. (2009). Carbon flow in the rhizosphere: carbon trading at the soil–root interface. *Plant Soil* 321, 5–33. doi: 10.1007/s11104-009-9925-0

Jones, D. R., Xing, X., Tingley, J. P., Klassen, L., King, M. L., Alexander, T. W., et al. (2020). Analysis of active site architecture and reaction product linkage chemistry reveals a conserved cleavage substrate for an endo-alpha-mannanase within diverse yeast mannans. *J. Mol. Biol.* 432, 1083–1097. doi: 10.1016/j.jmb.2019.12.048

Juggins, S. (2022). *rioja: Analysis of Quaternary Science Data* [Online]. Available online at: https://cran.r-project.org/package=rioja (accessed January 11, 2024).

Kavasch, E. B., and Baar, K. (1999). *American Indian Healing Arts: Herbs, Rituals, and Remedies for Every Season of Life*. Thorsons.

Kembel, S. W., Cowan, P. D., Helmus, M. R., Cornwell, W. K., Morlon, H., Ackerly, D. D., et al. (2010). Picante: R tools for integrating phylogenies and ecology. *Bioinformatics* 26, 1463–1464. doi: 10.1093/bioinformatics/btq166

Klassen, L., Reintjes, G., Li, M., Jin, L., Amundsen, C., Xing, X., et al. (2023). Fluorescence activated cell sorting and fermentation analysis to study rumen microbiome responses to administered live microbials and yeast cell wall derived prebiotics. *Front. Microbiol.* 13:1020250. doi: 10.3389/fmicb.2022.1020250

López-Mondéjar, R., Algora, C., and Baldrian, P. (2019). Lignocellulolytic systems of soil bacteria: a vast and diverse toolbox for biotechnological conversion processes. *Biotechnol. Adv.* 37:107374. doi: 10.1016/j.biotechadv.2019.03.013

Low, K. E., Tingley, J. P., Klassen, L., King, M. L., Xing, X., Watt, C., et al. (2023). Carbohydrate flow through agricultural ecosystems: implications for synthesis and microbial conversion of carbohydrates. *Biotechnol. Adv.* 69:108245. doi: 10.1016/j.biotechadv.2023.108245

Low, K. E., Xing, X., Moote, P. E., Inglis, G. D., Venketachalam, S., Hahn, M. G., et al. (2020). Combinatorial glycomic analyses to direct CAZyme discovery for the tailored degradation of canola meal non-starch dietary polysaccharides. *Microorganisms* 8:1888. doi: 10.3390/microorganisms8121888

Lu, J., Breitwieser, F. P., Thielen, P., and Salzberg, S. L. (2017). Bracken: estimating species abundance in metagenomics data. *PeerJ Comp. Sci.* 3:e104. doi: 10.7717/peerj-cs.104

Lugtenberg, B., and Kamilova, F. (2009). Plant-growth-promoting rhizobacteria. *Annu. Rev. Microbiol.* 63, 541–556. doi: 10.1146/annurev.micro.62.081307.162918

McMurdie, P. J., and Holmes, S. (2013). Phyloseq: an R package for reproducible interactive analysis and graphics of microbiome census data. *PLoS ONE* 8:e61217. doi: 10.1371/journal.pone.0061217

Moerman, D. E. (1998). *Native American Ethnobotany*. Portland, OR: Timber Press.

Muhidinov, Z. K., Bobokalonov, J. T., Ismoilov, I. B., Strahan, G. D., Chau, H. K., Hotchkiss, A. T., et al. (2020). Characterization of two types of polysaccharides from *Eremurus hissaricus* roots growing in Tajikistan. *Food Hydrocoll.* 105:105768. doi: 10.1016/j.foodhyd.2020.105768

Murphy, C. A., Foster, B. L., and Gao, C. (2016). Temporal dynamics in rhizosphere bacterial communities of three perennial grassland species. *Agronomy* 6:17. doi: 10.3390/agronomy6010017

Naylor, D., Degraaf, S., Purdom, E., and Coleman-Derr, D. (2017). Drought and host selection influence bacterial community dynamics in the grass root microbiome. *ISME J.* 11, 2691–2704. doi: 10.1038/ismej.2017.118

O'Brien, S. L., Gibbons, S. M., Owens, S. M., Hampton-Marcell, J., Johnston, E. R., Jastrow, J. D., et al. (2016). Spatial scale drives patterns in soil bacterial diversity. *Environ. Microbiol.* 18, 2039–2051. doi: 10.1111/1462-2920.13231

Ogle, D. H., Doll, J. C., Wheeler, A. P., and Dinno, A. (2023). *FSA: Simple Fisheries Stock Assessment Methods*. Available online at: https://CRAN.R-project.org/package$=$FSA (accessed January 11, 2024).

Oksanen, J. S. G., Blanchet, F., Kindt, R., Legendre, P., Minchin, P., O'hara, R., et al. (2023). *Vegan: Community Ecology Package*. Available online at: https://github.com/vegandevs/vegan (accessed January 11, 2024).

Or, D., Smets, B. F., Wraith, J. M., Dechesne, A., and Friedman, S. P. (2007). Physical constraints affecting bacterial habitats and activity in unsaturated porous media – a review. *Adv. Water Resour.* 30, 1505–1527. doi: 10.1016/j.advwatres.2006.05.025

Panchal, P., Preece, C., Peñuelas, J., and Giri, J. (2022). Soil carbon sequestration by root exudates. *Trends Plant Sci.* 27, 749–757. doi: 10.1016/j.tplants.2022.04.009

Pattathil, S., Avci, U., Miller, J. S., and Hahn, M. G. (2012). Immunological approaches to plant cell wall and biomass characterization: glycome profiling. *Methods Mol. Biol.* 908, 61–72. doi: 10.1007/978-1-61779-956-3_6

Peña, M. J., Kulkarni, A. R., Backe, J., Boyd, M., O'neill, M. A., and York, W. S. (2016). Structural diversity of xylans in the cell walls of monocots. *Planta* 244, 589–606. doi: 10.1007/s00425-016-2527-1

Pérez, J., Muñoz-Dorado, J., De La Rubia, T., and Martínez, J. (2002). Biodegradation and biological treatments of cellulose, hemicellulose and lignin: an overview. *Int. Microbiol.* 5, 53–63. doi: 10.1007/s10123-002-0062-3

Pettolino, F. A., Walsh, C. T., Fincher, G. B., and Bacic, A. (2012). Determining the polysaccharide composition of plant cell walls. *Nat. Protoc.* 7, 1590–1607. doi: 10.1038/nprot.2012.081

Plain Eagle, N. (2023). *Discussion About Sweetgrass Prevelance on the Reserve*.

Preece, C., Verbruggen, E., Liu, L., Weedon, J. T., and Peñuelas, J. (2019). Effects of past and current drought on the composition and diversity of soil microbial communities. *Soil Biol. Biochem.* 131, 28–39. doi: 10.1016/j.soilbio.2018.12.022

Pukalskas, A., Van Beek, T., Venskutonis, R., Linssen, J., Veldhuizen, A., and Groot, A. (2002). Identification of radical scavengers in Sweet Grass (*Hierochloe odorata*). *J. Agric. Food Chem.* 50, 2914–2919. doi: 10.1021/jf011016r

Robb, C. S., Hobbs, J. K., Pluvinage, B., Reintjes, G., Klassen, L., Monteith, S., et al. (2022). Metabolism of a hybrid algal galactan by members of the human gut microbiome. *Nat. Chem. Biol.* 18, 501–510. doi: 10.1038/s41589-022-00983-y

Rousk, J., Bååth, E., Brookes, P. C., Lauber, C. L., Lozupone, C., Caporaso, J. G., et al. (2010). Soil bacterial and fungal communities across a pH gradient in an arable soil. *ISME J.* 4, 1340–1351. doi: 10.1038/ismej.2010.58

Sasse, J., Martinoia, E., and Northen, T. (2018). Feed your friends: do plant exudates shape the root microbiome? *Trends Plant Sci.* 23, 25–41. doi: 10.1016/j.tplants.2017.09.003

Scheller, H. V., and Ulvskov, P. (2010). Hemicelluloses. *Annu. Rev. Plant Biol.* 61, 263–289. doi: 10.1146/annurev-arplant-042809-112315

Schimel, J., and Schaeffer, S. (2012). Microbial control over carbon cycling in soil. *Front. Microbiol.* 3:348. doi: 10.3389/fmicb.2012.00348

Schlatter, D. C., Paul, N. C., Shah, D. H., Schillinger, W. F., Bary, A. I., Sharratt, B., et al. (2019). Biosolids and tillage practices influence soil bacterial communities in dryland wheat. *Microb. Ecol.* 78, 737–752. doi: 10.1007/s00248-019-01339-1

Schneider, R. (2013). *Alberta's Natural Subregions Under a Changing Climate: Past, Present, and Future*. Edmonton, AB: University of Alberta.

Sharifi-Rad, J., Cruz-Martins, N., López-Jornet, P., Lopez, E. P., Harun, N., Yeskaliyeva, B., et al. (2021). Natural coumarins: exploring the pharmacological complexity and underlying molecular mechanisms. *Oxid. Med. Cell. Longev.* 2021:6492346. doi: 10.1155/2021/6492346

Shebitz, D. J., and Kimmerer, R. W. (2004). Population trends and habitat characteristics of Sweetgrass, *Anthoxanthum nitens*: integration of traditional and scientific ecological knowledge. *J. Enthnobiol.* 24, 93–111.

Shebitz, D. J., and Kimmerer, R. W. (2005). Reestablishing roots of a Mohawk community and a culturally significant plant: Sweetgrass. *Restor. Ecol.* 13, 257–264. doi: 10.1111/j.1526-100X.2005.00033.x

Smith, B. G., and Harris, P. J. (1999). The polysaccharide composition of Poales cell walls: Poaceae cell walls are not unique. *Biochem. Syst. Ecol.* 27, 33–53. doi: 10.1016/S0305-1978(98)00068-4

Strikes with a Gun (2022). *Sweetgrass Partner Ceremony*. Piikani Nation.

Swincer, G. D., Oades, J. M., and Greenland, D. J. (1969). "The extraction, characterization, and significance of soil polysaccharides," in *Advances in Agronomy*, ed. N. C. Brady (Academic Press), 195–235.

Ueyama, Y., Arai, T., and Hashimoto, S. (1991). Volatile constituents of ethanol extracts of *Hierochloe odorata* L. var. Pubescens kryl. *Flav. Fragr. J.* 6, 63–68. doi: 10.1002/ffj.2730060108

Vinnitskiy, D. Z., Ustyuzhanina, N. E., and Nifantiev, N. E. (2015). Natural bacterial and plant biomolecules bearing α-d-glucuronic acid residues. *Russian Chem. Bull.* 64, 1273–1301. doi: 10.1007/s11172-015-1010-7

Vives-Peris, V., De Ollas, C., Gómez-Cadenas, A., and Pérez-Clemente, R. M. (2020). Root exudates: from plant to rhizosphere and beyond. *Plant Cell Rep.* 39, 3–17. doi: 10.1007/s00299-019-02447-5

Vogel, J. (2008). Unique aspects of the grass cell wall. *Curr. Opin. Plant Biol.* 11, 301–307. doi: 10.1016/j.pbi.2008.03.002

Voiges, K., Adden, R., Rinken, M., and Mischnick, P. (2012). Critical re-investigation of the alditol acetate method for analysis of substituent distribution in methyl cellulose. *Cellulose* 19, 993–1004. doi: 10.1007/s10570-012-9663-y

Vranova, V., Rejsek, K., Skene, K. R., Janous, D., and Formanek, P. (2013). Methods of collection of plant root exudates in relation to plant metabolism and purpose: a review. *J. Plant Nutr. Soil Sci.* 176, 175–199. doi: 10.1002/jpln.201000360

Wickham, H. (2007). Reshaping data with the reshape package. *J. Stat. Softw.* 21, 1–20. doi: 10.18637/jss.v021.i12

Wickham, H. (2016). *Ggplot2: Elegant Gaphics for Data Analysis*. New York, NY: Springer-Verlag.

Wickham, H. (2023). *Forcats: Tools for Working With Categorical Variables (Factors)*. Available online at: https://forcats.tidyverse.org/ (accessed January 11, 2024).

Wickham, H. F. R., Henry, L., Müller, K., and Vaughan, D. (2023). *Dplyr: A Grammar of Data Manipulation*. Available online at: https://dplyr.tidyverse.org, https://github.com/tidyverse/dplyr

Winslow, S. R. (2000). Propagation protocol for *Hierochloe odorata* Sweetgrass. *Native Plants J.* 1, 102–103. doi: 10.3368/npj.1.2.102

Wolf, S., and Greiner, S. (2012). Growth control by cell wall pectins. *Protoplasma* 249 (Suppl. 2), S169–175. doi: 10.1007/s00709-011-0371-5

Wood, D. E., Lu, J., and Langmead, B. (2019). Improved metagenomic analysis with Kraken 2. *Genome Biol.* 20:257. doi: 10.1186/s13059-019-1891-0

Wood, J. A., Tan, H. T., Collins, H. M., Yap, K., Khor, S. F., Lim, W. L., et al. (2018). Genetic and environmental factors contribute to variation in cell wall composition in mature desi chickpea (*Cicer arietinum* L.) cotyledons. *Plant Cell Environ.* 41, 2195–2208. doi: 10.1111/pce.13196

Yu, L., Yakubov, G. E., Zeng, W., Xing, X., Stenson, J., Bulone, V., et al. (2017). Multi-layer mucilage of Plantago ovata seeds: rheological differences arise from variations in arabinoxylan side chains. *Carbohydr. Polym.* 165, 132–141. doi: 10.1016/j.carbpol.2017.02.038

Zhalnina, K., Louie, K. B., Hao, Z., Mansoori, N., Da Rocha, U. N., Shi, S., et al. (2018). Dynamic root exudate chemistry and microbial substrate preferences drive patterns in rhizosphere microbial community assembly. *Nat. Microbiol.* 3, 470–480. doi: 10.1038/s41564-018-0129-3

Zhou, X., Zhang, J., Khashi, U. R. M., Gao, D., Wei, Z., Wu, F., et al. (2023). Interspecific plant interaction via root exudates structures the disease suppressiveness of rhizosphere microbiomes. *Mol. Plant* 16, 849–864. doi: 10.1016/j.molp.2023.03.009

Frontiers in Microbiology

Explores the habitable world and the potential of microbial life

The largest and most cited microbiology journal which advances our understanding of the role microbes play in addressing global challenges such as healthcare, food security, and climate change.

Discover the latest Research Topics

See more →

Frontiers

Avenue du Tribunal-Fédéral 34
1005 Lausanne, Switzerland
frontiersin.org

Contact us

+41 (0)21 510 17 00
frontiersin.org/about/contact